

8-1-2012

# SPECIATION STUDIES FOR BIOGENIC VOLATILE ORGANIC COMPOUNDS AND SECONDARY ORGANIC AEROSOL GENERATED BY OZONOLYSIS OF VOLATILE ORGANIC COMPOUND MIXTURES

Hardik Surendra Amin

*Southern Illinois University Carbondale*, hardikamin82@gmail.com

Follow this and additional works at: <http://opensiuc.lib.siu.edu/dissertations>

---

## Recommended Citation

Amin, Hardik Surendra, "SPECIATION STUDIES FOR BIOGENIC VOLATILE ORGANIC COMPOUNDS AND SECONDARY ORGANIC AEROSOL GENERATED BY OZONOLYSIS OF VOLATILE ORGANIC COMPOUND MIXTURES" (2012).  
*Dissertations*. Paper 528.

This Open Access Dissertation is brought to you for free and open access by the Theses and Dissertations at OpenSIUC. It has been accepted for inclusion in Dissertations by an authorized administrator of OpenSIUC. For more information, please contact [opensiuc@lib.siu.edu](mailto:opensiuc@lib.siu.edu).

SPECIATION STUDIES FOR BIOGENIC VOLATILE ORGANIC COMPOUNDS AND  
SECONDARY ORGANIC AEROSOL GENERATED BY OZONOLYSIS OF VOLATILE  
ORGANIC COMPOUND MIXTURES

By

Hardik Surendra Amin

M.Sc. Ramnarain Ruia College, Mumbai University, 2005

A Dissertation

Submitted in Partial Fulfillment of the Requirements for the  
Degree of Doctor of Philosophy

Department of Chemistry and Biochemistry  
In the Graduate School  
Southern Illinois University Carbondale  
August, 2012

DISSERTATION APPROVAL

SPECIATION STUDIES FOR BIOGENIC VOLATILE ORGANIC COMPOUNDS AND  
SECONDARY ORGANIC AEROSOL GENERATED BY OZONOLYSIS OF VOLATILE  
ORGANIC COMPOUND MIXTURES

By

Hardik Surendra Amin

A Dissertation Submitted in Partial

Fulfillment of the Requirements

for the Degree of

Doctor of Philosophy

in the field of Chemistry

Approved by:

Dr. Kara E. Huff Hartz, Chair

Dr. Qingfeng Ge

Dr. Matthew E. McCarroll

Dr. Luke Tolley

Dr. Lizette R. Chevalier

Graduate School  
Southern Illinois University Carbondale  
May 2, 2012

## AN ABSTRACT OF THE DISSERTATION OF

Hardik Surendra Amin, for the Doctor of Philosophy degree in Chemistry, presented on April 26, 2012, at Southern Illinois University Carbondale.

**TITLE: SPECIATION STUDIES FOR BIOGENIC VOLATILE ORGANIC COMPOUNDS AND SECONDARY ORGANIC AEROSOL GENERATED BY OZONOLYSIS OF VOLATILE ORGANIC COMPOUND MIXTURES**

**MAJOR PROFESSOR: Dr. Kara E. Huff Hartz**

Aerosols are either emitted directly into the atmosphere or are generated in the atmosphere; the latter process forms secondary organic aerosol (SOA). One of the important sources for SOA is the oxidation of volatile organic compounds (VOCs) by OH radicals, NO<sub>x</sub>, and O<sub>3</sub>. The condensed portion of aerosol is called particulate matter (PM). The severe impact of PM on human health and climate drives the scientific community to investigate volatile organic compounds (VOCs) and their potential to form SOA, as well as the factors that alter the efficiency of SOA generation and the types of products. In a similar pursuit, the focus of this dissertation is to investigate the SOA formation and products formed during oxidation of VOC mixtures. Studies of VOC mixtures which can undergo concurrent reactions are important because the findings provide insight on SOA generation and products formed in real environment.

Chapter 1 introduces PM, VOCs present in atmosphere, SOA generation, and speciation of products generated from the ozonolysis of VOCs. A literature survey on biogenic VOC emissions and factors leading to their variability along with SOA generation from direct plant emissions and consumer products is presented.

Chapter 2 shows the impact of bark beetle infestation on VOC emissions in western United States. Increases in the total and the individual VOCs emitted by infested trees were measured. A

statistical analysis shows significant differences between the emissions from infested and healthy trees. A perspective is provided on potential impact of bark beetle infestation on regional SOA.

Chapter 3 describes the results of the SOA generation by ozonolysis of limonene and VOC mixtures containing limonene. The yield of PM as a function of VOC precursor mixture was measured with respect to VOC composition and is found to be characteristic of most concentrated VOC in the mixture. The speciation studies in context of this dissertation are limited to structural elucidation of the condensed phase SOA products formed during ozonolysis of VOC mixtures. The identification of these products can be used to assess the toxicological impact of SOA mixtures. The condensed-phase SOA products from different VOC mixtures are identified using GC/MS, and variation in amount of the SOA products formed is correlated to composition of VOC mixture. In Chapter 4, condensed-phase products sampled from SOA generated by the ozonolysis of  $\alpha$ -pinene and VOC mixtures containing  $\alpha$ -pinene, including two fir needle essential oils, are studied. The products generated from VOC mixtures are characteristic of the dominant VOC present in the mixture i.e. either limonene or  $\alpha$ -pinene. The distribution of SOA products is found to change as the composition of the SOA precursor mixture changes.

In Chapter 5, the UV-visible absorption characteristics of ammonium ion-aged SOA, generated from limonene based air freshener and Siberian fir needle oil are discussed. Ammonium ion aging of aerosol impacts the radiative properties of aerosol and has the potential to impact aerosol's role in climate change. The conclusions from all chapters are summarized in Chapter 6.

## DEDICATION

I dedicate this dissertation to my family. To my parents, Mr. Surendra D. Amin and Mrs. Swapnali S. Amin for all the support, belief, and teaching me that biggest goals can be achieved when approached one step at a time. To my loving wife, Puja, for being there with me throughout the graduate program. To my dear sister, Dhanashree, to have never left my side and is very special. To my parents-in-law Pramod and Medha Tendolkar for being encouraging and having stood by me.

To my respected advisor, Dr Kara E. Huff Hartz, this dissertation would not have been completed if not for your guidance, leadership and mentoring.

## ACKNOWLEDGMENTS

The time I have spent in the Department of Chemistry and Biochemistry at SIUC while pursuing my doctoral degree has been a joyous experience and made me proactive professionally. This phase of my life would not be complete without the cooperation of many individuals, involved either directly or indirectly in my research work. First and foremost I wish to express my gratitude towards my research advisor and mentor, Dr. Kara Huff Hartz. She has constantly motivated me and encouraged me to approach the research problems systematic manner. Her continued guidance, and patient input in numerous discussions on the research topics have been invaluable. Her work ethic and time management have been precious lessons for me which I look forward to passing on to the others in future.

I wish to thank Professors Luke Tolley, Qingfeng Ge, Matthew McCarroll, and Lizette Chevalier for serving on my research committee and providing valuable inputs and comments to my research.

I would like to thank my colleagues at the Huff Hartz group – Meagan Hatfield, Audrey Wagner, Weiwei Hua, Kyle Power, John Junge, James Dalton, Andy Carr, Amy Meeks, Christa Schaefer, Aaron Brown and Ruth Umlor – for making our lab an enjoyable place to work. All your encouragement, cooperation and support have made this journey smoother. I will miss you all and hope our paths cross again in near future.

I would like to thank our collaborators for all their input for the bark beetle infestation project. I would like to thank P.Tyson Atkins, Ian McCubbin, Dr. Craig Dodson and Dr. A. Gannet Hallar from Storm Peak Laboratory, for their support and all field work. I would like to thank Dr. Barkley Sive and Rachel Russo for their invaluable input with analysis of canister samples.

I would like to thank Dr. Punit Kohli and lab members for splitting time with me to use the UV-visible instrument in their lab.

I am also thankful to the staff members at the department of chemistry, SIUC, namely, Kristen Burton, Kim Doellman, Dan Parker, Chris Kraft, Joan Marie Looft, Terry Christian, Glenn Shaw and Douglas Coons for their help in many other aspects indirectly related to research.

I wish to thank my parents, wife, parent-in-laws, and all the extended family members who have always encouraged, supported and stood behind me. And finally, I would like to thank my dear friends and roommates who have put up with numerous things. To name a few, Mr. Bhushan Pendse, Mr. Tushar Gadge, Mr. Kedar Karmarkar, Mr. Aniket Datar, Dr. Dheepak Jayaraman, Dr. Kaushik Balakrishnan, Mr. Mitesh Patil, Mr. Sudhaunshu Purohit, Mr. Bhushan Deodhar, Mr. Adeep Bhojne, Mr. Swapnil Bhatkalkar, Mr. Parag Desai, Mr. Arun Gothekar, Mr. Siddharth Joshi, Dr. Saikat Talapatra, Mr. Ashish and Mrs. Snehal Choudhari, Mr. Milind Bisen, Mr. Swananad Kulkarni, Mr. Navneet Dogra, Mr. Annirudha Khedlekar, Ms Gauri Pitale, Ms. Arya Joshi, Dr. Shubash Khedekar and family.



## TABLE OF CONTENTS

<u>CHAPTER</u>	<u>PAGE</u>
ABSTRACT.....	i
DEDICATION.....	iii
ACKNOWLEDGMENTS .....	iv
LIST OF TABLES.....	xiii
LIST OF FIGURES .....	xvi
CHAPTERS	
CHAPTER 1 – Introduction.....	1
1.1 Air pollutants .....	1
1.2 Complexity of aerosols .....	2
1.3 Particulate matter .....	2
1.3.1 Chemical composition of atmospheric PM.....	3
1.3.2 Effects of PM on atmosphere.....	5
1.3.2.1 Health effects of PM .....	5
1.3.2.2 PM effects on climate .....	6
1.3.2.2a Direct radiative forcing .....	7
1.3.2.2b Indirect radiative forcing.....	7
1.3.2.2c Mix of direct and indirect radiative forcing .....	8
1.4 Volatile organic compounds (VOCs): source of SOA.....	8
1.4.1 VOCs in atmosphere .....	9
1.4.2 VOCs in indoor environment.....	10
1.5 SOA generation from ozonolysis of VOCs .....	11

1.5.1 Generation of SOA by ozonolysis of plant emissions .....	12
1.5.2 Generation of SOA in indoor environments .....	15
1.6 SOA partitioning models .....	17
1.7 Reaction mechanism for ozonolysis of monoterpene .....	19
1.8 Effect of physical parameters on SOA formation .....	21
1.8.1 Effect of temperature on SOA formation .....	22
1.8.2 Effect of relative humidity on SOA formation .....	23
1.8.3 Effect of UV radiation on SOA formation .....	25
1.8.4 Effect of radical scavenger during SOA formation .....	25
1.9 Concluding remarks .....	27
CHAPTER 2 – Effect of Bark Beetle Infestation on Secondary Organic Aerosol Precursor	
Emission .....	28
2.1 Importance of BVOCs or biogenic SOA precursors .....	28
2.1.1 Monoterpenes as plants defense mechanism .....	29
2.1.2 Bark beetle-host interactions .....	29
2.1.3 Climate change: increase in bark beetle epidemic .....	31
2.2 Experimental details .....	31
2.2.1 Sample site description .....	31
2.2.2 VOC sample collection .....	34
2.2.3 Solvent extraction of VOCs in the scent traps .....	36
2.2.4 Analysis of VOCs using GCMS .....	36
2.2.5 Identification and quantitation of VOCs .....	38
2.3 Results and discussion .....	39

2.3.1 Lodgepole pine emissions.....	39
2.3.1.1 Individual VOCs from healthy vs. infested plants of lodgepole pine.....	39
2.3.1.2 Comparison of total VOC concentrations.....	45
2.3.2 Engelmann spruce emissions .....	50
2.3.2.1 Individual VOCs emitted from healthy vs infested plants from Engelmann spruce .....	50
2.3.2.2 Comparison in total VOC concentrations .....	52
2.3.3 Potential impact of bark beetle infestation on SOA.....	54
2.4 Conclusion .....	56
CHAPTER 3 – SOA Formation and Speciation Studies for Limonene, Limonene VOC Mixtures and Limonene Based Air Freshener.....	57
3.1 Introduction.....	57
3.1.1 SOA generation from limonene ozonolysis.....	58
3.1.2 Chemical speciation for SOA ozonolysis products form limonene.....	59
3.1.3 SOA generation and product analysis from monoterpenes mixtures.....	63
3.1.4 Ozonolysis of limonene and limonene based commercial products in indoor environment.....	64
3.2 Experimental details.....	66
3.2.1. SIUC smog chamber .....	67
3.2.2 Monitoring physical parameters of the smog chamber.....	69
3.2.3 Ozone monitoring instrument .....	71
3.2.4 Scanning mobility particle sizer.....	71
3.2.5 Hydroxyl radical scavenger .....	72
3.2.6 Ozone generation system .....	73

3.2.7 Injection of VOC in the chamber .....	73
3.2.8 Collection of SOA filters for speciation studies .....	74
3.2.9 Solvent extraction of SOA filter samples .....	74
3.2.10 Silylation of SOA filter extracts .....	77
3.2.11 GC/MS analysis of SOA filter samples .....	77
3.2.12 Identification of VOCs in limonene based air freshener .....	78
3.2.13 Particle generation and SOA yield calculations.....	92
3.3 Results and discussion .....	94
3.3.1 SOA yields for VOC mixtures.....	94
3.3.1.1 SOA yields for limonene .....	94
3.3.1.2 SOA yields form limonene and p-cymene VOC mixtures .....	95
3.3.1.3 SOA yields form mixtures of limonene and other reactive VOC's .....	95
3.3.1.4 SOA yields from mixtures containing linalool .....	96
3.3.2 SOA yields for surrogate mixtures and limonene based air freshener.....	101
3.3.3 Volatility basis set.....	107
3.3.4 Conclusion on SOA yield studies .....	112
3.3.5 SOA speciation studies .....	113
3.3.5.1 Identification of SOA products.....	113
3.3.5.2 Quantification of SOA products and calculation of amount of SOA collected.....	114
3.3.5.3 Speciation studies for SOA generation from limonene .....	115
3.3.5.4 Speciation studies for SOA generation from limonene + p-cymene mixture.....	125
3.3.5.5 Speciation studies for SOA generated from limonene, p-cymene, $\alpha$ -pinene, and $\beta$ -pinene mixture .....	126

3.3.5.6 Speciation studies for SOA generated from linalool containing mixtures .....	127
3.3.5.7 Speciation studies for SOA generated from surrogates .....	128
3.3.5.8 Speciation studies for limonene based air freshener .....	129
3.4 Conclusions .....	131
CHAPTER 4 – Speciation Studies for Products Generated from Ozonolysis of $\alpha$ -pinene, $\alpha$ -pinene VOC Mixtures, and Fir Needle Oil .....	134
4.1 Introduction .....	134
4.1.1 SOA from $\alpha$ -pinene and ozone reactions .....	134
4.1.2 SOA generation from mixed VOC systems containing $\alpha$ -pinene .....	136
4.2 Experimental details .....	139
4.2.1 SOA generation experiments .....	139
4.3 Results and discussion .....	139
4.3.1 SOA filters from ozonolysis of $\alpha$ -pinene and VOC mixtures .....	139
4.3.2 SOA filters from ozonolysis of SFNO surrogates, SFNO, and CFNO .....	143
4.3.3 Speciation studies for SOA products .....	146
4.3.3.1 Speciation studies for SOA generated by ozonolysis of $\alpha$ -pinene .....	147
4.3.3.1.1 Mass fragmentation patterns for individual SOA products .....	148
4.3.3.1.2 Comparison of SOA product yields to other work .....	150
4.3.3.2 Speciation of SOA generated by ozonolysis of $\alpha$ -pinene + bornyl acetate mixtures .....	155
4.3.3.3 Speciation of SOA generated by ozonolysis of VOC mixtures containing camphene .....	159
4.3.3.4 Speciation of SOA generated by ozonolysis of $\alpha$ -pinene and $\beta$ -pinene mixtures .....	162
4.3.3.5 Speciation generated by ozonolysis of reactive VOC mixtures .....	163
4.3.3.6 Speciation for SOA generated by ozonolysis of SFNO surrogates .....	165

4.3.3.7 Speciation of SOA generated by ozonolysis of SFNO .....	166
4.3.3.8 Speciation of SOA generated by ozonolysis of CFNO.....	167
4.4 Conclusions.....	168
CHAPTER 5 – Effect of $\text{NH}_4^+$ Aging of SOA Generated from Lemon and Chamomile Air	
Freshener and Siberian Fir Needle Oil.....	171
5.1 Introduction.....	171
5.1.1 Elemental carbon and organic carbon as absorbing species .....	171
5.1.2 Chemical composition of light absorbing species in aerosols .....	172
5.1.3 Role of inorganic ions in absorption of radiation by aerosols .....	173
5.1.4 UV-visible absorbance by ammonium aged SOA .....	174
5.2 Experimental details.....	176
5.2.1 Generation of SOA from SFNO .....	177
5.2.2 Generation of SOA from limonene based air freshener.....	177
5.2.3 UV-visible spectroscopy .....	178
5.3 Results.....	179
5.3.1 SOA yields from SFNO .....	179
5.3.2 Absorbance spectra for blank filters .....	184
5.3.3 Limonene-based air freshener chamber blanks.....	186
5.3.4 Siberian fir needle oil chamber blanks.....	188
5.3.5 Limonene-based air freshener SOA filter samples .....	190
5.3.6 Siberian fir needle oil SOA filter samples .....	193
5.4 Calculation and discussions .....	195
5.4.1 Calculation of average absorption coefficients.....	195

5.4.2 Absorption coefficients for $\text{NH}_4^+$ aged limonene-based air freshener SOA .....	195
5.4.3 Absorption coefficients for $\text{NH}_4^+$ aged SFNO SOA .....	198
5.4.4 Comparison of absorption coefficients for $\text{NH}_4^+$ aged SFNO and limonene-based air freshener SOA.....	199
5.5 Conclusions.....	200
CHAPTER 6 – Summary and Conclusion.....	201
6.1 Research Amis .....	201
6.2 Research Findings.....	201
6.3 Future Direction.....	203
REFERENCES .....	204
APPENDICES	
Appendix I – Total VOCs from Individual Scent trap samples collected over the period of bark beetle project.....	237
Appendix II – Physical parameters for smog chamber experiments in Chapter 3 .....	242
Appendix III – Mass spectral fragmentation for SOA products identified from limonene VOC mixtures for Chapter 3 .....	246
Appendix IV – Mass spectral fragmentation patterns for SOA products identified from $\alpha$ -pinene VOC mixtures for Chapter 4.....	261
Appendix V – Permission to reproduce Figure 2.2 “The sampling assembly for collection of VOCs using scent traps” .....	273
VITA .....	274

## LIST OF TABLES

<u>TABLE</u>	<u>PAGE</u>
<b>Table 2.1</b> Location and description of sampled trees along with number of samples collected at each location .....	33
<b>Table 2.2</b> Monoterpenes used to make VOC calibration standards .....	39
<b>Table 2.3</b> Concentration $\pm$ standard error of the mean <sup>a</sup> (ng L <sup>-1</sup> ) of the major VOCs, averaged over the entire study, obtained from extracts of lodgepole pine samples .....	41
<b>Table 2.4</b> Concentration $\pm$ standard error of the mean <sup>a</sup> (ng L <sup>-1</sup> ) of the minor VOCs, averaged over the entire study, obtained from extracts of lodgepole pine samples .....	42
<b>Table 2.5</b> Summary of the total VOCs sampled by sorbent traps and detected by GCMS from lodgepole pine.....	46
<b>Table 2.6</b> Statistical comparison of the total VOCs sampled from lodgepole pine .....	49
<b>Table 2.7</b> Concentration $\pm$ standard error of the mean <sup>a</sup> (ng L <sup>-1</sup> ) of the major VOCs, averaged over the entire study for Engelmann spruce .....	51
<b>Table 2.8</b> Summary of the total VOCs sampled by sorbent traps and detected by GCMS for Engelmann spruce trees.....	53
<b>Table 3.1</b> List of compounds used as surrogate standards for quantification of SOA products. Deuterated standards are used as internal standards and calculate % recovery for SOA products .....	76
<b>Table 3.2</b> VOC standards used for calibration of amounts in limonene-based air freshener.....	80
<b>Table 3.3</b> Components Present in Limonene Based Air Freshener.....	85
<b>Table 3.4</b> VOC precursor concentrations and calculated SOA yields from limonene and other VOC mixtures .....	98



<b>Table 3.5</b> VOC precursor concentrations and calculated SOA yields for surrogates and limonene containing air freshener .....	103
<b>Table 3.6</b> Fitted $\alpha_i$ values and $C_i^*(\mu\text{g m}^{-3})$ for volatility basis set of limonene and air freshener .....	112
<b>Table 3.7</b> Summary of percent individual SOA product yields of SOA products generated by ozonolysis of limonene based precursors .....	117
<b>Table 3.8</b> Molar yields (%) for SOA products identified by Glasius et al. and this work .....	121
<b>Table 3.9</b> Molar yields for SOA products identified in this work.....	122
<b>Table 4.1</b> VOC precursor concentrations and amount of SOA collected on filters from ozonolysis of $\alpha$ -pinene and other VOC mixtures.....	142
<b>Table 4.2</b> VOC precursor concentrations and amount of SOA collected on filters from oxidation of SFNO surrogates, SFNO, and CFNO .....	145
<b>Table 4.3</b> Summary of percent individual SOA product yields of SOA products generated by ozonolysis of $\alpha$ -pinene based precursors.....	152
<b>Table 4.4</b> Comparison of molar yields for $\alpha$ -pinene SOA ozonolysis products in percentage (%). .....	154
<b>Table 5.1</b> Average absorption coefficient ( $\text{Lg}^{-1}\text{cm}^{-1}$ ) for monoterpenes reported by Bones et al. for sample treated with $0.008 \text{ mol L}^{-1}$ , obtained after 20 hours .....	176
<b>Table 5.2</b> Experimental parameters and amount of SOA collected on filters for SFNO .....	183
<b>Table 5.3</b> Average absorption for treated and untreated blank filter samples.....	186
<b>Table 5.4</b> Average absorption for treated and untreated chamber blanks for limonene-based air freshener .....	188

<b>Table 5.5</b> Average absorption for treated and untreated chamber blanks for Siberian fir needle oil.....	190
<b>Table 5.6</b> Average absorption for treated and untreated SOA filter generated from ozonolysis of limonene-based air freshener.....	192
<b>Table 5.7</b> Average absorption for treated and untreated SOA filter generated from ozonolysis of Siberian fir needle oil .....	194
<b>Table 5.8</b> Calculated and measured average absorbance Coefficients ( $\beta$ ) for Lemon and Chamomile Air Freshener.....	197
<b>Table 5.9</b> Average absorbance coefficients for Siberian fir needle oil .....	198

## LIST OF FIGURES

<u>FIGURE</u>	<u>PAGE</u>
<p><b>Figure 1.1</b> Average PM (<math>\leq 2.5 \mu\text{m}</math>) composition for St Louis, MO in 2002. The concentration of the components in decreasing order of concentration is organic carbon (38%), sulfates (24%), nitrates (12%), ammonium (11%), other species (mostly water, 6%) crustal material (5%) and elemental carbon (4%) .....</p>	4
<p><b>Figure 1.2</b> Reaction mechanism for the ozonolysis of <math>\alpha</math>-pinene. Adapted from Ma et al., and Jang and Kamens .....</p>	21
<p><b>Figure 2.1</b> Map of sampling region located in northwestern Colorado, USA. Base image provided by Google Earth 6.1.0.5001 .....</p>	32
<p><b>Figure 2.2</b> The sampling assembly for collection of VOCs using scent traps. ....</p>	35
<p><b>Figure 2.3</b> GCMS chromatogram of VOCs obtained from bark of (a) infested and (b) healthy lodgepole pine tree. The peak shown in red is for the internal standard <math>\text{d}^{22}</math>-decane .....</p>	40
<p><b>Figure 2.4</b> Box and whisker plots of the major VOCs found in the scent trap samples collected from the trunks of healthy (S1T1, S2T7, S3T9) and infested lodgepole pine trees (S1T2, S2T6, S3T10). The median, the 25<sup>th</sup> percentile, and the 75<sup>th</sup> percentile are denoted by the center line and the edges of the box, the 10<sup>th</sup> and 90<sup>th</sup> percentiles are denoted by the whiskers, and the mean is denoted by the symbols .....</p>	44
<p><b>Figure 2.5</b> Total VOC concentrations for all scent trap samples collected from lodgepole pine. The center line of the box is the median, the edges of the blocks are the 25<sup>th</sup> and 75<sup>th</sup> percentile, and the whiskers are the 10<sup>th</sup> and 90<sup>th</sup> percentile. The closed circles and open circles represent the average total VOCs sampled near the trunk and in the canopy, respectively. Trees labeled “I” on the x-axis are beetle infested. Inset: scale expansion for total VOC concentrations for non-infested trees .....</p>	47

<b>Figure 2.6</b> Box and whisker plots of the major VOCs found in the scent trap samples collected from the trunk of healthy spruce (S2T5) and infested spruce tree (S2T4). The median, the 25 <sup>th</sup> percentile, and the 75 <sup>th</sup> percentile are denoted by the center line and the edges of the box, the 10 <sup>th</sup> and 90 <sup>th</sup> percentiles are denoted by the whiskers, and the mean is denoted by the symbols.....	52
<b>Figure 3.1</b> Experimental set up for SOA generation.....	67
<b>Figure 3.2</b> PTFE access port (6 inches diameter). The big circles have diameter of 3/8 inches and the medium circles have a diameter of 1/4 inches; the smallest circles are the screws .....	68
<b>Figure 3.3</b> Total ion chromatogram for limonene-based air freshener for retention times ranging from 10.3 min to 29.6 min. The chromatogram is split in three panes the first ranging from 10.3 min to 17.3 min (Figure 3.3a), the second ranging from 17.3 min to 22.8 min (Figure 3.3b), and the third ranging from 22.8 min to 29.6 min (Figure 3.3c). No peaks other than from the solvent were observed prior to 10.5 min, and some polysiloxane peaks due to the column elute after 29.6 min, and these are not shown. 90±0.3 % by mass of the components in the air freshener was identified. Components were identified using retention time comparison with commercially available standard and mass spectral comparison to NIST library. VOCs were identified by mass spectral comparison and confirmed using Adams retention indices. The components are identified using probability based matching of mass spectra with NIST library. These peaks are either polysiloxane compounds or are present in the solvent chromatogram as well.....	79
<b>Figure 3.4</b> Best fit curve for Adams indices versus experimental retention times. The empty circles represent the standards. The dashed line represents the best fitting line, the equation of line is: $y = 0.004x^3 - 0.101x^2 + 0.962x + 2.122$ where x is the retention time of VOCs measured in our work, and y values are the Adams indices (2007).....	82

**Figure 3.5** PM generated by the reaction of  $367 \pm 48 \mu\text{g m}^{-3}$  limonene with  $530 \pm 33$  ppb of ozone. The temperature, pressure, and %RH are  $293.1 \pm 0.3$  K,  $0.984 \pm 0.001$  atm and  $3.0 \pm 1.8$  (%) respectively. The open circles indicate the PM concentration, measured by SMPS, as a function of time. The solid line is the best fit line obtained by using equation above. The dashed line represents the PM concentration corrected for losses to the walls where  $k_2 = 0$ . The values and error for PM,  $k_1$  and  $k_2$  are calculated using Sigma Plot 10.0 .....93

**Figure 3.6** SOA yield vs  $M_0$  for limonene, VOC mixtures, surrogates and air freshener. Yields are represented according to the following symbols: limonene only ( $\times$ ), limonene + p-cymene (Mixtures 2A, 2B, 2C, 2D) (red circles), limonene+ p-cymene +  $\alpha$ -pinene + $\beta$ -pinene mix (mixture 3) (green triangles, face up), limonene+ linalool + p-cymene +  $\alpha$ -pinene + $\beta$  -pinene mix (mixtures 4A and 4B) (blue squares), limonene +linalool (yellow square), surrogates 1, 2, 3 and 4 (maroon diamonds), air freshener trial 1 and trial 2 (dark green triangles with face down). The lines represent the volatility basis fit using parameters given in table below. Solid line: this work, Dotted line: Chen and Hopke;165 long dash and dot dash represent the work by Saathoff et al.; 92 for two different conditions, dot dot dash: Zhang et al.;101. The curves are corrected for density  $1\text{g cm}^{-3}$  by dividing the calculated values by reported density (Saathoff et al.,92 density =  $1.3\text{ g cm}^{-3}$ ; Chen and Hopke,165 density =  $1.5\text{ g cm}^{-3}$ ) .....109

**Figure 3.7 .** Expanded view of Figure 3.6 SOA yield vs  $M_0$  for limonene, VOC mixtures, surrogates and air freshener. Yields are represented according to the following symbols: limonene only ( $\times$ ), limonene + p-cymene (Mixtures 2A, 2B, 2C, 2D) (red circles), limonene+ p-cymene +  $\alpha$ -pinene + $\beta$ -pinene mix (mixture 3) (green triangles, face up), limonene+ linalool + p-cymene +  $\alpha$ -pinene + $\beta$  -pinene mix (mixtures 4A and 4B) (blue squares), limonene +linalool (yellow square), surrogates 1, 2, 3 and 4 (maroon diamonds), air freshener trial 1 and trial 2 (dark

green triangles with face down). The lines represent the volatility basis fit using parameters given in table below. Solid line: this work, dotted line: Chen and Hopke;<sup>165</sup> long dash and dot dash represent the work by Saathoff et al.;<sup>92</sup> for two different conditions, dot dot dash: Zhang et al.<sup>101</sup> The curves are corrected for density 1 g cm<sup>-3</sup> by dividing the calculated values by reported density (Saathoff et al.,<sup>92</sup> density = 1.3 g cm<sup>-3</sup>; Chen and Hopke,<sup>165</sup> density = 1.5 g cm<sup>-3</sup>). .....110

**Figure 3.8** Synthesis of 2-hydroxy-3-(prop-1-en-2-yl)pentanedial adapted from Walser et al. .124

**Figure 3.9** Structures for 5-oxohexanoic acid and 6-oxoheptanoic acid.....124

**Figure 3.10** Mass fragmentation pattern for C<sub>8</sub>H<sub>14</sub>O<sub>4</sub> a) fragments in EI mode, b) fragments in CI mode.....131

**Figure 3.11** Variation in composition of SOA products among various limonene precursors...133

**Figure 4.1** Decrease in SOA product concentrations with increase in bornyl acetate concentrations .....156

**Figure 5.1** SOA yield vs M<sub>0</sub> for Siberian fir needle oil. The experiments carried out for SOA generation (details Table 5.1) are represented by the two filled circles; the error in each parameter is shown. The error in SOA yields are calculated by propagation of uncertainties associated with VOC concentrations and M<sub>0</sub>. The error in M<sub>0</sub> is the standard error associated with curve-fit used for wall loss corrections used in this experiment. The additional lines represent the volatility basis set fit for  $\alpha$ -pinene SOA. Black dashed line: Chan et al. (2009); black solid line: Hatfield and Huff Hartz (2011); Gray dashed line Pathak et al. (2007); black dash dot line: Presto and Donahue (2006); black dotted line: Shilling et al (2009) .....182

**Figure 5.2** UV-visible absorption spectra of (a) untreated blank filter (b) NH<sub>4</sub><sup>+</sup> treated blank filter (c) difference in UV-visible absorption of treated and untreated blank filters (d) expanded view for part c, from wavelength 300 nm to 700 nm. Curves in each plot represent UV-visible

spectra at different times after addition of  $\text{NH}_4^+$ , black solid line represents 162 hours, dotted black line represents 138 hours, dash black line represents 66 hours, dark gray solid line represents 48 hours, dotted dark gray line represents 36 hours, dash dark gray line represents 24 hours, gray solid line represents 12 hours, and dotted gray line represents 0 hours.....185

**Figure 5.3** UV-visible absorption spectra of (a) untreated chamber blank of lemon and chamomile filter (b)  $\text{NH}_4^+$  treated chamber blank of lemon and chamomile filter (c) difference in UV-visible absorption of treated and untreated chamber blank of lemon and chamomile filter (d) expanded view for part c, from wavelength 300 nm to 700 nm. Curves in each plot represent UV-visible spectra at different times after the addition of  $\text{NH}_4^+$ , black solid line represents 162 hours, dotted black line represents 138 hours, dash black line represents 66 hours, dark gray solid line represents 48 hours, dotted dark gray line represents 36 hours, dash dark gray line represents 24 hours, gray solid line represents 12 hours, and dotted gray line represents 0 hours.....187

**Figure 5.4** UV-visible absorption spectra of (a) untreated chamber blank of SFNO filter (b)  $\text{NH}_4^+$  treated chamber blank of SFNO filter (c) difference in UV-visible absorption of treated and untreated chamber blank of SFNO filter (d) expanded view for part c, from wavelength 300 nm to 700 nm. Curves in each plot represent UV-visible spectra at different times after addition of  $\text{NH}_4^+$ , black solid line represents 162 hours, dotted black line represents 138 hours, dash black line represents 66 hours, dark gray solid line represents 48 hours, dotted dark gray line represents 36 hours, dash dark gray line represents 24 hours, gray solid line represents 12 hours, and dotted gray line represents 0 hours .....189

**Figure 5.5** UV-visible absorption spectra of (a) untreated lemon and chamomile SOA filter (b)  $\text{NH}_4^+$  treated lemon and chamomile SOA filter (c) difference in UV-visible absorption of treated and untreated lemon and chamomile SOA filter (d) expanded view for part c, from wavelength

300 nm to 700 nm. Curves in each plot represent UV-visible spectra at different times after addition of  $\text{NH}_4^+$ , black solid line represents 162 hours, dotted black line represents 138 hours, dash black line represents 66 hours, dark gray solid line represents 48 hours, dotted dark gray line represents 36 hours, dash dark gray line represents 24 hours, gray solid line represents 12 hours, and dotted gray line represents 0 hours.....191

**Figure 5.6** UV-visible absorbance spectra of (a) untreated SFNO SOA filter (b)  $\text{NH}_4^+$  treated SFNO SOA filter (c) difference in UV-visible absorption of treated and untreated SFNO SOA filter (d) expanded view for part c, from wavelength 300 nm to 700 nm. The curves in each plot represent UV-visible spectra at different times after addition of  $\text{NH}_4^+$ , where the black solid line represents 162 hours, dotted black line represents 138 hours, dash black line represents 66 hours, dark gray solid line represents 48 hours, dotted dark gray line represents 36 hours, dash dark gray line represents 24 hours, gray solid line represents 12 hours, and dotted gray line represents 0 hours.....193



## CHAPTER 1

### INTRODUCTION

#### 1.1 Air pollutants

Air is very important for sustainability and survival; without air, humans can last only for a small period of time. Polluted air can lead to declines in the health of human population. For example, the World Health Organization estimates that 2.4 million people die each year from causes directly attributable to air pollution.<sup>1</sup> Air pollution can damage trees, crops, plants, lakes, and thus, the ecosystem,<sup>2,3</sup> and can also affect the climate.<sup>4</sup> *“Air pollution is defined as contamination of the indoor or outdoor environment by any chemical, physical, or biological agent that modifies natural characteristics of the atmosphere”.*<sup>5</sup> The exact composition of “unpolluted” air is unknown to us. Over the period of thousands of years, anthropogenic and biogenic activities have influenced the composition of air.<sup>6,7</sup>

Air quality is degraded with even amounts of pollutants and contaminants. A contaminant is a compound that is present in higher concentration than it is found naturally. An air pollutant is a contaminant which is introduced in the air and is present in concentrations where it can cause detrimental effects to human and ecosystem health.

Currently in the United States, according to the Clean Air Act,<sup>8</sup> the EPA sets and monitors the National Ambient Air Quality Standards for the six most common air pollutants. These pollutants are called as criteria air pollutants and have the potential to harm human health, the environment, and cause property damage. The criteria air pollutants are particulate matter, ground-level ozone, carbon monoxide, sulfur oxides, nitrogen oxides, and lead. Due to the nature of their impact on health and environment, it is important to understand the sources and the

transformations of these pollutants in the atmosphere. The scope of this dissertation is limited to a fraction of particulate matter (PM) called secondary organic aerosol (SOA).

## **1.2 Complexity of aerosols**

An aerosol is a solid or a liquid particle surrounded by gases, where the gas phase and condensed phase components of the aerosol are in equilibrium. The condensed phase of aerosols is called PM. Aerosols vary in composition and phase because they are emitted into the atmosphere by various sources and undergo various chemical reactions and physical changes. Aerosols affect the climate<sup>9</sup> and have adverse effects on human health.<sup>10,11</sup> To minimize the negative effects of aerosols, it is important to set standards on the amount of aerosols and take actions to meet the standards. Meeting the standards is a challenging task, because it is difficult to control the numerous sources of aerosols and transformations in environment that lead to their formation.

## **1.3 Particulate matter**

PM is the condensed-phase portion of aerosol. Atmospheric PM is grouped according to diameter of the particle: less than 0.1  $\mu\text{m}$  ( $\text{PM}_{0.1}$ ), less than 2.5  $\mu\text{m}$  ( $\text{PM}_{2.5}$ ), and particles less than 10  $\mu\text{m}$  ( $\text{PM}_{10}$ ).<sup>12</sup>  $\text{PM}_{0.1}$  include nucleation mode particles (also known as primary particles) that result from direct emissions (e.g., combustion of fossil fuel or biomass burning) or are generated from condensable products in atmosphere (e.g., oxidation of monoterpenes).  $\text{PM}_{2.5}$  includes accumulation mode particles (or secondary particles). These particles are formed from the growth of nucleation mode particles via condensation and coagulation. The particles which are larger than 2.5  $\mu\text{m}$  ( $\text{PM}_{10}$ ) are called coarse mode particles. These particles are made from

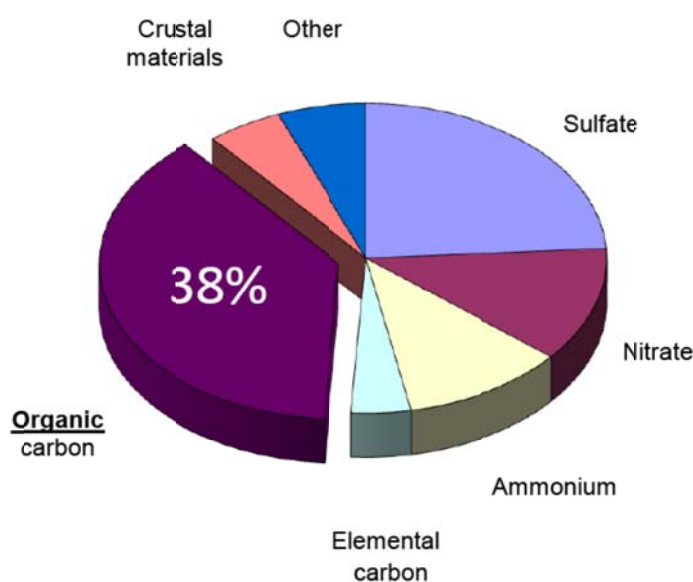
dust, pollen, mold, volcanic ash, and sea salt. Particles generated due to surface erosion, grinding of rocks, and mining processes also fall in this category.

The volume of atmospheric PM is dominated in by accumulation mode particles. The nucleation mode particles are short-lived in atmosphere and usually undergo coagulation and condensation to form accumulation mode particles. The coarse mode particles tend to settle as a result of gravitational deposition. Accumulation mode particles can reside in atmosphere for weeks and are lost via wet/dry deposition and heterogeneous processing. When compared to nucleation mode particles and coarse mode particles, the accumulation mode particles have longer life times and hence may travel long distances, and they are able to affect a larger population.

### **1.3.1 Chemical composition of atmospheric PM**

To understand the effects of PM on climate and health, it is important to know the chemical composition of the PM. A detailed study to characterize PM and to develop source-receptor-exposure-effect relationships was undertaken at various locations known as “supersites” under supervision of the USEPA in 2000.<sup>13</sup> The average PM ( $\leq 2.5 \mu\text{m}$ ) composition for St Louis, MO supersite during 2002 is shown in Figure 1.1.<sup>14</sup> The major source of these measurements were found to be anthropogenic activities. The highest contribution to the PM ( $\leq 2.5 \mu\text{m}$ ) composition was from organic carbon, around 38%. The next dominate species was sulfate which is known to dominate the PM in eastern North America.<sup>15</sup> The majority of sulfates are present in form of ammonium sulfate, generated by reaction of  $\text{SO}_2$  with ammonia (and water) in the atmosphere. Around 65% of primary  $\text{SO}_2$  is the result of electrical utilities emissions.<sup>16</sup> Highway vehicular emissions are major source of  $\text{NO}_x$ <sup>16</sup> and around 35%,  $\text{NO}_x$  reacts with ammonia to generate

ammonium nitrates. Nitrates dominate the PM ( $\leq 2.5 \mu\text{m}$ ) composition over western North America.<sup>15</sup> The majority of  $\text{NH}_3$ , around 85%, is generated by agricultural activities.<sup>16</sup> Other classes of compounds, like the crustal materials and elemental carbon, contributed to 10-15% of the total PM. The relative amounts for all the categories of  $\text{PM}_{2.5}$  show a dependence on geographical location and a seasonal dependence. The fraction of organic carbon in  $\text{PM}_{2.5}$  can range from 10-70%, and usually is the largest fraction of  $\text{PM}_{2.5}$  in non-marine areas.<sup>13</sup>



**Figure 1.1** Average PM ( $\leq 2.5 \mu\text{m}$ ) composition for St Louis, MO in 2002. The concentration of the components in decreasing order of concentration is organic carbon (38%), sulfates (24%), nitrates (12%), ammonium (11%), other species (mostly water, 6%) crustal material (5%) and elemental carbon (4%)<sup>14</sup>

This composition of  $\text{PM}_{2.5}$  is largely affected by primary sources of emissions. The composition of  $\text{PM}_{2.5}$  is dominated by organic carbon, which can be generated by oxidation of volatile organic carbon to form SOA. The SOA can undergo coagulation and condensation reactions to generate  $\text{PM}_{2.5}$ .  $\text{PM}_{2.5}$  has significant impact on climate and human health. Hence, it

important to investigate the SOA formation process and species generated during oxidation of VOCs.

### **1.3.2 Effects of PM on atmosphere**

#### **1.3.2.1 Health effects of PM**

SOA is solid or liquid PM surrounded by gases, and in this section we discuss the negative effects on health generated by PM and gases surrounding PM. Inhalation of particles can lead to detrimental cardiopulmonary health.<sup>10</sup> Deposition of particles in lungs and airways is dependent on size of the particles.<sup>18</sup> Particles above 10  $\mu\text{m}$  are filtered by the nose and throat and do not have serious effects when compared with smaller particles. Exposures to ultrafine particles,  $\text{PM}_{0.1}$ , prove more harmful to health. The ultrafine particles enter the lungs and embed into the gas-exchange regions within the lungs, causing a greater risk of inflammation and oxidative stress compared to larger particles.<sup>19,20</sup> Other health effects associated with PM exposure and increased risk of asthma, chronic bronchitis, decreased lung function, irregular heartbeat, heart attacks, airway inflammation, and premature death. Epidemiology studies summarized by Davidson et al.<sup>11</sup> show that the extent of the effects of PM on health varies with age, sex, and race, and the severity increases with preexisting medical condition. Weichenthal and Dufresne<sup>21</sup> suggested that asthmatic symptoms may be triggered in the children upon exposure to ultrafine particles. Brook and Rajagpalan<sup>22</sup> also have linked PM exposure to increased blood pressure.

The USEPA has designated PM as one of the six criteria pollutants (Section 1.2). The EPA has set a 24 hour standard of  $35 \mu\text{g m}^{-3}$  for ambient  $\text{PM}_{2.5}$ , which is measured as the 98<sup>th</sup> percentile for 24 hour measurements taken over a 3 year period. This  $\text{PM}_{2.5}$  standard was made

stringent, reducing it from  $65 \mu\text{g m}^{-3}$ , in 1997<sup>23</sup> to  $35 \mu\text{g m}^{-3}$  in 2006.<sup>24</sup> The number of US counties and population that live in non-attainment areas have decreased from 1997 to 2006.

Air fresheners and household cleaners which contain VOCs can react with oxidants indoors and form SOA. In addition to SOA, the oxidation of air fresheners and household cleaners can form gaseous products like formaldehyde, which is classified as carcinogen by USEPA.<sup>25</sup> Also, traces of acetaldehyde, acetone, glycoaldehyde, formic acid, and acetic acid have been identified in the gas-phase fraction of SOA.<sup>26,27</sup>

### **1.3.2.2 PM effects on climate**

The incoming radiation from the sun encounters the atmosphere before interacting with surface of the earth. Nearly 40% of the incoming radiation is absorbed and reflected by the atmosphere. PM contributes to the absorption and reflection by the atmosphere and the chemical composition of PM impacts the amount of light that is reflected and absorbed. The Intergovernmental Panel on Climate Change (IPCC)<sup>9</sup> defines radiative forcing as the change over time in the difference between incoming and outgoing solar radiation on the surface of earth. The term radiative forcing helps to evaluate the energy balance of the earth. The reflection of incoming radiation by PM causes decrease in net radiation incident on surface of earth, called negative radiative forcing. On the other hand, the greenhouse gases, such as water vapor,  $\text{CO}_2$ ,  $\text{CH}_4$ ,  $\text{N}_2\text{O}$ , and ozone, can trap and absorb solar radiation in the troposphere and cause the average temperature of the earth's surface to increase, leading to positive radiative forcing. PM affects the negative radiative forcing either directly or indirectly; both pathways are discussed in detail below.

### **1.3.2.2a Direct radiative forcing**

The radiative forcing resulting from absorption or reflection of solar radiation by PM itself is termed direct radiative forcing. The chemical composition of PM determines whether incoming solar radiation is absorbed or reflected. For example, PM consisting of elemental carbon (black carbon)<sup>28</sup> leads to absorption of light, whereas PM consisting of organic carbon (brown carbon)<sup>29</sup> partially absorbs and reflects or scatters most of the light. Thus the organic aerosols can lead to both positive radiative forcing by absorption and negative radiative forcing by scattering or reflecting the incoming solar radiation.

PM can scatter the solar radiation, which reduces the visibility of distant objects. This phenomenon is size dependent, and particles with varying diameters can scatter the incoming solar radiation. This effect is responsible for decrease in aesthetic value of national monuments.

### **1.3.2.2b Indirect radiative forcing**

The alteration of the light absorbing properties of clouds is called indirect radiative forcing. The cloud formation process starts when water vapor in the atmosphere condenses onto particles to create cloud droplets. These particles that become cloud droplets are cloud condensation nuclei (CCN), and without CCN there would be no clouds. The number concentration of CCN within an aerosol distribution affects the magnitude of the indirect effect by changing the reflectivity of the cloud, i.e. the cloud albedo. Regions with high density of CCN provide a larger surface area for condensation of water vapor. For a fixed amount of water vapor, higher PM creates a larger surface area and an increase in cloud albedo, and thus leading to negative forcing.<sup>9</sup>

### 1.3.2.2c Mix of direct and indirect radiative forcing

An intermediate between the direct and indirect radiative forcing has been suggested: mixing smaller sized CCN in presence of absorbing particles. An example of this would be combination of sulfates which are smaller in size and act as CCN leading to formation of clouds with increased albedo and hence causing negative radiative forcing. If, at the same time, elemental carbon is present in the atmosphere. It increases the temperature due the absorption of radiation preventing cloud condensation and hence less cloud condensation leads to fewer clouds. Thus, the presence of sulfates in presence of elemental carbon leads to absorption of solar radiation (direct forcing) and influences properties of clouds (indirect forcing).<sup>9</sup>

In Chapter 5 of this dissertation we investigated the UV-visible absorption characteristics of ammonium ion aged SOA generated by the ozonolysis of terpene mixtures. The ammonium ion aged SOA shows steady increase in the absorption coefficient, implying that the SOA generated by ozonolysis of these terpene mixtures can react with ammonium ions in atmosphere leading to formation of absorbing particles in UV-visible region.

## 1.4 Volatile organic compounds (VOCs): source of SOA

*“A VOC can be any compound of carbon excluding carbon monoxide, carbon dioxide, carbonic acid, metallic carbides or carbonates and ammonium carbonate, which participates in photochemical reactions, except those designated by EPA as having negligible photochemical reactivity”* (EPA).<sup>30</sup> VOCs are emitted by various anthropogenic activities. VOCs such as isoprene and monoterpenes are emitted by vegetation and are also present in indoor environment.<sup>31</sup>



### 1.4.1 VOCs in atmosphere

Almost every anthropogenic activity leads to the emission of organic species into the atmosphere. The emission of organic carbon compounds such as carbonyls, alcohols, alkanes, alkenes, esters, aromatics, ethers, and amides result from driving a car,<sup>32</sup> painting a house,<sup>33</sup> cooking,<sup>34</sup> making a fire,<sup>35</sup> cutting the grass,<sup>36</sup> and even breathing.<sup>37</sup> The VOCs emitted into the atmosphere as result of anthropogenic activities are called anthropogenic volatile organic compounds (AVOCs).

In addition to human activities, vegetation emits a large amount of organic gases into the atmosphere. The VOCs emitted in atmosphere by vegetation are classified as biogenic volatile organic compounds (BVOCs). In recent work by Liao et al.,<sup>38</sup> the BVOC concentrations in atmosphere are estimated to dominate AVOC emissions at least by a factor of four. Total emissions of non-methane BVOCs in the atmosphere are estimated to be up to 1150 Tg carbon per year,<sup>39</sup> and they account for approximately 90% of VOCs present in the atmosphere. Isoprenoids are the most dominant of nonmethane BVOCs emitted into the atmosphere.<sup>40-42</sup> Isoprenoids are classified into three primary classes: isoprene ( $C_5H_8$ ), monoterpenes ( $C_{10}H_{16}$ ), and sesquiterpenes ( $C_{15}H_{24}$ ). Almost half the BVOC mass is isoprene, and around 11% of the BVOC mass is monoterpenes. Of the fraction of monoterpenes,  $\alpha$ -pinene (25%) and limonene (16%) are greatest.<sup>43</sup>

The quantity and composition of emissions from a particular plant vary depending on the age and the health of a plant,<sup>44</sup> stress factors,<sup>45,46</sup> physical wounding,<sup>47</sup> light, and temperature.<sup>48</sup> Plant VOC emissions can also act as a defense mechanism against herbivore attack.<sup>49</sup> All these changes lead to variation in the BVOCs amounts and species emitted into the atmosphere. BVOCs emitted into atmosphere undergo various oxidation reactions which contribute to the

formation of secondary organic aerosol (SOA).<sup>50</sup> SOA has significant effects on human health and climate, which have been discussed in detail later in this chapter. Hence, the parameters that lead to variation in the amount of BVOCs emitted into atmosphere lead to uncertainties in estimation of global SOA. Furthermore, the amount of SOA generated by BVOCs is around 20 to 50 times more than SOA generated by AVOCs.<sup>51</sup>

The amount of BVOCs emitted into the atmosphere is significant and can vary due to wounding from herbivores.<sup>52,53</sup> Thus, insect infestation may lead to variation in the amount SOA produced in the insect infested environment. In the Chapter 2 of this dissertation, we investigate the effect of bark beetle infestation on VOC emissions in the western United States.

#### **1.4.2 VOCs in indoor environment**

VOCs are introduced in the indoor environment due to air exchange with outdoor air<sup>31</sup> or by indoor emissions sources. For example, materials used for construction emit chemicals into the indoor environment,<sup>54</sup> and flooring boards emit a mixture of terpenoids and aldehydes.<sup>31</sup> Paints are another major source of VOCs. For example, older latex paints contain chemicals like 3-hydroxy-2,2,4-trimethylpentyl-1-isobutyrate and 1-hydroxy-2,2,4-trimethylpentyl-3-isobutyrate.<sup>55</sup> Recently, increased use of green or natural paints has led to an increase in the amounts of unsaturated organic compounds in indoor atmosphere from the use of linseed oil and products that contain limonene and other terpenoids.<sup>56</sup> Cleaning products have followed a similar trend moving towards more green or natural products. In the past, cleaning products often contained glycol ethers have been used as the active agents.<sup>57</sup> The trend is to use greener cleaning reagents which contain terpenoids such as limonene,  $\alpha$ -terpinene,  $\alpha$ -terpineol, and linalool.<sup>58</sup> Air freshener are another important source of the terpenoids in the indoors, their

significance has increased as shown by the increase in sales of air fresheners, from \$0.9 billion in 2000 to \$1.5 billion in 2005.<sup>59</sup> Approximately 70% of households in the United States use an air freshener.<sup>31</sup> Other sources of VOCs in the indoor environment include appliances and cigarette smoking.<sup>31</sup> The effects of indoor pollution are amplified in comparison to outdoor pollution, because, on average, a person spends more time indoors (approx. 90%) than outdoors, the ventilation rate limits the removal of particles generated indoors, and people are in close proximity of the indoor sources.<sup>60</sup>

Terpenoids present in the natural paints, cleaners, and air fresheners can react with ozone leading to the generation of SOA.<sup>61-63</sup> Ozone/VOC chemistry occurs indoors because use of ozone-based deodorizers and because of ventilation with ozone-containing outdoor air.<sup>64</sup>

### **1.5 SOA generation from ozonolysis of VOCs**

VOCs undergo oxidation reactions in both indoor and outdoor environments. The major oxidants present in the atmosphere are hydroxyl radical (OH), ozone (O<sub>3</sub>), and nitrate radical (NO<sub>3</sub>). The second-order rate constants for reaction between oxidants and VOCs tend to be highest for OH, are followed by NO<sub>3</sub>, and are lowest for O<sub>3</sub> among the three.<sup>65</sup> However, the concentration of ozone ( $0.7\text{--}2.4 \times 10^{12}$  molecules cm<sup>-3</sup>)<sup>66</sup> is typically higher than concentrations of the more reactive OH radicals ( $0.4\text{--}10 \times 10^6$  molecules cm<sup>-3</sup>)<sup>67</sup> and NO<sub>3</sub> radicals ( $0.2\text{--}9 \times 10^9$  molecules cm<sup>-3</sup>).<sup>68</sup> The oxidants that tend to be most reactive towards VOCs contain carbon-carbon double bonds. The OH and NO<sub>3</sub> radicals form a reactive radical adduct with VOCs that contain double bonds. The radical adduct reacts with O<sub>2</sub> to form a peroxy radical. The peroxy radical undergoes decomposition in a series of steps, eventually yielding semivolatile products (SOA) which undergo condensation and coagulation. The high reactivity of OH radicals with

trace species in atmosphere leads to rapid consumption and thus the steady-state OH concentration in the atmosphere is smaller than the ozone concentration. The  $\text{NO}_3$  concentration tends to be at a minimum during the daytime, because  $\text{NO}_3$  photodissociates. However, during nighttime,  $\text{NO}_3$  concentrations are significant and  $\text{NO}_3$  competes with  $\text{O}_3$  for oxidation of VOCs. Oxidants are present in indoor air due to exchange with outdoor air. Ozone important oxidant in indoor environment as it is present due to exchange with outdoor air and can be generated by use of electrical appliances. In this contribution, we focus on the ozone/VOC chemistry.

Most of the current research is focused on the generation SOA by single precursor in presence of single oxidant. The literature for SOA formation from single monoterpenes like  $\alpha$ -pinene and limonene in presence of ozone are summarized in Chapter 3 and 4 respectively. In the following sections, background information for the studies on generation of SOA from real plant emissions and indoor VOCs in presence ozone are summarized.

### 1.5.1 Generation of SOA by ozonolysis of plant emissions

Biogenic sources comprise 90% of atmospheric VOC emissions.<sup>39</sup> BVOCs are a significant source of SOA in atmosphere. Most of the studies involve generation of particles from emissions of trees in the presence of oxidants. In a study by Hao et al.,<sup>69</sup> particles were generated from the emissions from Scots pine (*Pinus sylvestris* L.) seedlings. Ozone and a mixture of ozone/OH radical as the oxidant were used. The authors found that in presence of OH radical, nucleation processes were favored, while the presence of ozone was important to condensation and growth of particles. In later studies, Hao et al.,<sup>70</sup> compared the amount of particles generated by ozone and OH radical oxidation from real plant emissions of Scots pine (*Pinus sylvestris* L.) and Norway spruce (*Picea abies*), the studies also compared the yields to SOA formation from  $\alpha$ -

pinene. While the SOA yields from oxidation of  $\alpha$ -pinene were in agreement with previous work, the SOA yields from the real plant emissions were lower than the  $\alpha$ -pinene only experiments. The authors report that in the growth stage, the particles generated by the use of OH radical as oxidant were more volatile than when ozone was used. The authors also found that the particle phase products become less volatile upon aging and the aging process continues even after the gas-phase oxidants had been completely consumed.

The effect of isoprene ( $C_5H_8$ ) on new particle formation has been studied by Kiendler-Scharr et al.<sup>71</sup> In this study, the authors investigated three low isoprene emitting trees, silver birch (*Betula pendula* Linnaeus (L.)), European beech (*Fagus sylvatica* L.), and Norway spruce (*Picea abies* L.), and a high isoprene emitting tree, namely, English oak (*Quercus robur*), for the impact of isoprene on the number and volume of new particles produced during nucleation events. Experiments with the addition of isoprene in range of 2-30 ppb were also performed. It was found that as the ratio of isoprene to other VOCs increased, the amount of new particle formation decreased. When English oak was placed with low isoprene emitting trees, an inhibition of new particle formation was observed. The inhibition mechanism was attributed to consumption of OH radicals by isoprene.

van Reken et al.<sup>72</sup> reported particle formation and growth from ozonolysis of VOCs of Holm oak (*Quercus ilex*) and loblolly pine (*Pinus taeda*) trees and compared these to  $\alpha$ -pinene ozonolysis. In these experiments, the trees were placed under controlled conditions of relative humidity (RH) and temperature, and the emissions from the trees were transported to another chamber where the ozonolysis studies were performed. The ozonolysis of Holm oak emissions gave lower particle concentrations than the ozonolysis of loblolly pine emissions. The authors attributed the difference in particle concentration to composition of VOCs emitted by these trees.

Holm oak VOC emissions consisted of  $\alpha$ -pinene (40%) and  $\beta$ -pinene (40%).  $\beta$ -pinene reacts with ozone at a slower rate than  $\alpha$ -pinene and generates fewer particles. While loblolly pine emissions contained similar amount of  $\alpha$ -pinene as Holm oak emissions, loblolly pine emissions had a higher concentration of sesquiterpenes which can react rapidly with ozone and generate products that can condense to form particles.

Mentel et al.<sup>73</sup> used a similar experimental set up to van Reken et al.<sup>72</sup> Plants were held in one chamber, and the emitted VOCs were transported to the reaction chamber wherein the VOCs were exposed to oxidants like ozone and OH radicals. Mentel et al.<sup>73</sup> used emissions from pine (*Pinus sylvestris* L.), birch (*Betula pendula* L.), and spruce (*Picea abies* L.). Both the plant chamber and reaction chamber were equipped to control the physical parameters of relative humidity, temperature, and light. The authors investigated the effect of emission changes with variation in physical parameter in plant chamber and its subsequent effect towards particle formation in the reaction chamber. The authors reported that only a small fraction of monoterpenes and a larger fraction of sesquiterpenes react with ozone, and a larger fraction did not participate in new particle formation. Formation of the new particles only occurred in presence of OH radicals. The study also involved particle generation from  $\alpha$ -pinene as a reference. Using VOC mixing ratios, authors found that the nucleation thresholds, i.e. the amount of carbon which must be consumed before new particles can be detected, for plant emission oxidation were much lower than the nucleation thresholds for  $\alpha$ -pinene oxidation. The authors also suggested that  $\alpha$ -pinene might not be suitable model compound for studying new particle formation from emissions by real plants.

### 1.5.2 Generation of SOA in indoor environments

Particles are present in the indoor environment due to the exchange of indoor air with outdoor air and activities such as cooking, smoking, use of electrical appliances, etc. The particles can be generated due to reaction of VOCs, like monoterpenes, that are present in cleaning products and air fresheners. The ozone reactive components present in these products can generate SOA and hence lead to formation of PM.

Destailats et al.<sup>26</sup> performed bench scale studies in a chamber and investigated SOA formation from ozonolysis of a pine-oil cleaner, an orange-oil based degreaser, and a plug-in air freshener. These consumer products contained a significant amount of ozone reactive monoterpenes.<sup>58</sup> The authors found that the reaction between the volatilized consumer products and ozone lead to the formation of particles instantaneously. Gaseous products, like formaldehyde, acetaldehyde, acetone, glyceraldehydes, formic acid, and acetic acid, were also observed, and these products have health hazards. The authors found that the increase in particle concentration and gaseous products depend on the ozone concentration in the chamber and air exchange rate. Furthermore, the authors reported the formation of particle and gas-phase products from ozonolysis of dry residue of these consumer products, which implicates that cleaning products can react with oxidants when applied to a surface and need not be in gaseous form. Singer et al.<sup>27</sup> generated SOA from the same consumer products (pine-oil based cleaner, orange-oil degreaser, and a plug-in scented oil air freshener) in a 50 m<sup>3</sup> chamber, which simulated a residential room. The conditions were kept near to the conditions of a residential home (the air exchange rate of 1.0 per hour and an ozone concentration of 120 ppb were used). The consumer products were applied in quantities scaled to simulate the residential use rate. The air freshener showed weaker ozone consumption as compared to pine-oil cleaner and orange-oil

based degreaser. Heterogeneous reactions between sorbed air freshener and ozone generated SOA with yields of similar magnitude as compared to homogeneous reactions between the air freshener and ozone. Formaldehyde was generated as result of product use in presence of ozone. Cleaning product use in the presence of ozone generated substantial fine particle concentration (approximately  $100 \mu\text{g m}^{-3}$ ) in some experiments. Authors also report increased hydroxyl radical concentrations persisted for 10-12 h after brief cleaning events, thus implying that the secondary pollutants can last in the indoor atmosphere can last for extended period of times.

The constituents of air fresheners are also present in essential oils and can generate SOA upon reaction with ozone as shown by Hatfield and Huff Hartz.<sup>74</sup> The SOA yield generated from ozonolysis of Siberian fir needle oil was compared to SOA yields generated from single VOCs and artificial VOC mixtures. It was concluded that as the VOC composition of artificial mixtures approached the VOC composition of the Siberian fir needle oil, the SOA yields were found to be the same. Huang et al.<sup>75</sup> have also found SOA formation from Chinese herbal oils and lemon oil. The authors report that the evaporation of 1 mL of Chinese herbal oils in presence of 30 ppb ozone can lead to an increase of  $6.4 \mu\text{g m}^{-3}$  in PM levels of a typical room or office. The amount of SOA generated by ozonolysis of Chinese essential oils was found to be lower than SOA generated by ozonolysis of essential oil. Jutia et al.,<sup>76</sup> performed solid phase micro extraction (SPME) combined with gas chromatography–mass spectrometry (GC-MS) to identify and quantitate the volatile organic compounds (VOCs) formed in the degradative oxidation of linseed oil. The majority of the detected products originated from the oxidation of linolenic compounds, which dominate the composition of linseed oil, while 2-propenal, pentanal, hexanal, 2,4-decadienal, and hexanoic acid, among others, were released from linoleic compounds.



In Chapter 3 of this dissertation we compare the SOA yields generated by single VOC, limonene, to VOC mixtures containing limonene and eventually to a limonene-based commercially available air freshener. Previous studies on SOA generation, with the exception Hatfield and Huff Hartz,<sup>74</sup> from VOC mixtures do not investigate the contribution of single VOC towards SOA yields.

## 1.6 SOA partitioning models

When an oxidant reacts with a VOC, the condensation of SOA products begins once the SOA concentration reaches saturation concentrations. When the concentration of product equals its saturation concentration, the product is partitioned equally between the gas and condensed phase. The SOA yield is calculated as a fraction of the amount of VOC oxidized. The amount of PM formed for any given precursor-oxidant reaction can be characterized by calculating the SOA yield. For aerosol generated by the reaction of a gas phase precursor and oxidant, the SOA yield,  $Y$ , is calculated by dividing the amount of PM formed in  $\mu\text{g m}^{-3}$  to the amount of VOC precursor in  $\mu\text{g m}^{-3}$  (details in section 3.2.13). This method applies to the SOA generated from a single precursor or a mixture of precursors,<sup>74</sup> and this treatment assumes that the oxidation of the precursor (or precursors) leads to products which do not undergo any subsequent reactions. The above treatment of SOA assumes that the oxidation of one precursor leads to formation of one first generation product, which does not undergo any subsequent reactions.

SOA partitioning models are applied because they predict the amount of SOA generated from VOC emissions. A challenge for developing an accurate model is to consider the variety of physical parameters that impact SOA yields, like temperature and humidity. The challenge increases in real environment as the single precursor might undergo reaction with multiple

oxidants, the first generation products from this reaction may react with other products, other oxidants or other components of atmosphere generating a second/third generation of products.

SOA partitioning between the gas and condensed phase was described by Pankow<sup>77</sup> by using an absorption model. For each compound that partitions between absorbing organic material phase, Pankow has defined an absorption equilibrium constant ( $K_{p,i}$ ) as

$$K_{p,i} = \frac{F_{i,om}}{A_i TSP} \quad (1.1)$$

where  $F_{i,om}$  is the concentration of compound  $i$  in the organic material phase,  $A_i$  is the gas phase concentration of compound  $i$ , and TSP is the total suspended particulate concentration.

Odum et al.<sup>78</sup> addressed the semi-volatile nature of the SOA and incorporated the SOA yield in the partitioning model described by Pankow. The model assumes that two products with two differing volatilities are formed during the reaction. One product has a high molecular mass (less volatile) while other a low molecular mass (more volatile). The two-product model, in terms of SOA yield, is given in equation 1.2.

$$Y = M_o \sum_i \left( \frac{\alpha_i K_{om,i}}{1 + K_{om,i} M_o} \right) \quad (1.2)$$

The yield,  $Y$ , is equivalent to the sum of both partitioning coefficients,  $K_{om,i}$ , in the organic phase and  $\alpha_i$ , is the individual product yields.  $M_o$ , is the total aerosol organic mass concentration, for this work we will consider  $M_o$  as the mass concentration of reactive precursor. Odum et al.<sup>78</sup> found that the two-model product fit experimental data. The two-product model worked well because it considered the semivolatile nature of SOA and products with both high and low volatilities generated by VOC oxidation. However, in many cases the model overestimated the saturation concentration ( $C^*$ ) values for the products, and this is contradictory to fact that SOA particles are difficult to evaporate.

Volatility basis set is an alteration for two-product model suggested. Donahue et al.<sup>79</sup> and Stanier et al.<sup>80</sup> proposed the model, where equation 1.3 was solved for a set of saturation concentrations ( $C_i^*$ ) separated by order of magnitude from  $0.01 \mu\text{g m}^{-3}$  to  $100,000 \mu\text{g m}^{-3}$ . The SOA products formed during the reaction are grouped into a range of volatilities instead of determining the saturation concentration,  $C^*$ , for a given product.  $\alpha_i$  is the mass based yields of product i.

$$Y = \sum_{i=1}^n \frac{1}{1 + \frac{C_i^*}{M_0}} \alpha_i \quad (1.3)$$

The theoretical treatment of SOA in this manner showed that amount of condensed material verses the gas phase material will depend on the total concentration of aerosol, which is convenient for modeling the SOA contributions to existing PM. This modeling approach has shown that the SOA is more semivolatile than originally thought to be.

## 1.7 Reaction mechanism for ozonolysis of monoterpenes

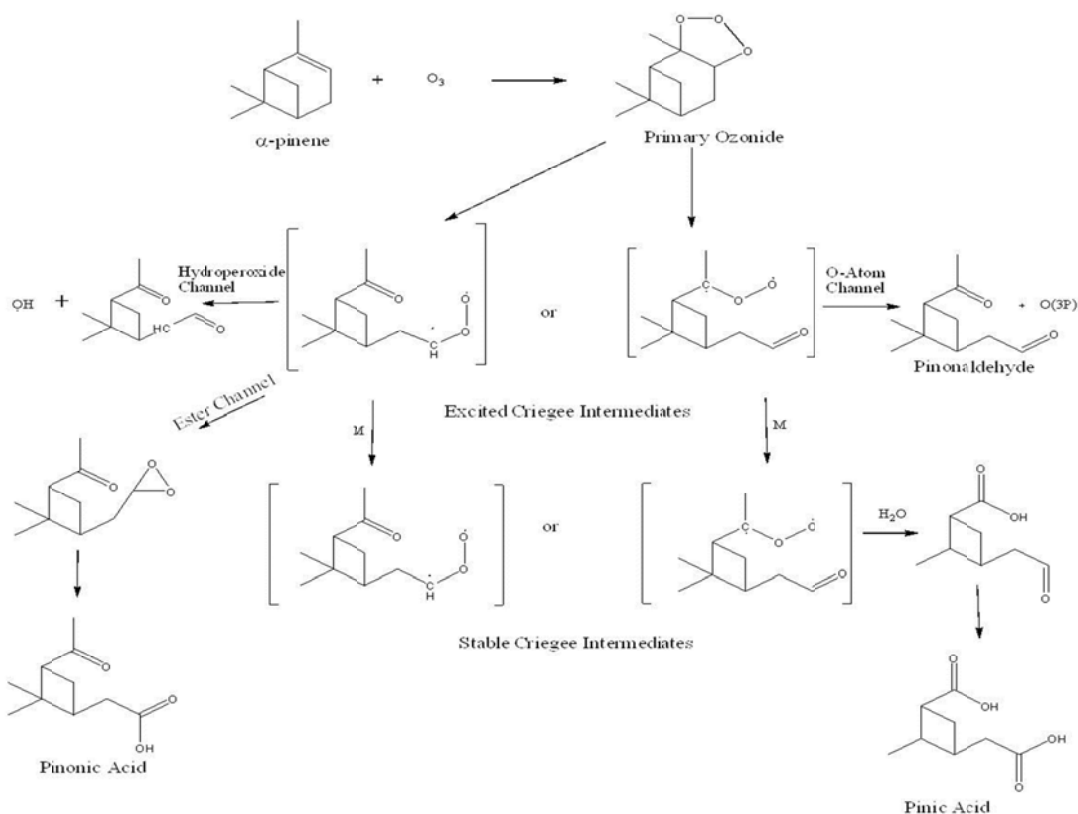
The word speciation in context of this dissertation describes the identification and quantification of condensed phase SOA generated by ozonolysis of VOCs and VOC mixtures. The products identified from the speciation studies can be used to predict the toxicity of SOA. In this section we discuss the mechanism for generation of SOA products by ozonolysis. The reaction of alkene VOCs with  $\text{O}_3$  proceeds via the addition of ozone across the carbon-carbon double bond to generate a primary ozonide. The primary ozonide ring is not stable, and cleavage of the carbon-oxygen and carbon-carbon bond occurs leading to the formation of a carbon-oxygen-oxygen bond, which further yields a Criegee biradical.<sup>81</sup> The Criegee biradical is unstable but can be stabilized through collisions with neutral gas molecules. Until recently, Criegee intermediates were neither separated nor directly detected. However, recently Welz et

al.,<sup>82</sup> have detected formation of the Criegee intermediate using mass spectrometry. The Criegee intermediate, formaldehyde oxide ( $\text{CH}_2\text{OO}$ ), was generated by low pressure photolytic reaction between diiodomethane ( $\text{CH}_2\text{I}$ ) and oxygen ( $\text{O}_2$ ). The decay rates for  $\text{CH}_2\text{OO}$  radical were then investigated with nitric oxide, nitrogen dioxide, and sulfur dioxide. The reaction rates reported are higher than the previously reported values calculated using theoretical studies. This work suggests that the intermediate plays a more important role in atmospheric chemistry than previously thought.

The consumption of Criegee biradical can take place by unimolecular rearrangement via an ester channel leading to formation of pinonic acid (Figure 1.2). Also, a fragmentation process like the hydroperoxide channel or the oxygen-atom elimination channel can occur, which leads to formation of pinic acid. Pinic acid and pinonic acid are major products formed during ozonolysis of  $\alpha$ -pinene.<sup>84</sup> The mechanisms for other minor condensed phase products, like pinalic-4-acid, norpinic acid, norpinonic acid, and 10-OH pinonic acid, formed during ozonolysis of  $\alpha$ -pinene are discussed by Ma et al.,<sup>85</sup> these products are formed as result of peroxy (ROO) and hydroperoxy (HOO) radical mechanisms with the Criegee intermediate. The stabilized Criegee biradical can also react with other gaseous species (like  $\text{H}_2\text{O}$ , OH,  $\text{SO}_2$ ,  $\text{NO}_x$ , etc.) to form a variety of SOA products which increases the quantity of SOA as well. The mechanism of ozonolysis of  $\alpha$ -pinene shown in Figure 1.2, it also shows mechanism for formation of pinonaldehyde, pinonic acid, and pinic acid.<sup>85,86</sup>

The condensed fraction of SOA products formed from the ozonolysis of individual VOCs have been identified in many studies.<sup>83,87</sup> However, very few studies have been done on the identification of SOA products generated by the ozonolysis of VOC mixtures.<sup>88</sup> In Chapters three and four of this dissertation we report the products generated by ozonolysis of individual VOCs

and VOC mixtures, and compare these products to the products generated from commercially available VOC mixtures like air freshener and essential oil.



**Figure 1.2** Reaction mechanisms for the ozonolysis of  $\alpha$ -pinene. Adapted from Ma et al.,<sup>85</sup> 2008 and Jang and Kamens, 1999.<sup>86</sup>

## 1.8 Effect of physical parameters on SOA formation

Physical conditions, like temperature, relative humidity, pressure, and radiation, have significant effects on the SOA formation process. As the atmospheric conditions are always changing, it is important in understanding how the individual parameters affect SOA production. Correlation between SOA formation and physical parameters is essential for development of accurate models and theory of SOA formation. The following sections discuss the effects of temperature, humidity, and UV light on aerosol generation by ozonolysis of monoterpenes.

### 1.8.1 Effect of temperature on SOA formation

SOA consists of semivolatile compounds. Temperature fluctuations perturb the partitioning between gases and solid/liquid particulate matter, and hence the amount of SOA generated. Furthermore, the kinetics of SOA formation (from VOC oxidation, intermediate lifetime, and product formation) depends on temperature. Also, the temperature in the atmosphere changes with time of day, location, weather, and altitude of a geographic location; thus it is important to understand the affect of variation in temperature on SOA formation. Pathak et al.<sup>89</sup> have investigated the temperature dependence on ozonolysis of  $\alpha$ -pinene and showed that SOA formation decreased with increasing temperature. Warren et al.,<sup>90</sup> reported the findings for the effects of temperature on SOA formation for ozonolysis of both cyclohexane and  $\alpha$ -pinene. The studies were carried out by cycling temperatures between 278 K, 300 K, and 318 K to determine if SOA formation was reversible. They concluded that there was inverse dependence between temperature and SOA formation. Stanier et al.<sup>91</sup> found that the aerosol volume concentration decreased with decrease in temperature and the mass concentration decreased by around 5-60% with increase in temperature from 22 to 35 °C.

Saathoff et al.<sup>92</sup> investigated the temperature dependence on SOA generated from the ozonolysis of  $\alpha$ -pinene and limonene in separate chambers. They found a decrease in the amount of SOA from both precursors occurred with an increase in temperature.  $\alpha$ -pinene SOA showed greater temperature dependence than limonene SOA. Pathak et al.<sup>93</sup> have investigated temperature dependence for  $\beta$ -pinene SOA generated by ozonolysis. The authors found SOA yields increased by two or three times as the temperature was reduced from 313 K to 273 K. von Hessberg et al.<sup>94</sup> also have shown similar temperature dependence for  $\beta$ -pinene and showed the SOA yields increased as the temperatures decreased from 303 K to 263 K. von Hessberg et al.<sup>94</sup>

also reported that SOA yields did not vary linearly as temperature was decreased. The studies were carried out at two different relative humidity (RH) conditions. Under high RH conditions the amount of SOA was found to increase with increasing temperature where as at low RH conditions the amount of SOA formed showed a decreasing trend.

Huang et al.<sup>61</sup> have investigated temperature dependence for SOA generated by the ozonolysis of a limonene-based cleaning product. Their results indicate that the total particle count increased as the temperature was increased from 15 °C to 23 °C, but as the temperature was increased to 30 °C, the total particle count decreased with an increase in the temperature. From these studies we could conclude that as the temperatures are increased, oxidation products do not condense and remain in gas phase, while at lower temperatures the oxidation products can undergo condensation to generate more particles.

In summary, the particle formation from oxidant-VOC reaction decreases with increase in temperature. For the experiments presented in this dissertation were carried out at room temperatures (18 °C -27 °C), the temperature was not controlled but was monitored during course of SOA generation experiment.

### **1.8.2 Effect of relative humidity on SOA formation**

SOA is formed by condensation of oxidation products generated from volatile precursors. The amount of SOA produced can be altered by altering the chemical mechanism<sup>95</sup> or perturbation of gas-particle thermodynamics.<sup>95,96</sup> Relative humidity alters the gas-particle thermodynamics and has been investigated as a factor in SOA formation.

Jonsson et al.<sup>95</sup> tested the effect of relative humidity (RH) on the ozonolysis of limonene, 3-carene, and  $\alpha$ -pinene. The studies were carried out by increasing RH from <2% to 85%. The

authors observed an increase in particle mass concentrations by factor of three with increasing RH, and the particle number concentrations increased by a factor of four to eight. The authors attribute this increase in mass and number concentration to formation of the water dimer with increased RH. The rate constant for reaction of water dimer and Criegee intermediate is faster than that of water monomer and Criegee intermediate. Thus, with increased RH, there is an increase in the concentration of the water dimer and hence the amount of particles formed.

Barley et al.<sup>97</sup> performed modeling studies for SOA formation under different RH conditions. They concluded that there is a significant increase in SOA mass with increasing RH. The authors suggested that the water uptake occurs in the organic phase, and the increasing water mole fraction (with increasing RH) in organic phase suppresses the organic partial pressures in that mixture. This model showed that the increase in amount of SOA with increasing RH is a consequence of Raoult's law.

Prisle et al.<sup>98</sup> investigated the effect of RH on SOA generated by  $\alpha$ -pinene/ozone reaction. The experiments showed that SOA from  $\alpha$ -pinene remains largely in a separate organic phase, even when an aqueous phase is present in the same particles. Also, Huang et al.<sup>61</sup> observed an increase in SOA generated from limonene-based cleaning product at RH of 50% and 80% when compared to RH of 30%.

In summary, these studies show that SOA formation increases with an increase in RH, indicating that higher RH facilitates the nucleation. In the work presented herein, we do not control the RH of the reaction but we monitor it continuously during the course of the reaction. Some minor variation in the amount of SOA generated (around 1%), which is very small and could be due to fluctuations in RH of the laboratory or house air in the reaction chamber used for SOA generation.



### 1.8.3 Effect of UV radiation on SOA formation

SOA formation takes place during daytime as well as during night time; i.e., both during the presence and absence of solar radiation. Presto et al.<sup>99</sup> investigated the effect of UV light on SOA formation from the ozonolysis of  $\alpha$ -pinene. In presence of UV light the SOA yield found to decrease by 20-40%. An investigation by Cao et al.<sup>100</sup> found that UV light decreases the SOA mass produced by oxidation of both toluene and 1,3,5-trimethylbenzene. Similar results were observed by Zhang et al.<sup>101</sup> for the ozonolysis of limonene, where the exposure to UV light led to decrease in SOA production. The decrease in amount of SOA upon exposure to UV light is attributed to photodissociation of nucleating agents such as diacyl peroxides; inhibition of nucleation prevents new particle formation. The stabilization of gas-phase species through photolysis has also been suggested as an alternate reason for the observed decrease.

The SOA generation experiments carried out in this dissertation were carried out in dark. The chamber was always covered with a black-out fabric hence the contribution of light towards the SOA yields would be insignificant. Furthermore, solar photolysis is not expected to occur indoors.

### 1.8.4 Role of radical scavenger during SOA formation

Radical scavengers are added to SOA generation experiments to curb the formation of secondary radicals which can react with precursors. The scavengers do not react with the primary oxidation product but with subsequent radical species. Criegee intermediates formed during primary oxidation reaction decompose to generate the OH radicals (for example, Figure 1.3).

<sup>102,103</sup> The OH radicals can affect the amount of SOA formed and final products generated by

reacting with other ozonolysis products and/or precursors. The use of radical scavenger reduces the complexity of the SOA generation reactions, because ozone/VOC chemistry is isolated.

Commonly used radical scavengers are cyclohexane,<sup>102,103</sup> CO,<sup>104</sup> and 2-butanol.<sup>105</sup> Each radical scavenger reacts differently, and there are differences in how the radical scavengers affect SOA formation. Cyclohexane and 2-butanol produce peroxy and alkoxy radicals through their reactions with the OH radical. The reaction of cyclohexane with OH radical produces higher amount of alkoxy radical, while reaction of 2-butanol with OH radical produces higher amount of peroxy radical. The product of reaction between CO and OH radicals is hydroperoxy radicals. The amount of alkoxy or peroxy radicals generated affect the amount of SOA formed, hence the amount of SOA formed varies with the type of radical scavenger used.<sup>106,107</sup> If radical scavengers are not used, higher SOA yields would be reported as secondary reactions with OH would produce higher concentration of lower volatility products.

The effect of OH radical scavengers, namely cyclohexane and 2-butanol, on SOA formation via ozonolysis of limonene, 3-carene, and  $\alpha$ -pinene has been investigated. The amount of SOA formed in terms of decreasing order was no scavenger>2-butanol>cyclohexane.<sup>108</sup> The lower SOA yields generated for when cyclohexane is used as opposed to 2-butanol is thought to be a result of differing ratios of peroxy/alkoxy radicals present. Na et al.<sup>109</sup> carried out experiments to study the effect of ammonia on the ozonolysis of  $\alpha$ -pinene using three radical scavengers (CO, cyclohexane, and 2-butanol) under dry and humid conditions. The authors found that the amount of SOA formed in terms of decreasing order was CO>cyclohexane>2-butanol. The authors suggest that the presence of increased amounts of alkoxy radicals suppressed amount of SOA formation. In our experiments, 2-butanol was the radical scavenger.

## 1.9 Concluding remarks

The impact of PM on human health and climate drives the need for investigation of VOCs and their potential to form SOA. The VOCs emitted into atmosphere are dominated by biogenic sources, and the amount of BVOCs emitted into atmosphere vary according to physical parameters (temperature, RH, exposure to light, stress, and insect infestation). These factors, which lead to variation of BVOCs, need to be investigated as BVOCs affect the global SOA budget. In this dissertation, we compare the amount and type of VOC compounds emitted by healthy and bark beetle infested trees in the western United States (Chapter 2).

In the atmosphere, multiple VOCs co-exist. Hence, it is important to understand SOA formation from realistic SOA mixtures. The oxidation products formed during ozonolysis reactions are important in understanding volatility distribution of products and the potency of VOCs to form SOA upon oxidation. We report the SOA yields and products generated from ozonolysis of commercially-available mixtures. We use an additive approach for building a surrogate VOC mixture as close in composition as possible to a commercially-available mixture. This study explains the variability in both SOA yields and products formed with respect to the type of VOC added to the mixture. We study a limonene-based air freshener for SOA yields and condensed phase products formed, with variation in component VOCs used for reaction with ozone (Chapter 3). We also study condensed phase products formed by ozonolysis of Siberian fir needle oil and VOCs present in it (Chapter 4).

SOA present in atmosphere mitigates the amount of incoming solar radiation and can affect the climate. In this dissertation, we report the UV-visible absorption characteristics for ammonium ion-aged SOA generated from ozonolysis of limonene-based air freshener and Siberian fir needle oil (Chapter 5).

## CHAPTER 2

### EFFECT OF BARK BEETLE INFESTATION ON SECONDARY ORGANIC AEROSOL PRECURSOR EMISSIONS

#### 2.1 Importance of BVOCs or biogenic SOA precursors

As discussed in Chapter 1, atmospheric aerosols can impact climate through direct and indirect radiative forcing, degrade air quality, and cause detrimental effects on human health.<sup>10,110,111</sup> The oxidation of BVOCs provide major reaction pathway for formation of SOA.<sup>112,113,114</sup> In United States, BVOC emissions are estimated to be four times larger than the AVOC emissions<sup>38</sup>. Globally, Tsigaridis and Kakakidou<sup>115</sup> suggested that BVOCs dominate AVOCs in the production of SOA. The total biogenic SOA fluxes are estimated around 12-70 Tg yr<sup>-1</sup>,<sup>43</sup> and the anthropogenic fluxes are estimated to be smaller, 2-12 Tg yr<sup>-1</sup>.<sup>116</sup> To understand the impact of aerosols on climate, health, and atmospheric chemical processing, the aerosol formation pathways, specifically via BVOC production mechanisms, must be known.<sup>117</sup> It is important to understand the emission changes of BVOC concentrations (due to increasing global temperatures, increased insect infestation etc.) with respect to various and potential impact on climate change. In the regions dominated by coniferous tree species the BVOC emissions are dominated by monoterpenes.<sup>118</sup> Globally, coniferous trees are responsible for approximately 10% of monoterpenes emission.<sup>39</sup> Specifically for the lodgepole pine tree the emissions are dominated by  $\alpha$ -pinene,  $\beta$ -pinene, and limonene.<sup>118</sup> For the Engelmann spruce the samples collected from the bole and foliage have shown emissions dominated by  $\alpha$ -pinene,  $\beta$ -pinene, and 3-carene.<sup>119</sup>

### 2.1.1 Monoterpenes as plants defense mechanism

The production of monoterpenes takes place within plastids, the site of photosynthesis within a plant. Specifically in conifers, monoterpenes synthesis occurs within specialized cells in the needles and resin canals of the bark.<sup>53</sup> Monoterpenes represent the main fraction of essential oils that are produced and stored in plant secretory organs like resin ducts.<sup>44</sup> As a result of this storage mechanism, the tree exhibits a large storage pool of monoterpenes compared to the emission rates.<sup>120</sup> Hence, the emission of monoterpenes via volatilization out of storage organs is related to the vapor pressure and to the transport resistance along the diffusion path.<sup>44</sup>

The main ecological roles for monoterpenes in conifers are to deter feeding or oviposition by generalist herbivore and to acts as toxins against fungal pathogens.<sup>121,122</sup> Also, monoterpenes may act as a solvent for high molecular weight defense compounds which would otherwise be unable to flow to an attacked site.<sup>120,123</sup> Monoterpenes are not particularly toxic to herbivores,<sup>124</sup> but they provide trees with physical protection against herbivores as the sheer volume of monoterpenes can clog the mouthpart of the bark beetles.<sup>125</sup>

Priemé et al.<sup>53</sup> have showed that weevil (*Strophosoma melanogrammum*) attacks on spruce trees in Denmark had a significant effect on local monoterpene emissions. In fact, a single weevil induced a three-fold increase in monoterpene emissions and the response lasted for several weeks. Furthermore, large pine weevil (*Hylobius abietis*) feedings on Scots pine seedlings (*Pinus sylvestris*) induced a nearly three-fold increase in monoterpene emissions.<sup>126</sup>

### 2.1.2 Bark beetle-host interactions

Across Western North America, there is currently a sudden large-scale population increase in mountain pine beetles (*Dendroctonus ponderosae*). The lodgepole pines (*Pinus contorta* var. *latifolia*) are the primary host for this beetles.<sup>127</sup> The female beetles select a tree and bore

through the bark into the phloem. While boring into the tree, the female beetle processes the host monoterpenes into pheromones to attract male beetles.<sup>52</sup> The male then helps clear out the entrance gallery.<sup>128</sup> While doing so the beetle severs the pine tree's resin canals, and resin flows into the wound to slow down the beetle, as a part of defense mechanism. The resin contains monoterpenes, which are toxic to the beetle, but not at the concentration encountered in the resin.<sup>129</sup> However, the plants defense mechanism is exhausted by repetitive attack by multiple bark beetles in the population.<sup>130</sup> If a sufficient number of beetles arrive at a rate that exceeds the resistance capacity of a particular tree, then colonization is successful. The second strategy of bark beetle attack includes transfer of various strains of blue stain fungi to the plants. The bark beetles have a mutual relationship with blue stain fungi.<sup>131</sup> The blue stain fungi germinate quickly and penetrate the living cells in both phloem and xylem<sup>132</sup> causing desiccation and disruption of transpiration,<sup>133</sup> effectively terminating the production of resin by trees. If the beetle proceeds through the resin, the female beetle then lays eggs in ovipositional galleries under the bark.<sup>134</sup> The resulting larvae develop by feeding on the phloem and fungi.<sup>128</sup> The pine tree responds to the beetle-fungal attack with a broad chemical defense, including increases in monoterpenes<sup>52</sup>. Miller et al.<sup>135</sup> inoculated lodgepole pine stands with a mountain pine beetle in the Colville National Forest and repeated these experiments in the St. Joe National Forest. They found a 4-fold increase of monoterpenes in the phloem tissue surrounding the inoculation site over the course of three days. In a similar study, Raffa and Berryman<sup>136</sup> investigated the chemical change in the phloem of lodgepole pines when attacked by mountain pine beetles, and its symbiotic fungus, *Euophium clavigerum*. In this study, all trees were inoculated, and as a result, an increase was observed in the monoterpene output. The response was rapid (i.e. within three days of inoculations), and the response appeared localized near the infection point. Only

one study in literature was found which indicates that the Engelmann spruce can be infested by bark beetles.<sup>137</sup> The authors report that during a large bark beetle epidemic it is likely that the mountain pine beetle can infest the Engelmann spruce tree and colonize. The authors indicate that this infestation may be result of milder resistance provided by the Engelmann spruce trees when compared to lodgepole pine.

### **2.1.3 Climate change: increase in bark beetle epidemic**

The current mountain pine beetle outbreak has resulted in wide scale tree mortality, which can be related to increase in average summer and winter temperatures. For example, the current beetle epidemic in British Columbia, Canada is an order of magnitude larger than all previously recorded outbreaks.<sup>138,139</sup> The infestation has increased in area from 164,000 ha in 1999 to more than 11 million ha in 2007.<sup>140</sup> One reason for this outbreak is changes in winter and summer temperatures and reduced summer precipitation in recent decades. Climate change has allowed for the outbreak to expand northward and into higher elevation forests.<sup>139,141,142</sup>

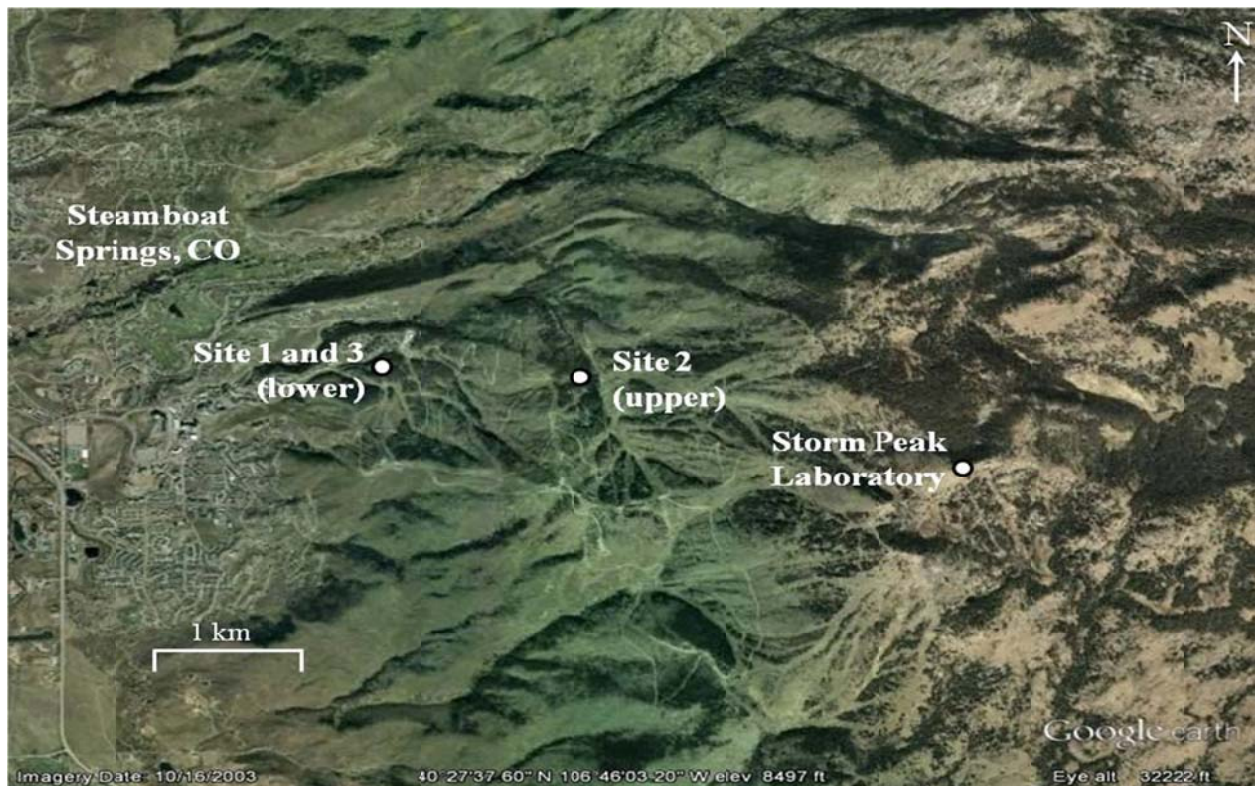
**In this chapter we investigate the changes in BVOC emissions that have potential to contribute to SOA formation and address the impact of mountain pine beetle epidemic on SOA.**

## **2.2 Experimental details**

### **2.2.1 Sample site description**

The samples were collected at Storm Peak Laboratory (SPL), 3210 m AMSL (Above Mean Sea Level). This facility is owned and operated by Desert Research Institute (DRI), it is located on west summit of Mt. Werner in the Routt National Forest in northwestern Colorado. SPL is located approximately 1150 m above Steamboat Springs, Colorado (population 9,500).<sup>143,144</sup> This

alpine site is at treeline, and the dominant tree species are Engelmann spruce (*Picea engelmannii*) and American aspen (*Populus tremuloides*). Below the laboratory (2700 m AMSL), the dominant tree species is lodgepole pine (*Pinus contorta* var. *latifolia*), currently facing beetle infestation. On the mountain below and to the West of SPL, nine sampling locations were selected. The first site (site 1) is at 2300 m AMSL, located 3.6 km west of SPL and was primarily a lodgepole pine stand. The second site (site 2) is at 2600 m AMSL, located 2.3 km west of SPL and consisted of lodgepole pine and Engelmann spruce trees. The trees selected for sampling at site 1 were logged mid-September during the campaign. After logging, a third site (site 3) was selected, and is located at site 1. The sites are shown in Figure 2.1, which is a Google Earth image (ver 6.1.0.5001).



**Figure 2.1** Map of sampling region located in northwestern Colorado, USA. Base image provided by Google Earth 6.1.0.5001.



Three lodgepole pine trees were selected for sampling at each site, giving a total of nine lodgepole pine trees. For lodgepole pine trees, at each site an infested tree and one or two healthy trees without current infestation were selected, some healthy trees are recovered from previous bark beetle attacks by spraying of carbaryl, a beetle insecticide. At site 1 and site 3, some of the healthy trees had old pitch tubes (resin deposits on the trunk indicating prior beetle infestation). At site 2, a deceased tree with pitch tubes was also selected for sampling. Also at site 2, two Engelmann spruce trees, one infested with pitching out and one healthy were selected for sampling. From nine lodgepole pine trees selected, five were healthy trees, three trees with current infestation and one deceased tree. Table 2.1 gives the details on description and locations of the sampled trees along with the number of scent trap samples collected from each tree.

**Table 2.1.** Location and description of sampled trees along with number of samples collected at each location

Description	abbreviation	number of scent trap samples collected from trunk, canopy
site 1		
healthy lodgepole pine, recovered from prior infestation, old pitch tubes present	S1T1	15,15
infested lodgepole pine	S1T2	18,15
healthy lodgepole pine, sprayed with carbaryl	S1T3	15,15
site 2		
infested, pitching out, Engelmann Spruce	S2T4	0,15 <sup>a</sup>
healthy Engelmann Spruce	S2T5	0,14 <sup>a</sup>
infested lodgepole pine	S2T6	37,34
healthy lodgepole pine	S2T7	37,37
deceased lodgepole pine, old pitch tubes present indicating prior infestation	S2T8	19,19
site 3		
healthy lodgepole pine, recovered from prior infestation, old pitch tubes present	S3T9	18,15
infested lodgepole pine	S3T10	18,0
healthy lodgepole pine, recovered from prior attack, old pitch tubes present, and sprayed with carbaryl	S3T11	18,18

<sup>a</sup> The number of samples is corrected by removing one outlier, Q tests were performed before removing the outliers

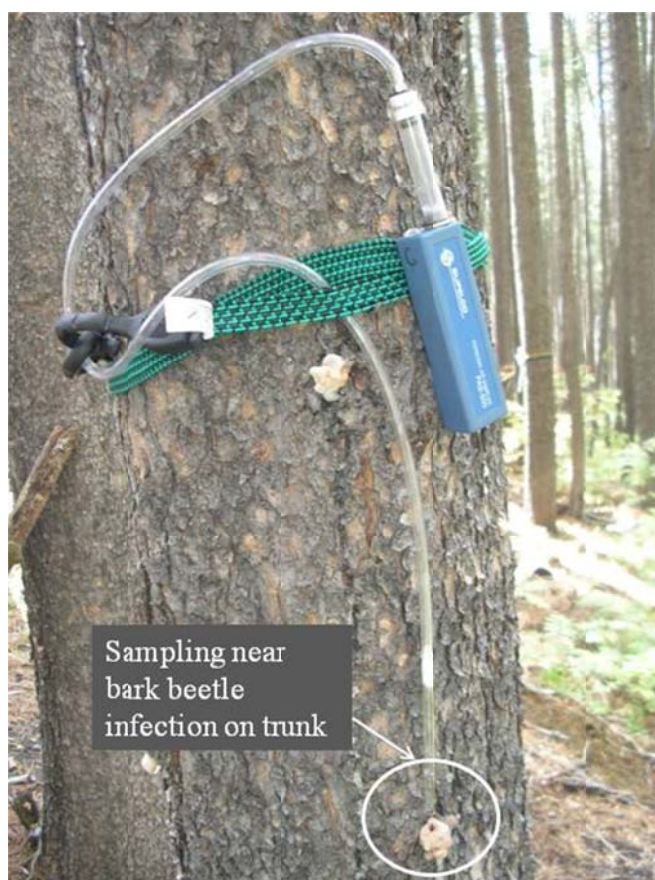
### 2.2.2 VOC sample collection

Air samples were collected at the trunk and canopy by dynamic sampling. This method was adapted from the work of Raguso and Pellmyr.<sup>145</sup> Scent traps were prepared in the Huff Hartz research lab using 5 3/4" glass Pasteur pipet (Fisher Scientific). The Pasteur pipets were plugged near the neck by placing 3 mm plug of deactivated borosilicate glass wool (Restek) 110 mg of Porapak Q sorbent (divinylbenzene/ethylvinylbenzene polymer, 80/110 mesh, Grace Davidson) was placed on top of the glass wool, and the sorbent was packed using another piece of glass wool on top. The trap was then rinsed with 5-6 volumes of n-hexane (GC Resolv, Fisher). The scent traps were then air dried overnight and then wrapped in pre-fired aluminium foil.

The scent traps were shipped to SPL where the VOC samples were collected by our collaborator, A. Gannett Hallar and coworkers. The sample collections were done using a PAS-500 (Spectrex) micro air sampler that was attached to each scent trap using 1/4" ID Tygon tubing 1 m in length. The flow rate of the PAS-500 was adjusted to 400 mL min<sup>-1</sup> using a Gilibrator air flow calibrator, and the flow rate was checked between the sample collections. Samples were collected simultaneously at the trunk and canopy. For trunk sampling, the PAS-500, tubing, and trap were placed so the inlet of the trap was near (<1 cm) the tree trunk between 0.5 – 1.5 m off the ground. The scent traps are placed as close to infested sites as possible while collecting samples from infested tree trunks. The set up for collecting the samples near the trunk is shown in Figure 2.2.

The canopy samples were collected using a sling-shot to place a line in the upper most branches of the tree (approximately 30 m high). The sampler, tubing and the trap were hoisted into the upper branches of the tree using this sling line. Air was sampled through each trap for 2 hours. After sampling, each trap was wrapped in two layers of pre-fired Al-foil and stored on ice

for overnight shipping. Blank scent traps were collected by taking traps to the sampling site and unwrapping them, but no vacuum was applied for the blank samples. The samples were collected approximately one day each week between 8/1/2009 and 10/31/2009. Samples were collected at both the canopy and trunk on all three trees simultaneously, with the exception of the infested tree at site 3. All samples were collected for two hours each starting at 8 AM, 11 AM, and 2 PM. Thus, a total of three to six samples were collected for each tree per day. The total number of samples collected during this period is listed in Table 2.1.



**Figure 2.2** The sampling assembly for collection of VOCs using scent traps.

In addition to scent traps, a few whole-air canister samples were collected and analyzed by multi-channel GC/FID/MS in Barkley Sive's lab at University of New Hampshire. These

samples were used as secondary confirmation of the identity of VOCs in the scent traps. The details of those samples and results are discussed in Amin et al.,<sup>146</sup> and will not be discussed in this dissertation.

### **2.2.3 Solvent extraction of VOCs in the scent traps**

The scent traps were stored in the freezer at -18 °C upon arrival at the Huff Hartz lab after shipping from SPL, and the traps were extracted within 1-2 weeks. For extraction, the scent traps were spiked with 75 µL of 10 ppm d<sup>22</sup>-decane (99%, Cambridge Isotope Laboratories), which acts as a recovery standard. The analytes were extracted using 1.5 mL n-hexane in three portions. After draining the last aliquot of n-hexane, positive pressure was applied on top of the Pasteur pipet, using the pipet bulb, to ensure complete collection of extraction solvent in the vial. The extracts were collected in pre-weighed 2 mL Target DP vials with Teflon-lined caps (National Scientific). The vials were weighed again with the extracts in them. The weights of extract obtained were converted to exact volumes and used in the calculation of percent recovery of the internal standards. The vials were stored in the freezer until gas chromatography and mass spectrometer (GCMS) analysis. After extraction, the scent traps were reconditioned with 5-6 volumes of n-hexane, air dried overnight and reused for sample collection.

### **2.2.4 Analysis of VOCs using GCMS**

The extracts were analyzed using a Saturn 2100 GCMS, which is equipped with a 3900 gas chromatograph and 2100T ion trap mass spectrometer. The extracts were injected via autosampler (8400), which is cooled to 10 °C using a water bath and prevents the loss of volatile compounds prior to injection. A 2.0 µL aliquot of each extract and standard was injected in the

splitless mode for 0.5 s with the inlet temperature at 220 °C. Ultrahigh purity helium (99.999%, Air Gas-Mid America) was used as the carrier gas at a flow rate of 1.0 mL/min. The analytes were separated with a method adapted from Adams, using a 5% diphenyl/95% dimethylpolysiloxane capillary column (VF-5MS, Varian Factor Four; 30 m x 0.25 mm x 0.25  $\mu$ m). For initial screening studies the analytes were separated using the temperature gradient described by Adams<sup>147</sup>: initial temperature of 60 °C, ramped to final temperature of 246 °C at rate of 3 °C/min, giving a total runtime of 62 min. However, no analytes eluted after 30 minutes and hence the temperature gradient was modified to give a total runtime of 45 minutes. The modified temperature gradient is as follows: initial temperature 60 °C, 3 °C/min ramp to 180 °C, followed by a second ramp to 246 °C with a rate of 30 °C/min. The analytes were detected in electron ionization mode (70 eV) scanning from 40-400 m/z. The temperature parameters for the mass spectrometer were as follows: trap temperature: 170 °C, manifold temperature: 40 °C and transfer line temperature: 240 °C. The GCMS data were collected and processed using the Varian Workstation software (ver. 6.9). After injection of samples, the vials were stored in the freezer and new septa were used to seal the vials.

The recovery of the analytes from the sorbent trap was estimated using the peak area for the  $d^{22}$ -decane in each chromatogram and comparing to the  $d^{22}$ -decane peak area in an extracted lab blank and adjusting for the differences in the extract volumes. The  $d^{22}$ -decane recovery average and standard deviation for the entire study was  $97 \pm 10\%$ . The peak areas obtained from GCMS are converted into concentration units using the calibration standard curves. The concentration is corrected for the blanks and further reported in ng of VOC per liter of air sampled using the flow rate and time for which the vacuum is applied.

### 2.2.5 Identification and quantitation of VOCs

The analytes in the extract were identified using standards, listed in Table 2.2, where the peaks were identified by comparison with retention times and mass spectra. For compounds without commercially-available authentic standards, the Adams<sup>147</sup> retention time indices were used followed by probability-based matching using the NIST/EPA/NIH 2005 mass spectral library for additional confirmation.

For analyte quantification, a VOC standard was made by mixing  $\alpha$ -pinene,  $\beta$ -pinene, 3-carene, limonene, terpinolene, estragole, p-cymene, and eucalyptol (Table 2.2) using n-hexane as the solvent. The standard solutions with concentrations 0.05, 0.1, 0.2, 0.5, 1.0, and 2.5 ppm were used to calculate the amounts of VOCs in the mixture. The most abundant ion mass fragments for each compound were selected, which reduces the interference of acetophenone contaminants found in the sorbent polymer.<sup>148</sup> The concentrations of analytes that lacked commercially-available standards like  $\beta$ -phellandrene, tricyclene, and sabinene were estimated using surrogate standards limonene,  $\alpha$ -pinene, and  $\alpha$ -pinene respectively and the selection of suurogates was based on the basis of chemical structure and retention time.

Limonene was found in the VOC canister samples but not in the scent trap samples. Limonene and  $\beta$ -phellandrene were not resolved on the VF-5ms column used for the separation of scent trap samples. For scent trap samples, the difference between electron impact mass spectra of  $\beta$ -phellandrene and limonene was used: limonene's dominant product ion is m/z 68, and  $\beta$ -phellandrene does not form ion fragments with m/z 68 to a significant extent. Limonene could have been present in the scent trap samples, but the lack of m/z 68 in the mass spectra indicates that it was not detected. However, limonene and  $\beta$ -phellandrene were resolved on OV-624 column used for analysis of VOC canister samples by multi-channel GC/FID/MS.

details of GC system used for identification of VOCs from canister samples are given elsewhere.<sup>149,150</sup> From analysis of scent trap samples it was concluded that concentration of  $\beta$ -phellandrene was higher than limonene and hence the mass spectra was similar to that of  $\beta$ -phellandrene, this was consistent with findings from the analysis of canister samples.<sup>146</sup>

**Table 2.2** Monoterpenes used to make VOC calibration standards.

VOC Standard	Manufacturer	CAS #	Molecular Weight <sup>a</sup> (g mol <sup>-1</sup> )	Purity <sup>a</sup>
(1R)-(+)- $\alpha$ -pinene	Aldrich	7785-70-8	136.23 $\pm$ 0.05	0.99 $\pm$ 0.05
(1S)-(+)- $\beta$ -pinene	Aldrich	18172-67-3	136.23 $\pm$ 0.05	0.99 $\pm$ 0.05
eucalyptol (1,8-cineole)	SAFC	470-82-6	154.25 $\pm$ 0.05	0.99 $\pm$ 0.05
(R)-(+)-limonene	Aldrich	5989-27-5	136.23 $\pm$ 0.05	0.985 $\pm$ 0.005
(1S)-(+)-3-carene	Aldrich	498-15-7	136.23 $\pm$ 0.05	0.99 $\pm$ 0.005
terpinolene	Fluka	586-62-9	136.23 $\pm$ 0.05	0.95 $\pm$ 0.05
p-cymene	Fluka	498-15-7	134.22 $\pm$ 0.05	0.995 $\pm$ 0.005
estragole	Fluka	470-82-6	148.20 $\pm$ 0.05	0.965 $\pm$ 0.05

<sup>a</sup>The error is estimated on the number of significant digits provided by manufacturer.

## 2.3 Results and discussion

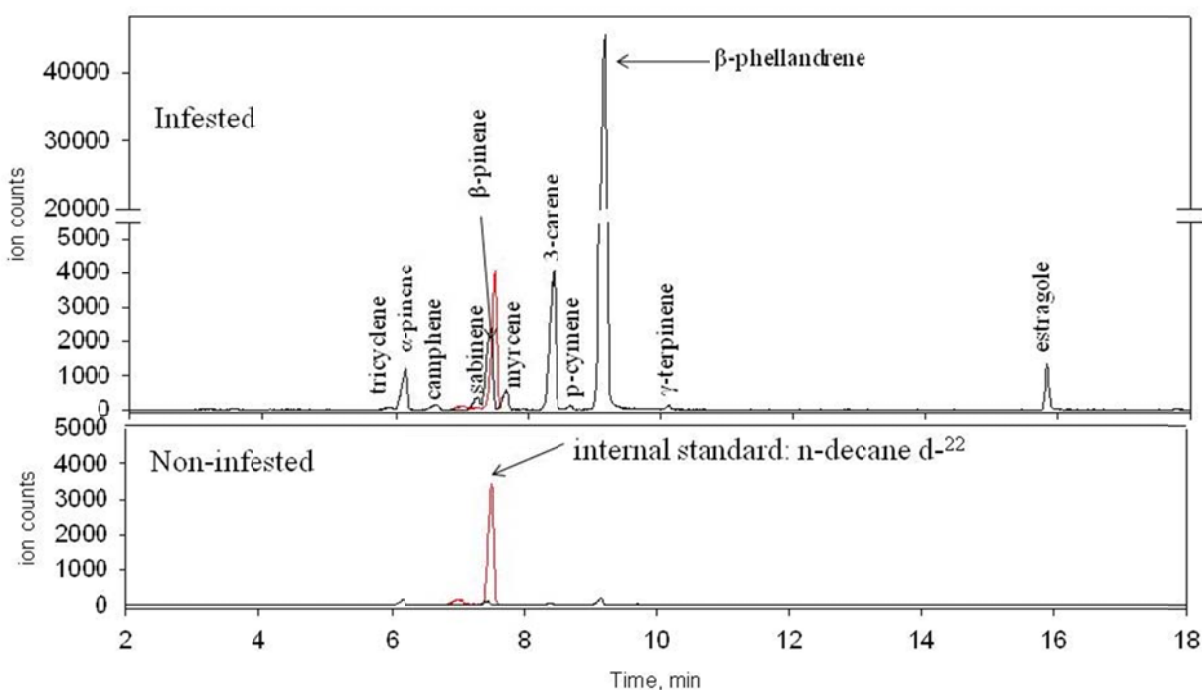
The results and discussion section is split in two parts in the first part discussion on emissions from lodgepole pine is presented and the second part presents the discussion on emissions from Engelmann spruce.

### 2.3.1 Lodgepole pine emissions

#### 2.3.1.1 Individual VOCs from healthy vs infested plants of lodgepole pine

A total of thirteen VOCs were identified from the extract trap samples. Amongst the identified VOCs major components were monoterpene isomers:  $\alpha$ -pinene, camphene,  $\beta$ -pinene, 3-carene, and  $\beta$ -phellandrene, with concentrations ranging from 1 ng L<sup>-1</sup> to greater than 50 ng L<sup>-1</sup>. Other minor VOCs included monoterpene isomers: tricyclene, camphene, sabinene,

myrcene,  $\gamma$ -terpinene, and terpinolene, a monoterpene derivative, 1,4-cineole, and aromatic VOCs, estragole and p-cymene, were sometimes found in the samples at concentrations less than  $2 \text{ ng L}^{-1}$ . Figure 2.3 shows GCMS chromatogram for VOCs observed for trunk of infested and trunk of healthy lodgepole pine tree. The peak shown in red is for the internal standard  $\text{d}^{22}$ -decane. From the chromatogram, it is evident that amount of VOCs emitted from trunk of infested trees are higher than amount of VOCs emitted from trunk of non-infested trees.



**Figure 2.3** GCMS chromatogram of VOCs obtained from bark of (a) infested and (b) healthy lodgepole pine tree. The peak shown in red is for the internal standard  $\text{d}^{22}$ -decane.

The average concentrations of major VOC species, which include monoterpene isomers ( $\alpha$ -pinene, camphene,  $\beta$ -pinene, 3-carene, and  $\beta$ -phellandrene), and aromatic VOCs (estragole and p-cymene), over the entire study are listed in Table 2.3. The total VOC concentration for individual samples collected at site 1, site 2, and site 3 are listed in Appendix I (A-I Table 1 to A-I Table 3).



**Table 2.3** Concentration  $\pm$  standard error of the mean<sup>a</sup> (ng L<sup>-1</sup>) of the major VOCs, averaged over the entire study, obtained from extracts of lodgepole pine samples

	$\alpha$ -pinene	camphene	$\beta$ -pinene	3-carene	$\beta$ -phellandrene	estragole	p-cymene
S1T1							
Trunk	1.4 $\pm$ 0.6	0.06 $\pm$ 0.03	0.50 $\pm$ 0.20	0.24 $\pm$ 0.08	2.3 $\pm$ 0.6	nd	0.01 $\pm$ 0.01
Canopy	1.1 $\pm$ 0.54	0.02 $\pm$ 0.02	0.03 $\pm$ 0.03	0.08 $\pm$ 0.04	1.4 $\pm$ 0.5	nd	nd
S1T2							0.38 $\pm$ 0.0.0
Trunk	4.4 $\pm$ 1.0	0.16 $\pm$ 0.05	6.8 $\pm$ 1.2	8.4 $\pm$ 1.7	69 $\pm$ 12	2.6 $\pm$ 0.4	7
Canopy	1.5 $\pm$ 0.6	0.09 $\pm$ 0.04	nd	0.15 $\pm$ 0.06	1.7 $\pm$ 0.6	nd	nd
S1T3							
Trunk	5 $\pm$ 3	1.2 $\pm$ 0.7	0.5 $\pm$ 0.3	1.5 $\pm$ 0.7	0.8 $\pm$ 0.3	nd	0.10 $\pm$ 0.04
Canopy	0.21 $\pm$ 0.11	0.02 $\pm$ 0.01	0.06 $\pm$ 0.06	1.0 $\pm$ 1.0	0.8 $\pm$ 0.5	nd	nd
S2T6							
Trunk	8 $\pm$ 3	1.5 $\pm$ 0.7	4.2 $\pm$ 1.5	13 $\pm$ 5	43 $\pm$ 17	0.20 $\pm$ 0.09	0.20 $\pm$ 0.06
Canopy	2.6 $\pm$ 0.9	0.5 $\pm$ 0.2	0.6 $\pm$ 0.2	0.9 $\pm$ 0.4	1.2 $\pm$ 0.4	nd	0.06 $\pm$ 0.02
S2T7							
Trunk	2.2 $\pm$ 0.8	0.5 $\pm$ 0.2	0.5 $\pm$ 0.2	0.4 $\pm$ 0.2	1.5 $\pm$ 0.6	nd	0.04 $\pm$ 0.01
Canopy	2.7 $\pm$ 1.1	0.6 $\pm$ 0.3	0.5 $\pm$ 0.2	0.8 $\pm$ 0.4	1.0 $\pm$ 0.3	nd	0.06 $\pm$ 0.03
S2T8							
Trunk	0.3 $\pm$ 0.3	0.09 $\pm$ 0.09	0.18 $\pm$ 0.10	0.06 $\pm$ 0.04	1.4 $\pm$ 0.6	nd	0.35 $\pm$ 0.09
Canopy	nd	0.01 $\pm$ 0.01	0.07 $\pm$ 0.05	0.24 $\pm$ 0.22	0.04 $\pm$ 0.02	nd	0.05 $\pm$ 0.03
S3T9							
Trunk	11 $\pm$ 3	2.5 $\pm$ 0.7	1.1 $\pm$ 0.4	4.2 $\pm$ 1.5	0.9 $\pm$ 0.3	nd	0.09 $\pm$ 0.04
Canopy	9 $\pm$ 3	1.0 $\pm$ 0.4	0.53 $\pm$ 0.20	5.4 $\pm$ 1.9	0.8 $\pm$ 0.3	nd	0.17 $\pm$ 0.07
S3T10							
Trunk	5.3 $\pm$ 2	1.1 $\pm$ 0.4	4.7 $\pm$ 1.3	5.0 $\pm$ 1.2	43 $\pm$ 12	0.36 $\pm$ 0.07	0.22 $\pm$ 0.07
Canopy <sup>b</sup>	-	-	-	-	-	-	-
S3T11							
Trunk	8 $\pm$ 3	2.2 $\pm$ 0.9	1.0 $\pm$	2.4 $\pm$ 0.8	0.7 $\pm$ 0.2	nd	0.15 $\pm$ 0.05
Canopy	2.2 $\pm$ 1.5	0.7 $\pm$ 0.5	0.4 $\pm$ 0.4	1.7 $\pm$ 1.0	0.21 $\pm$ 0.17	nd	0.03 $\pm$ 0.03

<sup>a</sup>standard error of the mean was calculated by standard deviation divided by  $n^{1/2}$ , where n is the number of samples given in Table 2.2. <sup>b</sup>no canopy samples were collected at S3T10. nd = not detected.

For the minor monoterpenes, tricyclene, sabinene, myrcene,  $\gamma$ -terpinene, and terpinolene, and a monoterpene derivative, 1,4-cineole, the average concentrations over the course of the study are listed in Table 2.4.

**Table 2.4** Concentration  $\pm$  standard error of the mean<sup>a</sup> (ng L<sup>-1</sup>) of the minor VOCs, averaged over the entire study, obtained from extracts of lodgepole pine samples

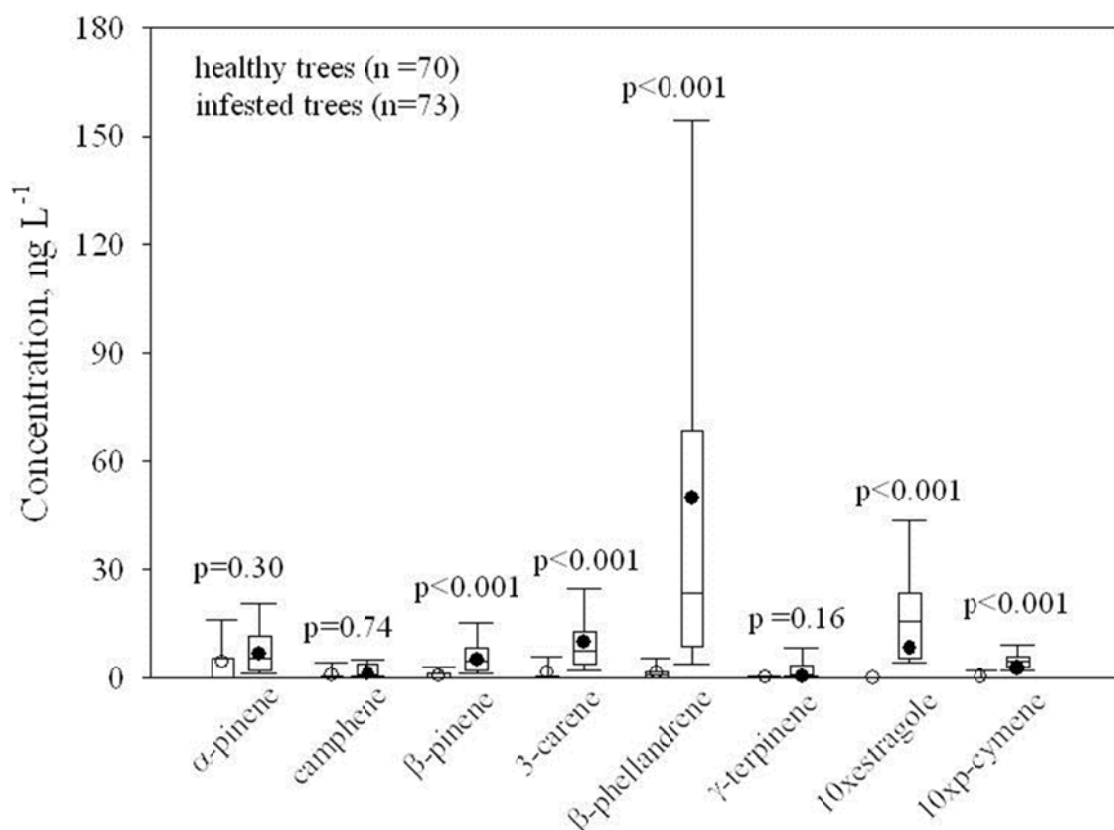
	tricyclene	sabinene	myrcene	$\gamma$ - terpinene	terpinolene	1,4- cineole
S1T1						
trunk	nd	nd	nd	Nd	nd	nd
canopy	nd	nd	nd	Nd	nd	nd
S1T2						
trunk	0.05 $\pm$ 0.02	0.47 $\pm$ 0.12	0.6 $\pm$ 0.2	0.14 $\pm$ 0.07	0.51 $\pm$ 0.15	nd
canopy	nd	nd	nd	Nd	nd	nd
S1T3						
Trunk	0.26 $\pm$ 0.15	0.005 $\pm$ 0.01	nd	0.11 $\pm$ 0.07	nd	nd
canopy	0.003 $\pm$ 0.002	0.004 $\pm$ 0.006	nd	Nd	0.04 $\pm$ 0.04	nd
S2T6						
trunk	0.4 $\pm$ 0.2	0.5 $\pm$ 0.2	0.7 $\pm$ 0.4	0.5 $\pm$ 0.3	0.23 $\pm$ 0.11	nd
canopy	0.15 $\pm$ 0.06	0.006 $\pm$ 0.007	0.035 $\pm$ 0.02	0.05 $\pm$ 0.05	nd	nd
S2T7						
trunk	0.11 $\pm$ 0.05	0.004 $\pm$ 0.005	0.020 $\pm$ 0.012	0.02 $\pm$ 0.02	0.009 $\pm$ 0.009	nd
canopy	0.12 $\pm$ 0.06	0.01 $\pm$ 0.01	0.023 $\pm$ 0.013	0.07 $\pm$ 0.05	nd	nd
S2T8						
trunk	0.03 $\pm$ 0.03	0.0003 $\pm$ 0.0003	0.039 $\pm$ 0.021	Nd	nd	nd
canopy	0.3 $\pm$ 0.3	nd	0.041 $\pm$ 0.022	Nd	nd	nd
S3T9						
trunk	0.43 $\pm$ 0.12	0.04 $\pm$ 0.02	nd	0.43 $\pm$ 0.21	nd	nd
canopy	0.22 $\pm$ 0.09	0.04 $\pm$ 0.03	nd	0.47 $\pm$ 0.18	nd	0.05 $\pm$ 0.21
S3T10						
trunk	0.23 $\pm$ 0.10	0.22 $\pm$ 0.09	0.48 $\pm$ 0.15	0.30 $\pm$ 0.19	0.17 $\pm$ 0.17	nd
canopy	nd	nd	nd	-	nd	nd
S3T11						
trunk	0.47 $\pm$ 0.17	0.01 $\pm$ 0.01	nd	0.20 $\pm$ 0.08	nd	nd
canopy	0.13 $\pm$ 0.10	0.007 $\pm$ 0.007	nd	0.07 $\pm$ 0.05	nd	nd

<sup>a</sup> standard error of the mean was calculated by standard deviation divided by  $n^{1/2}$ , where n is the number of samples given in Table 2.2. nd = not detected.

Statistical tests were performed to compare samples from infested trees to samples from trees that were not infested. For each test, an independent, two-sample t-test was performed, and the null hypothesis tested was that the averages were the same. The result of the t-test is the probability (p) that the averages of the populations are equal. A low p-value indicates that it is unlikely that the average VOC concentrations for a species emitted from the infested trees and

non-infested trees are the same. Prior to each t-test, an F-test was used to compare the standard deviations. When the F-test indicated the difference in standard deviation of the two populations was not significant at the 99% confidence level, the standard deviations were pooled. Standard mean of error were calculated by taking ratio of the standards deviation to the square root of the number of samples.

Figure 2.4 shows that the individual VOC sample concentrations were higher at the trunks of infested trees than healthy trees. Statistically significant increases ( $p < 0.001$ ) were observed for  $\beta$ -pinene, 3-carene,  $\beta$ -phellandrene, estragole, and p-cymene. The  $\beta$ -phellandrene concentrations measured near infested pine trunks were more than thirty times higher than healthy pine trunks.



**Figure 2.4.** Box and whisker plots of the major VOCs found in the scent trap samples collected from the trunks of healthy (S1T1, S2T7, S3T9) and infested lodgepole pine trees (S1T2, S2T6, S3T10). The median, the 25<sup>th</sup> percentile, and the 75<sup>th</sup> percentile are denoted by the center line and the edges of the box, the 10<sup>th</sup> and 90<sup>th</sup> percentiles are denoted by the whiskers, and the mean is denoted by the symbols.

The types and distributions of monoterpenes observed in healthy and infested samples are generally consistent with prior work. The major monoterpenes found by Rhoades (1990) emitted from the undamaged trunks of lodgepole pine trees were  $\beta$ -phellandrene,  $\beta$ -pinene,  $\alpha$ -pinene, p-cymene, and an unidentified oxygenated monoterpene. Similar monoterpenes were found by Gara et al.<sup>151</sup> in lodgepole pine trunks infested with heartwood decay fungi ( $\beta$ -phellandrene,  $\beta$ -pinene,  $\alpha$ -pinene, and p-cymene). The types of VOCs and the observed increases are generally consistent with the work of Jost et al.,<sup>152</sup> where the bark from lodgepole, hybrid, and jack pine trees were inoculated with three types of blue stain fungi, a symbiotic species associated with

mountain pine beetle infestation. The gas emissions from bark samples that were inoculated with fungi contained eight monoterpenes ( $\alpha$ -pinene, camphene,  $\beta$ -pinene, sabinene,  $\alpha$ -phellandrene, myrcene, limonene,  $\beta$ -phellandrene) and p-cymene. Jost et al.<sup>152</sup> observed species-dependent increases and decreases in the relative monoterpene concentrations. For the lodgepole pine, camphene, limonene, and  $\alpha$ -pinene emissions decreased while the  $\beta$ -phellandrene emissions increased with fungi inoculation.

### **2.3.1.2 Comparison of total VOC concentrations**

The total VOC concentrations for each scent trap sample were calculated by summing the concentrations of each VOC that was sampled by scent trap, extracted, and detected by the GCMS. The averages and the standard errors of the means of the total VOC concentration at each tree for the entire study are listed in Table 2.5. For individual samples, the total VOC concentrations range from approximately 800 ng L<sup>-1</sup> to below the detection limit (estimated 0.1 ng L<sup>-1</sup> for total VOCs). The average total VOC concentrations differ by a factor of up to 100, with the lowest concentrations found in the canopy of a dead pine tree (0.7 ng L<sup>-1</sup>) (S2T8) and the highest concentrations found near the trunk of infested pine trees (>90 ng L<sup>-1</sup>) (S1T2). Total VOC emissions from the canopy are lower than those from the trunk.

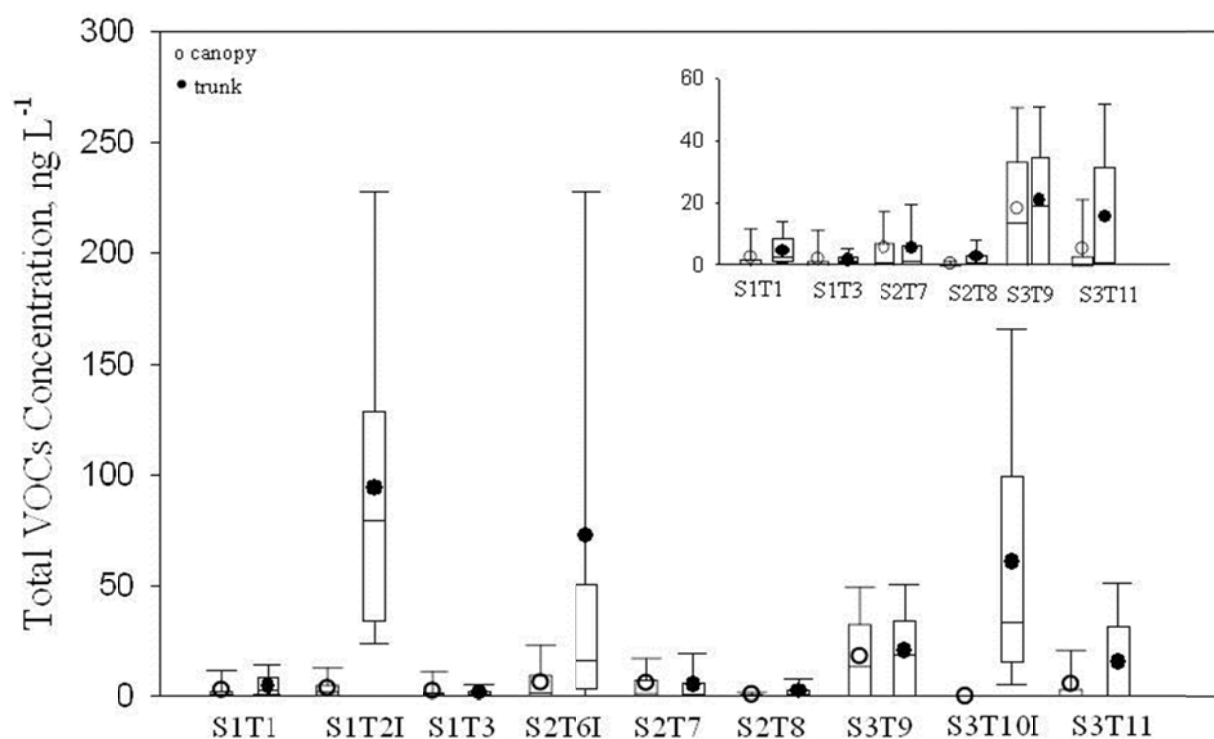
**Table 2.5** Summary of the total VOCs sampled by sorbent traps and detected by GCMS from lodgepole pine

	trunk average±standard error of the mean <sup>a</sup> , ng/L	canopy average±stand ard error of the mean <sup>a</sup> , ng/L	$F_{DIST}$ (trunk vs. canopy) <sup>c</sup>	$p$ (trunk vs. canopy)
site 1				
healthy pine, prior infestation S1T1	4.5±1.3	2.7±1.1	$2.1 \times 10^{-1}$	0.89
pine, active infestation S1T2	94.2±16.4	3.5±1.2	$1.1 \times 10^{-16}$	$3.8 \times 10^{-5}$
healthy pine, sprayed S1T3	1.6±0.5	2.2±1.7	$2.4 \times 10^{-5}$	0.72
site 2				
pine, active infestation S2T6	72.7±27.2	6.0±1.7	$1.8 \times 10^{-34}$	0.019
healthy pine S2T7	5.4±1.6	5.8±2.3	$2.6 \times 10^{-2}$	0.99
deceased pine, prior infestation S2T8	2.5±1.0	0.7±0.5	$2.3 \times 10^{-3}$	0.098
site 3				
healthy pine S3T9, prior infestation	20.6±5.6	17.9±4.9	$1.9 \times 10^{-1}$	0.97
pine, active infestation S3T10	60.9±15.4	- <sup>b</sup>	- <sup>b</sup>	- <sup>b</sup>
healthy pine, prior infestation, sprayed S3T11	15.4±5.4	5.4±3.3	$2.5 \times 10^{-2}$	0.86

<sup>a</sup>standard error of the mean was calculated by standard deviation divided by  $n^{1/2}$ , where n is the number of samples given in Table 2.2. <sup>b</sup>no canopy samples were collected at S3T10. <sup>c</sup> $F_{DIST}$  is the F probability distribution value calculated using the FDIST function in Excel and evaluated at  $s_1^2/s_2^2$  where  $s_1$  and  $s_2$  are the standard deviations for population 1 and 2 and  $s_1 > s_2$ . For t-testing, standard deviations are pooled when  $F_{DIST} > 1 \times 10^{-2}$ .

Variations in the total VOC concentrations from biogenic emissions are expected, in part because emissions vary with season, solar radiation, and temperature. To compare the total VOC concentrations found at each site, the samples were grouped according to the location of the sampling (trunk vs. canopy) and the tree at each site. Figure 2.5 shows the distribution of the total VOC concentration as a box and whiskers plot, where the center line of the box is the median, the edges of the blocks are the 25th and 75th percentile, the whiskers are the 10th and 90th percentile, and the average total VOCs sampled near the trunk and in the canopy is shown with closed and open circles, respectively. The concentrations of the total VOCs overlap with

the exception of the samples collected at the trunks of infested trees (S1T2, S2T6, S3T10). The healthy site 3 trees tended to have higher total VOC concentrations than the other healthy trees. Logging at this site prior to sample collection could cause an increase to background VOC concentrations.



**Figure 2.5** Total VOC concentrations for all scent trap samples collected from lodgepole pine. The center line of the box is the median, the edges of the blocks are the 25<sup>th</sup> and 75<sup>th</sup> percentile, and the whiskers are the 10<sup>th</sup> and 90<sup>th</sup> percentile. The closed circles and open circles represent the average total VOCs sampled near the trunk and in the canopy, respectively. Trees labeled “I” on the x-axis are beetle infested. Inset: scale expansion for total VOC concentrations for non-infested trees.

The total VOC concentrations from samples collected at the canopy and trunk at each tree are compared in Table 2.6. The average total VOCs from trunks of infested trees (S1T2, S2T6) are significantly greater than the average total VOCs from their canopy samples, (S1T2  $p = 3.8 \times 10^{-5}$ ; S2T6  $p = 0.019$ ). In contrast, there is no significant difference in the averages of canopy

and trunk total VOC concentrations for healthy, dead, or healthy and recovered trees. This suggests that there is a correlation between active beetle infestation, which occurs in the trunk of the tree, and an increase in total VOC emissions. The higher VOC concentrations found near the trunks of infested trees could be due to the pitch tubes of the infested pine trees, which likely provide a direct route for VOCs to be emitted from the trunk, and/or additional VOCs are generated due to beetle infestation.

In addition to comparisons between the distributions of total VOCs from the trunk and canopy from the same tree, the total VOC concentrations from healthy and infested trees were compared, refer Table 2.6. Trees from the same site were compared in order to reduce differences in VOC emissions resulting from homogeneities in temperature and solar radiation. There is a statistically significant difference ( $p = 0.022$ ) between the total VOCs sampled from the trunks of healthy vs. infested trees at the same site. However, the canopies of healthy and infested trees show no significant difference in the total VOC concentration sampled ( $p = 0.54$ ).



**Table 2.6** Statistical comparison of the total VOCs sampled from lodgepole pine

	$F_{DIST}$ trunk <sup>a</sup>	$p$ trunk	$F_{DIST}$ canopy <sup>a</sup>	$p$ canopy
healthy vs. infested				
healthy pine with prior infestation vs. infested pine (S1T1 vs. S1T2)	$4.2 \times 10^{-3}$	$4.4 \times 10^{-5}$	$3.6 \times 10^{-1}$	0.62
healthy pine, sprayed vs. infested pine (S1T3 vs. S1T2)	$1.5 \times 10^{-19}$	$2.9 \times 10^{-5}$	$9.8 \times 10^{-2}$	0.54
healthy pine vs. infested pine (S2T7 vs. S2T6)	$2.9 \times 10^{-35}$	0.018	$4.7 \times 10^{-2}$	0.996
healthy pine with prior infestation vs. infested pine (S3T9 vs. S3T10)	$6.8 \times 10^{-5}$	0.022	_ <sup>b</sup>	_ <sup>b</sup>
healthy pine, sprayed vs. infested pine (S3T11 vs. S3T10)	$1.2 \times 10^{-6}$	0.011	_ <sup>b</sup>	_ <sup>b</sup>
deceased vs. healthy or infested				
deceased pine vs. infested pine (S2T8 vs. S2T6)	$1.2 \times 10^{-25}$	0.016	$1.5 \times 10^{-9}$	0.0057
deceased pine vs. healthy pine (S2T8 vs. S2T7)	$1.7 \times 10^{-4}$	0.14	$8.7 \times 10^{-12}$	0.033

<sup>a</sup> $F_{DIST}$  is the F probability distribution value calculated using the FDIST function in Excel and evaluated at  $s_1^2/s_2^2$  where  $s_1$  and  $s_2$  are the standard deviations for population 1 and 2 and  $s_1 > s_2$ . For t-testing, standard deviations are pooled when  $F_{DIST} > 1 \times 10^{-2}$ . <sup>b</sup>no canopy samples were collected at S3T10, hence no  $F_{DIST}$  values or  $p$  values for canopy

Gara et al.<sup>151</sup> found that the total monoterpenes emitted per day increased nearly five times i.e. from  $6.8 \mu\text{g m}^{-2} \text{day}^{-1}$  to  $32.38 \mu\text{g m}^{-2} \text{day}^{-1}$ , from the trunks of pine trees (*Pinus contorta murryana*) with heartwood decay fungi present compared to trunks with no fungi present. In comparison, for this study at site 1, the total VOC concentrations increased by 21 times (from  $4.5 \text{ ng L}^{-1}$  at a healthy tree to  $94.2 \text{ ng L}^{-1}$  at an infested tree). At site 2, the total VOC concentrations increased by 13 times (from  $5.4 \text{ ng L}^{-1}$  at a healthy tree to  $72.7 \text{ ng L}^{-1}$  at an infested tree). At site 3, the total VOC concentrations increased by three times (from  $20.6 \text{ ng L}^{-1}$  at a healthy tree to  $60.9 \text{ ng L}^{-1}$  at an infested tree). Although the heartwood decay fungi is not the same type of fungi associated with bark beetles, the observation of the increases in VOC emissions are consistent with the work of Gara et al.<sup>151</sup>

Samples were collected at site 2 from a deceased pine tree that was caused by beetle infestation, and the total VOC concentrations from this tree were found to be lower than the other samples at the same site. There was a significant difference between the average total VOC concentrations (Table 2.7) of the deceased and infested pine both at the trunk ( $p = 0.016$ ) and the canopy ( $p = 0.0057$ ). However, the differences between the total VOC concentrations of the deceased and healthy pine were lower, thus the probabilities that the average total VOC concentrations at the trunk ( $p = 0.14$ ) and the canopy ( $p = 0.033$ ) were higher, indicating very little difference. The total VOC samples at the deceased tree could be affected by emissions from nearby infested and healthy trees. If the deceased tree only emits a negligible concentration of VOCs, nearby infested and healthy trees could cause an overestimation of the VOC emissions from the deceased tree, which leads to a less significant difference between deceased tree's and healthy tree's total VOC concentrations. Decomposition by fungi within the deceased tree could lead to additional VOC emissions, but these increased emissions were not observed at this tree.

### **2.3.2 Engelmann spruce emissions**

#### **2.3.2.1 Individual VOCs emitted from healthy vs infested plants from Engelmann spruce**

Two Engelmann spruce trees were used to collect the samples near the trunk of one infested and one healthy tree. Of the thirteen VOCs identified from the lodgepole pine extracts of scent trap samples, twelve were identified for emissions from Engelmann spruce. Estragole, detected in emissions of infested lodgepole pine, was not detected in extracts of trap samples originating from trunks either infested or healthy spruce trees. Of the eleven VOCs were identified, which include monoterpene species like  $\alpha$ -pinene, camphene,  $\beta$ -pinene, 3-carene,  $\beta$ -phellandrene, tricyclene, camphene, sabinene, myrcene,  $\gamma$ -terpinene, terpinolene 1,4-cineole,

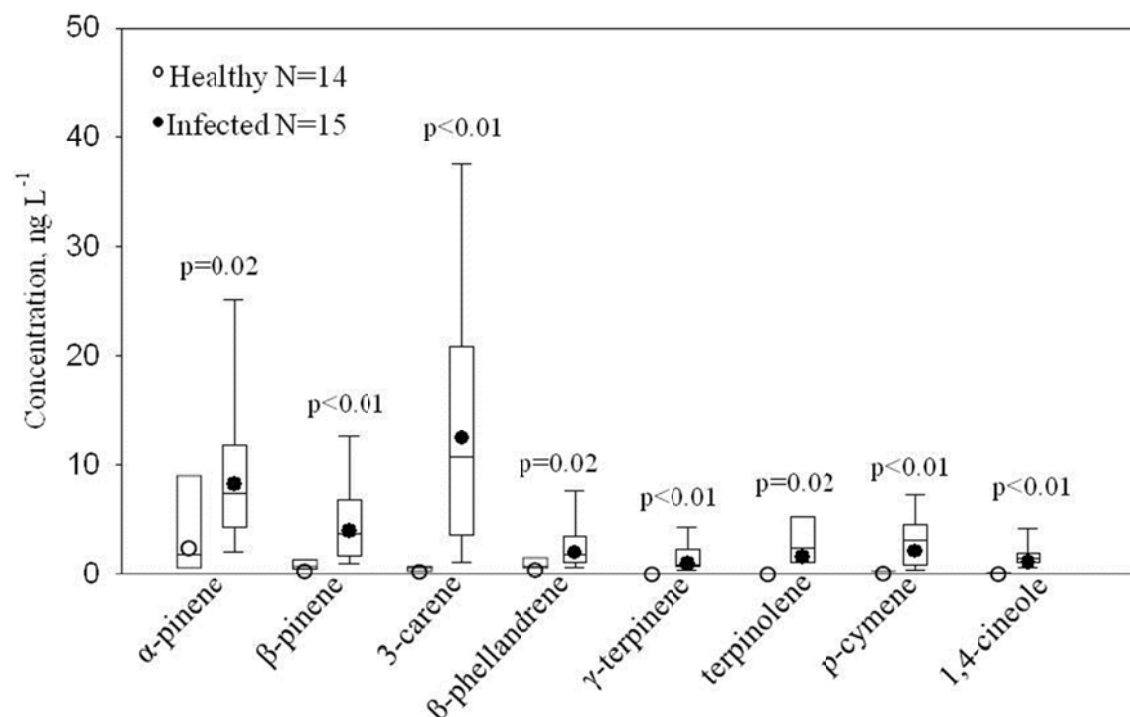
and p-cymene, the concentrations ranged from around 0.1 ng L<sup>-1</sup> to 13 ng L<sup>-1</sup>. The average concentrations of the VOC species is listed in Table 2.7. The total VOC concentrations for individual samples collected at site 2 for the Engelmann spruce are listed in Appendix I (A-I Table 4)

**Table 2.7** Concentration  $\pm$  standard error of the mean<sup>a</sup> (ng L<sup>-1</sup>) of the major VOCs, averaged over the entire study for Engelmann spruce

	$\alpha$ -pinene	camphene	$\beta$ -pinene	3-carene	$\beta$ -phellandrene	p-cymene
S2T4 Trunk	8.5 $\pm$ 2.1	1.1 $\pm$ 0.4	4.1 $\pm$ 1.0	13 $\pm$ 3	1.9 $\pm$ 0.6	2.2 $\pm$ 0.6
S2T5 Trunk	2.4 $\pm$ 0.6	0.47 $\pm$ 0.12	0.26 $\pm$ 0.07	0.20 $\pm$ 0.05	0.36 $\pm$ 0.09	0.05 $\pm$ 0.01
	tricyclene	sabinene	myrcene	$\gamma$ -terpinene	terpinolene	1,4-cineole
S2T4 Trunk	0.42 $\pm$ 0.12	1.9 $\pm$ 0.6	0.01 $\pm$ 0.01	1.0 $\pm$ 0.3	1.6 $\pm$ 0.6	1.08 $\pm$ 0.3
S2T5 Trunk	0.10 $\pm$ 0.02	0.11 $\pm$ 0.02	nd	nd	0.5 $\pm$ 0.1	0.056 $\pm$ 0.004

<sup>a</sup>Standard error of the mean was calculated by standard deviation divided by  $n^{1/2}$ , where n is the number of samples given in Table 2.2.

Similar to lodgepole pine data analysis, statistical tests were performed to compare if the average of the individual concentration of VOCs emitted from healthy and infested spruce trees were the same. Figure 2.6 shows that the individual VOC sample concentrations were higher at the trunks of the infested trees than the healthy spruce trees (only major VOCs are shown). Statistically, significant increases ( $p < 0.001$ ) were observed for  $\beta$ -pinene, 3-carene,  $\gamma$ -terpinene, 1,4-cineole, and p-cymene. For other monoterpenes, the p-values were calculated:  $\alpha$ -pinene ( $p = 0.02$ ), camphene ( $p = 0.2$ ), tricyclene ( $p = 0.02$ ), sabinene ( $p = 0.01$ ), myrcene ( $p = 0.3$ ), terpinolene ( $p = 0.02$ ).



**Figure 2.6.** Box and whisker plots of the major VOCs found in the scent trap samples collected from the trunk of healthy spruce (S2T5) and infested spruce tree (S2T4). The median, the 25<sup>th</sup> percentile, and the 75<sup>th</sup> percentile are denoted by the center line and the edges of the box, the 10<sup>th</sup> and 90<sup>th</sup> percentiles are denoted by the whiskers, and the mean is denoted by the symbols.

From our work we see that the average concentration of 3-carene and β-pinene change the most, for samples collected healthy and infested trees. The 3-carene concentration increases around more than 50 times while concentration of β-pinene increases by more than ten times. While the β-phellandrene emissions are found to be increase five times. When compared to Figure 2.4, the individual VOCs emitted by infested Engelmann spruce are found to be lower than those emitted by infested lodgepole pine. This difference is due to different species of tree also lodgepole pine is a preferred tree for bark beetle infestation.

### 2.3.2.2 Comparison in total VOC concentrations

The total VOC concentrations for each scent trap sample were calculated by summing the concentrations of each VOC that was sampled by scent trap, extracted, and detected by the

GCMS. The averages and the standard errors of the means of the total VOC concentration at each of the two spruce trees for the entire study are listed in Table 2.8. For infested spruce tree, the total VOC concentration was found to be  $37 \pm 7 \text{ ng L}^{-1}$  and for the healthy spruce tree the total VOC concentration was  $3.9 \pm 0.1 \text{ ng L}^{-1}$ . The average total VOC concentrations emitted by infested spruce trees increase approximately by a factor of ten (infested spruce vs. healthy spruce  $p = 2.9 \times 10^{-4}$ ). Only samples near the trunk of these trees were collected hence no canopy vs trunk emission comparisons are made in this section.

**Table 2.8** Summary of the total VOCs sampled by sorbent traps and detected by GCMS for Engelmann spruce trees

	trunk average $\pm$ standard error of the mean <sup>a</sup> , ng/L	$F_{DIST}$ (healthy vs. infested) <sup>b</sup>	$p$ (healthy vs. infested)
site 2			
infested spruce S2T4, pitching out	$37 \pm 7$	$2.7 \times 10^{-7}$	$2.9 \times 10^{-4}$
healthy spruce S2T5	$3.9 \pm 1.0$		

<sup>a</sup>standard error of the mean was calculated by standard deviation divided by  $n^{1/2}$ , where  $n$  is the number of samples given in Table 2.2. <sup>b</sup> $F_{DIST}$  is the F probability distribution value calculated using the FDIST function in Excel and evaluated at  $s_1^2/s_2^2$  where  $s_1$  and  $s_2$  are the standard deviations for population 1 and 2 and  $s_1 > s_2$ . For t-testing, standard deviations are pooled when  $F_{DIST} > 1 \times 10^{-2}$ .

The total VOCs emitted by infested spruce tree (S2T4),  $37 \pm 7 \text{ ng L}^{-1}$ , are lower than the total VOCs emitted by the infested lodgepole pine tree (S1T2=  $94.2 \pm 16.4 \text{ ng L}^{-1}$ , S2T6=  $72.7 \pm 27.2 \text{ ng L}^{-1}$ , S3T10=  $60.9 \pm 15.4 \text{ ng L}^{-1}$ ). However, this finding is based on VOC concentrations of one infested spruce trees, data set involving higher number of infested spruce trees may support this comparison better.

### 2.3.3 Potential impact of bark beetle infestation on SOA

The analysis of the scent trap samples suggests that upon bark beetle infestation, lodgepole pine trees show increases in total VOC emissions and a shift in the types of VOCs emitted, i.e., from a mixture of monoterpenes containing  $\alpha$ -pinene,  $\beta$ -pinene, and 3-carene in healthy trees to a monoterpene mixture that is dominated by  $\beta$ -phellandrene in infested trees. These results suggest that SOA concentrations could increase from bark beetle infestation because the concentrations of SOA precursors increase. The magnitude of this increase is difficult to predict at this time because very few studies have addressed SOA from  $\beta$ -phellandrene, possibly due to the lack of a high purity compound that is commercially available.  $\beta$ -phellandrene is a cyclic monoterpene and contains two carbon-carbon double bonds, one exo and one endo with respect to the ring. The oxidation kinetics of  $\beta$ -phellandrene with respect to OH ( $1.7 \times 10^{-10} \text{ molec}^{-1} \text{ cm}^3 \text{ s}^{-1}$ ),  $\text{O}_3$  ( $4.7 \times 10^{-17} \text{ molec}^{-1} \text{ cm}^3 \text{ s}^{-1}$ ), and  $\text{NO}_3$  ( $8.0 \times 10^{-12} \text{ molec}^{-1} \text{ cm}^3 \text{ s}^{-1}$ ) are similar to the major monoterpenes emitted from non-infested trees, including:  $\alpha$ -pinene (OH,  $5.2 \times 10^{-11} \text{ molec}^{-1} \text{ cm}^3 \text{ s}^{-1}$ ;  $\text{O}_3$ ,  $8.4 \times 10^{-17} \text{ molec}^{-1} \text{ cm}^3 \text{ s}^{-1}$ ; and  $\text{NO}_3$   $6.2 \times 10^{-12} \text{ molec}^{-1} \text{ cm}^3 \text{ s}^{-1}$ ),  $\beta$ -pinene (OH,  $7.4 \times 10^{-11} \text{ molec}^{-1} \text{ cm}^3 \text{ s}^{-1}$ ;  $\text{O}_3$ ,  $1.5 \times 10^{-17} \text{ molec}^{-1} \text{ cm}^3 \text{ s}^{-1}$ ; and  $\text{NO}_3$   $6.16 \times 10^{-12} \text{ molec}^{-1} \text{ cm}^3 \text{ s}^{-1}$ ), and 3-carene (OH,  $8.8 \times 10^{-11} \text{ molec}^{-1} \text{ cm}^3 \text{ s}^{-1}$ ;  $\text{O}_3$ ,  $3.7 \times 10^{-17} \text{ molec}^{-1} \text{ cm}^3 \text{ s}^{-1}$ ; and  $\text{NO}_3$   $9.1 \times 10^{-12} \text{ molec}^{-1} \text{ cm}^3 \text{ s}^{-1}$ ).<sup>65</sup> Thus, we expect the oxidation kinetics of the VOCs emitted from infested lodgepole pine trees that form SOA will have at least the same order of magnitude as the oxidation kinetics as healthy trees, and as a result, a change in the types of VOCs emitted will not inhibit SOA formation.

The efficacy of VOCs to form SOA depends on the structure and concentration of VOC, the type and concentration of oxidant, and the environmental conditions (i.e., temperature, relative humidity). The results in this work suggest that upon bark beetle infestation, the concentration of

total VOCs increase and the dominant VOCs change from monoterpenes with one carbon-carbon double bond ( $\alpha$ -pinene,  $\beta$ -pinene, 3-carene) to  $\beta$ -phellandrene, which has two double bonds. The ratio of the SOA produced per VOC oxidized is termed the SOA yield, and VOCs with higher SOA yields are more likely to produce higher amounts of SOA. Only one measure of SOA yield from  $\beta$ -phellandrene is available. Surratt et al.<sup>153</sup> generated OH-initiated SOA from a  $\beta$ -phellandrene/limonene mixture (in the presence of  $\text{NO}_x$ ) and using an acidic  $\text{MgSO}_4/\text{H}_2\text{SO}_4$  seed aerosol. The average SOA volume produced from  $\sim 100$  ppb of a 40/60 mixture of  $\beta$ -phellandrene/limonene was  $169 \mu\text{m}^3/\text{cm}^3$ . The average SOA volume produced from 86 ppb limonene under similar conditions was  $186 \mu\text{m}^3/\text{cm}^3$ . SOA yields depend on  $\text{NO}_x$  concentrations, and the sampling sites may have lower  $\text{NO}_x$  concentrations than the  $\text{NO}_x$  concentrations used by Surratt et al. If the SOA yields from individual monoterpenes are additive in a mixture, this indicates that the OH-initiated SOA yield from  $\beta$ -phellandrene is significant. The relative yield is slightly less than the yield from limonene under similar conditions but greater than  $\alpha$ -pinene and  $\beta$ -pinene. Thus, we might expect the SOA yields to increase when bark beetle infestations occur, especially since we saw an overall increase in VOC concentration due to infestation.

For Engelmann spruce, the emissions from infested trees are higher in concentration of 3-carene,  $\alpha$ -pinene, and  $\beta$ -pinene. Increase in 3-carene,  $\alpha$ -pinene, and  $\beta$ -pinene emissions from the infested spruce trees is by  $12.8 \text{ ng L}^{-1}$ ,  $6.1 \text{ ng L}^{-1}$ , and  $3.8 \text{ ng L}^{-1}$  respectively (Table 2.8). The increased concentrations of these species will lead to increase in regional SOA concentrations. The SOA yields for 3-carene,  $\alpha$ -pinene, and  $\beta$ -pinene have been discussed in presence of  $\text{NO}_x$  and  $\text{O}_3$  by various groups.<sup>112,154,155</sup> All three compounds have potential to form SOA, and hence can lead to increase in amount of regional SOA concentrations.

## 2.4 Conclusions

From this work, we can observe that the total VOCs emitted from the trunks of bark beetle infested trees were higher than the total VOCs emitted from the trunks of healthy, non-infested lodgepole pine and Engelmann spruce trees. The emissions for the dominant monoterpene,  $\beta$ -phellandrene, emitted from infested lodgepole pine trees increased by a factor of thirty.  $\beta$ -phellandrene reacts with oxidants on an atmospherically-relevant time scale and forms SOA with significant yields, higher SOA concentrations due to bark beetle infestation may occur. Similarly, Engelmann spruce trees emit increased quantities of 3-carene (more than fifty fold increase),  $\alpha$ -pinene (approximately four-fold increase), and  $\beta$ -pinene (approximately fifteen-fold increase), which are known to contribute towards SOA formation. Hence it is reasonable to assume that the bark beetle infestation in Western United States has led to higher monoterpene concentrations and also higher SOA concentrations and yields. The higher SOA concentration and yields impacts the background particulate matter concentrations, deleterious health effects due to increased particulate matter concentrations, and may impact radiative forcing in the atmosphere.



## CHAPTER 3

### SOA FORMATION AND SPECIATION STUDIES FOR LIMONENE, LIMONENE VOC MIXTURES AND LIMONENE BASED AIR FRESHENER

#### 3.1 Introduction

As mentioned in Chapter 2, monoterpenes are estimated to account for 11% of the 1150 Tg C annual natural organic compound emissions on a global basis.<sup>39</sup> In the United States, more of than half of monoterpene emissions which come from conifers and crops are composed of  $\alpha$ -pinene,  $\beta$ -pinene, and limonene.<sup>118,156</sup> Studies by Millet et al.<sup>157</sup> on primary organic carbon and elemental carbon show that SOA may range from 20 to 70% of total organic aerosol depending upon the season and location in the United States. Globally, Tsigaridis and Kakakidou<sup>51</sup> suggested that BVOCs dominate AVOCs in the production of SOA. The limonene concentration may be as high as 5% by mass in some areas, but it may account for more than 20% of the terpene SOA depending on vegetative species distribution.<sup>50,158</sup>

Limonene is present in the indoor environment due to its use in series of consumer products. Limonene is present in large amount in peels of citrus fruits,<sup>159</sup> air fresheners, household cleaning agents,<sup>58</sup> wood surface furnishings, and waxes.<sup>31</sup> Limonene is also present in pine needle oils and turpentine.<sup>57</sup> These limonene containing products can react with ozone present indoors to generate SOA.<sup>64</sup> Indoor limonene concentrations, largely due to use of surface cleaning and treatment reagents, have been reported to exceed 80 ppb.<sup>160,161</sup> From the studies above we can conclude that limonene is important SOA precursor not only outdoors and but also indoors.

The presence of limonene in both the indoor and outdoor atmospheres in significant concentrations is driving force for interest of scientific community to study the SOA generation

process via limonene oxidation. In next section we summarize the studies which use ozone as the oxidant for SOA formation.

### 3.1.1 SOA generation from limonene ozonolysis

Many studies have been done to investigate SOA yields by hydroxyl radical (OH) oxidation of limonene in presence of NO<sub>x</sub><sup>112,113,162,163</sup> However, given that the focus of this chapter is SOA from limonene ozonolysis, these studies are not discussed in this chapter.

Limonene is a monoterpene containing two carbon-carbon double bonds, one endocyclic bond and one exocyclic bond, and it has higher potential to form SOA than  $\alpha$ -pinene. Leungsakul et al.<sup>164</sup> have reported SOA yields (i.e., the mass of particulate matter generated relative to the mass of limonene oxidized) from reaction between limonene and ozone, and the yields were found to vary between 0.43 to 0.94 depending upon the concentration of limonene and ozone. The authors report the product generation mechanistic in details which are discussed in later section. Zhang et al.<sup>101</sup> investigated the effect of NO<sub>x</sub>, and UV light on SOA generation of limonene from ozonolysis. Limonene was found to generate higher SOA yields than  $\alpha$ -pinene + ozone reactions under similar conditions. The authors report that in presence of ozone (zero/low NO<sub>x</sub> conditions), oxidation occurs at the endocyclic carbon-carbon double bond first, followed by oxidation at the exocyclic double bond. The initial step, ozone reaction at the endocyclic carbon-carbon double bond, is the rate-limiting step. In the presence of ozone and NO<sub>x</sub> the oxidation of exocyclic double bond in limonene dominates. The chemistry of oxidation involving exocyclic double bond reaction is slower when compared to reaction of the oxidant and endocyclic double bonds. Though slower chemistry is observed, reaction across either double bond present in limonene generates products with low volatility.

Saathoff et al.<sup>92</sup> investigated effect of humidity on limonene-ozone SOA yields. The authors report SOA yields and parameters for two product model<sup>78</sup>, for temperatures ranging from 253-313 K. The authors also studied variability of the RH on SOA yield, and for this temperature range, the SOA yields were found to increase with decreasing temperature. Chen and Hopke<sup>165</sup> reported SOA yields and parameters for one-product model for SOA generated from ozonolysis limonene. The experiments were carried out at conditions relevant to indoor environment in terms of temperature, air exchange rate, and reactant concentrations. The SOA yields generated by R-(+)-limonene and S-(-)-limonene were similar. In the experiments performed in this chapter, the R-(+)-limonene isomer is used as the VOC.

### 3.1.2 Chemical speciation for SOA ozonolysis products from limonene

A mechanism on ozonolysis of  $\alpha$ -pinene is shown in Chapter 1 (Figure 1.2). A similar mechanism is followed for the ozonolysis for limonene at the endocyclic carbon-carbon double bond. The ozone is added across the endocyclic double bond to form ozonide, which decomposes forming a reactive biradical, called Criegee intermediate, which undergoes various reactions and decomposes to generate the various SOA products. The chemical identities of the SOA products are difficult to predict from the reaction mechanism alone, because the composition of the products is affected by the reaction conditions and not all of the products are known. Several groups have reported speciation studies of limonene ozonolysis, and these are discussed below.

Some of the early work on the SOA products generated by ozonolysis of limonene was done by Grosjean et al.<sup>166</sup>. The authors report the identification of formaldehyde and 4-acetyl-1-methylcyclohexene (limona ketone) as ozonolysis products of limonene. The carbonyl reaction products were identified a 2,4-dinitrophenyl hydrazones by sampling the chamber air

with C18-cartridges coated with 2,4-dinitrophenylhydrazine as derivatizing agent. The products were identified using high performance liquid chromatography (HPLC)-UV, at an absorbance wavelength of 360 nm. The product 4-acetyl-1-methylcyclohexene can undergo further reaction. The authors report a generalized mechanism for formation of C<sub>9</sub> and C<sub>10</sub> polyfunctional oxygenates formed from the reactions of biradicals. The formaldehyde yield indicates that at least 10% of time the exocyclic double bond reacts with ozone under these experimental conditions.

Calogirou et al.<sup>167</sup> reviewed the earlier efforts in field of the SOA product analysis using all three oxidants OH, NO<sub>3</sub> and O<sub>3</sub>. The reaction between an alkene and O<sub>3</sub> is highly exothermic and electrophilic addition of ozone across C=C depends on number and nature of substituents at the C=C bond. The terminal bonds are less susceptible to ozonolysis as compared to cyclic double bonds, presence of electron-withdrawing groups in vicinity of the C=C are also not favorable for ozonolysis.

Glasius et al.<sup>83</sup> investigated product formation from ozonolysis of five different terpenes:  $\alpha$ -pinene,  $\beta$ -pinene, 3-carene, sabinene, and limonene. The products were characterized using GC/MS and HPLC/MS. Four classes of products were identified: carboxylic acid, dicarboxylic acid, oxocarboxylic acids, and hydroxyketocarboxylic acids. For limonene the major products identified include limonic acid, limononic acid, and isomers of 7-hydroxy limononic acid.

Around same time, Koch et al.<sup>87</sup> reported formation of new particles in ozonolysis reactions of limonene and four other terpenes. The authors found that upon ozonolysis of limonene, the major product formed is a C<sub>9</sub> dicarboxylic acid i.e. limonic acid.

Larsen et al.<sup>168</sup> investigated the gas-phase oxidation of limonene in presence of OH radicals, the concentration for gas phase and condensed phase products are identified and quantified using

HPLC/MS and GC/MS. The authors report limonaldehyde (gas phase) and ketolimaldehyde (condensed phase) as the major products. The other products identified include hydroxy limononic acids, which were most concentrated, with minor concentrations of limononic acid, limonic acid, ketolimononic acid, and norlimonic acid.

Leungsakul et al.<sup>164</sup> developed a reaction mechanism for predicting the SOA formation from the reaction of limonene with ozone. The model provides comprehensive kinetic mechanisms for ozonolysis of limonene and the model was developed based on the data collected from the smog chambers and identified using GC/MS. The SOA products are dominated by limonaldehyde, followed by limonaketone, ketolimaldehyde, limononic acid, and ketolimononic acid.

Jaoui et al.<sup>169</sup> performed an extensive chamber study for the identification of products in SOA generated from photooxidation of limonene in presence of NO<sub>x</sub>. The method used different derivatization methods to distinguish between the products which predominantly contain one or more of -OH, -COOH, -CHO, and >CO groups. The products were identified using GC/MS (Gas chromatography/Mass spectrometry) in EI (Electroionization) and methane-CI (Chemical ionization mode), and a total of 28 of 103 peaks were identified and structure was assigned. The products identified from the chamber studies were then used to identify limonene-SOA products in field samples. The analysis field sample showed presence of 21 of the limonene-SOA products, indicating that limonene SOA is significantly present in the atmosphere. The authors also report 3-carboxyheptanedioic acid and an unknown compound unique to limonene-NO<sub>x</sub> SOA (the earlier work from same research group did not show these compounds in SOA generated from  $\alpha$ -pinene and  $\beta$ -pinene) and hence these compounds can be used as tracer for limonene.

Most of the oxidation products identified from the above work are between mass ranges of 138-202 m/z. Walser et al.<sup>170</sup> observed higher molecular weight components in SOA from limonene ozonolysis using high resolution electrospray ionization mass spectrometry. The authors suggested the reaction mechanisms for the first generation of SOA molecular compounds includes isomerization and addition reactions of carbonyl oxide intermediates generated during ozonolysis of limonene. The authors also found evidence for isomerization reactions which yield numerous products with progressively increasing number of alcohol and carbonyl groups. The authors also reported formation of smaller molecules by C-C bond scission in alkoxy radicals. These mechanisms for generation of higher and lower molecular weight compounds were disregarded in previous studies.

High molecular weight SOA products can also be formed by reaction of low molecular weight neutral molecules with Criegee intermediates and hydroperoxides.<sup>171,172</sup> Bateman et al.<sup>173</sup> suggested the importance of Criegee and hemi-acetal reaction pathways for formation of high molecular weight SOA compounds in limonene ozonolysis.

Kundu et al. (2012, ACPD) used Fourier transform ion cyclotron resonance (FT-ICR) mass spectrometry for determining molecular composition of SOA products from limonene ozonolysis. The authors observed both high molecular weight products and low molecular weight products. The high molecular weight products generated are predominantly formed via hydroperoxide, Criegee, and hemi-acetal reaction pathways rather than aldol condensation and esterification processes. The generation of small molecules takes place via elimination reactions for Criegee radicals, reactions between alkoxy and peroxy radicals, and scission of alkoxy radicals resulting from the Criegee radicals.

### 3.1.3 SOA generation and product analysis from monoterpene mixtures

Although a number of experiments have been performed on SOA generation from limonene and cleaning products (mentioned in section below), only a couple of papers have been published for SOA generation from monoterpene mixtures. Li et al.<sup>174</sup> merged separate kinetic models for oxidation models of limonene and  $\alpha$ -pinene reactions and closely simulated the formation and timing for SOA mass concentrations in an outdoor smog chamber. The results showed that SOA yields from the reaction are dependent on initial  $\alpha$ -pinene/limonene ratios.

Warring et al.<sup>175</sup> investigated SOA formation from ozone reactions with both single terpenoids and mixtures of limonene,  $\alpha$ -pinene, and  $\alpha$ -terpineol. Experiments were conducted at two levels of initial ozone concentrations: 25 ppb and 100 ppb. At ozone concentrations of 100 ppb, the SOA generated from single terpenoids and mixtures follows a linear trend as a function of the initial rate of reaction. The particle number concentrations, at the higher level of ozone, reported in following order: mixture of limonene/ $\alpha$ -pinene/ $\alpha$ -terpineol > limonene/ $\alpha$ -terpineol >  $\alpha$ -terpineol > limonene. This was expected as the mixtures contained reactive VOC concentrations higher than the individual terpenes. At lower ozone concentrations (25 ppb), particle number concentrations decreased in the following order: limonene > limonene/ $\alpha$ -pinene/ $\alpha$ -terpineol >  $\alpha$ -pinene/ $\alpha$ -terpineol > limonene/ $\alpha$ -terpineol >  $\alpha$ -pinene >  $\alpha$ -terpineol. This data show that at ozone-limiting concentrations, the nucleation potential of d-limonene is higher as individual and upon addition of other terpenoids the nucleation potential is reduced. A similar trend is not observed for higher ozone concentrations (100 ppb). The authors explain large observed nucleation event may be due to formation of secondary ozonides at ozone-limiting concentrations as observed by Nøjgaard et al.<sup>176</sup>. These observations imply that the nucleation and mass formation potential of products may not be related.

To our knowledge no other work on ozonolysis of limonene containing non-commercial mixtures has been carried out. Jaoui et al.<sup>177</sup> investigated mixture of  $\alpha$ -pinene and  $\beta$ -pinene for products formed this work will be discussed in Chapter 4.

**The goal of this chapter is to study SOA yields and speciation of condensed phase SOA products generated by ozonolysis from limonene and limonene containing VOC mixtures and compare the findings to commercially available limonene-based air freshener. We use an additive approach to make VOC mixtures in same VOC ratios as present in the air freshener. We investigate the condensed phase SOA products generated during ozonolysis of VOC precursors, the speciation studies will help in understanding volatility distribution of products.**

### **3.1.4 Ozonolysis of limonene and limonene based commercial products in indoor environment**

As mentioned earlier, limonene can be present in the indoor environment due to various sources. A typical concentration of limonene in indoor environment is around 80 ppb and has been reported to increase to 175 ppb after applying spray wax to coffee table for a period of 15 s.<sup>161</sup> The indoor ozone concentration can be around 20-70% of outdoor ozone concentration Weschler,<sup>64</sup> and can be emitted by photocopiers, printers, and some ozone-based air purifiers.<sup>27</sup> Particle generation by limonene-ozone reaction in indoor environment been reported by Weschler and Shields<sup>63</sup>. Particles generated were monitored in size range of 0.1-0.2  $\mu\text{m}$ , the experiments were performed in office set-up. The authors found that when limonene and ozone were added to the office set up, new particle formation was observed. The particle concentration was 20 times higher in comparison to a control office set up. In another set of experiments, only



limonene introduction to an office (no added ozone) yielded 10 times the particle concentration as compared to the control office. This implies that ozone may be present in indoor environment due to exchange with outside air. These studies indicated that limonene-ozone reactions are important source of particle formation. Weschler and Shields<sup>178</sup> have reported that the indoor particle sizes formed from reaction of limonene with ozone decrease with increasing air exchange rates, and the maximum particle count is reached in quicker times.

Wainman et al.<sup>179</sup> conducted chamber experiments for limonene-ozone reactions and found increase in formation of particles between ranges of 0.1-0.2  $\mu\text{m}$  and 0.2-0.3  $\mu\text{m}$  with addition of ozone. The results of this study show that secondary particles between 0.2-0.3  $\mu\text{m}$  are formed from reaction of primary particles of 0.1-0.2  $\mu\text{m}$  and ozone. Rohr et al.<sup>180</sup> conducted chamber studies for particle generation from limonene-ozone reactions. The authors compared the particle formation with respect to air exchange rates in a chamber, the particle formation was found to be much faster than air exchange rates. The precursors studied were isoprene,  $\alpha$ -pinene, and limonene. The authors reported that isoprene ozonolysis generated a smaller concentration of particles as compared to  $\alpha$ -pinene and limonene.

Sarwar and Corsi<sup>181</sup> conducted experiments to investigate the secondary particle formation resulting from limonene/ozone reactions. The experiments also included an indoor quality model to predict the dynamic particle mass concentrations based on homogeneous chemical mechanisms and partitioning of semivolatile products to particles. The predicted particle mass concentrations were approximately within 25% of experimental results, once steady-state conditions were reached. The authors reported that lowering of air exchange rates with outdoor air increase particle mass concentrations and size particles are formed. The computational results also implied that particle concentration in indoor air can increased with higher outdoor ozone

concentrations, higher outdoor particle concentrations, higher indoor limonene emission rates, and lower indoor temperatures.

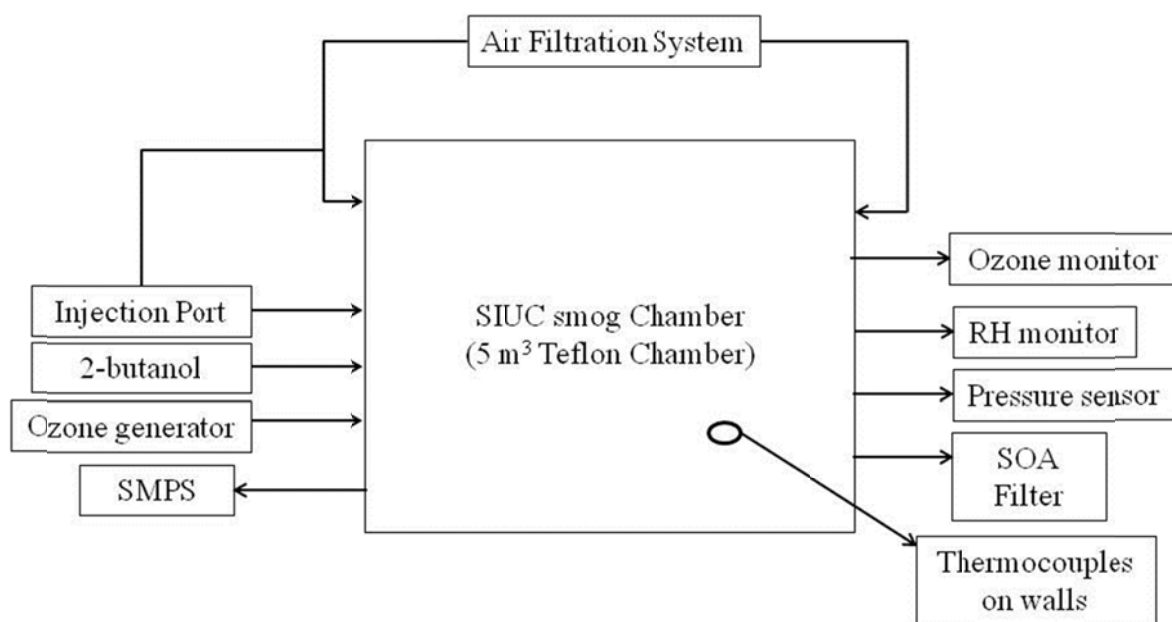
As mentioned earlier in Chapter 1, Singer et al.<sup>58</sup> reported emission of terpenoids, limonene,  $\alpha$ -terpinene, terpinolene, and  $\alpha$ -terpineol along with chemical species like formaldehyde, 2-butoxyethanol, and glycol ethers from use of pinene based oil degreaser. During air freshener use, the authors found emission of limonene, dihydromyrcenol, linalool, linalyl acetate, and  $\beta$ -citronellol. The experiments were done in the chamber which mimics indoor environment, and also included plywood floor and wooden furniture to provide surface for application of cleaners. Singer et al.<sup>27</sup> reported SOA formation from using a pine-oil based cleaner, an orange oil-based degreaser, and a plug-in scented oil air freshener in presence of ozone. The authors found the application of each product to surfaces resulted in ozone consumption along with formation of SOA and hydroxyl radicals (product of reaction between monoterpenes and ozone). The SOA and hydroxyl radicals formed lasted in the indoor environment for period of 10-12 hours. The reactions increased indoor concentration of formaldehyde by 10 ppb. The authors also reported that the ozone consumption by the air freshener was lower as compared to the pine oil based cleaner and orange oil based degreaser. The reaction rate of sorbed air freshener and ozone was similar in magnitude as homogeneous reaction between the air freshener and ozone. In this work, the SOA formation is reported for limonene based liquid air freshener in presence of ozone.

### 3.2 Experimental details

The general procedure for generation of SOA and identification of SOA products began with cleaning the smog chamber so the particle number concentration is less than  $1.0 \text{ cm}^{-3}$ . Instruments for monitoring ozone concentration, particle size and concentrations, internal

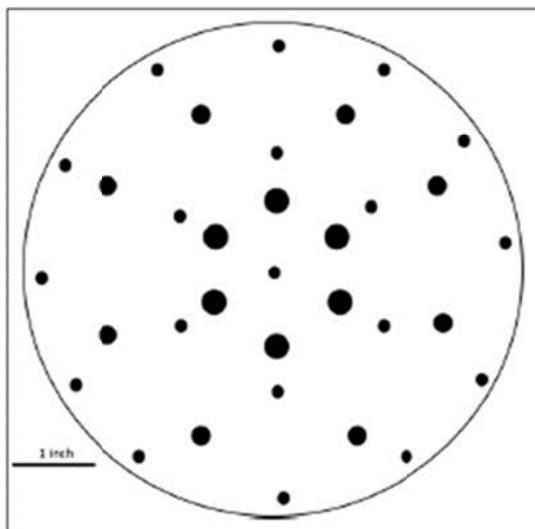
pressure of the chamber, temperature, and RH were used. A radical scavenger, 2-butanol, was introduced in the chamber. Ozone was added to the smog chamber and allowed to mix with chamber air until the concentration the stabilized. A blank filter was sampled after stabilization of ozone. In separate experiments, the VOC, VOC mixture, or air freshener was injected in the chamber to initiation SOA and particle formation. A filter sample was collected 300±30 min after injection of the precursor. Each of the steps is described in detail in the following sections. The laboratory set-up for SOA generation has been previously discussed in detail.<sup>74,182</sup>

### 3.2.1 SIUC smog chamber



**Figure 3.1** Experimental set up for SOA generation

The smog chamber set up has been previously described in detail.<sup>74</sup> Figure 3.1 schematically represents the SIUC chamber. SOA was generated in conducted in a 5.5 m<sup>3</sup> Teflon® polytetrafluoroethylene 200 LP (2.5 m x 1.3 m x 1.7 m, thickness 50 µm) smog chamber (Welch Fluorocarbon). The surface area to volume ratio for this chamber is 3.5 m<sup>-1</sup>.



**Figure 3.2** PTFE access port (6 inches diameter). The big circles have diameter of 3/8 inches and the medium circles have a diameter of 1/4 inches; the smallest circles are the screws.

The chamber was suspended from the ceiling using trolleys supported on a Unistrut metal framing, and the trolleys allowed for lateral movement of chamber enabling expansion and contraction. The bottom part of smog chamber rested on top of the table. The chamber had a large access port in the bottom of side wall (approx. 13 inches) allowing rapid emptying of filled chamber while cleaning the chamber and also provided access to the interior of the chamber. Two opposite walls of chambers had polytetrafluoroethylene (PTFE) access ports manufactured by the SIU Central Research Shop.

The PTFE ports (Figure 3.2) were installed so the wall of the chamber was sandwiched between the two discs of the port. The discs were held together by Teflon-coated eighteen screws. The PTFE discs had fourteen pre-drilled holes for tubing, six holes were 3/8" and eight

holes were 1/4" in diameter. The PTFE plates were held in place using hollow metal rods screwed to the outside PTFE discs. The corners of the chamber were reinforced, to avoid tearing, using polyimide Kapton film tape (McMaster-Carr). During all the experiments, the chamber was covered with black out fabric, which reduces light and therefore photo-oxidization reactions during experiments.

Air for the chamber was provided by two in-house purified air lines. The air was connected to smog chamber using Teflon® tubing (outer diameter 3/8") and through the PTFE port. The house air was used for cleaning the chamber and volatilization of VOC precursors in the chamber. The air was purified using three filters. First, a carbon filter (Whatman) reduced the concentration of organics in the air. Second, a silica gel desiccant (Drierite) filter (Fisher) reduced the water vapor concentration in the air lines. Third, a high-efficiency particulate air filter (TSI) removed particles from the house air. Thus, the house air was purified for organics, moisture, and particulates. Each air line introduced the air, on opposite sides of the chamber, with flow rate of approximately 20 L min<sup>-1</sup>.

### **3.2.2 Monitoring physical parameters of the smog chamber**

Physical parameters such as temperature, pressure and relative humidity have an impact on the amount of SOA formed and hence require monitoring. The internal pressure of the chamber was measured by an Omega pressure sensor, and this sensor recorded internal pressure of the chamber every five seconds. The sensor was connected to the chamber through a 1/4" NPT fitting, using a hole in the PTFE port. To calibrate the pressure sensor, a built-in calibration wizard in the Omega engineering OM-CP data logging software (version 2.00.70) was used. For calibration to be performed, the average experimental pressure value was obtained by recording

the outdoor pressure for one hour. The experimental average was then entered in the software along with pressure value obtained from National Weather Service (NWS, the values are obtained by NWS at Southern Illinois airport and can be obtained from [www.nws.noaa.gov](http://www.nws.noaa.gov)). The offset or gain was calculated by the calibration wizard, thus calibrating the instrument. The pressure sensor was set-up and initially calibrated by undergraduate researcher, Aaron Brown. The pressure data were saved to the computer using Omega Engineering OM-CP data logging software.

The external temperature of the chamber was continuously monitored by three type K thermocouples and a digital thermometer (Omega, part# SA1-K). Two thermocouples are placed on the sides of the chamber and one thermo couple is placed on bottom of the chamber. The digital thermometer was placed near the chamber but was not attached to any of the walls of the chambers. The temperature probes were calibrated by comparison with room temperature recorded by digital thermometer. The thermocouples were connected to data logging software using a high-speed USB carrier (National Instruments, part # 192558C-01). The data from the thermocouples and ozone monitor were monitored and recorded using a LabVIEW (student edition version 8.5) program, which was developed in our lab by undergraduate researcher John Junge.

The relative humidity of the chamber was measured using a HUMICAP® probe (Vaisala) that was interfaced to a humidity meter (Vaisala Model MI70). The data logging for humidity and temperature data was done using MI70 Link software (version 1.10). The flow to the probe was generated using house vacuum, controlled by a flow meter (Omega) at  $0.3 \text{ L min}^{-1}$ . The other end of the humidity sensor was attached to the smog chamber using a 3/8" hole on the PTFE port. The calibration of the humidity meter was checked using saturated aqueous solutions of salts:

NaCl, MgCl<sub>2</sub>, LiCl, and KCl. A few grams of each salt was placed at bottom of an amber vial leaving enough head space for the probe. The salt was then wetted with distilled water, and the RH and temperature values are then monitored for thirty minutes. The measured values were similar to standard values for saturated salts solutions. The initial calibration for the humidity meter was performed by undergraduate researcher Aaron Brown.

### **3.2.3 Ozone monitoring instrument**

The ozone concentration was monitored using a Teledyne API (Model # 450) continuous ozone analyzer. The concentration is recorded for 5 second intervals. As mentioned above, the data from this instrument are recorded by using in-house, LabVIEW program. The operation of this instrument is based on Beer-Lambert law, and the ratio of intensity of transmitted light between a sample air cell to the cell containing ozone scrubbed gas is used calculate ozone concentration. The instrument samples air from inside the smog chamber (access from PTFE port) at rate of 3.0 L min<sup>-1</sup>. The instrument has a mercury lamp which uses ultra-violet light at 254 nm to determine ozone concentration.

### **3.2.4 Scanning mobility particle sizer**

A scanning mobility particle sizer (SMPS) (TSI, Model# 3936) was used to monitor the size and number distribution of suspended particles in the chamber. The SMPS comprises of a long dynamic mobility analyzer (DMA, 3080) and a condensation particle counter (CPC, 3010). As the particles enter the DMA, they pass through a Krypton-85 charger/neutralizer (TSI, Model #3077) and gain a bipolar charge distribution. The particles are separated according to their electrical mobility, which directly relates to particle diameter, by voltage applied to DMA. After

the particles are separated on the basis of diameter, the particles are counted by the CPC. As the particles pass into the CPC, 1-butanol condenses onto them, making particles large enough to be counted optically. The particle diameter and particle number concentration from the SMPS is recorded using Aerosol Instrument Manager (AIM) software (ver. 8.0.0.0). The DMA sheath flow rate and aerosol flow rate were set to of  $3.00 \text{ L min}^{-1}$  and  $1.00 \text{ L min}^{-1}$ , respectively, and the particles diameters that were sampled ranged from 13.8 nm to 749.9 nm. The mass concentration was calculated from the particles number concentration in each diameter bin, assuming the particles were spherical and had an average density of  $1 \text{ g cm}^{-3}$ .

### 3.2.5 Hydroxyl radical scavenger

The ozonolysis of the monoterpenes which contain carbon-carbon double bond proceeds via the formation of an ozone-alkene adduct, called the primary ozonide. The primary ozonide then decomposes to form a Criegee biradical which, upon isomerization to the vinyl hydroperoxide and then further decomposition, yields the hydroxyl radical (OH). The hydroxyl radicals may react with the secondary ozonolysis products or the VOCs (i.e., limonene) which would affect the SOA yields and the composition of final ozonolysis products formed. While hydroxyl radical reactions are important in the atmosphere during photooxidation (i.e. daytime), in our experiments, we focus on ozone oxidation (i.e., indoor but also nighttime chemistry) and therefore limit hydroxyl radical reactions. In the experiments mentioned herein, 2-butanol was used as hydroxyl radical scavenger. 2-butanol kinetically competes with other VOCs for the hydroxyl radical produced by ozonolysis of monoterpenes. For all the SOA generation experiments mentioned in this chapter, a pre-calculated volume of 2-butanol (250  $\mu\text{L}$  or 750  $\mu\text{L}$ ) is volatilized in the smog chamber by placing it in an Erlenmeyer flask with side arm. An air line



was attached to the side arm and a glass tube attached on sealed top of the flask carried 2-butanol vapors to the smog chamber. The volume of 2-butanol was varied so greater than 85% of maximum possible hydroxyl radical generated would be consumed.<sup>184</sup>

### **3.2.6 Ozone generation system**

Ozone was used as the oxidant for SOA generation in all experiments. Ozone was generated from ultra-high purity oxygen (99.999%) (Airgas, Mid-America) using a corona discharge ozone generator (Azco Industries, HTU-500 AC). Ozone concentrations were approximately 500 ppb for most of the experiments. For increased amounts of VOC concentration in reactive precursors, experiments were carried out at higher ozone concentrations (up to 1700 ppb). For all experiments, the ratio of ozone to VOC was greater than 2:1 and no more than 5:1.

### **3.2.7 Injection of VOC in the chamber**

The VOCs were injected in the chamber via volatilization using a custom built injection port. The injection port was assembled by using Swagelok compression fittings and 1/4" O.D. stainless steel tubing, coated with Siltek®/Sulfinert® (Restek P/N 22509) which reduces VOC losses. A stainless steel Swagelok tee (Part # SS-400-3) was fitted to opposite ends of the Siltek® tubing. The two air lines were attached to the injection port with help of another Swagelok tee and two Swagelok reducing unions (part # SS-400-1-6RT). The precursors were injected and volatilized by air flow into the chamber via a third tee joint. This tee joint had a 9 mm ice blue septum (Restek), is held in place by a cap and back ferrule. Hamilton microliter syringes were used for injection of VOC precursors. To facilitate the volatilization of VOCs, the injection port tee was heated with heating tape set at approximately 50 °C.

### 3.2.8 Collection of SOA filters for speciation studies

A portion of the SOA that is generated from the ozonolysis of VOCs condenses to form particulate matter with a complex chemical composition. Filter samples of the particulate matter were collected during each ozonolysis experiment so that the composition of the particulate matter, and hence the condensed phase portion of the SOA, could be analyzed offline. For each experiment, two filter samples were collected. A blank filter was collected prior to injection of the VOCs in the chamber, and a second filter was collected  $300 \pm 30$  min after the injection of VOC. Pallflex Tissuquartz filters (VWR, 47 mm diameter) were used to collect the SOA, and these filters were housed in a Gelman stainless steel filter holder. Prior to each experiment, the filters were heated to  $185\text{ }^{\circ}\text{C}$ , for 4-8 hours, to remove any volatile contaminants, if present. The SOA species were collected on the filter at a flow rate of  $40 \pm 1\text{ L min}^{-1}$  (Gast, part # 0823-1010-SG608X), monitored using an Omega flow meter (FL-2017). The flow was supplied for 30-60 min, so at least  $100\text{ }\mu\text{g}$  of SOA was collected on each filter. Aluminum foil was used to store the filters. After sample collection, the filters were stored in air tight containers, at temperature of  $-18\text{ }^{\circ}\text{C}$ , until they were procured for solvent extraction.

### 3.2.9 Solvent extraction of SOA filter samples

Particulate matter on filters was analyzed by extracting the material with solvent and analyzing by GCMS. Prior to extraction, the amount of PM collected on filters was calculated using mass concentration data from the SMPS. The amount of PM collected on the filter varies around  $100 \pm 30\text{ }\mu\text{g}$ . The filters were then spiked with a deuterated standard mixture includes n-pentadecane d-32, myristic acid (methyl d-3), palmitic acid d-31, n-eicosane d-42, and n-tetracosane d-50 (Cambridge Isotope Labs).<sup>185,186</sup>  $10\text{ }\mu\text{g}$  of each deuterated standard was spiked

on the filter. After spiking with deuterated standards, the filter samples were transferred to a 30 mL, glass centrifuge tube 10 mL of the extraction solvent [dichloromethane: acetone: hexanes (2:3:5) (v/v)] was added to each tube using a tilt pipette. The tubes were then sonicated at 30 °C for 15 min. The supernatant was collected in a different test tube. The extraction process was repeated twice, and the supernatant fractions were combined (30 mL). The supernatant contained fibrils from the filter paper, and these were removed by settling. The supernatant containing SOA products was transferred to a 250 mL round bottom flask, taking care that none of the residual fibrils are transferred. The sedimentation method is different from the previously described filtration method by Huff Hartz et al.<sup>186</sup>, which used 0.45 µm PTFE membrane filters. The average percent recovery for standards (listed in Table 3.1), was 96% when the sedimentation method is used. The average percent recovery for the same standards upon use of filtration method was 68%. Hence, to avoid loss of SOA products during filtration, the sedimentation method was preferred for removal of debris from the extracted solvent.

**Table 3.1** List of compounds used as surrogate standards for quantification of SOA products. Deuterated standards are used as internal standards and calculate % recovery for SOA products.

Standard	CAS #	Purity (%)	Manufacturer
Linear alkanes			
Pentadecane	629-62-9	99	Sigma-Aldrich
Hexadecane	544-76-3	99	Sigma-Aldrich
Octadecane	593-45-3	99	Sigma-Aldrich
Eicosane	112-95-8	99	Sigma-Aldrich
Tetracosane	646-31-1	99	Sigma-Aldrich
Carboxylic acids			
Cis-pinonic acid	61826-55-9	98	Sigma-Aldrich
Dodecanoic acid	143-07-7	98	Sigma-Aldrich
Sebacic acid	111-20-6	99	Sigma-Aldrich
Palmitic acid	57-10-3	99	Sigma-Aldrich
Dodecanedioic acid	693-23-2	99	Sigma-Aldrich
Deuterated standards			
Pentadecane(D-32)	36340-20-2	98	Cambridge Isotope Labs
Myristic acid(methyl-D3)	NA	98	Cambridge Isotope Labs
Eicosane(D-42)	62369-67-9	98	Cambridge Isotope Labs
Palmitic acid(D-31)	NA	98	Cambridge Isotope Labs
Tetracosane(D-50)	16416-32-3	98	Cambridge Isotope Labs

The extract in the round bottom flask was concentrated using a rotary evaporator (Yamato RE500) until the volume was reduced to 1 mL, and the concentrated extract was transferred to a GC/MS vial using a Pasteur pipette. The volume of the extract was further reduced to 400  $\mu$ L using a gentle stream of the nitrogen gas (grade 5.0, Airgas, further purified using a molecular sieve vapor trap Supelco product # 20618). 0.1 g of anhydrous sodium sulfate (Sigma Aldrich) was added to the vial to remove water from the extract, which improves the efficiency of the silylating reagent.

### 3.2.10 Silylation of SOA filter extracts

Immediately prior to GC/MS analysis, 100  $\mu\text{L}$  of the extract was transferred into a pre-cleaned, silanized polyspring vial inserts (National Scientific), and the insert was placed in a GC/MS vial. 125  $\mu\text{L}$  of N,O-bis(trimethylsilyl)trifluoroacetamide (BSTFA) in 1% trimethylchlorosilane (TMCS) (Thermo Pierce) was added followed by the addition of 15  $\mu\text{L}$  of pyridine catalyst (99%, ACS grade, ACROS). The vial was sealed using a polypropylene cap equipped with a PTFE/Silicon septum (National Scientific) and incubated at 65  $^{\circ}\text{C}$ , for 2 hours.

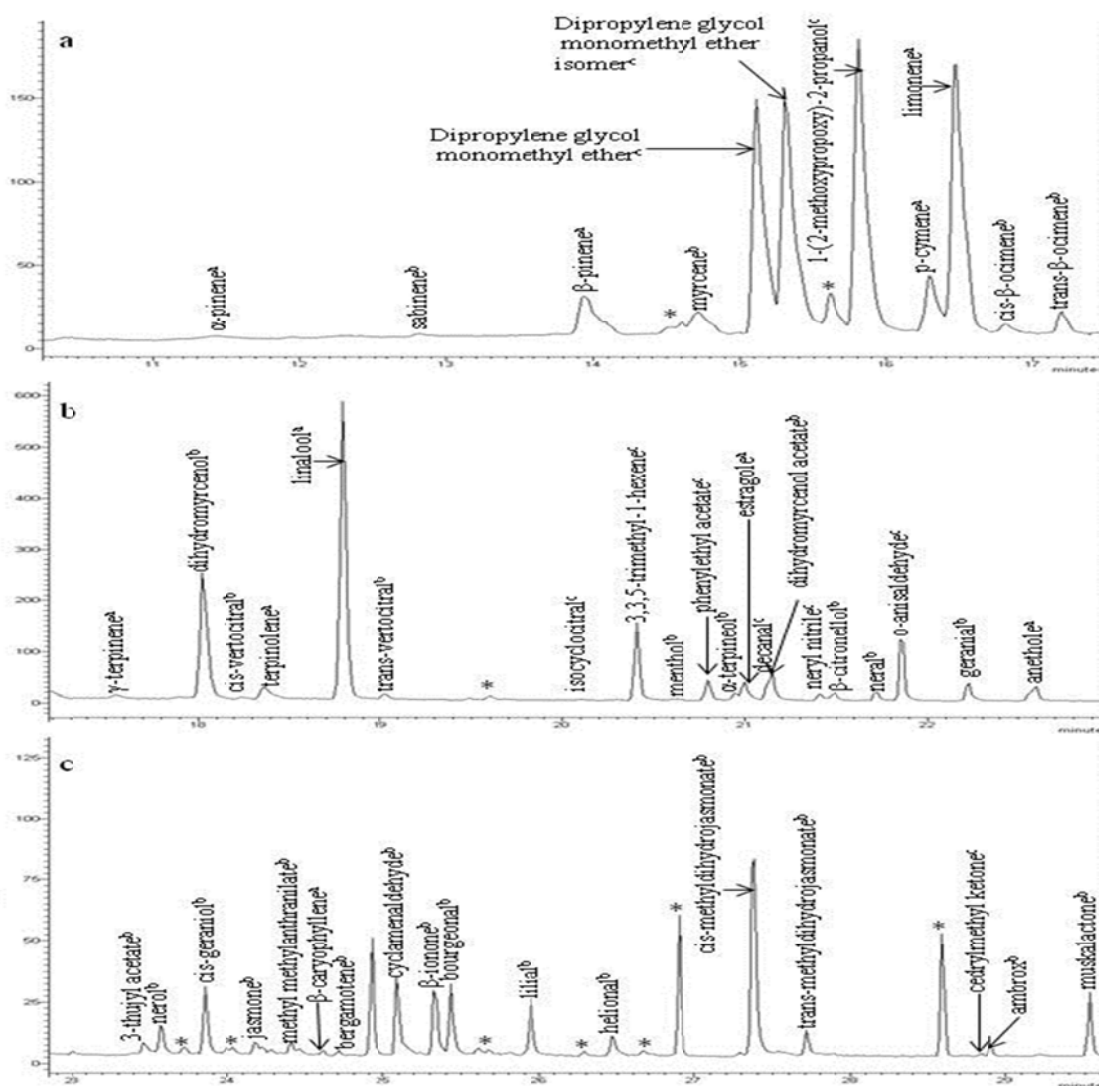
### 3.2.11 GC/MS analysis of SOA filter samples

SOA species extracted from the filters were analyzed using a Varian Saturn 2100 GC/MS, which was equipped with a 3900 gas chromatograph and 2100T ion trap mass spectrometer. The 2.0  $\mu\text{L}$  solution was injected using an autosampler (Varian, 8400) using a 10  $\mu\text{L}$  syringe (Hamilton), and the temperature of inlet was maintained at 250  $^{\circ}\text{C}$ . A constant flow rate of helium (Airgas, Mid-America, 99.999%) was maintained at 1.0 mL/min. Before entering the GC/MS, helium gas was stripped of any moisture, oxygen, or organics using GC/MS filter (Varian, CP17973). The autosampler was cooled to 10-12  $^{\circ}\text{C}$  using a water bath, cooling of autosampler prevents loss of semivolatile species between replicate injections. The separation column was 5% diphenyl/95% dimethylpolysiloxane capillary column (Varian FactorFour<sup>TM</sup>; 30 m x 0.25 mm x 0.25  $\mu\text{m}$ ), using a temperature gradient as follows: initial column temperature was held at 50  $^{\circ}\text{C}$  for 10 min, and ramped to 80  $^{\circ}\text{C}$  at a rate of 5  $^{\circ}\text{C min}^{-1}$ . A second temperature ramp of 10  $^{\circ}\text{C min}^{-1}$  was used to reach final temperature of 320  $^{\circ}\text{C}$ , with a final hold for 20 min, giving a total runtime of 59 min. The mass spectrometric data for the samples were obtained in electro ionization (EI) mode (70 eV) and by chemical ionization mode (CI) using acetonitrile as

CI reagent (CI-ACN). The temperature parameters for MS were trap temperature: 170 °C, manifold temperature: 40 °C, and transferline temperature: 320 °C. The MS was used for continuous monitoring for ions ranging from 40 to 650 m/z. The GCMS data were collected and processed using the Varian Workstation software (ver. 6.9).

### **3.2.12 Identification of VOCs in limonene based air freshener**

A 2.0 µL of 50 ppm solution of the limonene-based liquid air freshener and VOC standards were injected on the GC/MS. The instrumental conditions and temperature programming used are same as mentioned above (section 3.2.11). The MS was operated in EI mode only. The total ion chromatogram obtained from the limonene-based air freshener is shown in Figure 3.3. For components with low mass contents, like  $\alpha$ -pinene, the peak may not be distinguishable in total ion chromatogram, but can easily observed, identified, and quantified after extracting characteristic ions for the species (for example m/z 93, 121, and 136 for  $\alpha$ -pinene).



**Figure 3.3** Total ion chromatogram for limonene-based air freshener for retention times ranging from 10.3 min to 29.6 min. The chromatogram is split in three panes the first ranging from 10.3 min to 17.3 min (Figure 3.3a), the second ranging from 17.3 min to 22.8 min (Figure 3.3b), and the third ranging from 22.8 min to 29.6 min (Figure 3.3c). No peaks other than from the solvent were observed prior to 10.5 min., and some polysiloxane peaks due to the column elute after 29.6 min., and these are not shown.  $90 \pm 0.3$  % by mass of the components in the air freshener were identified. <sup>a</sup>Components were identified using retention time comparison with commercially available standard and mass spectral comparison to NIST library. <sup>b</sup>VOCs were identified by mass spectral comparison and confirmed using Adams retention indices. <sup>c</sup>The components are identified using probability based matching of mass spectra with NIST library. \*These peaks are either polysiloxane compounds or are present in the solvent chromatogram as well.

**Table 3.2** VOC standards used for calibration of amounts in limonene based air freshener

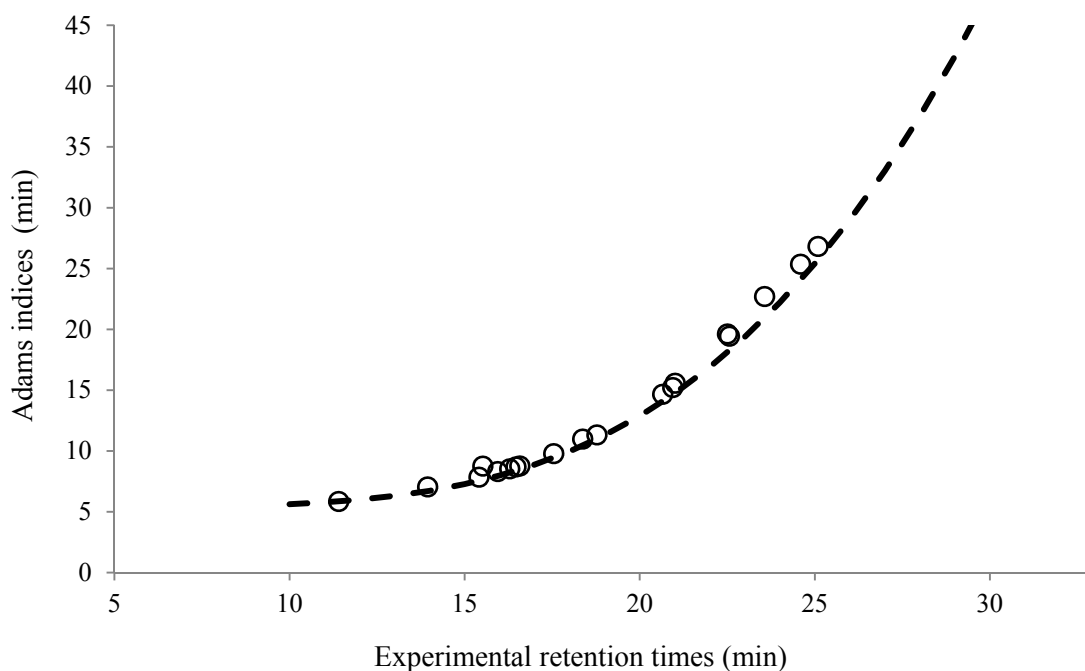
VOC Standard <sup>a</sup>	CAS #	Manufacturer	Density <sup>b</sup> (g cm <sup>-3</sup> )	Molecular Weight <sup>b</sup> (g mol <sup>-1</sup> )	Purity <sup>b</sup>
(1R)-(+)- $\alpha$ -pinene	7785-70-8	Aldrich	0.858 $\pm$ 0.005	136.23 $\pm$ 0.05	0.99 $\pm$ 0.05
(1S)-(+)- $\beta$ -pinene	18172-67-3	Aldrich	0.871 $\pm$ 0.005	136.23 $\pm$ 0.05	0.99 $\pm$ 0.05
eucalyptol	470-82-6	SAFC-Global	0.921 $\pm$ 0.005	154.25 $\pm$ 0.05	0.99 $\pm$ 0.05
$\alpha$ -terpinene	99-85-4	TCI-America	0.837 $\pm$ 0.005	136.23 $\pm$ 0.05	0.90 $\pm$ 0.005
$\alpha$ -phellandrene	99-83-2	SAFC-Global	0.85 $\pm$ 0.05	136.23 $\pm$ 0.05	0.995 $\pm$ 0.005
$\alpha$ -humulene	6753-98-6	Fluka	0.89 $\pm$ 0.05	204.36 $\pm$ 0.05	0.98 $\pm$ 0.05
$\gamma$ -terpinene	99-85-4	TCI-America	0.85 $\pm$ 0.05	136.23 $\pm$ 0.05	0.95 $\pm$ 0.05
eugeneol	97-53-0	Aldrich	1.067 $\pm$ 0.005	164.20 $\pm$ 0.05	0.99 $\pm$ 0.05
(R)-(+)-limonene	5989-27-5	Aldrich	0.843 $\pm$ 0.005	136.23 $\pm$ 0.05	0.985 $\pm$ 0.005
(-)-linalool	126-91-0	Aldrich	0.862 $\pm$ 0.005	154.25 $\pm$ 0.05	0.95 $\pm$ 0.05
(1S)-(+)-3-carene	498-15-7	Fluka	0.864 $\pm$ 0.005	136.23 $\pm$ 0.05	0.99 $\pm$ 0.005
terpinolene	586-62-9	Fluka	0.861 $\pm$ 0.005	136.23 $\pm$ 0.05	0.95 $\pm$ 0.05
p-cymene	498-15-7	Fluka	0.86 $\pm$ 0.05	134.22 $\pm$ 0.05	0.995 $\pm$ 0.005
(-)- $\beta$ -caryophyllene	87-44-5	Fluka	0.902 $\pm$ 0.005	204.351 $\pm$ 0.005	0.97 $\pm$ 0.05
(-)-bornyl acetate	5644-61-8	Acros	0.982 $\pm$ 0.005	196.28 $\pm$ 0.05	0.97 $\pm$ 0.05
$\alpha$ -terpineol	10482-56-1	SAFC-Global	0.93 $\pm$ 0.05	154.25 $\pm$ 0.05	0.96 $\pm$ 0.05
4-allylanisole	140-67-0	Fluka	0.965 $\pm$ 0.005	148.20 $\pm$ 0.05	0.985 $\pm$ 0.005
(+/-)-terpinen-4-ol	562-74-3	Acros	0.934 $\pm$ 0.005	154.25 $\pm$ 0.05	0.95 $\pm$ 0.05
anethole	4180-23-8	Fluka	0.988 $\pm$ 0.005	148.20 $\pm$ 0.05	0.995 $\pm$ 0.005
2-methylcyclohexanone	583-60-8	Acros	0.924 $\pm$ 0.005	112.17 $\pm$ 0.05	0.99 $\pm$ 0.05

<sup>a</sup>Some of the VOC standards were mixtures of enantiomers, however, separation of the enantiomers could not have been achieved on the achiral column used in this GC/MS. <sup>b</sup>The error is estimated on the number of significant digits provided by manufacturer.



The standards listed in Table 3.2 were used to identify some of the components of the air freshener (Table 3.3). The components present in the air fresheners include: linalool, limonene,  $\beta$ -pinene, p-cymene, estragole, anethole,  $\alpha$ -terpineol,  $\gamma$ -terpinene, terpinolene, and  $\alpha$ -pinene. The identification of components was done by matching the retention times and mass fragmentation patterns with standards. Additional confirmation was provided by using probability based matching to spectra in the NIST/EPA/NIH 2005 mass spectral database. The amount of each species in the air freshener was calculated using slope and intercept obtained for corresponding standard.

For components that lacked authentic standards, the Adams Index <sup>147</sup> was used for identification. Out of the 47 components identified, 32 were identified using retention indices in this library. Adams indices are retention times for VOCs, measured on a DB-5 column (5% phenyl, 95% methylpolysiloxane) which is the same as the column used in our method. Adams retention indices were obtained using different GC temperature programming. Hence, we do not expect a directly linear relationship. Instead, a best fit curve for Adams indices against the retention time values obtained by our temperature program using the authentic standards (Figure 3.4). From the equation of this best fitting line we calculated the Adams indices for compounds which did not have authentic standards available. The calculated Adams indices were used to identify unknown components. Additional identification was done by comparing the mass fragmentation patterns acquired experimentally to one in the NIST/EPA/NIH 2005 spectral database and digitized library for Adams Index.



**Figure 3.4** Best fit curve for Adams indices versus experimental retention times. The empty circles represent the standards. The dashed line represents the best fitting line, the equation of line is:  $y = 0.004x^3 - 0.101x^2 + 0.962x + 2.122$  where  $x$  is the retention time of VOCs measured in our work, and  $y$  values are the Adams indices (2007).

VOCs that lacked authentic standards and that were not listed in Adams library were identified by probability-based matching using the NIST/EPA/NIH 2005 spectral database. The components that were identified using probability-based matching were dipropylene glycol methyl ether, 1-(2-methoxypropoxy)-2-propanol, 3,3,5-trimethyl-1-hexene, helional, and neryl nitrile. For limonene-based air freshener we observe two peaks at retention time 15.11 min and 15.30 min, NIST library search of both these peaks identifies them as dipropylene glycolmethyl ether. It is likely that one of the components is isomer of dipropylene glycolmethyl ether. Dipropylene glycolmethyl ether is commonly used as a solvent/carrier in many floor cleaners.<sup>187</sup> It vaporizes slowly, is a good solvent for many organics, and does not have a characteristic smell which could mask the scent of other VOCs. 1-(2-methoxypropoxy)-2-propanol is a volatile

alcohol and can also be assumed to work as a carrier for VOCs in the air freshener.<sup>188</sup> The other three compounds 3,3,5-trimethyl-1-hexene (2.2%), helional (0.4%), and neryl nitrile (0.4%) do not possess any characteristic odor of lemon or chamomile.

Some of the VOCs that comprise the limonene-based air freshener will react with ozone to generate SOA. Limonene is the most reactive and dominant VOC in the air freshener and generates high yields of SOA.  $\alpha$ -pinene is most abundant monoterpene emitted in the atmosphere<sup>118</sup> and has a significant SOA yield and hence cannot be neglected. Other studies indicate  $\beta$ -pinene<sup>89</sup>, linalool,<sup>203</sup> and terpinolene<sup>201</sup> also form SOA upon oxidation with ozone, however the yields from these VOCs are lower when compared to SOA yields generated by limonene and  $\alpha$ -pinene. In the air freshener, p-cymene is one of the least ozone reactive species, we have included it VOC mixtures to study the effect of non-reactive species on SOA generation.

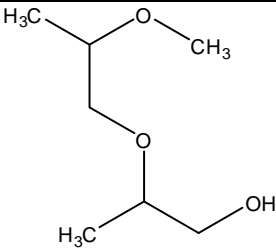
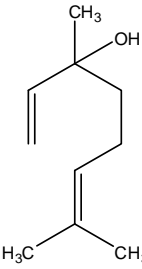
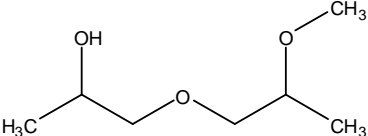
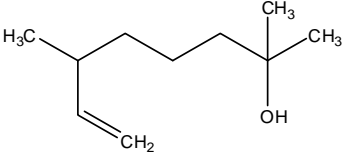
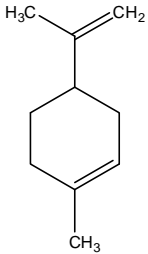
The half-lives of the VOCs were calculated to distinguish between the reactive and non-reactive VOCs (Table 3.3). The half-lives of VOCs were calculated at an ozone concentration of 500 ppb,<sup>182</sup> using ozone-VOC reaction rate constants published in various research articles the references are cited at bottom of the Table 3.3. The experimental kinetic values were not available for some components of the air freshener, and for these cases, the reaction rates were obtained from using the USEPA's Estimated Program Interface (EPI website ver 1.4).<sup>189</sup> One component of the air freshener, 3,3,5-trimethyl-1-hexene, could not be estimated by EPI. The substitution about the carbon-carbon double bond for this alkene is similar in structure to 3,3-dimethyl-1-butene, thus we estimated the half-life for 3,3,5-trimethyl-1-hexene using the second-order rate constant for 3,3-dimethyl-1-butene.<sup>190</sup>

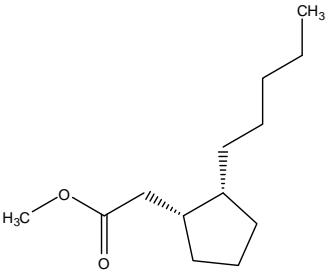
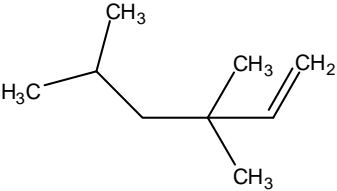
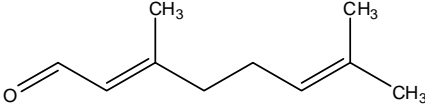
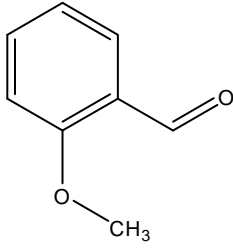
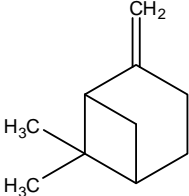
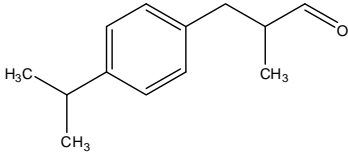
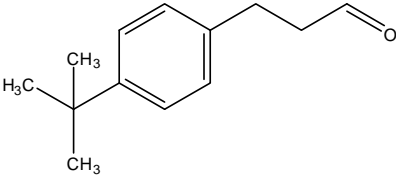
The identification of the compounds in the limonene-based air freshener can be compared to the previous analysis of the essential oils and extract that are used to make this type of air freshener. This air freshener is called lemon and chamomile scented by the manufacturer, thus one might expect lemon essential oils and chamomile extracts to be used in the air freshener. Sabinene,  $\alpha$ -pinene, myrcene, p-cymene, eucalyptol, limonene,  $\beta$ -ocimene,  $\gamma$ -terpinene, terpinolene,  $\alpha$ -terpineol, terpinen-4-ol, and  $\beta$ -caryophyllene have been reported to be present in chamomile extract from Estonia by Orav et al.<sup>191</sup> In addition to these VOCs, Mierendorff et al.,<sup>192</sup> have identified other VOCs in commercial cape chamomile oil, these VOCs include, nerol, geranial, linalyl acetate, eugenol, neryl acetate, geranyl acetate,  $\beta$ -caryophyllene,  $\alpha$ -humulene, and aromadendrene. Verzera et al.<sup>193</sup> analyzed the composition of the volatile fraction of essential oils of *Citrus meyerii* Y. Tan. and *Citrus medica* L. cv. Diamante and two new lemon hybrids obtained by cross-breeding them. Around 30 VOCs from the above three references for citrus and chamomile essential oils have been identified to be present in the air freshener.

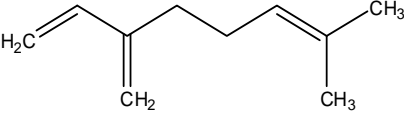
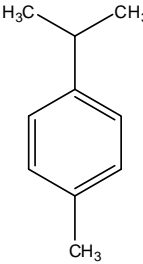
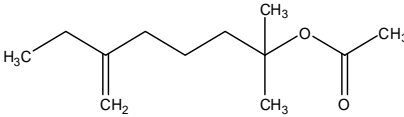
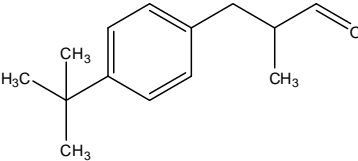
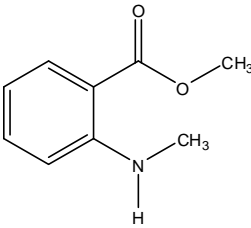
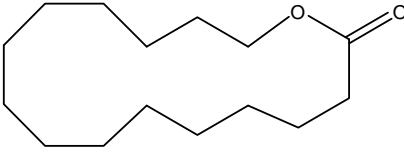
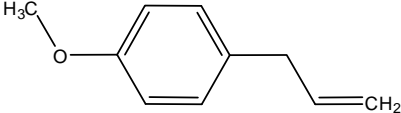
The VOCs identified in the limonene-based air freshener are listed in Table 3.3. The components are listed in descending order of percent composition. The determination of the fraction of VOCs recovered is a measure of the mass closure of the analysis. A 50.2 ppm solution of air freshener was injected on the GC/MS. After quantitative analysis, the sum of the concentrations for all components was  $45 \pm 1$  ppm. Therefore, 90% of the VOCs by mass in the air freshener have been determined. Steinemann et al.<sup>194</sup> performed head space analysis of eight different air fresheners in form of sprays gels, solids and deodorant skins using GC/MS. The authors report presence of very volatile organic compounds like acetaldehyde, acetone, ethanol, ethyl butanoate, ethyl acetate, and benzaldehyde in head space of the air freshener, with some of them contributing as much as 10% (w/v) towards composition. These compounds cannot be

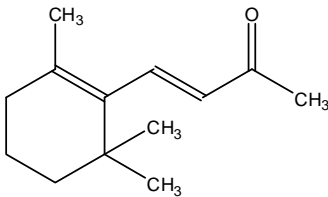
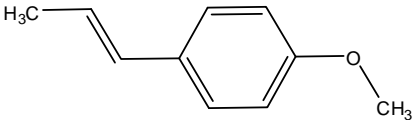
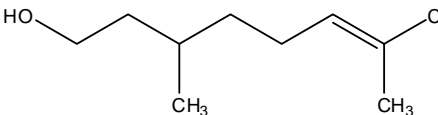
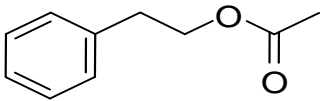
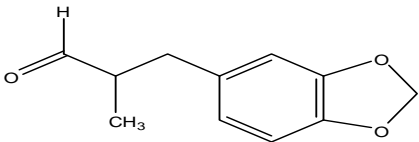
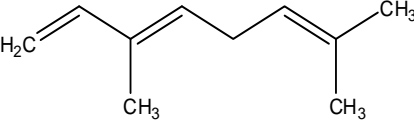
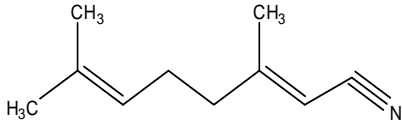
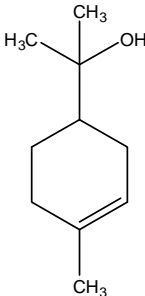
detected with the methodology used in this work and hence can lead to underestimation of total VOCs in the air freshener.

**Table 3.3** Components Present in Limonene Based Air Freshener.

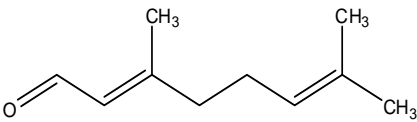

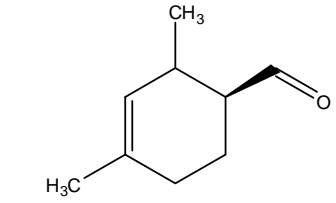
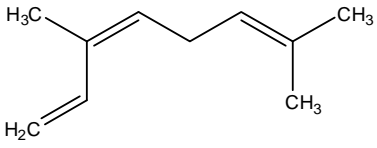
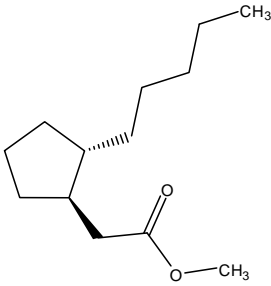
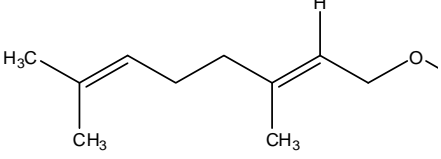
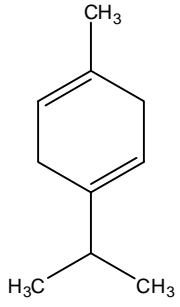
VOC	Structure	% composition <sup>d</sup>	VOC <sup>e</sup> ( $\mu\text{g m}^{-3}$ )	$t_{1/2}$ <sup>f</sup> (min)
dipropylene glycol methyl ether and isomer <sup>b</sup>		19.3±0.8	1108±71	>9500 <sup>p</sup>
linalool <sup>a</sup>		14.4±0.3	839±53	2.2 <sup>g</sup>
1-(2-methoxypropoxy)- 2-propanol <sup>b</sup>		12.8±0.5	744±47	>9500 <sup>p</sup>
dihydromyrcenol <sup>c</sup>		9.8±0.3	500±36	4670 <sup>h</sup>
limonene <sup>a</sup>		6.2±0.2	317±23	4.5 <sup>i</sup>

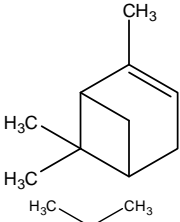
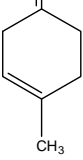
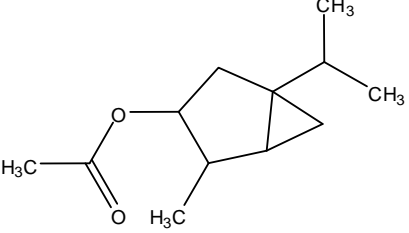
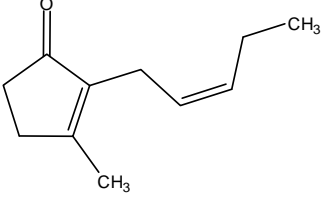
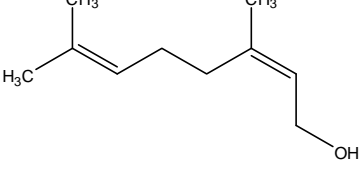
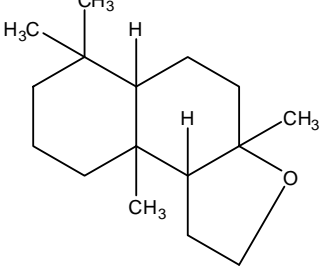
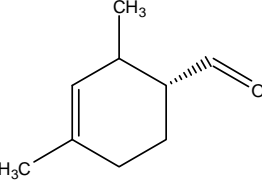
VOC	Structure	% composition <sup>d</sup>	VOC <sup>e</sup> ( $\mu\text{g m}^{-3}$ )	$t_{1/2}$ <sup>f</sup> (min)
cis-methyl-dihydrojasmonate <sup>c</sup>		2.6±0.1	153±13	>9500 <sup>p</sup>
3,3,5-trimethyl-1-hexene <sup>b</sup>		2.20±0.1	129±8	2500 <sup>q</sup>
geranial <sup>c</sup>		2.1±0.1	112±8	2.1 <sup>j</sup>
o-anisaldehyde <sup>c</sup>		1.7±0.1	108±7	>9500 <sup>p</sup>
$\beta$ -pinene <sup>a</sup>		1.6±0.1	84±6	63 <sup>k</sup>
cyclamenaldehyde <sup>c</sup>		1.37±0.03	77±5	>9500 <sup>p</sup>
bourgeonal <sup>c</sup>		1.15±0.03	66±4	>9500 <sup>p</sup>

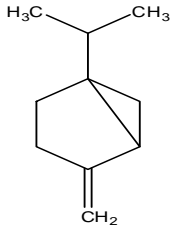
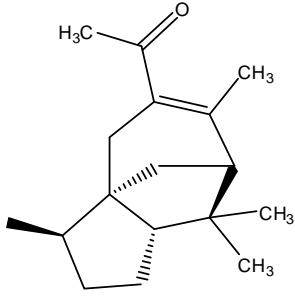
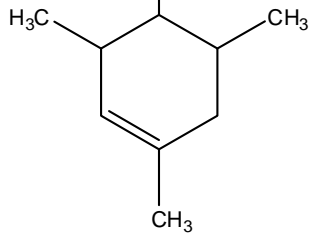
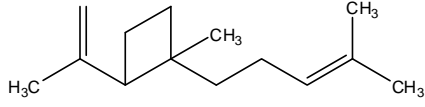
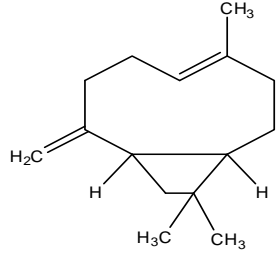
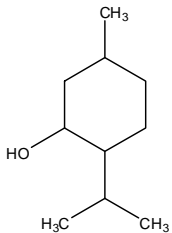
VOC	Structure	% composition <sup>d</sup>	VOC <sup>e</sup> ( $\mu\text{g m}^{-3}$ )	$t_{1/2}$ <sup>f</sup> (min)
myrcene <sup>c</sup>		0.99±0.03	47±4	2.0 <sup>i</sup>
p-cymene <sup>a</sup>		0.97±0.03	50±3	18800 <sup>k</sup>
dihydromyrcenyl acetate <sup>c</sup>		0.90±0.04	47±3	78 <sup>j</sup>
lilial <sup>c</sup>		0.84±0.04	47±3	>9500 <sup>p</sup>
methyl methylantranilate <sup>c</sup>		0.78±0.03	53±3	>9500 <sup>p</sup>
muskalactone <sup>c</sup>		0.78±0.02	42±3	>9500 <sup>p</sup>
estragole <sup>a</sup>		0.76±0.05	39±3	78 <sup>j</sup>

VOC	Structure	% composition <sup>d</sup>	VOC <sup>e</sup> ( $\mu\text{g m}^{-3}$ )	$t_{1/2}$ <sup>f</sup> (min)
$\beta$ -ionone <sup>c</sup>		$0.72 \pm 0.03$	$41 \pm 3$	$49^l$
anethole <sup>a</sup>		$0.57 \pm 0.02$	$34 \pm 2$	$6.9^j$
$\beta$ -citronellol <sup>c</sup>		$0.527 \pm 0.02$	$31 \pm 2$	$3.9^m$
2-phenylethyl acetate <sup>c</sup>		$0.50 \pm 0.03$	$28 \pm 2$	$>9500^p$
helional <sup>b</sup>		$0.44 \pm 0.03$	$25 \pm 2$	$>9500^p$
trans- $\beta$ -ocimene <sup>c</sup>		$0.41 \pm 0.02$	$20 \pm 2$	$1.7^g$
neryl nitrile <sup>b</sup>		$0.40 \pm 0.02$	$21 \pm 1$	$1.1^g$
$\alpha$ -terpineol <sup>a</sup>		$0.38 \pm 0.03$	$22 \pm 1$	$3.1^n$



VOC	Structure	% composition <sup>d</sup>	VOC <sup>e</sup> ( $\mu\text{g m}^{-3}$ )	$t_{1/2}$ <sup>f</sup> (min)
neral (isomer of Citral) <sup>c</sup>		0.35±0.02	19±1	2.1 <sup>j</sup>
decanal <sup>c</sup>		0.27±0.02	15±1	>9500 <sup>p</sup>
trans-vertocitral <sup>c</sup>		0.26±0.01	15±1	200 <sup>p</sup>
cis- $\beta$ -ocimene <sup>c</sup>		0.23±0.01	11±1	1.7 <sup>i</sup>
trans-methyldihydrojas monate <sup>c</sup>		0.23±0.01	14±1	>9500 <sup>p</sup>
cis-geraniol <sup>c</sup>		0.23±0.02	12±1	1.0 <sup>o</sup>
$\gamma$ -terpinene <sup>a</sup>		0.19±0.01	10±1	6.7 <sup>i</sup>

VOC	Structure	% composition <sup>d</sup>	VOC <sup>e</sup> ( $\mu\text{g m}^{-3}$ )	$t_{1/2}$ <sup>f</sup> (min)
$\alpha$ -pinene <sup>a</sup>		0.18±0.01	9±1	11 <sup>i</sup>
terpinolene <sup>a</sup>		0.14±0.01	7.3±0.5	0.5 <sup>i</sup>
thujyl acetate <sup>c</sup>		0.139±0.003	7.8±0.5	>9500 <sup>p</sup>
jasmone <sup>c</sup>		0.115±0.01	6.5±0.4	1.4 <sup>j</sup>
nerol <sup>c</sup>		0.107±0.005	5.7±0.4	1.1 <sup>j</sup>
ambrox <sup>c</sup>		0.098±0.003	5.7±0.4	>9500 <sup>p</sup>
cis-vercitolal <sup>c</sup>		0.075±0.002	4.2±0.3	200 <sup>p</sup>

VOC	Structure	% composition <sup>d</sup>	VOC <sup>e</sup> ( $\mu\text{g m}^{-3}$ )	$t_{1/2}$ <sup>f</sup> (min)
sabinene <sup>c</sup>		0.062±0.006	3.2±0.2	11 <sup>i</sup>
cedryl methyl ketone <sup>c</sup>		0.043±0.005	2.5±0.2	0.4 <sup>j</sup>
isocyclocitral <sup>c</sup>		0.034±0.005	1.9±0.1	2.2 <sup>j</sup>
bergamotene <sup>c</sup>		0.033±0.002	1.7±0.1	2.1 <sup>j</sup>
$\beta$ -caryophyllene <sup>c</sup>		0.028±0.003	1.5±0.1	0.1 <sup>j</sup>
menthol <sup>c</sup>		0.007±0.001	0.38±0.0 3	>9500 <sup>p</sup>

<sup>a</sup>VOCs identified using authentic standards <sup>b</sup> VOCs identified using mass spectral comparison to for these components NIST MS library, <sup>c</sup>VOCs identified using mass spectra and Adams indices <sup>d</sup>The percent composition values calculated by dividing individual concentration values of components by total concentrations, the error in percent composition is calculated from the standard deviation in peak area for multiple injections on GC/MS <sup>e</sup>The uncertainty in VOC concentration is calculated by error propagation of uncertainty in VOC concentration, density of VOC, and syringe uncertainty. <sup>f</sup>The half-life for VOCs was calculated from pseudo first order reaction rates constants between VOCs and 500 ppb ozone at 298 K. <sup>g</sup> Reaction rate constant obtained from Atkinson et al.,<sup>194</sup> <sup>h</sup>Forester et al.,<sup>195</sup> <sup>i</sup>Atkinson, R.; Arey, J.,<sup>65</sup> <sup>j</sup>The values are calculated using AOPWIN in EPIWEB 1.4 suite<sup>189</sup> <sup>k</sup>Atkinson et al.,<sup>197</sup> <sup>l</sup>Forester et al.,<sup>198</sup> <sup>m</sup>Ham et al.,<sup>199</sup> <sup>n</sup>Wells et al.,<sup>200</sup> <sup>o</sup>Forester et al.,<sup>198</sup> <sup>p</sup> Reaction rate constant<sup>196</sup> are estimated from structurally similar compounds like saturated carbonyls or unsaturated carbonyls. <sup>q</sup>estimated from a structurally similar compound, 3,3-dimethyl-1-butene<sup>190</sup>.

### 3.2.13 Particle generation and SOA yield calculations

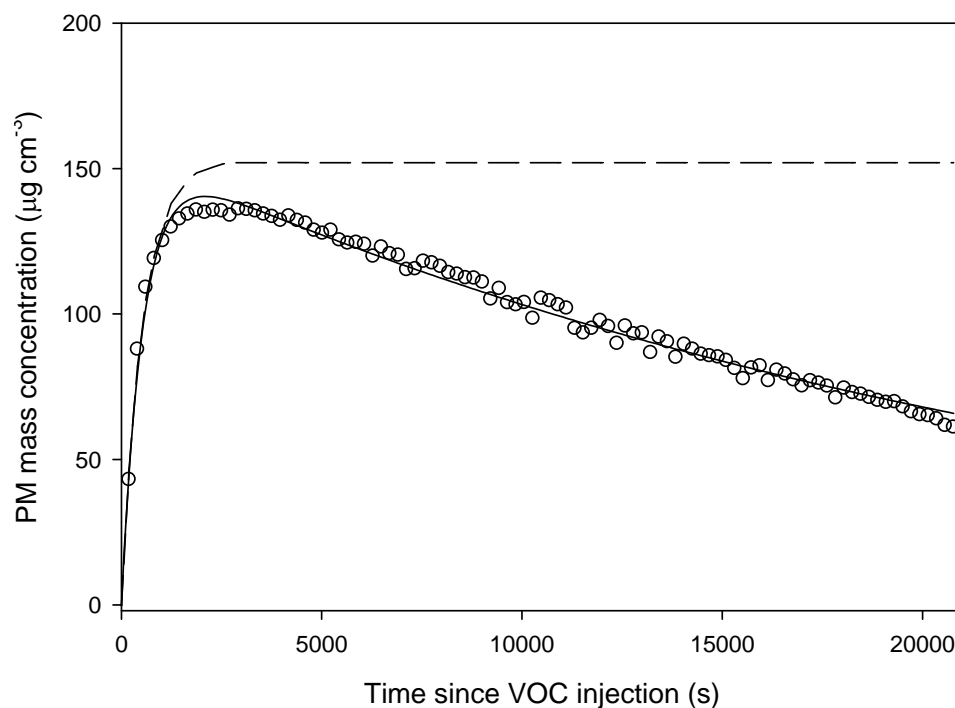
Aerosol can be visualized as semivolatile particulate matter (PM) in equilibrium with surrounding vapor phase. In smog chambers, the formation of aerosol can be modeled using a three-step process. First, a VOC (or mixture of VOCs) reacts with an oxidant to form condensable organic carbon (COC). Next, a portion of COC condenses to form PM. Last, the PM deposits on the walls of the chamber. In our experiments, the ozone is in stoichiometric excess and the oxidation of VOC is rapid relative to condensation and PM loss. Thus, the particle formation process can be represented by equation given below: <sup>99</sup>

$$PM_t = \frac{k_1 M_o}{k_2 - k_1} (e^{-k_1 t} - e^{-k_2 t})$$

$PM_t$  is the concentration of PM at time  $t$ ,  $k_1$  is rate constant for particle formation while  $k_2$  is rate constant for wall loss.  $M_o$  is the concentration of COC that partitions into PM at equilibrium and in the absence of the chamber walls; this is the wall-loss corrected amount of PM that is formed. The amount of PM formed in the chamber during oxidation reaction is done by fitting the above equation to  $PM_t$  mass concentration (measured by SMPS) as function of time, the final

amount of PM formed  $M_o$  is calculated by correcting for wall losses. Figure 3.5 shows an example of the fit of the data from equation above. The SOA yield is calculated by dividing this  $M_o$  value with mass concentration of reactive VOC precursor ( $[VOC]$ ) oxidized.

$$\text{SOA yield} = \frac{M_o}{[VOC]}$$



**Figure 3.5.** PM generated by the reaction of  $367 \pm 48 \mu\text{g m}^{-3}$  limonene with  $530 \pm 33$  ppb of ozone. The temperature, pressure, and %RH are  $293.1 \pm 0.3$  K,  $0.984 \pm 0.001$  atm and  $3.0 \pm 1.8$  (%) respectively. The open circles indicate the PM concentration, measured by SMPS, as a function of time. The solid line is the best fit line obtained by using equation above. The dashed line represents the PM concentration corrected for losses to the walls where  $k_2 = 0$ . The values and error for PM,  $k_1$  and  $k_2$  are calculated using Sigma Plot 10.0.

### 3.3 Results and discussion

#### 3.3.1 SOA yields for VOC mixtures

##### 3.3.1.1 SOA yields for limonene

As seen from the Table 3.3, the two most abundant monoterpenes in the air freshener are limonene and linalool. The limonene/ozone rate constant is higher in comparison to other monoterpenes.<sup>65</sup> Limonene has two double bonds which are susceptible to oxidation, and limonene also generates higher SOA yields when compared to other monoterpenes.<sup>101</sup> For these reasons the limonene in the VOC mixtures to contribute the most to the SOA yield and composition. Hence, prior to studying limonene in mixtures, it is important to consider limonene alone as a base case and study the SOA production under our experimental conditions. We generated SOA at three different occasions (Table 3.4) from  $367 \pm 48 \mu\text{g m}^{-3}$  limonene. The SOA yields generated for all three experiments from limonene were  $0.53 \pm 0.07$ ,  $0.54 \pm 0.07$ , and  $0.42 \pm 0.05$ . These measured yields are similar to previous work. Chen and Hopke<sup>165</sup> measured SOA yields between 0.4 and 0.6 (limonene concentration = 166 to  $550 \mu\text{g m}^{-3}$ ,  $\text{O}_3=30\text{-}100$  ppb) where the limonene concentrations were the similar or twice the concentration used in this work, the ozone concentrations used were around 50-100 ppb. Saathoff et al.<sup>92</sup> measured SOA yields between 0.54 (limonene concentration =  $78 \mu\text{g m}^{-3}$ ) to 0.69 (limonene concentration =  $222 \mu\text{g m}^{-3}$ ) (at  $T=293.3$  K and  $\text{RH}=39\text{-}44\%$ ,  $\text{O}_3=100\text{-}300$  ppb). The limonene concentration used in Saathoff et al.<sup>92</sup> was lower than used in work presented herein, the higher SOA yields for their work can be attributed to higher RH (%) than our work (typical RH 4-8%).

### 3.3.1.2 SOA yields from limonene and p-cymene VOC mixtures

The air freshener that is used as a model of the complex mixtures contains VOCs that, alone, do not react with ozone to a measurable extent. However, it is not known if the non-reactive VOCs can react with the intermediates or products of the reactive VOCs. One of the least reactive VOCs present in air freshener is p-cymene.<sup>65</sup> The null hypothesis is that because p-cymene doesn't react with ozone, adding p-cymene to limonene should not change the SOA yields. The ratio of p-cymene to limonene (Table 3.4, mix 2A) is similar to in the ratio in the air freshener. The SOA yields for mixture 2A were  $0.49 \pm 0.06$  and  $0.47 \pm 0.06$ , which is slightly lower than SOA yields generated by limonene alone (Student's  $t$   $p=0.71$ ) ( $0.53 \pm 0.07$ ,  $0.54 \pm 0.07$  and  $0.42 \pm 0.05$ ). As seen from the  $p$  value associated with the SOA yields, from the two precursors we can say that the yields are not significantly different. The concentration of p-cymene in this mixture is low ( $\sim 8 \mu\text{g m}^{-3}$ ), and hence to further confirm the hypothesis, p-cymene has no effect on SOA yields, concentration of p-cymene was increased ten times ( $\sim 80 \mu\text{g m}^{-3}$ ) in next set of experiments (Table 3.4, mix 2B, 2C, 2D). The yields were found to be a slightly lower (Student's  $t$   $p=0.24$  with limonene and  $p=0.22$  with mix 2A) ( $0.43 \pm 0.06$ ,  $0.38 \pm 0.05$  and  $0.48 \pm 0.06$ ), but not statistically different, when compared to yields generated by limonene and earlier limonene and p-cymene mixtures. Thus, p-cymene, a non-reactive VOC, does not significantly affect SOA yields.

### 3.3.1.3 SOA yields from mixtures of limonene and other reactive VOCs

After confirming that the SOA yields generated from a mixture containing p-cymene and limonene are similar to SOA yields generated from only limonene experiments, the next set of experiments were done by generating SOA from a mixture of limonene, p-cymene,  $\alpha$ -pinene, and

$\beta$ -pinene. In this VOC mixture,  $\alpha$ -pinene contributes approximately 2% by mass,  $\beta$ -pinene contributes nearly 7% by mass, while p-cymene and limonene contribute 2% and 89% respectively. The monoterpene ratios were similar to monoterpene ratios in the air freshener (Table 3.3). In this mixture,  $\alpha$ -pinene is more reactive than  $\beta$ -pinene<sup>65</sup> and also yields more SOA than  $\beta$ -pinene.<sup>202</sup> The SOA yields generated from experiments for this mixture is  $0.44 \pm 0.06$  and  $0.43 \pm 0.06$ , which is statistically similar to the SOA yields generated by limonene alone ( $p=0.24$ ) and limonene and p-cymene mixtures ( $p=0.5$ ). These results indicate that the contribution of  $\alpha$ -pinene and  $\beta$ -pinene at these concentrations towards the SOA yield is negligible.

#### 3.3.1.4 SOA yields from mixtures containing linalool

Experiments were carried out using VOC mixtures containing linalool, limonene,  $\alpha$ -pinene,  $\beta$ -pinene, and p-cymene. Linalool readily reacts with ozone as indicated from its half life, (Table 3.3).<sup>194</sup> Linalool is also a dominant VOC in these mixtures: 35% in Mixture 4A and 4B and 73% in Mixture 4C. The average SOA yield for linalool-containing mixtures is  $0.46 \pm 0.10$ , while the average SOA yield generated from non-linalool containing mixtures is  $0.46 \pm 0.08$ . Hence, we can conclude that linalool does not contribute towards SOA yield under the reaction conditions used for this work. The SOA yields from linalool reported in the literature are found to be low as well. For example, Lee et al.,<sup>154</sup> Chen and Hopke,<sup>165</sup> and Ng et al.,<sup>162</sup> measured low SOA yields 0.01, 0.003-0.02, and 0.012, respectively, when cyclohexane was used as OH scavenger. In our work we observe that with the addition of linalool to limonene generates a SOA yield of  $0.38 \pm 0.05$  (refer Table 3.4), which is lower than yields generated by all earlier mixtures thus ascertaining the fact that linalool does not contribute to SOA formation. Hence for further mixtures we will treat linalool as a non-reactive VOC, and will not include the linalool



concentration in the SOA yield calculation. One of the reasons for linalool not contributing significantly towards yield may be the linear structure of the molecule. Moreover, terpenes like  $\alpha$ -pinene form SOA products which are 9 or 10 carbon atoms in length, whereas linalool products are 5 to 7 carbon atoms in length. Linalool products have lower molecular weights and tend to be more volatile than other terpene products. Thus, the potential for SOA formation from linalool is lower in comparison to other terpenes.<sup>203</sup>

**Table 3.4** VOC precursor concentrations and calculated SOA yields from limonene and other VOC mixtures

Reactive precursor	Non-reactive species	Injection volume (μL)	Reactive VOC concentration <sup>a</sup> (μg m <sup>-3</sup> )	M <sub>o</sub> <sup>b</sup> (μg m <sup>-3</sup> )	SOA yield <sup>c</sup>	Ozone concentration <sup>d</sup> (ppb)	Mass of SOA collected on filter (μg) <sup>e</sup>	% of OH consumed by 2-butanol
1. Limonene (367±48 μg m <sup>-3</sup> )								
limonene	-	2.4±0.1	367±48	193±3	0.53±0.07	530±33	76.7	91
limonene	-	2.4±0.1	367±48	199±2	0.54±0.07	539±18	173	
limonene	-	2.4±0.1	367±48	153±1	0.42±0.05	515±10	115 <sup>f</sup>	
Mixture 2A. Limonene (374±48 μg m <sup>-3</sup> ) and p-cymene (8.4±1 μg m <sup>-3</sup> )								
limonene	p-cymene	2.5±0.1	374±48	182±1	0.49±0.06	510±4	112	91
limonene	p-cymene	2.5±0.1	374±48	175±1	0.47±0.06	443±9	108	
Mixture 2B. Limonene (310±40 μg m <sup>-3</sup> ) and p-cymene (72±9 μg m <sup>-3</sup> )								
limonene	p-cymene	2.5±0.1	310±40	134±1	0.43±0.06	421±12	74.1	90
Mixture 2C. Limonene (372±47 μg m <sup>-3</sup> ) and p-cymene (87±11 μg m <sup>-3</sup> )								
limonene	p-cymene	3.0±0.1	372±47	142±1	0.38±0.05	452±13	95.5	90
Mixture 2D. Limonene (374±48 μg m <sup>-3</sup> ) and p-cymene (85±11 μg m <sup>-3</sup> )								
limonene	p-cymene	3.0±0.1	374±48	181±2	0.48±0.06	494±10	99.0	90
Mixture 3. Limonene (379±48 μg m <sup>-3</sup> ), p-cymene (10±1 μg m <sup>-3</sup> ), α-pinene (10±1 μg m <sup>-3</sup> ) and β-pinene (30±4 μg m <sup>-3</sup> )								
limonene + α-pinene +β-pinene	p-cymene	2.8±0.1	419±54	185±2	0.44±0.06	474±1	119	90
limonene +α-pinene +β-pinene	p-cymene	2.8±0.1	419±54	180±2	0.43±0.06	450±5	122	

Reactive precursor	Non-reactive species	Injection volume (μL)	Reactive VOC concentration <sup>a</sup> (μg m <sup>-3</sup> )	M <sub>o</sub> <sup>b</sup> (μg m <sup>-3</sup> )	SOA yield <sup>c</sup>	Ozone concentration <sup>d</sup> (ppb)	Mass of SOA collected on filter (μg) <sup>e</sup>	% of OH consumed by 2-butanol
Mixture 4A. Limonene (377±47 μg m <sup>-3</sup> ), Linalool (236±29 μg m <sup>-3</sup> ), p-cymene (9±1 μg m <sup>-3</sup> ), α-pinene (10±1 μg m <sup>-3</sup> ) and β-pinene (33±4 μg m <sup>-3</sup> )								
limonene	linalool							
+α-pinene	+p-	4.3±0.1	420±52	189±2	0.45±0.06	504±2	89.6 <sup>f</sup>	
+β-pinene	cymene							86
limonene	linalool							
+α-pinene	+p-	4.3±0.1	420±52	203±3	0.48±0.04	494±7	111	
+β-pinene	cymene							
Mixture 4B. Limonene (368±46 μg m <sup>-3</sup> ), Linalool (238±30 μg m <sup>-3</sup> ), p-cymene (11±1 μg m <sup>-3</sup> ), α-pinene (11±1 μg m <sup>-3</sup> ) and β-pinene (36±4 μg m <sup>-3</sup> )								
limonene	linalool							
+α-pinene	+p-	4.3±0.1	415±52	190±2	0.46±0.04	505±3	97.0	
+β-pinene	cymene							89
limonene	linalool							
+α-pinene	+p-	4.3±0.1	415±52	149±2	0.36±0.05	1568±11	106 <sup>f</sup>	
+β-pinene	cymene							
Mixture 4C. Limonene (370±46 μg m <sup>-3</sup> ), Linalool (1138±140 μg m <sup>-3</sup> ), p-cymene (11±1 μg m <sup>-3</sup> ), α-pinene (10±1 μg m <sup>-3</sup> ) and β-pinene (29±4 μg m <sup>-3</sup> )								
limonene	linalool							
+α-pinene	+p-	10.0±0.1	410±50	230±5	0.56±0.07	1735±9	121	
+β-pinene	cymene							89
limonene	linalool							
+α-pinene	+p-	10.0±0.1	410±50	172±3	0.42±0.05	1512±9	115	
+β-pinene	cymene							
Mixture 5. Limonene (368±46 μg m <sup>-3</sup> ) and Linalool (234±29 μg m <sup>-3</sup> )								
limonene	linalool	3.9±0.1	368±46	140±2	0.38±0.05	488±5	121	86

<sup>a</sup>The uncertainties in VOC concentration calculated by propagation of uncertainty associated with syringe used for VOC injection, density of VOC and uncertainty in volume of chamber (estimated 10%) <sup>b</sup>The error in  $M_{o,}$  is the standard error associated with curve fit used for wall-loss corrections used in these experiments <sup>c</sup>The uncertainties associated with SOA yield are calculated by error propagation using uncertainties in VOC concentration and standard error in  $M_o$  <sup>d</sup>The ozone concentration is calculated by averaging the ozone concentration readings obtained from the ozone analyzer for twenty minutes prior to injection of VOC, and the uncertainty in the measurement is the standard deviation. <sup>e</sup>The amount of SOA collected on the filter is the PM concentration measured by the SMPS averaged over the time that the vacuum was applied, flow rate of the vacuum. <sup>f</sup>These filters were utilized for SOA toxicity experiments conducted by undergraduate student Megan Czerniejewski. Thus they will not be discussed later in the sections covering SOA products analyzed from the filter

### 3.3.2 SOA yields for surrogate mixtures and limonene based air freshener

To confirm that SOA generation is an additive process, SOA yields from air freshener and surrogate were compared, and found to be similar. SOA formation experiments were carried out using surrogates to mimic the VOCs in limonene-based air freshener as closely as possible hence a mixture containing ten different VOCs was made. The different terpenes that were selected for making the surrogates include; limonene, linalool, estragole,  $\gamma$ -terpinene,  $\alpha$ -terpineol,  $\beta$ -pinene, terpinolene, p-cymene,  $\alpha$ -pinene, and anethole. Among these, the reactive terpenes are limonene,  $\alpha$ -pinene, terpinolene, and  $\beta$ -pinene. The remaining terpenes, linalool, p-cymene, estragole, anethole,  $\gamma$ -terpinene, and  $\alpha$ -terpineol, are not reactive and/or do not produce significant amounts of SOA. Surrogate 1 and 2 are similar to each other, and they have near identical VOC concentrations. Surrogate 3 is different from surrogate 1 and 2, where the concentration of linalool in surrogate 3 is approximately five times higher than in surrogate 1 and 2. Surrogate 3's linalool concentration is a better match the content in the air freshener. For first three surrogate experiments the VOC concentrations were similar to when 33  $\mu$ L of limonene based air freshener is injected in the chamber. One surrogate experiment was carried by injecting lower volume of surrogate 3, in this case the VOC concentrations are equal to those present when 20  $\mu$ L of limonene based air freshener.

The SOA yields for Surrogate 1, Surrogate 2, and Surrogate 3 are calculated to be  $0.50 \pm 0.03$ ,  $0.46 \pm 0.03$  and  $0.42 \pm 0.05$  (Table 3.5) respectively. These yields were found to be in agreement with the SOA yields obtained for experiments conducted with 33  $\mu$ L of air freshener-trial 2 ( $0.36 \pm 0.03$ ,  $0.38 \pm 0.04$  and  $0.40 \pm 0.03$ ) ( $p=0.06$ ).

In another set of experiments, the SOA yields generated from the ozonolysis of a lower injected volume of surrogate 3 were  $0.29 \pm 0.04$ . The SOA yield for this surrogate experiment is in

agreement with the SOA yields from three experiments of 20  $\mu\text{L}$  of ( $p=0.3$ ) limonene-based air freshener-trial 1 ( $0.33\pm0.02$ ,  $0.28\pm0.03$ , and  $0.34\pm0.03$ ). The agreement between the SOA yields of the surrogates and the air freshener is expected, because the surrogates are mixtures of VOCs that are prepared with VOC mass percentages similar to that of the limonene based air freshener. Around 95% of reactive VOCs present in the air freshener (Table 3.3) were added to the surrogate, hence it is expected that the SOA yields would be similar for surrogate and air freshener.

Two more experiments were performed at higher volume of air freshener (50  $\mu\text{L}$ ) the yields of these experiments were found to be higher,  $0.85\pm0.10$  and  $0.80\pm0.09$ , than all the earlier experiments for air freshener as well as limonene and its VOC mixtures. The higher SOA yields for this experiment of air freshener can be explained by comparing the amount of OH radicals scavenged by 2-butanol. In trial 1 and trial 2 of the air freshener 750  $\mu\text{L}$  of 2-butanol was used as radical scavenger while for trial 250  $\mu\text{L}$  of the 2-butanol was used. In the first two trials the amount of OH radicals scavenged by 2-butanol is 92% and 86% respectively. In trial 3, around 60% of OH radicals are scavenged. Thus during trial 3, the amount of OH radicals present in the chamber is higher than the first two trials. Jonsson et al.<sup>204</sup> have shown that in absence of radical scavenger OH radical pathways exist which lead to generation of higher amounts of SOA. The filters generated in trial 3 were used in UV-visible experiments in Chapter 5 of this dissertation and hence the filters will not be discussed in the SOA speciation section of this chapter.

**Table 3.5** VOC precursor concentrations and calculated SOA yields for surrogates and limonene containing air freshener

Reactive Precursor	Injection volume (μL)	Reactive VOC concentration <sup>a</sup> (μg m <sup>-3</sup> )	M <sub>o</sub> <sup>b</sup> (μg m <sup>-3</sup> )	SOA yield <sup>c</sup>	Ozone concentration <sup>d</sup> (ppb)	Mass of SOA collected on filter (μg) <sup>e</sup>	% of OH consumed by 2-butanol
Surrogate 1. Limonene (375±47 μg m <sup>-3</sup> ), Linalool (225±28 μg m <sup>-3</sup> ), Estragole (107±13 μg m <sup>-3</sup> ), γ-terpinene (85±11 μg m <sup>-3</sup> ), α-terpineol (52±6 μg m <sup>-3</sup> ), β-pinene (31±4 μg m <sup>-3</sup> ), terpinolene (22±3 μg m <sup>-3</sup> ), p-cymene (11±1 μg m <sup>-3</sup> ), α-pinene (9±1 μg m <sup>-3</sup> ) and anethole (20±3 μg m <sup>-3</sup> ) <sup>h</sup>							
limonene +α-pinene +β-pinene +terpinolene	5.4±0.1	437±52	217±4	0.50±0.03	598±2	124	89
Surrogate 2. Limonene (368±46 μg m <sup>-3</sup> ), Linalool (239±30 μg m <sup>-3</sup> ), Estragole (110±14 μg m <sup>-3</sup> ), γ-terpinene (84±10 μg m <sup>-3</sup> ), α-terpineol (50±6 μg m <sup>-3</sup> ), β-pinene (40±5 μg m <sup>-3</sup> ), terpinolene (23±3 μg m <sup>-3</sup> ), p-cymene (10±1 μg m <sup>-3</sup> ), α-pinene (10±1 μg m <sup>-3</sup> ) and anethole (20±3 μg m <sup>-3</sup> ) <sup>h</sup>							
limonene +α-pinene +β-pinene +terpinolene	5.5±0.1	441±53	201±3	0.46±0.03	586±4	158	96
Surrogate 3. Limonene (350±43 μg m <sup>-3</sup> ), Linalool (1086±134 μg m <sup>-3</sup> ), Estragole (76±9 μg m <sup>-3</sup> ), γ-terpinene (22±3 μg m <sup>-3</sup> ), α-terpineol (24±3 μg m <sup>-3</sup> ), β-pinene (99±12 μg m <sup>-3</sup> ), terpinolene (23±3 μg m <sup>-3</sup> ), p-cymene (62±8 μg m <sup>-3</sup> ), α-pinene (16±2 μg m <sup>-3</sup> ) and anethole (43±5 μg m <sup>-3</sup> ) <sup>h</sup>							
limonene +α-pinene +β-pinene +terpinolene	11.5±0.1	488±61	207±3	0.42±0.05	578±9	144	95

Reactive Precursor	Injection volume (μL)	Reactive VOC concentration <sup>a</sup> (μg m <sup>-3</sup> )	M <sub>o</sub> <sup>b</sup> (μg m <sup>-3</sup> )	SOA yield <sup>c</sup>	Ozone concentration <sup>d</sup> (ppb)	Mass of SOA collected on filter (μg) <sup>e</sup>	% of OH consumed by 2-butanol
Surrogate 3. Limonene (201±25 μg m <sup>-3</sup> ), Linalool (623±77 μg m <sup>-3</sup> ), Estragole (43±5 μg m <sup>-3</sup> ), γ-terpinene (12±2 μg m <sup>-3</sup> ), α-terpineol (14±2 μg m <sup>-3</sup> ), β-pinene (57±7 μg m <sup>-3</sup> ), terpinolene (13±2 μg m <sup>-3</sup> ), p-cymene (35±4 μg m <sup>-3</sup> ), α-pinene (9±1 μg m <sup>-3</sup> ) and anethole (24±3 μg m <sup>-3</sup> ) <sup>h</sup>							
limonene +α-pinene +β-pinene +terpinolene	6.6±0.1	280±35	81±1	0.29±0.03	650±8	76.1	98
Limonene based air freshener-Trial 1: limonene (201±25 μg m <sup>-3</sup> ), β-pinene (53±6 μg m <sup>-3</sup> ), terpinolene (5±1 μg m <sup>-3</sup> ), α-pinene (6±1 μg m <sup>-3</sup> ) <sup>h</sup>							
limonene +α-pinene +β-pinene +terpinolene	20±0.5	265±38	88±1	0.33±0.02	567±3	112	93
limonene +α-pinene +β-pinene +terpinolene	20±0.5	265±38	74±1	0.28±0.03	600±2	82.9	97
limonene +α-pinene +β-pinene +terpinolene	20±0.5	265±38	91±2	0.34±0.03	~500 <sup>g</sup>	109	97



Reactive Precursor	Injection volume (μL)	Reactive VOC concentration <sup>a</sup> (μg m <sup>-3</sup> )	M <sub>o</sub> <sup>b</sup> (μg m <sup>-3</sup> )	SOA yield <sup>c</sup>	Ozone concentration <sup>d</sup> (ppb)	Mass of SOA collected on filter (μg) <sup>e</sup>	% of OH consumed by 2-butanol
Limonene based air freshener-Trial 2: limonene (322±40 μg m <sup>-3</sup> ), β-pinene (89±9 μg m <sup>-3</sup> ), terpinolene (8±1 μg m <sup>-3</sup> ), α-pinene (10±1 μg m <sup>-3</sup> ) <sup>h</sup>							
limonene +α-pinene +β-pinene +terpinolene	33.3±0.2	427±54	155±1	0.36±0.03	450±2	226 <sup>f</sup>	89
limonene +α-pinene +β-pinene +terpinolene	33.3±0.2	427±54	162±1	0.38±0.04	425±6	143	96
limonene +α-pinene +β-pinene +terpinolene	33.3±0.2	427±54	170±1	0.40±0.03	469±5	142	96
Limonene based air freshener-Trial 3: limonene (477±46 μg m <sup>-3</sup> ), β-pinene (126±10 μg m <sup>-3</sup> ), terpinolene (11±1 μg m <sup>-3</sup> ), α-pinene (14±1 μg m <sup>-3</sup> ) <sup>h</sup>							
limonene +α-pinene +β-pinene +terpinolene	50±0.2	628±90	532±10	0.85±0.10	1428±7	1700	60
limonene +α-pinene +β-pinene +terpinolene	50±0.2	628±90	499±7	0.80±0.09	1236±8	1800	60

<sup>a</sup>The uncertainties in VOC concentration calculated by propagation of uncertainty associated with syringe used for VOC injection, density of VOC and uncertainty in the volume of chamber(estimated 10%) <sup>b</sup>The error in  $M_o$ , is the standard error associated with curve fit used for wall-loss corrections used in these experiments <sup>c</sup>The uncertainties associated with SOA yield are calculated by error propagation using uncertainties in VOC concentration and standard error in  $M_o$  <sup>d</sup>The ozone concentration is calculated by averaging ozone concentration readings obtained from the ozone analyzer twenty minutes prior to injection of VOC, and the uncertainty in the measurement is the standard deviation between these values. <sup>e</sup>The amount of SOA collected on the filter is the mean value obtained by multiplying the time for vacuum applied, flow rate of the vacuum, and mass of particles recorded by SMPS. <sup>f</sup>These filters were utilized for other experiments beyond the scope of this dissertation. <sup>g</sup>Ozone was added after addition of air freshener to chamber, thus the accuracy of this value is limited because the ozone concentration in the absence of reactive VOCs was not measured. <sup>h</sup>For list of non reactive VOCs in the surrogates refer text in section 3.3.2 and for non reactive VOCs in air freshener refer Table 3.3

### 3.3.3 Volatility basis set

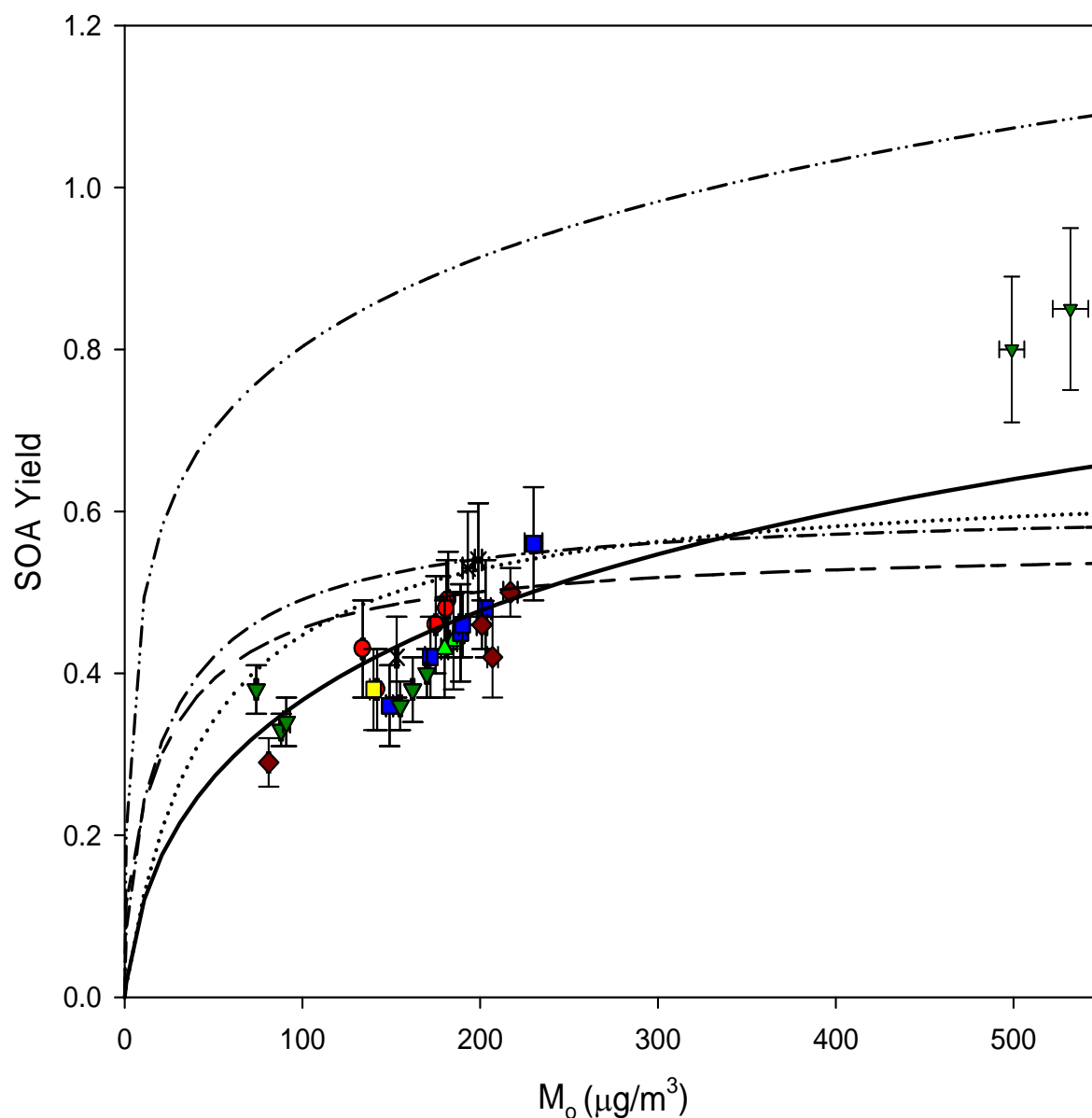
According to SOA yields from limonene, VOC mixtures, surrogates, and limonene-based air freshener (Table 3.4 and Table 3.5), the SOA yields are affected by the amount of precursor oxidized. All the precursor mixtures contain limonene and the concentration of limonene in these mixtures is at least 3.5 times, if not more, than the next more concentrate reactive precursor  $\beta$ -pinene. From these two observations, we can conclude that the SOA yields depend on the amount of limonene present in precursor mixtures.

Figure 3.6 shows a plot of SOA yield for all the mixtures mentioned in Table 3.4 and Table 3.5 as a function of aerosol mass concentration ( $M_o$ ). This plot shows the impact of VOC mixtures on SOA yields, as a function of VOCs added to make the mixtures. For example, if p-cymene, which is a non-reactive VOC under these reaction conditions, were to impact the SOA formation, the SOA yields measured from precursors containing p-cymene would deviate from the SOA yields measured from precursors that do not contain p-cymene. The SOA generated from ozonolysis of VOC mixtures have different volatilities, the volatility distribution of SOA can be predicted using volatility basis set. Experimental SOA yields (Table 3.5)  $M_o$  were fit to equation below<sup>79</sup> and the best fit was determined by minimizing the sum of squares. The SOA yields from all the mixtures except air freshener trial 3 were used to generate the best fit (air freshener trial 3 had lower amount of radical scavenger used). Treating the measured yields as part of the same data set allows for the determination of mass-based yields,  $\alpha$ , using the VBS analysis (Chapter 1, section 1.6). The magnitude of mass-based yields,  $\alpha$ , describes the fraction of total semi-volatile products that fall in each bin. This treatment of the data accounts for many products that can form the semi-volatile nature of SOA by grouping the products into volatility bins separated by order of magnitude.<sup>79,80</sup> These products should not be confused with single

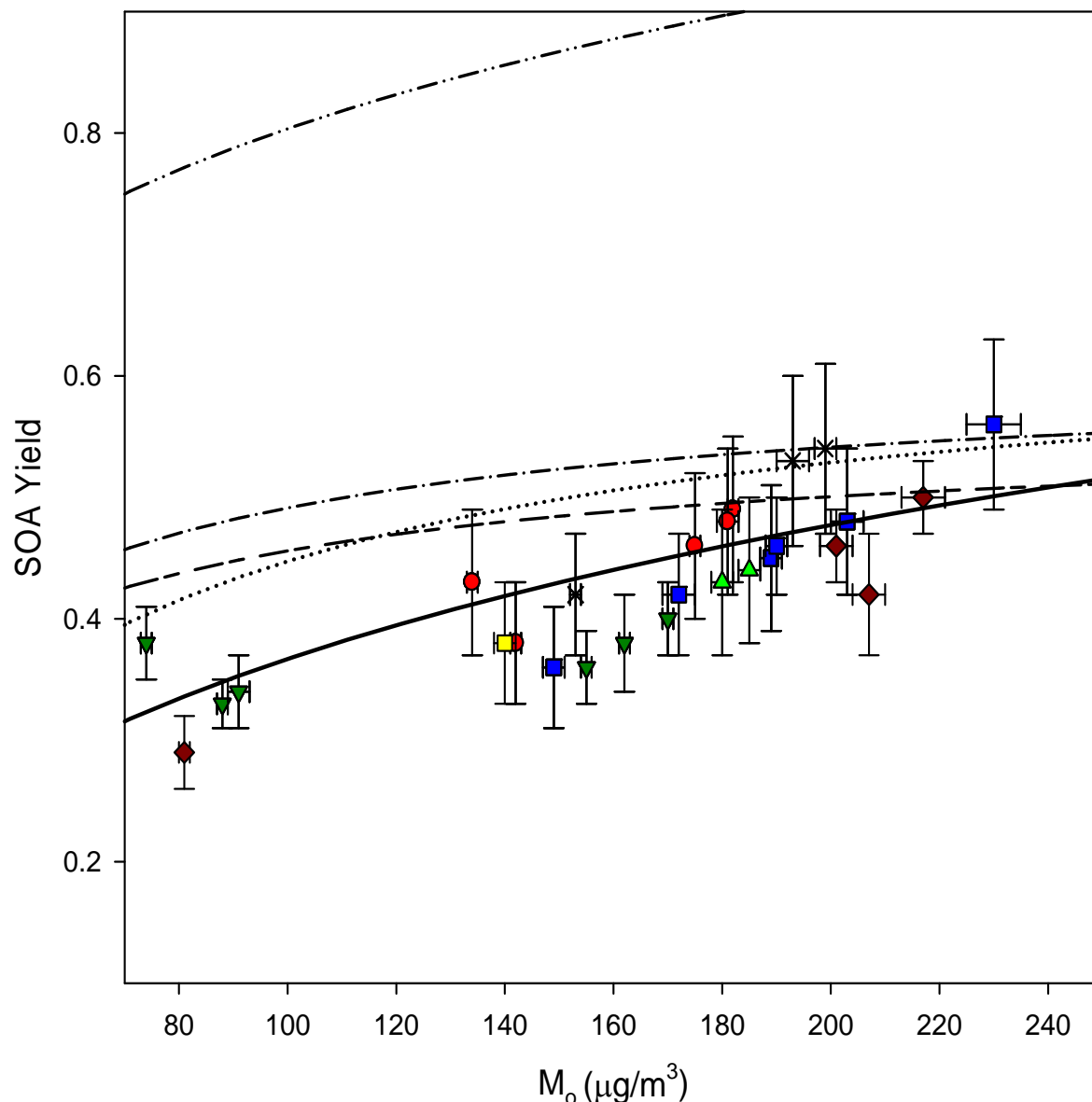
species generated during ozonolysis. The mass-based yields for the data were calculated for saturation vapor pressures ranging from 0.1 to 1000  $\mu\text{g m}^{-3}$ , and  $\alpha$  values were {0.0, 0.0, 0.001, 0.1500, 0.3500, 0.5998}. The values were zero within the uncertainty of the fit for first two bins, which correspond to the lowest saturation concentration and highest volatility products. No data were collected at low VOC concentrations. The mass-based yields increased with increasing saturation concentration from 0.1 to 1000  $\mu\text{g m}^{-3}$  and the highest mass-based yield of 0.5998 was obtained for a saturation concentration of 1000  $\mu\text{g m}^{-3}$ .

$$Y = \sum_{i=1}^n \frac{1}{1 + \frac{C_i^*}{M_0}} \alpha_i$$

The solid line shown in Figure 3.6 represents the best fit of the data, and most of the measured yields agree with the best fit within the range of their uncertainties. The data for air freshener trial 2 in this graph is lower than the surrogates (1, 2, and 3), which may be due to slightly higher concentration of reactive precursors in surrogates ( $455 \pm 57 \mu\text{g m}^{-3}$ ) as compared to air freshener ( $427 \pm 54 \mu\text{g m}^{-3}$ ). From Figure 3.6 and 3.7 we observe that all SOA yields occurred on the portion of the curve with a small slope. This part of the curve shows the saturation behavior of the semivolatile SOA products generated by use of high concentration of limonene as a SOA precursor. In this part of the curve, changes in the VOC concentrations leads to only small changes in the yield. The deviation of SOA yields from the best fit line may be due to the variation in concentration of reactive precursors or due to variations in physical parameters during the respective experiments. The SOA products generated in this work by the ozonolysis of limonene-based precursor mixtures tend to have low volatility.



**Figure 3.6.** SOA yield vs  $M_0$  for limonene, VOC mixtures, surrogates and air freshener. Yields are represented according to the following symbols: limonene only ( $\times$ ), limonene + p-cymene (Mixtures 2A, 2B, 2C, 2D) (red circles), limonene+ p-cymene +  $\alpha$ -pinene +  $\beta$ -pinene mix (mixture 3) (green triangles, face up), limonene+ linalool + p-cymene +  $\alpha$ -pinene +  $\beta$ -pinene mix (mixtures 4A and 4B) (blue squares), limonene + linalool (yellow square), surrogates 1, 2, 3 and 4 (maroon diamonds), air freshener trial 1 and trial 2 (dark green triangles with face down). The lines represent the volatility basis fit using parameters given in table below. Solid line: this work, Dotted line: Chen and Hopke;<sup>165</sup> long dash and dot dash represent the work by Saathoff et al.;<sup>92</sup> for two different conditions, dot dot dash: Zhang et al.;<sup>101</sup>. The curves are corrected for density 1g/cc by dividing the calculated values by reported density (Saathoff et al.,<sup>92</sup> density = 1.3 g  $\text{cm}^{-3}$ ; Chen and Hopke,<sup>165</sup> density = 1.5 g  $\text{cm}^{-3}$ )



**Figure 3.7.** Expanded view of Figure 3.6 SOA yield vs  $M_0$  for limonene, VOC mixtures, surrogates and air freshener. Yields are represented according to the following symbols: limonene only ( $\times$ ), limonene + p-cymene (Mixtures 2A, 2B, 2C, 2D) (red circles), limonene+ p-cymene +  $\alpha$ -pinene +  $\beta$ -pinene mix (mixture 3) (green triangles, face up), limonene+ linalool + p-cymene +  $\alpha$ -pinene +  $\beta$ -pinene mix (mixtures 4A and 4B) (blue squares), limonene + linalool (yellow square), surrogates 1, 2, 3 and 4 (maroon diamonds), air freshener trial 1 and trial 2 (dark green triangles with face down). The lines represent the volatility basis fit using parameters given in table below. Solid line: this work, dotted line: Chen and Hopke;<sup>165</sup> long dash and dot dash represent the work by Saathoff et al.;<sup>92</sup> for two different conditions, dot dot dash: Zhang et al.<sup>101</sup> The curves are corrected for density  $1 \text{ g cm}^{-3}$  by dividing the calculated values by reported density (Saathoff et al.,<sup>92</sup> density =  $1.3 \text{ g cm}^{-3}$ ; Chen and Hopke,<sup>165</sup> density =  $1.5 \text{ g cm}^{-3}$ ).

The VBS parameters for limonene SOA from previous work are listed in Table 3.6, and the corresponding curves are shown in Figure 3.6. Chen and Hopke<sup>165</sup> used a one product model, indicated by the dotted line in Figure 3.6. Saathoff et al.<sup>92</sup> used a two-product model using two different relative humidities; the long dash short dash represent data generated at RH = 0.02%, and the data with dot dash represent data for RH = 40%. Zhang et al.<sup>101</sup> used a VBS analysis for  $C_i^*$  of 0.1 to 1000  $\mu\text{g m}^{-3}$ , represented by the dot dot dash curve. For the higher  $M_0$  values, there is reasonable agreement between our work and the VBS curves from Chen and Hopke and Saathoff et al. At lower  $M_0$  values, our SOA yields tend to be lower than VBS curves reported by Chen and Hopke<sup>165</sup> and Saathoff et al.<sup>92</sup> This may be due the fact that few of the experiments in this work were performed at lower precursor concentration values.

The limonene yields reported here are the significantly lower than the yields measured by Zhang et al.<sup>101</sup> The  $\alpha$  values given in this reference for  $C_i^*$  of 0.1 to 1000  $\mu\text{g m}^{-3}$  are {0, 0.03, 0.29, 0.31, 0.3, 0.6}. The volatility bins are similar for  $C_i^*$  values of 100  $\mu\text{g m}^{-3}$  and 1000  $\mu\text{g m}^{-3}$ . In work by Zhang et al.,<sup>101</sup> a larger chamber (10  $\text{m}^3$ ) was used and for all experiments mentioned by Zhang et al.,<sup>101</sup> the volume of 2-butanol introduced in the chamber remained constant even for higher concentrations of limonene in the chamber. It is possible that lower amount of OH radicals are scavenged and may lead to increase in SOA yields. All the mass-based yields calculated as described in text above are listed in Table 3.6 below.

**Table 3.6** Fitted  $\alpha_i$  values and  $C_i^*(\mu\text{g m}^{-3})$  for volatility basis set of limonene and air freshener

$C_i^*$	Zhang et al. <sup>a</sup>	This work <sup>a</sup>
	$\alpha_i$	$\alpha_i$
0.01	0	0
0.1	0.03	0
1	0.29	0.0031
10	0.31	0.15
100	0.3	0.35
1000	0.6	0.55
Chen and Hopke 2009 <sup>b</sup>		
	$\alpha_i$	
44.4	0.969	-
Saathoff et al. 2009 <sup>c</sup>		
	$\alpha_i$	
T = 293.3 K and RH = 0.02%		
0.714	0.171	-
24.39	0.618	-
T = 293.4 K and RH = 40%		
2.340	0.171	-
24.39	0.556	-

<sup>a</sup> Density of 1 g cm<sup>-3</sup> used<sup>b</sup> Density of 1.5 g cm<sup>-3</sup><sup>c</sup> Density of 1.3 g cm<sup>-3</sup>

### 3.3.4 Conclusion on SOA yield studies

To conclude, SOA yield generation studies were carried out for limonene and VOC mixtures containing limonene. The VOCs in the mixtures were in the same ratio as present in the air freshener. The SOA yields generated from limonene and p-cymene mixtures were statistically similar to SOA yields obtained from limonene alone experiments. The other reactive VOCs present in the mixture ( $\alpha$ -pinene and  $\beta$ -pinene) generated the statistically similar yields as limonene alone and limonene p-cymene mixtures. Linalool though present in large quantities in the mixture did not contribute significantly towards SOA yield, upon ozonolysis linalool may



generate small linear chain products which could not be condense to generate PM. The SOA yields from surrogates though statistically similar were higher than the SOA yields from limonene based air freshener experiments with similar SOA content. The mass based yields,  $\alpha$ , were calculated and compared to previous literature.

### 3.3.5 SOA speciation studies

#### 3.3.5.1 Identification of SOA products

Filters collected from SOA generation experiments were extracted and analyzed by GC/MS (section 2.11). Many of the SOA species generated by ozonolysis of limonene do not have authentic standards and their identification is based on the interpretation of mass spectra of the derivatized compound in complimentary EI mode and CI mode. Initial identification was done using mass spectra in CI mode, where mass fragments and adduct fragments were used for initial determination of number of functional groups and molecular weight of the silylated derivative. Following the initial identification, confirmation of compounds was done by analyzing the mass fragmentation pattern in EI mode. Identification of trimethylsilyl derivatives has been discussed in detail by Rontani and Aubert<sup>205</sup>, and Rontani and Aubert.<sup>206</sup> BSTFA reacts with  $-\text{COOH}$  and  $-\text{OH}$  groups to form trimethylsilyl esters and ethers, respectively. These characteristic ions have  $m/z$  values of 73 ( $\text{Si}(\text{CH}_3)_3^+$ ), 89 ( $\text{OSi}(\text{CH}_3)_3^+$ ), and 117 ( $((\text{C}(\text{O})\text{OSi}(\text{CH}_3)_3)^+$ ). Fragment ions of trimethylsilyl derivatives observed in EI mode include  $m/z$  values  $\text{M}^+$  (where M is the molecular weight of silylated compound),  $(\text{M}-15)^+$ ,  $(\text{M}-73)^+$ ,  $(\text{M}-89)^+$ , and  $(\text{M}-117)^+$ . Adduct ions are observed in the CI mode,  $(\text{M}+1)^+$  and  $(\text{M}+73)^+$ . Previous work by Jaoui et al.,<sup>207</sup> have reported other adduct ions,  $(\text{M}+29)^+$  due to  $(\text{C}_2\text{H}_5)^+$  and  $(\text{M}+41)^+$  due to  $(\text{C}_3\text{H}_7)^+$  in CI mode are

characteristic when methane is used as a CI reagent. However, neither of these adducts were observed as in this work acetonitrile is used as CI reagent.

### **3.3.5.2 Quantification of SOA products and calculation of amount of SOA collected**

All the observed SOA products were identified using surrogate standards. The SOA products that were observed have either one or two polar hydrogen atoms which were replaced by trimethylsilyl derivative upon reaction with BSTFA. For products with one replaceable hydrogen, cis-pinonic acid or dodecanoic acid were used as the surrogate standard. For SOA products with two replaceable hydrogen atoms, sebacic acid or dodecanedioic acid was used as the surrogate standard. The appropriate surrogate standard was also selected on the basis of the retention time match to the SOA products. The quantity of SOA product calculated was corrected for the percent of SOA recovered from the filter by the average percent recovery of palmitic acid (d-31) and myristic acid (methyl, d-3). The corrected amount of SOA product was divided by amount of SOA collected on filters and multiplied by one hundred, to give percentage of respective product identified for each filter sample. Table 3.8 summarizes these values. The total percent of SOA observed is obtained by summing up the individual SOA product percentage. The total percentage of SOA identified varies from 13% to 40%. The amount of SOA products identified is less than 100%, as positive (ca. 60%) and negative (ca. 40%) artifacts exist for the amount of SOA collected on filter.<sup>208</sup> Also, though utmost care was taken, the time between collection of filter samples and their actual analysis using GC/MS may have lead to loss of some SOA.

### 3.3.5.3 Speciation studies for SOA generated from limonene

SOA that is generated from the ozonolysis of limonene comprises at least fifteen products, and these tend to be oxygenated ring-opening products. Since few authentic standards exist for these compounds, identification has been based on previous work on limonene-ozone SOA product analysis and mass spectral identification based on ion fragmentation patterns.<sup>209</sup> The compounds that were tentatively identified are listed according to their retention time: 2-hydroxy-3-(prop-1-en-2-yl)pentanedial, 5-oxohexanoic acid, 6-oxoheptanoic acid, ketolimononic acid, limononic acid, ketonorlimonic acid, limonic acid, ketolimononic acid, 5-hydroxy limononic acid, 7-hydroxy limononic acid, compound with molecular formula  $C_9H_{14}O_4$ , 7-hydroxy limonaldehyde, limonic acid, 5-hydroxy ketolimononic acid, 7-hydroxy ketolimononic acid. The structures and mass spectra of EI and CI modes are listed in appendix III. These products are consistent with previous work on limonene SOA.<sup>83</sup> We do not detect 3-isopropenyl-6-oxoheptanal or 5-methyl-5-vinyltetrahydrofuran-2-ol which has been reported as major oxidized SOA product generated by ozonolysis of limonene,  $\alpha$ -pinene,  $\beta$ -pinene and linalool.<sup>167</sup> The products are more volatile than the carboxylic compounds mentioned above and hence are not detected by the methodology used in this work.

Filter samples for two experiments of limonene were extracted and analyzed, the percent individual SOA product yields are listed in Table 3.7. The numbers discussed in the text are numbers averaged for the two experiments. Limononic acid was the most dominant product identified products (13.7% on average). The least dominant product was 5-hydroxylimononic acid (0.1% on average).

Table 3.8 compares the limonene SOA molar yields to the work done by Glasius et al.<sup>83</sup>. A molar yield is the ratio of moles of SOA product formed to moles of monoterpene reacted. The

molar yields for this work are calculated by dividing the moles of product formed by the moles of monoterpene injected in the chamber, assuming the entire amount of monoterpene is reacted. The products which are detected in this work, 2-hydroxy-3-(prop-1-en-2-yl)pentanedial 5-oxohexanoic acid, 6-oxoheptanoic acid, keto norlimonic acid,  $C_9H_{14}O_4$  and limonalic acid, but not mentioned in Glasius et al.<sup>83</sup> are the molar yields for these products are listed in Table 3.9. The yields of products for which positional isomers are identified (e.g., 5-hydroxyketolimononic acid and 7-hydroxyketolimononic acid) in this work are added to find the total amount of compounds (OH-ketolimononic acid) represented in Glasius et al.<sup>83</sup>

**Table 3.7** Summary of percent individual SOA product yields of SOA products generated by ozonolysis of limonene based precursors

2-hydroxy-3-(prop-1-en-2-yl)pentanedial	5-oxohexanoic acid	6-oxoheptanoic acid	C <sub>8</sub> H <sub>14</sub> O <sub>3</sub>	ketolimononic acid	limononic acid	ketonorlimonic acid	limonic acid	ketolimononic acid	5-hydroxy limononic acid	7-hydroxy limononic acid	C <sub>9</sub> H <sub>14</sub> O <sub>4</sub>	7-hydroxylimonalddehyde	limonic acid	5-hydroxyketolimononic acid	7-hydroxyketolimononic acid	Total SOA identified (%)
Mixture 1. Limonene (367±48 µg m <sup>-3</sup> )																
2.36	0.577	0.488	n.d.	5.55	14.3	0.417	0.785	2.85	0.060	1.74	0.996	1.68	1.21	0.571	0.443	34.0
1.34	0.376	0.327	n.d.	3.21	13.0	0.637	0.551	3.39	0.140	2.21	1.63	1.16	1.04	0.532	0.686	30.2
<i>1.85</i>	<i>0.48</i>	<i>0.488</i>	<i>n.d.</i>	<i>4.38</i>	<i>13.6</i>	<i>0.527</i>	<i>0.668</i>	<i>3.12</i>	<i>0.037</i>	<i>1.97</i>	<i>1.314</i>	<i>1.42</i>	<i>1.13</i>	<i>0.552</i>	<i>0.565</i>	<i>32.1</i>
Mixture 2A. Limonene (374±48 µg m <sup>-3</sup> ) and p-cymene (8.4±1 µg m <sup>-3</sup> ) <sup>a</sup>																
1.55	0.426	0.410	n.d.	4.64	18.2	0.815	0.803	4.62	0.154	2.66	1.93	1.48	2.08	1.05	1.00	41.8
1.49	0.374	0.354	n.d.	3.74	15.63	0.642	0.588	3.66	0.304	2.67	1.5	1.01	1.29	0.650	0.614	34.5
Mixture 2B, 2C and 2D Limonene (374±48 µg m <sup>-3</sup> ) and p-cymene (approx. 80±10 µg m <sup>-3</sup> ) <sup>b</sup>																
1.99	0.508	0.516	n.d.	5.48	13.7	0.662	0.724	3.48	0.304	2.16	0.996	1.85	1.84	0.730	0.647	35.6
0.541	0.447	0.326	n.d.	4.83	14.3	0.903	0.683	3.92	0.365	3.02	1.29	1.01	1.61	0.650	0.727	34.6
1.59	0.492	0.351	n.d.	4.46	17.0	0.535	0.490	2.42	0.106	1.86	1.16	1.51	1.20	0.494	0.482	34.2
<i>1.46</i>	<i>0.449</i>	<i>0.391</i>	<i>n.d.</i>	<i>4.63</i>	<i>15.8</i>	<i>0.711</i>	<i>0.658</i>	<i>3.62</i>	<i>0.247</i>	<i>2.48</i>	<i>1.36</i>	<i>1.37</i>	<i>1.60</i>	<i>0.715</i>	<i>0.694</i>	<i>36.1</i>

2-hydroxy-3-(prop-1-en-2-yl)pentanedial	5-oxohexanoic acid	6-oxoheptanoic acid	$C_8H_{14}O_3$	ketolimononic acid	limononic acid	ketonorlimonic acid	limonic acid	ketolimononic acid	5-hydroxy limononic acid	7-hydroxy limononic acid	$C_9H_{14}O_4$	7-hydroxylimonaldehyde	limonic acid	5-hydroxyketolimononic acid	7-hydroxyketolimononic acid	Total SOA identified (%)
Mixture 3. Limonene ( $379 \pm 48 \mu g m^{-3}$ ), p-cymene ( $10 \pm 1 \mu g m^{-3}$ ), $\alpha$ -pinene ( $10 \pm 1 \mu g m^{-3}$ ) and $\beta$ -pinene ( $30 \pm 4 \mu g m^{-3}$ )																
1.53	0.427	0.468	n.d.	5.12	5.95	1.01	2.69	5.38	0.215	3.18	2.65	1.89	2.66	1.19	1.34	35.7
1.72	0.509	0.475	n.d.	4.84	7.95	1.04	2.56	5.02	0.401	2.69	2.43	1.26	1.64	0.991	0.971	34.5
<i>1.62</i>	<i>0.468</i>	<i>0.472</i>	n.d.	<i>4.98</i>	<i>6.95</i>	<i>1.03</i>	<i>2.63</i>	<i>5.20</i>	<i>0.308</i>	<i>2.934</i>	<i>2.54</i>	<i>1.57</i>	<i>2.15</i>	<i>1.09</i>	<i>1.2</i>	<i>35.2</i>
Mixture 4A. Limonene ( $377 \pm 47 \mu g m^{-3}$ ), Linalool ( $236 \pm 29 \mu g m^{-3}$ ), p-cymene ( $9 \pm 1 \mu g m^{-3}$ ), $\alpha$ -pinene ( $10 \pm 1 \mu g m^{-3}$ ) and $\beta$ -pinene ( $33 \pm 4 \mu g m^{-3}$ ) <sup>c</sup>																
1.07	0.412	0.374	n.d.	4.51	4.74	0.893	1.98	3.69	0.157	2.33	1.52	1.30	1.71	0.799	1.01	26.5
Mixture 4B. Limonene ( $368 \pm 46 \mu g m^{-3}$ ), Linalool ( $238 \pm 30 \mu g m^{-3}$ ), p-cymene ( $11 \pm 1 \mu g m^{-3}$ ), $\alpha$ -pinene ( $11 \pm 1 \mu g m^{-3}$ ) and $\beta$ -pinene ( $36 \pm 4 \mu g m^{-3}$ ) <sup>c</sup>																
0.766	0.319	0.275	n.d.	4.58	3.18	0.760	1.95	3.59	0.268	2.04	0.888	1.09	1.54	0.764	0.690	22.7
Mixture 4C. Limonene ( $370 \pm 46 \mu g m^{-3}$ ), Linalool ( $1138 \pm 140 \mu g m^{-3}$ ), p-cymene ( $11 \pm 1 \mu g m^{-3}$ ), $\alpha$ -pinene ( $10 \pm 1 \mu g m^{-3}$ ) and $\beta$ -pinene ( $29 \pm 4 \mu g m^{-3}$ ) <sup>c</sup>																
0.460	0.251	0.179	n.d.	3.96	2.91	0.823	2.03	3.75	0.113	1.70	1.01	0.738	1.26	0.654	0.774	20.6
n.d.	0.308	0.225	n.d.	2.97	2.40	0.895	1.27	4.25	0.208	2.30	1.21	0.841	1.27	0.679	0.846	19.7
<i>0.766</i>	<i>0.319</i>	<i>0.275</i>	n.d.	<i>4.00</i>	<i>3.31</i>	<i>0.843</i>	<i>1.81</i>	<i>3.82</i>	<i>0.187</i>	<i>2.09</i>	<i>1.16</i>	<i>0.992</i>	<i>1.44</i>	<i>0.724</i>	<i>0.829</i>	<i>22.3</i> <i>7</i>
Mixture 5. Limonene ( $368 \pm 46 \mu g m^{-3}$ ) and Linalool ( $234 \pm 29 \mu g m^{-3}$ )																
0.562	0.377	0.320	n.d.	4.03	3.56	0.980	0.632	4.67	0.123	1.40	2.23	1.73	1.86	0.918	0.708	24.1

2-hydroxy-3-(prop-1-en-2-yl)pentanedial	5-oxohexanoic acid	6-oxoheptanoic acid	C <sub>8</sub> H <sub>14</sub> O <sub>3</sub>	ketolimononic acid	limononic acid	ketonorlimonic acid	limonic acid	ketolimononic acid	5-hydroxy limononic acid	7-hydroxy limononic acid	C <sub>9</sub> H <sub>14</sub> O <sub>4</sub>	7-hydroxylimonaldehyde	limonic acid	5-hydroxyketolimononic acid	7-hydroxyketolimononic acid	Total SOA identified (%)
Surrogate 1. Limonene (375±47 µg m <sup>-3</sup> ), Linalool (225±28 µg m <sup>-3</sup> ), Estragole (107±13 µg m <sup>-3</sup> ), γ-terpinene (85±11 µg m <sup>-3</sup> ), α-terpineol (52±6 µg m <sup>-3</sup> ), β-pinene (31±4 µg m <sup>-3</sup> ), terpinolene (22±3 µg m <sup>-3</sup> ), p-cymene (11±1 µg m <sup>-3</sup> ), α-pinene (9±1 µg m <sup>-3</sup> ) and anethole (20±3 µg m <sup>-3</sup> )																
0.287	0.475	0.010	n.d.	4.73	2.97	1.54	3.45	5.09	0.396	4.64	2.75	0.715	3.89	1.55	1.53	34.0
Surrogate 2. Limonene (368±46 µg m <sup>-3</sup> ), Linalool (239±30 µg m <sup>-3</sup> ), Estragole (110±14 µg m <sup>-3</sup> ), γ-terpinene (84±10 µg m <sup>-3</sup> ), α-terpineol (50±6 µg m <sup>-3</sup> ), β-pinene (40±5 µg m <sup>-3</sup> ), terpinolene (23±3 µg m <sup>-3</sup> ), p-cymene (10±1 µg m <sup>-3</sup> ), α-pinene (10±1 µg m <sup>-3</sup> ) and anethole (20±3 µg m <sup>-3</sup> )																
0.237	0.472	n.d.	n.d.	5.51	2.96	1.41	2.95	6.56	0.418	4.71	2.10	1.28	4.24	1.47	1.66	36.0
Surrogate 3. Limonene (350±43 µg m <sup>-3</sup> ), Linalool (1086±134 µg m <sup>-3</sup> ), Estragole (76±9 µg m <sup>-3</sup> ), γ-terpinene (22±3 µg m <sup>-3</sup> ), α-terpineol (24±3 µg m <sup>-3</sup> ), β-pinene (99±12 µg m <sup>-3</sup> ), terpinolene (23±3 µg m <sup>-3</sup> ), p-cymene (62±8 µg m <sup>-3</sup> ), α-pinene (16±2 µg m <sup>-3</sup> ) and anethole (43±5 µg m <sup>-3</sup> )																
0.196	0.523	0.019	n.d.	5.43	2.88	1.66	3.53	5.20	0.315	4.61	2.64	0.964	3.97	1.48	1.60	35.0
0.240	0.505	0.015	n.d.	4.55	2.55	1.50	3.06	5.51	0.381	4.52	2.38	0.938	3.89	1.30	1.39	32.7

2-hydroxy-3-(prop-1-en-2-yl)pentanedial	5-oxohexanoic acid	6-oxoheptanoic acid	C <sub>8</sub> H <sub>14</sub> O <sub>3</sub>	ketolimononic acid	limononic acid	ketonorlimonic acid	limonic acid	ketolimononic acid	5-hydroxy limononic acid	7-hydroxy limononic acid	C <sub>9</sub> H <sub>14</sub> O <sub>4</sub>	7-hydroxylimonaldehyde	limonic acid	5-hydroxyketolimononic acid	7-hydroxyketolimononic acid	Total SOA identified (%)
Surrogate 3. Limonene (201±25 µg m <sup>-3</sup> ), Linalool (623±77 µg m <sup>-3</sup> ), Estragole (43±5 µg m <sup>-3</sup> ), γ-terpinene (12±2 µg m <sup>-3</sup> ), α-terpineol (14±2 µg m <sup>-3</sup> ), β-pinene (57±7 µg m <sup>-3</sup> ), terpinolene (13±2 µg m <sup>-3</sup> ), p-cymene (35±4 µg m <sup>-3</sup> ), α-pinene (9±1 µg m <sup>-3</sup> ) and anethole (24±3 µg m <sup>-3</sup> )																
n.d.	0.138	n.d.	n.d.	1.38	0.965	0.855	1.94	2.60	0.108	1.71	0.676	0.504	1.17	0.529	0.541	13.1
Limonene based air freshener-Trial 1: limonene (201±25 µg m <sup>-3</sup> ), β-pinene (53±6 µg m <sup>-3</sup> ), terpinolene (5±1 µg m <sup>-3</sup> )α-pinene (6±1 µg m <sup>-3</sup> ) <sup>h</sup>																
0.094	0.192	n.d.	9.27	1.27	0.841	0.619	1.06	2.39	0.163	1.70	0.774	0.549	1.41	0.562	0.520	21.4
n.d.	0.304	0.121	8.65	1.21	0.997	0.749	1.70	3.30	0.206	2.50	0.977	0.470	1.26	0.459	0.384	23.3
<i>0.094</i>	<i>0.248</i>	<i>0.121</i>	<i>8.96</i>	<i>1.24</i>	<i>0.919</i>	<i>0.684</i>	<i>1.38</i>	<i>2.85</i>	<i>0.184</i>	<i>2.10</i>	<i>0.875</i>	<i>0.509</i>	<i>1.33</i>	<i>0.510</i>	<i>0.452</i>	<i>22.4</i>
Limonene based air freshener-Trial 2: limonene (322±40 µg m <sup>-3</sup> ), β-pinene (89±9 µg m <sup>-3</sup> ), terpinolene (8±1 µg m <sup>-3</sup> ), α-pinene (10±1 µg m <sup>-3</sup> ) <sup>h</sup>																
n.d.	0.550	n.d.	14.4	2.53	1.39	1.40	2.33	5.17	0.396	4.13	2.02	0.788	3.43	0.713	0.777	40.0
n.d.	0.452	0.038	13.1	1.63	1.46	1.52	2.88	6.14	0.398	3.82	2.18	0.842	2.57	1.13	0.968	39.1
n.d.	0.536	0.030	12.8	1.62	1.35	1.29	2.48	5.17	0.470	3.99	2.38	0.801	3.63	1.28	0.729	38.5
<i>n.d.</i>	<i>0.513</i>	<i>0.034</i>	<i>13.4</i>	<i>1.93</i>	<i>1.40</i>	<i>1.40</i>	<i>2.56</i>	<i>5.49</i>	<i>0.421</i>	<i>3.98</i>	<i>2.19</i>	<i>0.810</i>	<i>3.21</i>	<i>1.04</i>	<i>0.825</i>	<i>39.2</i>



**Table 3.8** Molar yields (%) for SOA products identified by Glasius et al. and this work

	limonene concentration ( $\mu\text{g m}^{-3}$ )	Ozone concentration (ppb)	limonic acid	keto limonic acid	nor limonic acid	limononic acid	keto-limononic acid	nor-limononic acid	OH-limononic acid	OH-keto-limononic acid	limonaldehyde	OH-limononaldehyde
Glasius et al 2000	21000	3600	0.03	0.005	0.001	0.1	trace	0.005	0.2	0.02	0.3	0.04
	10000	1600	0.09	0.01	0.002	0.1	0.002	0.02	0.2	0.02	0.22	0.02
	345	56	0.007	0.0003	0.00003	0.01	trace	0.002	n.a. <sup>c</sup>	n.a. <sup>c</sup>	n.a. <sup>c</sup>	n.a. <sup>c</sup>
	473 <sup>a</sup>	46	0.003	0.0002	trace	0.003	trace	0.001	n.a. <sup>c</sup>	n.a. <sup>c</sup>	n.a. <sup>c</sup>	n.a. <sup>c</sup>
This work	367 <sup>b</sup>	500	0.03	0.2	n.d. <sup>d</sup>	0.8	0.2	n.d. <sup>d</sup>	0.1	0.1	n.d. <sup>d</sup>	0.07
	367 <sup>b</sup>	539	0.1	0.04	n.d. <sup>d</sup>	0.4	0.2	n.d. <sup>d</sup>	0.1	0.01	n.d. <sup>d</sup>	0.1

<sup>a</sup> methyl cyclohexane is used as radical scavenger, other experiments did not use any radical scavenger <sup>b</sup> 2-butanol is used as radical scavenger <sup>c</sup> these compounds were not analyzed <sup>d</sup> these compounds were not detected

**Table 3.9** Molar yields for SOA products identified in this work

	limonene concentration ( $\mu\text{g m}^{-3}$ )	Ozone concentration (ppb)	2-hydroxy-3-(prop-1-en-2-yl)pentanediol	5-oxohexanoic acid	6-oxoheptanoic acid	ketonorlimonic acid	$\text{C}_9\text{H}_{14}\text{O}_4$	limononic acid
This work <sup>a</sup>	367	500	0.1	0.04	0.03	0.03	0.1	0.07
	367	539	0.08	0.02	0.02	0.09	0.2	0.2

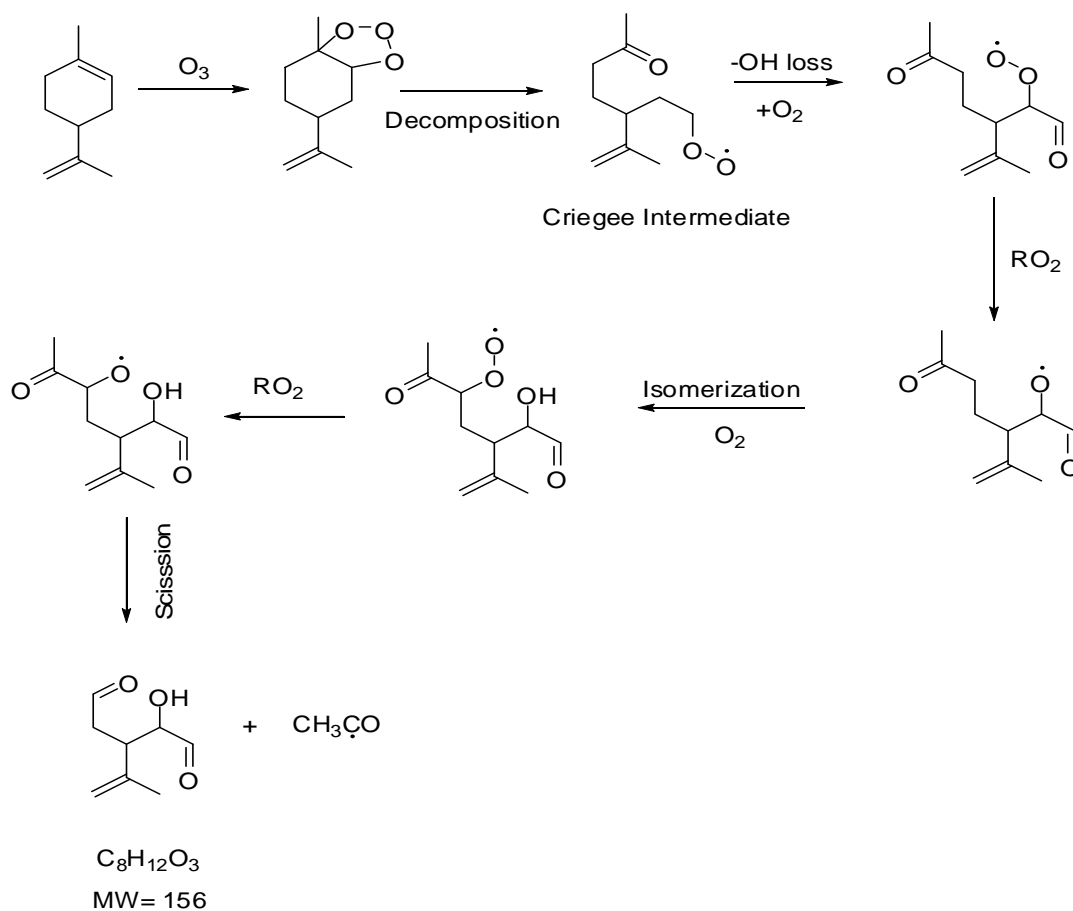
<sup>a</sup>2-butanol is used as radical scavenger <sup>c</sup> these compounds were not analyzed

From the work of Glasius et al.,<sup>83</sup> we observe that the amount of organic compounds detected is only a few percent of the reacted terpenes on a per mole basis. The molar yield calculations may be attributed to different terpene, ozone, and radical scavenger concentrations. From molar yields obtained in this work and from Glasius et al.,<sup>83</sup> we observe that the dominant oxidation product in condensed phase SOA is limononic acid. Limonaldehyde is another major product reported by Glasius et al.,<sup>83</sup> which is detected in gas phase of the SOA, and cannot be detected by the methodology used in this dissertation. All the products identified in this work were found to be in the same magnitude as reported by earlier work. Discrepancy if any may be due the use of different type of filters used for SOA sampling and the physical parameters of the experiment. TissuQuartz filters were used in this work while Glasius et al.,<sup>83</sup> use PTFE filter for SOA collection. In addition, the experiments by Glasius et al.<sup>83</sup> were performed at higher RH (40-55%), and our experiments are performed at lower RH conditions (4-5%). Higher RH conditions lead to fast nucleation and condensation of the particles and increasing the effective particle size of SOA

Since amounts of the precursor and  $O_3$  are much higher than ambient levels, the SOA product yields do not necessarily give accurate estimation of the ambient yields. However, the products formed and the reaction mechanisms followed for their formation remain same as in ambient conditions, because terpene ozone chemistry is independent of concentrations.<sup>210</sup>

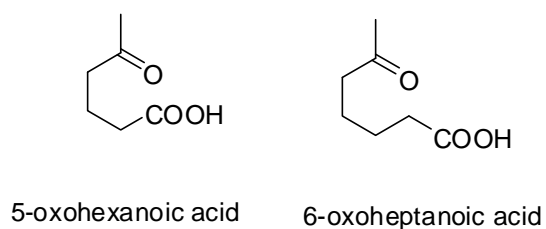
For all the limonene SOA products identified, the products from the ring opening dominates; i.e. the endocyclic double bond reacts with ozone. This reaction pathway is a dominant pathway for limonene ozone reactions.<sup>164</sup> The reaction mechanisms for ketolimononic acid, 5-hydroxyketolimononic acid, and 7-hydroxyketolimononic acid were discussed by Jaoui et al.,<sup>169</sup> and the mechanisms for limononic acid, limonic acid and limonalic acid were discussed by Leungsakul et al.<sup>164</sup> Mechanisms for products other than 4-ethyl-5-methylhexe-5-enoic acid, 5-oxohexanoic acid and 6-oxoheptanoic acid are discussed by Glasius et al. (2000) and Jaoui et al.<sup>207</sup>. To our knowledge, none of the studies have reported these three products in the SOA generated during oxidation of limonene.

A suggested mechanism for synthesis of 2-hydroxy-3-(prop-1-en-2-yl)pentanedial is shown in Figure 3.8 below. The exo bond of limonene is attacked by ozone to generate an ozonide which undergoes decomposition to generate a Criegee biradical. The Criegee biradical then undergoes a rearrangement with loss of  $-OH$  radical and is attacked by oxygen atom to form a peroxy radical which is converted to alkoxy radical by abstraction using  $RO_2$ , in or set up this by radical can be an alkyl peroxy radical. This radical is then attacked by a oxygen atom undergoes a second cycle of peroxy radical to alkoxy radical conversion. The alkoxy radical then losses an acetyl radical due to transfer of a free electron transfer.<sup>170</sup>



**Figure 3.8** Synthesis of 2-hydroxy-3-(prop-1-en-2-yl)pentanedial adopted from Walser et al.<sup>170</sup>

The next two products were tentatively identified as 5-oxohexanoic acid and 6-oxoheptanoic acid. These two products have been identified as ozonolysis products of cyclohexene.<sup>176</sup>



**Figure 3.9** Structures for 5-oxohexanoic acid and 6-oxoheptanoic acid

### 3.3.5.4 Speciation studies for SOA generated from limonene + p-cymene mixture

For second set of experiments we added p-cymene to limonene this mixture was made to investigate the effect of non-reactive VOC on limonene SOA products. Reaction rate for p-cymene with ozone is negligible,<sup>65</sup> and thus does p-cymene does not contribute to formation of the particles. The experiments were performed in two parts for first part experiments with p-cymene concentration of  $8 \mu\text{g m}^{-3}$  and limonene concentration of  $374 \mu\text{g m}^{-3}$ , which is approximately same ratio they are in the limonene based air freshener. For second part experiments with the concentration of p-cymene was increased by a factor of 10, so the ratio of p-cymene:limonene was 10:45, the p-cymene concentration being  $80 \mu\text{g m}^{-3}$  and limonene concentration being  $374 \mu\text{g m}^{-3}$ . In both cases, we found that addition of p-cymene did not lead to formation of any different species in comparison to the limonene-only experiment. Furthermore, the percent individual SOA product yields that were calculated for p-cymene limonene precursor mixtures were similar to that calculated from limonene as precursor alone, and the lower and higher concentrations of p-cymene do not impact the product yields of the SOA. The highest yielding product for the limonene/p-cymene precursor mixture was limononic acid and the lowest was 5-hydroxylimononic acid, and this is the same as the limonene only experiments. All other products follow a close trend when compared to limonene SOA products.

To confirm the hypothesis that presence of p-cymene with limonene does not affect the SOA products formed by limonene alone statistical two-tailed student's t-test to compare the percent individual SOA product yield for the products generated by limonene experiments and limonene and p-cymene mixture were performed. With the probability values (p) obtained from this helps in evaluating if there is significant difference in individual yields of products, we use null hypothesis ( $p < 0.05$ ). In case of limonene and p-cymene mixtures, the lowest probability value

was found for limonic acid ( $p=0.057$ ). Hence, we conclude that, there is no significant difference between the product yields generated by oxidizing limonene alone and limonene and p-cymene mixtures.

### **3.3.5.5 Speciation studies for SOA generated from limonene, p-cymene, $\alpha$ -pinene, and $\beta$ -pinene mixture**

Two filter samples containing condensed phase SOA from ozonolysis of VOC mixture containing limonene ( $379 \mu\text{g m}^{-3}$ ), p-cymene ( $10 \mu\text{g m}^{-3}$ ),  $\alpha$ -pinene ( $10 \mu\text{g m}^{-3}$ ), and  $\beta$ -pinene ( $30 \mu\text{g m}^{-3}$ ) were solvent extracted and analyzed, this mixture involves other reactive VOCs  $\alpha$ -pinene and  $\beta$ -pinene. The SOA products generated by this precursor mixture are listed in Table 3.8. The GC/MS analysis of the extracts of these filters did not show generation of any characteristic ozonolysis products for  $\alpha$ -pinene and  $\beta$ -pinene. Limonene is the most concentrated reactive species in this mixture nearly 30 times more concentrated than  $\alpha$ -pinene and more than ten times concentrated than  $\beta$ -pinene, hence the products generated from ozonolysis of this VOC mixture are more characteristic of limonene. Moreover, the GC/MS methodology is not able to distinguish between structurally close structures generated by oxidation of different terpenes<sup>211</sup> (eg.: pinic acid and limonic acid have similar structures and co-elute on the GC column).

A two tail student's t-test were performed to compare the percent individual SOA product yields obtained from ozonolysis of this mixture to percent individual SOA product yields obtained from ozonolysis of limonene. The hypothesis tested is presence of other reactive precursor should lead to increase in individual SOA product yields for all the components. The results obtained from t-test show that the six products show probability of  $p<0.05$ , indicating that there is statistically significant difference between these products upon addition of  $\alpha$ -pinene and

$\beta$ -pinene. The yield for product 6-oxoheptanoic acid increased from 0.39 % for limonene and limonene+p-cymene mixtures to 0.47 % for this precursor ( $p < 0.04$ ). A largest decrease was observed in the individual yields of limononic acid ( $p < 0.01$ ), from 15.2 % for limonene and limonene+p-cymene mixtures to 7.0% for this VOC mixture. A small but a significant ( $p < 0.05$ ) increase was observed in the percent yields of ketonorlimonic acid (0.7% to 1.0%), limonic acid (0.7% to 2.6%), ketolimononic acid (3.6% to 5.2%), and  $C_9H_{14}O_4$  (1.4% to 2.7%). Thus presence of  $\alpha$ -pinene and  $\beta$ -pinene with limonene leads to increase in individual yields of some of the products. This increase may be due to contribution from products generated by ozonolysis of  $\alpha$ -pinene and  $\beta$ -pinene. However, the decrease in concentration of limononic acid is may be due to reaction between the Criegee intermediate and the terpenes as mentioned by Heaton et al. The Criegee intermediates can react with oxidation products and generate oligomers which may not be detected by the GC/MS methods used in this dissertation.

### 3.3.5.6 Speciation studies for SOA generated from linalool containing mixtures

In linalool-containing mixtures, there are three mixtures: one which is a mixture of five terpenes mixtures in same ratio as they would be present in the air freshener (limonene  $377 \mu\text{g m}^{-3}$ , linalool  $236 \mu\text{g m}^{-3}$ ,  $\alpha$ -pinene  $10 \mu\text{g m}^{-3}$ ,  $\beta$ -pinene  $33 \mu\text{g m}^{-3}$ , and p-cymene  $9 \mu\text{g m}^{-3}$ ), in second mixture the concentration of linalool is increased by five times (limonene:  $370 \mu\text{g m}^{-3}$ , linalool  $1130 \mu\text{g m}^{-3}$ ,  $\alpha$ -pinene  $11 \mu\text{g m}^{-3}$ ,  $\beta$ -pinene  $36 \mu\text{g m}^{-3}$ , and p-cymene  $11 \mu\text{g m}^{-3}$ ), and a third containing two terpenes (limonene  $377 \mu\text{g m}^{-3}$ , and linalool  $234 \mu\text{g m}^{-3}$ ). Linalool is a major VOC (14.4% by mass) present in limonene based air freshener and has ozone reaction rates comparable to limonene. However, from chamber studies we found that linalool does not contribute towards SOA formation. Hence to confirm this finding multiple mixtures with varying

amounts of linalool were made. SOA filters were obtained from each type of linalool mixture. This VOC mixture did not generate any characteristic SOA products upon ozonolysis. Total of five SOA filters were extracted and analyzed using GC/MS for linalool containing mixtures refer, Table 3.7. A two tailed Student's t-test was performed to study the variation in individual SOA product yields as an effect of linalool addition, comparison was made between the limonene,  $\alpha$ -pinene,  $\beta$ -pinene and p-cymene. The percent individual SOA product yields for seven ozonolysis products were found to be significantly different than when generated in the limonene,  $\alpha$ -pinene,  $\beta$ -pinene and p-cymene mixture ( $p < 0.05$ ). The oxidation products, 2-hydroxy-3-(prop-1-en-2-yl)pentanedial, 5-oxohexanoic acid, 6-oxoheptanoic acid, showed small decrease in individual SOA product yields while a larger decrease is seen in the yield of limononic acid. The limononic acid yield is lower (3.35 %) than the yield observed (7.0 %) in case of limonene,  $\alpha$ -pinene,  $\beta$ -pinene and p-cymene mixture in section 3.5.5. The other products with  $p < 0.05$  are ketonorlimonic acid, limonic acid and 5-ketohydroxyketolimononic acid, refer Table 3.7, all these products show a slight increase in the percent yield. The possible explanation for reduction in the SOA product yields of limononic acid may be due to reaction of SOA products with Criegee intermediates to generate oligomers which may be not detected by this method. The percent SOA product yield for limononic acid are found decrease further upon addition of linalool than in the limonene,  $\alpha$ -pinene,  $\beta$ -pinene and p-cymene mixture.

### 3.3.5.7 Speciation studies for SOA generated from surrogates

Surrogates 1, 2, and 3 had the same limonene concentration as the all other mixtures discussed so far (approx.  $370 \mu\text{g m}^{-3}$ ). A Student's t test was performed on the percent individual SOA yields, generated from this surrogate mixtures and linalool, limonene,  $\alpha$ -pinene,  $\beta$ -pinene



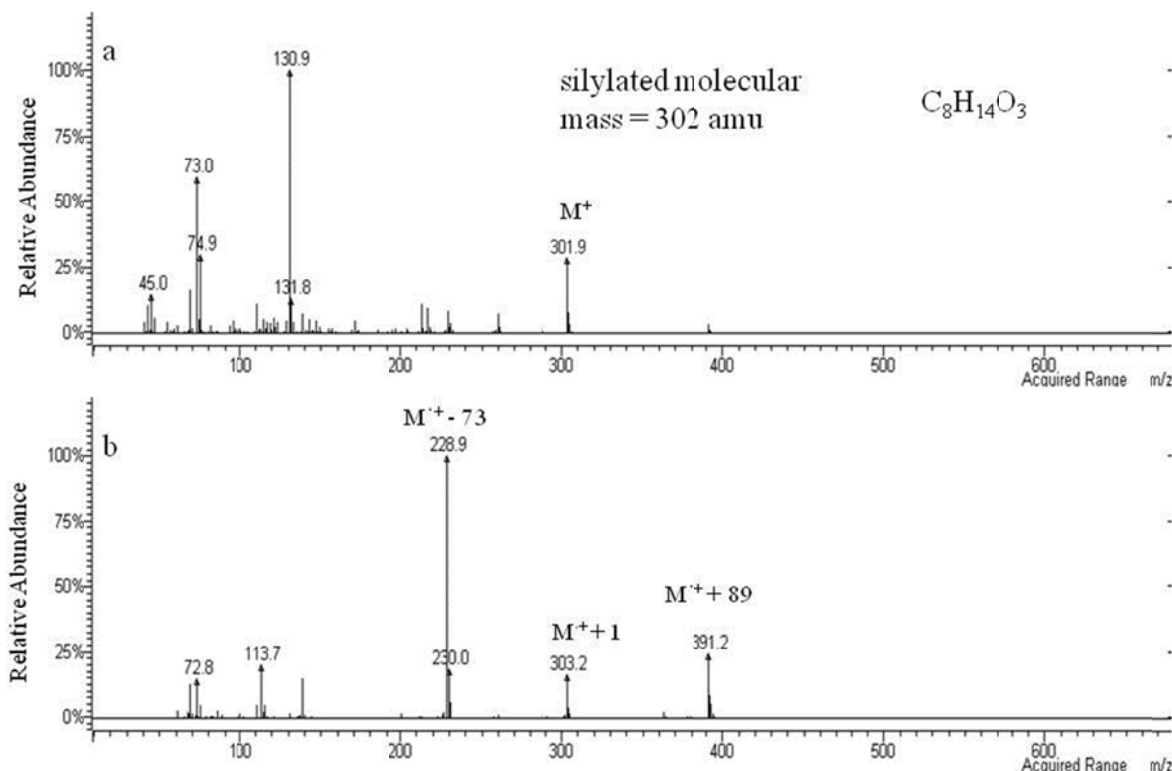
and p-cymene VOC mixture. The testing shows all products have  $p < 0.05$ , and hence the individual SOA product yields are found to be significantly different for surrogate standards 1, 2, and 3. The yield of limononic acid showed a significance difference and a decrease to 2.9% from the linalool containing mixtures (approx. 3.2%). All the other components showed an increase by a factor of 1.5 to 2; the exceptions were 2-hydroxy-3-(prop-1-en-2-yl)pentanedial and 6-oxoheptanoic acid, which showed a decrease from linalool containing VOC mixtures. The surrogate has ten VOC's present in them (refer Table 3.7). The decrease in product individual SOA yield for limononic acid might be correlated to increase in concentration of other VOCs. An experiment for surrogate 3 with lower injection volume was performed the SOA filter was extracted and analyzed. SOA generated from a lower concentration VOC surrogate generated products similar to VOC surrogate with higher concentrations. The products yields were found to be lower for this experiment corresponding to lower concentration of VOCs in surrogate.

### **3.3.5.8 Speciation studies for limonene based air freshener**

The individual SOA product yields generated from surrogates 1, 2, and 3 theoretically should be same as limonene based air freshener trial 2, as this trial of air freshener contains same concentration of reactive VOCs as those present in surrogates 1, 2, and 3. However, most of the products have lower individual SOA product yields percentages 2-hydroxy-3-(prop-1-en-2-yl)pentanedial, 5-oxohexanoic acid, 6-oxoheptanoic acid, ketolimononic acid, limonoic acid, 5-OH limonic acid, 7-OH limonic acid, limonalic acid, 5-OH ketolimononic acid and 7-OH ketolimononic acid than the surrogates ( $p < 0.05$ ). Some products stay at the same percentage yield those are ketonorlimonic acid, limonic acid, ketolimononic acid,  $C_9H_{14}O_4$ , and 7-OH limonaldehyde. The variation in the amount of products is found to be very random. The

lowering of individual SOA product yield lead may be related to the lowering of SOA yields from the chamber experiments.

An additional peak was observed in the chromatograms of extracted SOA generated from limonene-based air freshener in comparison to extracted SOA from limonene mixtures. The mass spectrum for the compound is shown in Figure 3.10 below. The mass spectra obtained do not follow the same fragmentation rules which have been discussed in earlier section 3.5.2. For structure elucidation the molecular ion peak is considered to be at 303 m/z in CI mode, the corresponding spectra in the EI mode does not show presence of  $M^+ - 15$ , but  $M^+$  is observed. In CI mode  $M^+ - 73$  and  $M^+ + 89$  are observed. Hence it is hard to identify the structure for the molecule, using the classical fragmentation pattern for the silyl derivative. Fragmentation pattern in the CI mode is used along with knowledge of other SOA products formed this product is tentatively suggested to have a formula of  $C_8H_{14}O_3$ .  $C_8H_{14}O_3$  has the highest percentage individual yield of SOA products generated by ozonolysis of the air freshener. However, inadequate mass spectral fragmentation pattern prevents from structural elucidation of this compound.



**Figure 3.10** Mass fragmentation pattern for  $C_8H_{14}O_4$  a) fragments in EI mode, b) fragments in CI mode

### 3.4 Conclusions

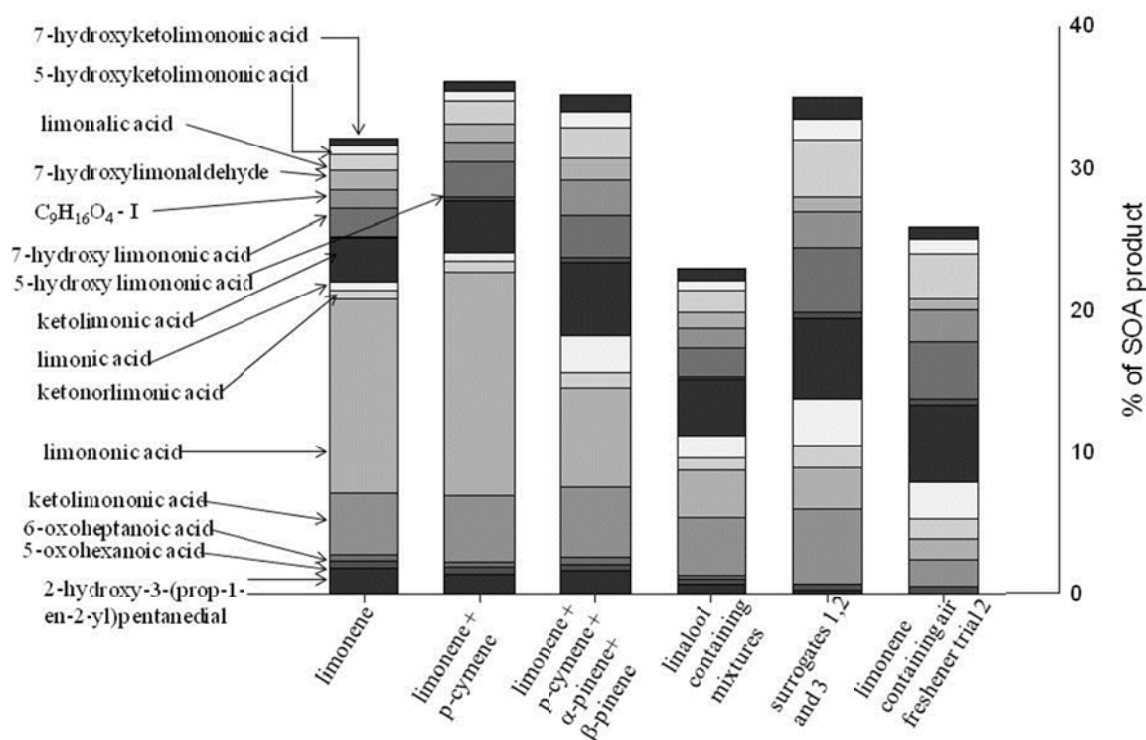
SOA yield studies were carried out for limonene, limonene containing VOC mixtures, and commercially available limonene based air freshener. The SOA yields were found to be statistically similar for limonene and various limonene containing mixtures. This implies that when limonene is a most concentrated VOC in a mixture the SOA generated can be characteristic of limonene. Linalool though present in large concentrations did not contribute towards SOA yields. The products from linalool oxidation are small chain compounds and may not condense to a significant extent to count towards generation of SOA. The yields for surrogates were found to be higher than the SOA yields generated by air freshener.

The individual SOA product yields were found to be similar for limonene and limonene+p-cymene mixtures, indicating that p-cymene is a non-reactive VOC that does not take part in SOA generation or alter the course of reaction. The VOC mixture containing limonene, p-cymene,  $\alpha$ -pinene and  $\beta$ -pinene showed an increase in SOA product yields: when compared to product yields from limonene only experiments, for 6-oxo-heptanoic acid (from 0.4% to 0.5%), ketonorlimonic acid (from 0.7% to 1.0%), limonic acid (from 0.7% to 2.6%), ketolimononic acid (from 3.6% to 5.2%), and  $C_9H_{14}O_4$  (from 1.4% to 2.7%). These small differences imply that  $\alpha$ -pinene and  $\beta$ -pinene contribute towards increase in yields of these products. For linalool containing mixtures the oxidation products, decreases in products were observed: 2-hydroxy-3-(prop-1-en-2-yl)pentanedial (from 1.5% to 0.7%), 5-oxohexanoic acid (from 0.5% to 0.3%), 6-oxoheptanoic acid (from 0.4% to 0.3%). These changes were small decreases in the individual SOA product yields in comparison to individual mass based SOA product yields. However, a larger decrease was observed for limononic acid (from 15.2% to 3.3%).

The individual SOA product yields for limonene-based air freshener were found to be lower than those found in surrogates. The total SOA mass identified for surrogates is 35% while for air freshener the total mass of SOA products identified are 30%. The ozonolysis of limonene based air freshener yielded a new product which had not been detected as an oxidation product for any of the earlier VOC mixtures. The suggested tentative molecular formula for this product is suggested as  $C_8H_{14}O_3$ .

Figure 3.11 is a graphical version of the data given in Table 3.8, and it shows variation in composition of the SOA obtained from limonene alone and mixtures of limonene and other VOCs. The SOA precursor or precursor mixture is noted on the x-axis, and the yields of individual SOA products are represented by different shades on a gray scale. The observed

products for each mixture are also observed in limonene with the exception of 5-hydroxy limonic acid which was present in very small yields for limonene SOA, and hence to be visually distinguishable is marked on the second bar of the graph. The VOC mixtures for p-cymene at both higher and lower concentration are grouped together. All the data obtained from five SOA filters of linalool containing mixtures are grouped together.



**Figure 3.11** Variation in composition of SOA products among various limonene precursors

From the figure we observe that there is a decrease in amount of limononic acid as the number of VOCs used to make a limonene containing mixtures increases. This decrease in yield can be explained by formation of oligomers among the Criegee radical with one of the ozonolysis products, which could not have been identified with the methodology used in this dissertation.

## CHAPTER 4

### SPECIATION STUDIES FOR SOA PRODUCTS GENERATED FROM OZONOLYSIS OF $\alpha$ -PINENE, $\alpha$ -PINENE VOC MIXTURES, AND FIR NEEDLE OIL

#### 4.1 Introduction

In Chapter 3, we discussed the formation of SOA and condensed phase SOA products generated from limonene, VOC mixtures containing limonene and commercially available limonene based air freshener. In this chapter, speciation studies will be discussed for  $\alpha$ -pinene, VOC mixtures containing  $\alpha$ -pinene, and two essential oils, Siberian fir needle oil (SFNO), and Canadian fir needle oil (CFNO).

##### 4.1.1 SOA from $\alpha$ -pinene and ozone reactions

The most dominant monoterpene emitted in the atmosphere is  $\alpha$ -pinene. The presence of endocyclic double bond makes it susceptible to oxidation reactions with OH, NO<sub>3</sub>, and O<sub>3</sub> in the atmosphere. Hence, owing to its high concentrations in atmosphere and ability to undergo oxidation to generate low volatility products,  $\alpha$ -pinene ozone chemistry has been investigated by many research groups<sup>50,83,84,112,177,204,212</sup>

Hoffmann et al.<sup>112</sup> reported SOA yields for experiments for several terpenes, including  $\alpha$ -pinene, in presence of ozone and NO<sub>x</sub>. The authors report that for the reaction of  $\alpha$ -pinene (and other terpenes) with ozone under dark conditions, the SOA yields were found to be higher than when SOA was generated by photo-oxidation and in presence of NO<sub>x</sub>. Yu et al.,<sup>84</sup> carried out a series of smog chamber experiments for ozonolysis of  $\alpha$ -pinene, 3-carene,  $\beta$ -pinene, and sabinene. The authors report that more than ten ozonolysis products were generated from  $\alpha$ -pinene experiments, and the products were compounds containing carbonyl, hydroxyl, and

carboxyl functional groups. The analysis of products was done by GC/MS. The compounds were separated and identified as an oxime-derivative or a silyl-derivative. The authors reported molar yields for both gas-phase and condensed phase products generated during the reactions. The authors report that the combined identified gas-phase and condensed phase products account for more than 90% of aerosol mass generated during  $\alpha$ -pinene and ozone reactions. The authors also estimate that the error associated with the amount of ozonolysis products can be as high as 50%. The authors found that the highest concentration of the condensed-phase SOA products generated from  $\alpha$ -pinene were pinonic acid and pinic acid, while pinonaldehyde and OH-pinonaldehyde were the most concentrated products generated in the gas phase.

Glasius et al.<sup>83</sup> analyzed the SOA generated from five individual monoterpenes including  $\alpha$ -pinene, the SOA was analyzed by GC/MS and HPLC/MS. The authors reported that there are three major classes of compounds formed from the ozonolysis reactions: dicarboxylic acids, oxocarboxylic acids, and hydroxyketocarboxylic acids. The most abundant products generated from ozonolysis of  $\alpha$ -pinene were found to be pinic acid, pinonic acid, and 10-OH pinonic acid. The authors also report structurally similar products generated from other monoterpenes like 3-carene, limonene,  $\beta$ -pinene, and sabinene. Koch et al.<sup>87</sup> had similar results, where the most dominant species generated by ozonolysis of  $\alpha$ -pinene,  $\beta$ -pinene, sabinene, 3-carene, and limonene was corresponding C<sub>9</sub>-dicarboxylic acid. The authors also suggest a hydroperoxide channel for generation of C<sub>9</sub>-dicarboxylic acid, example pinonic acid if the precursor is  $\alpha$ -pinene (Refer Figure 1.2). Presto et al.<sup>99</sup> also suggested similar product formation as earlier studies where dominant species were organic acids, keto acids, and hydroxy keto acids.

Jaoui and Kamens<sup>213</sup> carried out oxidation reactions for  $\alpha$ -pinene in presence of NO<sub>x</sub> and sunlight. The authors reported that more than 16 products were identified and quantified in this

study. On average, measured gas and particle phase products accounted for 54% to 71% of the carbon reacted in  $\alpha$ -pinene. Also, 10-hydroxypinonic acid, 10-hydroxypinonaldehyde, 4-oxopinonic acid, and 10-oxopinonic acid were observed in the early stage in the aerosol phase and may play an important role in the early formation of secondary aerosols.

Ma et al.<sup>212</sup> investigated the dependence of the product yields of various condensed phase products (pinic acid, pinonic acid, norpinonic acid, norpinic acid, norpinalic acid, pinalic-3-acid, 4-OH-pinalic-3-acid) on reaction conditions. Measuring the variation in the amount of products as a function of the reaction conditions helps elucidate the reaction mechanism between  $\alpha$ -pinene and ozone. Like limonene ozonolysis,  $\alpha$ -pinene ozonolysis can lead to generation of oligomers which have been reported by Gao et al..<sup>217</sup> The authors found that more than 50% products were present in oligomeric form. In this work we do not observe any oligomer or dimer formed from ozonolysis of  $\alpha$ -pinene.

#### 4.1.2 SOA generation from mixed VOC systems containing $\alpha$ -pinene

Only four studies of  $\alpha$ -pinene mixtures have been reported in literature.<sup>175,177,215</sup> Warring et al.,<sup>175</sup> investigated SOA formation from ozone reactions with both single terpenoids and mixtures of limonene,  $\alpha$ -pinene, and  $\alpha$ -terpineol. The particle number concentration, at higher level of ozone (100 ppb), were reported in following order, mixture of limonene/ $\alpha$ -pinene/ $\alpha$ -terpineol > limonene/ $\alpha$ -terpineol >  $\alpha$ -terpineol > limonene. This was expected as the mixtures contained reactive VOC concentrations higher than the individual terpenes. At lower ozone concentrations (25 ppb), particle number concentrations decreased in following order, limonene > limonene/ $\alpha$ -pinene/ $\alpha$ -terpineol >  $\alpha$ -pinene/ $\alpha$ -terpineol > limonene/ $\alpha$ -terpineol >  $\alpha$ -pinene >  $\alpha$ -terpineol. This data show that at limiting ozone concentrations the nucleation potential of d-



limonene is higher as individual and upon addition of other terpenoids the nucleation potential is reduced. A similar trend is not observed for higher ozone concentrations (100ppb). The authors explain large observed nucleation event may be due to formation of secondary ozonides at ozone-limiting concentrations as observed by Nøjgaard et al.<sup>176</sup> These findings imply that the nucleation and particle mass formation potential of products may not be related.

Jaoui and Kamens<sup>177</sup> have performed SOA generation and product identification studies for SOA generated from ozonolysis of a monoterpene mixture containing  $\alpha$ -pinene and  $\beta$ -pinene. The authors identified and quantified more than twenty-nine products in this study. On average, the combined measured gas and particle phase products accounted for  $\sim 74$  to  $\sim 80\%$  of the reacted  $\alpha$ -pinene/ $\beta$ -pinene mixture carbon. The products formed from  $\beta$ -pinene predominantly are present in the gas phase or were structurally similar to SOA products generated from  $\alpha$ -pinene.

Forester and Wells<sup>216</sup> carried out studies with to quantify the OH radical formation during ozonolysis reactions of  $\alpha$ -pinene, limonene and  $\alpha$ -terpineol. This process is important as generation of OH radicals upon terpene ozone reaction, adds to the additional reactivity as OH can further react with VOCs leading to increase in the oxygenated species formed. The authors conducted experiments to investigate the OH yields from these terpenes individually and as two-component terpene mixtures, they compare the OH yields with pine oil cleaning product. The authors found that the OH radicals generated from individual experiments were equal for limonene and  $\alpha$ -terpineol and highest for  $\alpha$ -pinene. Overall the hydroxyl radical yields were highest for a binary mixture of limonene/ $\alpha$ -pinene, followed by pine oil cleaner and lowest OH yields were obtained for mixture of  $\alpha$ -terpineol/  $\alpha$ -pinene and  $\alpha$ -terpineol/limonene.

Jaoui et al.<sup>215</sup> measured the effect of added isoprene and/or SO<sub>2</sub> on SOA production from the photooxidation of  $\alpha$ -pinene/toluene/NO<sub>x</sub> mixture. The purpose of this work was to determine how the addition of isoprene and/or SO<sub>2</sub> affected not only the mass concentration of SOA formed but also the chemical composition of the SOA formed. The results showed that the addition of isoprene to the base  $\alpha$ -pinene/toluene/NO<sub>x</sub> case decreased the concentration of SOA formed by 51%. It was suggested that since isoprene has a rapid reaction rate with OH, the addition of isoprene would affect the radical concentrations, which affects the chemical composition of photooxidation products at steady state. The presence of isoprene leads to a decrease in the amount of HNO<sub>3</sub> produced from the gas-phase reaction NO<sub>2</sub> and OH. A decrease in the amount of toluene reacted was observed, likely a result of a lack of OH present. This led to a reduction in the concentration of toluene oxidation products (benzaldehyde and glyoxal) at steady state and an increase in the concentration of isoprene oxidation products (carbonyl and dicarbonyl products) at steady state. The addition of SO<sub>2</sub> slightly increased the amount of SOA formed by 15%.

In this chapter, the products extracted from the SOA filters obtained from chamber experiments performed by Meagan Hatfield are discussed. The chamber experiments involved filters from ozonolysis of  $\alpha$ -pinene, VOC mixtures containing  $\alpha$ -pinene, and two essential oils namely, Siberian fir needle oil (SFNO) and Canadian fir needle oil (CFNO)<sup>74</sup>.

**The goal of this chapter is to study speciation of condensed phase SOA products generated by ozonolysis from  $\alpha$ -pinene and VOC mixtures containing  $\alpha$ -pinene and compare the findings to commercial essential oils namely Siberian fir needle oil and Canadian fir needle oil. These VOC mixtures are made to match the composition of**

**$\alpha$ -pinene and other VOCs in the essential oils and hence are different from the limonene dominating mixtures discussed in Chapter 3.**

## **4.2 Experimental details**

### **4.2.1 SOA generation experiments**

The chamber setup and methods used to generate SOA from  $\alpha$ -pinene and other VOC mixtures were similar to those used for limonene (refer section 3.2) and the procedures described by Hatfield and Huff Hartz.<sup>74</sup> The SOA filter samples used for speciation studies in this chapter were collected during SOA generation experiments performed by Meagan Hatfield. The samples were procured from a freezer where the samples were stored at -18 °C, in an air tight container. The filters were solvent extracted, the extracts were silylated and analyzed by using GC/MS methodologies described in Chapter 3. The experimental parameters and yields for SOA generation experiment for different  $\alpha$ -pinene precursors are discussed in Hatfield and Huff Hartz<sup>74</sup> and Hatfield.<sup>182</sup>

## **4.3 Results and discussion**

### **4.3. 1 SOA filters from ozonolysis of $\alpha$ -pinene and VOC mixtures**

The SOA filters extracted and analyzed for  $\alpha$ -pinene and VOC mixtures are listed in Table 4.1, and the amounts of SOA collected from each of these experiments are also given. The amount of SOA collected on the filter is the PM concentration, measured by the SMPS, averaged over the time that the vacuum was applied, multiplied by the average flow rate measured by the flow meter. The filters were collected during chamber experiments performed by Meagan Hatfield, and the SOA yields and experimental parameters were given in Hatfield and Huff

Hartz.<sup>74</sup> After SOA filter collection, the samples were stored at -18 °C, and were extracted within maximum period of one year after SOA generation experiment. The filter samples in Table 4.2 in this chapter are from Table 2 in the publication.

The speciation for the simplest system was analyzed: a total of four SOA filter samples were collected for  $\alpha$ -pinene-only SOA generation experiments (refer Table 4.1). The next sets of filters were obtained from SOA generation experiments performed on mixtures containing  $\alpha$ -pinene and bornyl acetate. Bornyl acetate does not react with ozone and, under the conditions for SOA generation given by Hatfield and Huff Hartz,<sup>74</sup> does not affect the SOA yield. The speciation of three mixtures containing varying amount of bornyl acetate were analyzed. . The first mixture (Table 4.1, mixture 6a, numbering continued from Chapter 3) contained  $280 \pm 10 \mu\text{g m}^{-3}$  of  $\alpha$ -pinene and  $400 \pm 10 \mu\text{g m}^{-3}$  of bornyl acetate, where the concentrations represent the initial amount of VOC injected into the chamber prior to ozone reaction and particle generation. A second experiment was done with increased injection volume for the same mixture, hence leading to  $\alpha$ -pinene concentration of  $300 \pm 20 \mu\text{g m}^{-3}$  and bornyl acetate concentration of  $420 \pm 20 \mu\text{g m}^{-3}$ . These two experiments generated one filter sample each and were used for SOA speciation in this chapter. A second mixture (Table 4.1, mixture 6b) with  $310 \pm 10 \mu\text{g m}^{-3}$  of  $\alpha$ -pinene and  $2860 \pm 90 \mu\text{g m}^{-3}$  bornyl acetate yielded three filter samples. A last set of filter for from this mixture was obtained for an experiment (Table 4.1, mixture 6c) with  $\alpha$ -pinene concentration of  $350 \pm 20 \mu\text{g m}^{-3}$  and bornyl acetate concentration of  $8900 \pm 500 \mu\text{g m}^{-3}$ .

Two additional SOA filter samples, with other non-reactive VOCs were analyzed. An SOA filter sample, obtained from a mixture (mixture 7) of  $\alpha$ -pinene ( $290 \pm 20 \mu\text{g m}^{-3}$ ), bornyl acetate ( $400 \pm 20 \mu\text{g m}^{-3}$ ), and camphene ( $180 \pm 10 \mu\text{g m}^{-3}$ ) and two SOA filters, obtained from mixture

(mixture 8) of  $\alpha$ -pinene ( $280 \pm 10 \mu\text{g m}^{-3}$ ), bornyl acetate ( $400 \pm 20 \mu\text{g m}^{-3}$ ), camphene ( $177 \pm 8 \mu\text{g m}^{-3}$ ), and borneol ( $23 \pm 1 \mu\text{g m}^{-3}$ ), were extracted and speciated.

In all the mixtures mentioned so far the only reactive precursor, under experimental conditions was  $\alpha$ -pinene. The next set of filter samples was collected from SOA generated from reactive precursor mixtures, where  $\beta$ -pinene, 3-carene, and limonene were added to  $\alpha$ -pinene. One SOA filter was obtained from the  $\alpha$ -pinene and  $\beta$ -pinene mixture experiments (Mixture 9). Three filter samples, one for each of three SOA generation experiments, were for VOC mixtures containing  $\alpha$ -pinene,  $\beta$ -pinene, and 3-carene (mixture 10). One filter sample was obtained for SOA generated from ozonolysis of a mixture of  $\alpha$ -pinene,  $\beta$ -pinene, 3-carene, and limonene (mixture 11). The mixtures containing reactive VOCs other than  $\alpha$ -pinene should increase the quantity and number of SOA products and generate products that are characteristic of the added VOC.

**Table 4.1** VOC precursor concentrations and amount of SOA collected on filters from ozonolysis of  $\alpha$ -pinene and other VOC mixtures

Reactive precursor	Non-reactive species	Injection volume ( $\mu\text{L}$ )	Reactive VOC concentration <sup>a</sup> ( $\mu\text{g m}^{-3}$ )	Mass of SOA collected on filter ( $\mu\text{g}$ ) <sup>b</sup>
$\alpha$ -pinene ( $230 \pm 20 \mu\text{g m}^{-3}$ )				
$\alpha$ -pinene	-	$1.5 \pm 0.1$	$230 \pm 20$	27.7
$\alpha$ -pinene	-	$1.5 \pm 0.1$	$230 \pm 20$	26.9
$\alpha$ -pinene ( $280 \pm 20 \mu\text{g m}^{-3}$ )				
$\alpha$ -pinene	-	$1.8 \pm 0.1$	$280 \pm 20$	22.6
$\alpha$ -pinene	-	$1.8 \pm 0.1$	$280 \pm 20$	20.7
Mixture 6a $\alpha$ -pinene ( $280 \pm 10 \mu\text{g m}^{-3}$ ) and bornyl acetate ( $400 \pm 10 \mu\text{g m}^{-3}$ )				
$\alpha$ -pinene	bornyl acetate	$4.2 \pm 0.1$	$280 \pm 10$	23.9
$\alpha$ -pinene	bornyl acetate	$4.3 \pm 0.1$	$300 \pm 20$	35.0
Mixture 6b $\alpha$ -pinene ( $310 \pm 10 \mu\text{g m}^{-3}$ ) and bornyl acetate ( $2860 \pm 90 \mu\text{g m}^{-3}$ )				
$\alpha$ -pinene	bornyl acetate	$19 \pm 0.2$	$310 \pm 10$	30.3
$\alpha$ -pinene	bornyl acetate	$19 \pm 0.2$	$310 \pm 10$	45.7
$\alpha$ -pinene	bornyl acetate	$19 \pm 0.2$	$310 \pm 10$	51.3
Mixture 6c $\alpha$ -pinene ( $350 \pm 20 \mu\text{g m}^{-3}$ ) and bornyl acetate ( $8900 \pm 500 \mu\text{g m}^{-3}$ )				
$\alpha$ -pinene	bornyl acetate	$55 \pm 0.3$	$350 \pm 20$	49.6
Mixture 7 $\alpha$ -pinene ( $290 \pm 20 \mu\text{g m}^{-3}$ ), bornyl acetate ( $400 \pm 20 \mu\text{g m}^{-3}$ ) and camphene ( $180 \pm 10 \mu\text{g m}^{-3}$ )				
$\alpha$ -pinene	bornyl acetate + camphene	$5.9 \pm 0.1$	$280 \pm 10$	52.5
Mixture 8 $\alpha$ -pinene ( $280 \pm 10 \mu\text{g m}^{-3}$ ), bornyl acetate ( $400 \pm 20 \mu\text{g m}^{-3}$ ), camphene ( $177 \pm 8 \mu\text{g m}^{-3}$ ) and borneol ( $23 \pm 1 \mu\text{g m}^{-3}$ )				
$\alpha$ -pinene	bornyl acetate + camphene + borneol	$6.1 \pm 0.1$	$280 \pm 10$	22.4
$\alpha$ -pinene	bornyl acetate + camphene + borneol	$6.1 \pm 0.1$	$280 \pm 10$	30.4
Mixture 9 $\alpha$ -pinene ( $280 \pm 10 \mu\text{g m}^{-3}$ ) and $\beta$ -pinene ( $30 \pm 1 \mu\text{g m}^{-3}$ )				
$\alpha$ -pinene + $\beta$ -pinene	-	$2.0 \pm 0.1$	$310 \pm 20$	44.3

Reactive precursor	Non-reactive species	Injection volume (μL)	Reactive VOC concentration <sup>a</sup> (μg m <sup>-3</sup> )	Mass of SOA collected on filter (μg) <sup>c</sup>
Mixture 10 α-pinene (280±10 μg m <sup>-3</sup> ), β-pinene (30±1 μg m <sup>-3</sup> ) and 3-carene (190±10 μg m <sup>-3</sup> )				
α-pinene +β-pinene +3-carene	-	3.3±0.1	500±20	69.5
α-pinene +β-pinene +3-carene	-	3.3±0.1	500±20	139
α-pinene +β-pinene +3-carene	-	3.3 ± 0.1	500±20	104
Mixture 11 α-pinene (280±10 μg m <sup>-3</sup> ), β-pinene (30±1 μg m <sup>-3</sup> ), 3-carene (150±10 μg m <sup>-3</sup> ) and limonene (30±1 μg m <sup>-3</sup> )				
α-pinene +β-pinene +3-carene +limonene	-	3.2±0.1	490±20	110

<sup>a</sup>The uncertainties in VOC concentration calculated by propagation of uncertainty associated with syringe used for VOC injection, density of VOC and uncertainty in volume of bag (estimated 10%). <sup>b</sup>The amount of SOA collected on the filter is the PM concentration measured by the SMPS averaged over the time that the vacuum was applied, flow rate of the vacuum. The mixtures 1-5 are numbered for limonene containing mixtures in Chapter 3

#### 4.3.2 SOA filters from ozonolysis of SFNO surrogates, SFNO, and CFNO

The filters that were analyzed for SOA product analysis from SFNO surrogates, SFNO, and CFNO are listed in Table 4.2, and the details for these experiments were given in Table 4 and Table 5 of Hatfield and Huff Hartz.<sup>74</sup> All VOCs present and their concentrations in the SFNO surrogates are shown in the row of Table 4.2, the reactive precursors are listed in the column. The data for SFNO surrogates and CFNO are listed in Table 4 of the publication. Experiment for SFNO trial 1 is listed in Table 4 and the other trial 2 is listed in Table 5 of the publication. In these two trials for SFNO, a different volume of SFNO was injected in the chamber. The only reactive precursors for SFNO and CFNO are listed in the Table 4.2, and the non-reactive

precursors have been discussed in detail in Hatfield and Huff Hartz<sup>74</sup> and in theses of Meagan L. Hatfield.<sup>182</sup>



**Table 4.2** VOC precursor concentrations and amount of SOA collected on filters from oxidation of SFNO surrogates, SFNO, and CFNO

Reactive precursor	Injection volume (μL)	Reactive VOC concentration <sup>a</sup> (μg m <sup>-3</sup> )	Mass of SOA collected on filter (μg) <sup>b</sup>
SFNO Surrogate 1: α-pinene (290±20 μg m <sup>-3</sup> ), bornyl acetate (410±53 μg m <sup>-3</sup> ), camphene (310±20 μg m <sup>-3</sup> ), 3-carene (160±10 μg m <sup>-3</sup> ), limonene (35±3 μg m <sup>-3</sup> ), borneol (24±2 μg m <sup>-3</sup> ), β-pinene (31±4 μg m <sup>-3</sup> ), β-caryophyllene (6.6±0.5 μg m <sup>-3</sup> ), terpinolene (8.0±0.7 μg m <sup>-3</sup> ), α-caryophyllene (6.2±0.5 μg m <sup>-3</sup> ), and p-cymene (3.7±0.2 μg m <sup>-3</sup> )			
α-pinene +3-carene +limonene +β-pinene	7.6±0.1	540±30	82.6
SFNO Surrogate 2: α-pinene (200±10 μg m <sup>-3</sup> ), bornyl acetate (450±20 μg m <sup>-3</sup> ), camphene (290±20 μg m <sup>-3</sup> ), 3-carene (157±8 μg m <sup>-3</sup> ), limonene (70±4 μg m <sup>-3</sup> ), borneol (27±2 μg m <sup>-3</sup> ), β-pinene (28±3 μg m <sup>-3</sup> ), β-caryophyllene (14±2 μg m <sup>-3</sup> ), terpinolene (8±2 μg m <sup>-3</sup> ), α-caryophyllene (7±2 μg m <sup>-3</sup> ), p-cymene (4±2 μg m <sup>-3</sup> ), camphor (2±2 μg m <sup>-3</sup> ) and α-terpinene (29±2 μg m <sup>-3</sup> )			
α-pinene +3-carene +limonene +β-pinene	8.6±0.1	510±20	176
SFNO trial 1: Refer to Table 1 Hatfield and Huff Hartz (2011) for composition			
α-pinene +3-carene +limonene +β-pinene	7.0±0.1	430±10	129
α-pinene +3-carene +limonene +β-pinene	7.0±0.1	430±10	146
SFNO trial 2: Refer to Table 1 Hatfield and Huff Hartz (2011) for composition			
α-pinene +3-carene +limonene +β-pinene	9.0±0.1	560±20	164
CFNO: Refer to Table 1 Hatfield and Huff Hartz (2011) for composition			
α-pinene +3-carene +limonene +β-pinene	4.3 ± 0.1	530 ± 70	216

<sup>a</sup>The uncertainties in VOC concentration calculated by propagation of uncertainty associated with syringe used for VOC injection, density of VOC and uncertainty in volume of bag (estimated 10%). <sup>b</sup>The amount of SOA collected on the filter is the PM concentration measured by the SMPS averaged over the time that the vacuum was applied, flow rate of the vacuum.

#### 4.3.3 Speciation studies for SOA products

The details on identification of SOA products remain the same as discussed in section 3.3.5.1 of this dissertation. To summarize, the chromatograms of SOA filter extracts were compared to the chromatograms of chamber filter extracts to identify the peaks that occur due to condensed-phase SOA products. The extracted condensed-phase SOA products were identified using the mass fragmentation patterns obtained in EI and CI-ACN mode used in a complementary manner. The fragmentation patterns in CI-ACN mode revealed the silylated molecular ion  $(M+1)^+$  and trimethyl silyl adduct  $(M+73)^+$ . The EI mode was used to further ascertain the molecular weight of the product, and the fragments observed in EI mode were  $(M-15)^+$ , formed by loss of a methyl group, and  $M^+$ , which is the molecular ion of the silylated product. The other ions used in EI mode for confirming the molecular weight were  $(M-73)^+$ ,  $(M-89)^+$ , and  $(M-117)^+$ , formed by loss of,  $(-\text{Si}(\text{CH}_3)_3)$ ,  $(-\text{OSi}(\text{CH}_3)_3)$ , and  $(-\text{COOSi}(\text{CH}_3)_3)$  respectively.<sup>84</sup>

Quantitative analysis of the SOA products was done in similar manner as discussed in Chapter 3. The ions  $M^+$  and  $(M-15)^+$  of standards were used to extract the peak area from total ion chromatogram, and this peak area was used to create calibration curves. An authentic standard for pinonic acid was available. The other SOA products were quantified using surrogate standards, and the surrogate standards were chosen depending upon the number of replaceable hydrogen atoms present in the structure. Monoprotic acids were quantified using either cis-pinonic acid or dodecanoic acid, where the choice depended on how closely the retention time of the standard matched the retention time of the analyte. Diprotic acids and monoprotic acids with hydroxy groups were quantified using sebacic acid as a surrogate standard. Due to lack of authentic standards use of surrogate standards for quantification of oxidation products is very common. After quantitative analysis, the amount of product formed

was corrected for the percent recoveries obtained for the internal standard. The percent individual SOA product yield, which is percent of mass of each product were recovered from SOA collected on the filter and should not be confused with SOA yield.

#### 4.3.3.1 Speciation studies for SOA generated by ozonolysis of $\alpha$ -pinene

Four filters that were sampled for  $\alpha$ -pinene SOA were solvent extracted and analyzed, and the percent individual SOA product yield for the individual condensed phase SOA products generated from ozonolysis of  $\alpha$ -pinene are summarized in Table 4.4. On an average, 61 % mass of SOA collected on filter was identified. The identified products include: (i) monoprotic acids such as pinalic-4-acid, norpinonic acid, pinonic acid, and norpinic acid; (ii) diprotic acids such as pinic acid; (iii) hydroxy-carboxylic acid such as 10-OH norpinonic acid and 10-OH pinonic acid; and (iv) an unknown product. The identified products are consistent with prior work. Hoffmann et al. (1998) reported the presence of pinic acid, norpinic acid, and pinonic acid in SOA generated from  $\alpha$ -pinene/ozone reaction. Other studies<sup>83,84,86,99</sup> reported the identification of hydroxypinonic acid, norpinonic acid and pinalic-4-acid. Jaoui and Kamens<sup>88</sup> reported 10-OH norpinonic acid as one of the products of  $\alpha$ -pinene ozonolysis. The unknown compound has derivatized molecular ion with a  $m/z$  244, which gives a molecular weight of  $172 \text{ g mol}^{-1}$  for the underivatized form for this compound if it contains only one replaceable hydrogen. From this mass spectral information and assumption the compound is tentatively identified as  $\text{C}_9\text{H}_{16}\text{O}_3$ . In this work we do not observe any pinonaldehyde or hydroxypinonaldehyde which have been reported as a major SOA product in previous studies,<sup>83,84</sup> but both these aldehyde compounds are more volatile than their carboxylic acid and alcohol counterparts, and partition predominantly to the gas phase. High molecular weight oligomers have also been reported to be generated during

ozonolysis of  $\alpha$ -pinene by Gao et al.,<sup>217</sup> and Hall and Johnston.<sup>215</sup> However, in this work all products have an unsilylated mass of less than 250 m/z, thus no oligomer products were observed, the highest temperature on GC program ramp was 320 °C. A discussion of the details of the product identification follows.

#### 4.3.3.1.1 Mass fragmentation patterns for individual SOA products

The SOA products that have been identified in this work are characteristic of  $\alpha$ -pinene ozonolysis and the mass spectra for all the products are given in Appendix IV. The first and second products eluted from the GC column have been identified as the structural isomers pinalic-4-acid and norpinonic acid (Figures A-IV-1 and 2). The mass fragmentation patterns for both analytes in CI mode show the presence of  $(M+1)^{+\cdot}$  at 243 m/z and  $(M-15)^{+\cdot}$  at 227 m/z. The trimethylsilyl adduct  $(M+73)^{+\cdot}$  at 315 m/z was not observed for pinalic-4-acid but was observed for norpinonic acid. In EI mode, the 242 m/z ion was observed for both analytes and is correlated to the molecular ion peak for the silylated forms,  $M^+$ . Next ion is observed at  $M^+-15$  which forms from loss of methyl group from derivatized molecular ion at 227 m/z. Pinalic-4-acid and norpinonic acid have the same molecular weight, but they separate on the 5% diphenyl/95% dimethylsiloxane column, and the elution order of these compounds, according to the work of Jaoui and Kamens<sup>177</sup>, was used to distinguish these compounds.

The next compound that was eluted is pinonic acid, which is one of the dominant SOA products from  $\alpha$ -pinene/ozonolysis<sup>83</sup>. The identification of this compound is done by retention time comparison with retention time of the available standard. In CI mode, the major peaks observed were 257 m/z and 329 m/z which correspond to  $(M+1)^{+\cdot}$  and  $(M+73)^{+\cdot}$  ions. In EI

mode, the most intense peak occurs at 241 m/z which corresponds to  $(M-15)^+$ . In addition we observe fragments at 256 m/z and 329 m/z, which represent the  $M^+$  and  $(M+73)^+$ , respectively.

The diprotic acid, norpinic acid, eluted next. In CI mode, peaks were observed at m/z values of 317, 389, and 227 which corresponded to the doubly- trimethylsilylated molecule ions  $(M+1)^+$ ,  $(M+73)^+$ , and  $(M-89)^+$  respectively. The  $(M-89)^+$  is attributed to loss of  $-\text{OSiMe}_3$  from the molecular ion, and this has been observed previously<sup>88</sup>. In the EI mode, the characteristic  $M^+$  and  $(M-15)^+$  ions are observed at 316 and 301 m/z respectively.

The next  $\alpha$ -pinene SOA product to elute is the unknown compound (Figure A-IV 8). The mass spectrum of this peak shows only two intense ions at 245 and 229 m/z which correspond to  $(M+1)^+$  and  $(M-15)^+$  respectively in the CI mode with no other dominating ions. The corresponding EI mode mass spectrum shows the fragments at 244 and 229 m/z for  $M^+$  and  $(M-15)^+$  respectively. The molecule is tentatively given a molecular formula of  $\text{C}_9\text{H}_{16}\text{O}_3$  which is consistent with the molecular ion identification.

The next  $\alpha$ -pinene SOA product that eluted is 10-OH norpinonic acid (Figure A-IV 9). The mass spectrum for this peak showed ions at 403, 331, 315 and 241 m/z in CI mode, which correspond to  $(M+73)^+$ ,  $(M+1)^+$ ,  $(M-15)^+$  and  $(M-89)^+$ . In EI mode, the dominant ion occurs at 315 m/z which corresponds to  $(M-15)^+$  and a very low intensity ion also occurs at 330 m/z representing  $M^+$ . The mass fragmentation pattern of 10-OH pinonic acid is similar to pinic acid, which is the compound that elutes next, the elution order for these products is also matches the elution order from work by Jaoui and Kamens.<sup>88</sup>

Pinic acid, which is one of the major products of  $\alpha$ -pinene ozonolysis, eluted next (Figure A-IV 10). The ions from this peak observed in CI mode are similar to ions observed for 10-OH

norpinonic acid. In EI mode along with  $(M-15)^+$  ion at 315 m/z,  $M^+$  at 330 m/z and  $(M+73)^+$  at 403 m/z are observed. Pinic acid is a dominant product formed from ozonolysis of  $\alpha$ -pinene.

The last  $\alpha$ -pinene SOA product observed in this study was 10-OH pinonic acid (Figure A-IV 11). 10-OH pinonic acid co-elutes with deuterated myristic acid (methyl d3), an internal standard, and thus the ions from the internal standard are marked with asterisk. These ions were identified by comparing the mass spectrum of the peak with mass spectrum of the peak from a blank filter (Figure A-IV-12). In CI mode, the ions attributed to 10-OH pinonic acid are 417, 345, and 329 m/z were observed, and these correspond to  $(M+73)^+$ ,  $(M+1)^+$ , and  $(M-15)^+$ . In EI mode fragment ions  $(M-15)^+$  ion at 329 m/z and  $(M+73)^+$  at 417 m/z are observed.

#### 4.3.3.1.2 Comparisons of SOA product yields to other work

Glasius et al.<sup>83</sup> and Yu et al.<sup>84</sup> reported molar yields for SOA products generated from  $\alpha$ -pinene ozonolysis. Glasius et al. used  $\text{BF}_3$ -methanol for formation of methyl esters from polar carboxylic acids, in conjunction with HPLC-MS<sup>n</sup> analysis for quantification of SOA products. In method used by Yu et al.<sup>84</sup>, the carbonyl groups were derivatized using O-(2,3,4,5,6-pentafluorobenzyl) hydroxylamine (PFBHA), and the carboxylic acid and the alcohol groups were derivatized using BSTFA to give trimethylsilyl (TMS) derivatives. Molar yields for SOA products are calculated by dividing the moles of product formed by the moles of terpene reacted to compare our work to the work of Glasius et al.<sup>83</sup> and Yu et al.<sup>84</sup> In general, the molar yields for SOA products generated in this work were similar to both of these previous studies (Refer Table 4.4).

The molar yields were similar in comparison to previous work. The percent molar yields for pinic acid (1.2) and pinonic acid (2.5) were dominant in our work and also in the work by

Glasius et al.<sup>83</sup> and Yu et al.,<sup>84</sup> (Table 4.4). Yu et al.<sup>84</sup> reported higher percent molar yields for SOA products formed for norpinonic acid and OH-pinonic acid. However, the molar yields for these two products are same as reported by Glasius et al.<sup>83</sup> Yu et al.<sup>84</sup> reported the molar yield for norpinonic acid as the sum of norpinonic acid and its isomer, the isomer is not observed in our work or work by Glasius et al.<sup>83</sup>

**Table 4.3** Summary of percent individual SOA product yields of SOA products generated by ozonolysis of  $\alpha$ -pinene based precursors

	pinic-4-acid	nor-pinonic acid	nor-3-caralic acid	camphene unknown 1	pinonic acid	nor pinic acid	camphene unknown 2	$\alpha$ -pinene unknown	10-OH norpinonic acid	pinic acid	10-OH pinonic acid	Total SOA identified (%)
$\alpha$ -pinene ( $230 \pm 20 \mu\text{g m}^{-3}$ )												
	0.810	0.521	n.d.	n.d.	24.5	0.524	n.d.	1.18	0.49	28.2	1.23	57.4
	0.960	0.456	n.d.	n.d.	23.3	0.490	n.d.	1.22	0.65	27.3	1.96	56.3
$\alpha$ -pinene ( $280 \pm 20 \mu\text{g m}^{-3}$ )												
	0.954	0.351	n.d.	n.d.	32.0	0.570	n.d.	1.22	0.41	31.6	1.06	68.3
	0.739	0.884	n.d.	n.d.	25.2	0.780	n.d.	2.30	0.55	29.3	2.24	62.0
Avg	0.866	0.553	n.d.	n.d.	26.2	0.591	n.d.	1.48	0.526	29.1	1.62	61.0
Mixture 6a $\alpha$ -pinene ( $290 \pm 10 \mu\text{g m}^{-3}$ ) and bornyl acetate ( $410 \pm 15 \mu\text{g m}^{-3}$ )												
	0.625	0.890	n.d.	n.d.	24.2	0.756	n.d.	1.93	0.911	25.2	1.86	56.3
	0.575	0.786	n.d.	n.d.	26.2	0.986	n.d.	2.36	0.867	27.3	2.17	61.2
Avg	0.600	0.838	n.d.	n.d.	25.2	0.871	n.d.	2.14	0.890	26.2	2.0	58.7
Mixture 6b $\alpha$ -pinene ( $310 \pm 10 \mu\text{g m}^{-3}$ ) and bornyl acetate ( $2860 \pm 90 \mu\text{g m}^{-3}$ )												
	0.524	0.346	n.d.	n.d.	23.4	0.342	n.d.	0.408	0.411	17.80	0.99	44.2
	1.000	1.445	n.d.	n.d.	22.5	0.388	n.d.	1.36	0.304	12.82	1.32	41.2
	0.766	0.352	n.d.	n.d.	21.7	0.377	n.d.	0.856	0.459	15.34	1.17	41.0
Avg	0.763	0.714	n.d.	n.d.	22.5	0.369	n.d.	0.369	0.391	15.32	1.16	42.1
Mixture 6c $\alpha$ -pinene ( $350 \pm 20 \mu\text{g m}^{-3}$ ) and bornyl acetate ( $8900 \pm 500 \mu\text{g m}^{-3}$ )												
Avg	0.436	0.165	n.d.	n.d.	17.9	0.287	n.d.	0.465	0.336	11.6	0.77	32.0
Mixture 7 $\alpha$ -pinene ( $290 \pm 20 \mu\text{g m}^{-3}$ ), bornyl acetate ( $400 \pm 20 \mu\text{g m}^{-3}$ ) and camphene ( $180 \pm 10 \mu\text{g m}^{-3}$ )												
Avg	0.510	1.58	n.d.	1.41	17.5	0.829	2.94	1.62	1.03	24.5	1.60	53.5
Mixture 8 $\alpha$ -pinene ( $280 \pm 10 \mu\text{g m}^{-3}$ ), bornyl acetate ( $400 \pm 20 \mu\text{g m}^{-3}$ ), camphene ( $177 \pm 8 \mu\text{g m}^{-3}$ ) and borneol ( $23 \pm 1 \mu\text{g m}^{-3}$ )												
	0.291	1.210	n.d.	1.084	14.3	0.829	3.03	1.30	1.42	27.9	0.926	52.3
	0.378	0.976	n.d.	0.857	15.6	0.780	3.56	1.12	1.26	28.5	0.756	53.7
Avg	0.335	1.093	n.d.	0.970	14.9	0.805	3.30	1.21	1.34	28.2	0.841	52.9
Mixture 9 $\alpha$ -pinene ( $280 \pm 10 \mu\text{g m}^{-3}$ ) and $\beta$ -pinene ( $30 \pm 1 \mu\text{g m}^{-3}$ )												
	0.335	0.664	n.d.	n.d.	16.3	0.775	n.d.	1.52	0.619	29.6	1.19	51.1
Mixture 10 $\alpha$ -pinene ( $280 \pm 10 \mu\text{g m}^{-3}$ ), $\beta$ -pinene ( $30 \pm 1 \mu\text{g m}^{-3}$ ) and 3-carene ( $190 \pm 10 \mu\text{g m}^{-3}$ )												
	0.960	0.456	3.26	n.d.	14.3	0.490	n.d.	1.220	0.650	27.3	1.96	50.6
	0.954	0.351	2.93	n.d.	15.6	0.570	n.d.	1.219	0.411	31.6	1.07	54.7
	0.739	0.884	2.96	n.d.	14.2	0.780	n.d.	2.300	0.550	29.3	2.24	54.0
Avg	0.884	0.564	3.05	n.d.	14.7	0.613	n.d.	1.580	0.537	29.4	1.76	53.1



pinalic-4-acid	nor-pinonic acid	nor-3-carelic acid	camphene unknown 1	pinonic acid	nor pinic acid	camphene unknown 2	$\alpha$ -pinene unknown	10-OH norpinonic acid	pinic acid	10-OH pinonic acid	Total SOA identified (%)
Mixture 11 $\alpha$ -pinene ( $280 \pm 10 \mu\text{g m}^{-3}$ ), $\beta$ -pinene ( $30 \pm 1 \mu\text{g m}^{-3}$ ), 3-carene ( $150 \pm 10 \mu\text{g m}^{-3}$ ) and limonene ( $30 \pm 1 \mu\text{g m}^{-3}$ )											
0.368	1.28	4.43	<i>n.d.</i>	9.49	1.10	<i>n.d.</i>	2.33	6.72	30.2	1.48	57.4
SFNO Surrogate 1: $\alpha$ -pinene ( $290 \pm 20 \mu\text{g m}^{-3}$ ), bornyl acetate ( $410 \pm 53 \mu\text{g m}^{-3}$ ), camphene ( $310 \pm 20 \mu\text{g m}^{-3}$ ), 3-carene ( $160 \pm 10 \mu\text{g m}^{-3}$ ), limonene ( $35 \pm 3 \mu\text{g m}^{-3}$ ), borneol ( $24 \pm 2 \mu\text{g m}^{-3}$ ), $\beta$ -pinene ( $31 \pm 4 \mu\text{g m}^{-3}$ ), $\beta$ -caryophyllene ( $6.6 \pm 0.5 \mu\text{g m}^{-3}$ ), terpinolene ( $8.0 \pm 0.7 \mu\text{g m}^{-3}$ ), $\alpha$ -caryophyllene ( $6.2 \pm 0.5 \mu\text{g m}^{-3}$ ), and p-cymene ( $3.7 \pm 0.2 \mu\text{g m}^{-3}$ )											
0.311	1.232	5.19	0.558	8.37	1.43	4.43	1.43	6.66	29.5	1.64	60.7
SFNO Surrogate 2: $\alpha$ -pinene ( $200 \pm 10 \mu\text{g m}^{-3}$ ), bornyl acetate ( $450 \pm 20 \mu\text{g m}^{-3}$ ), camphene ( $290 \pm 20 \mu\text{g m}^{-3}$ ), 3-carene ( $157 \pm 8 \mu\text{g m}^{-3}$ ), limonene ( $70 \pm 4 \mu\text{g m}^{-3}$ ), borneol ( $27 \pm 2 \mu\text{g m}^{-3}$ ), $\beta$ -pinene ( $28 \pm 3 \mu\text{g m}^{-3}$ ), $\beta$ -caryophyllene ( $14 \pm 2 \mu\text{g m}^{-3}$ ), terpinolene ( $8 \pm 2 \mu\text{g m}^{-3}$ ), $\alpha$ -caryophyllene ( $7 \pm 2 \mu\text{g m}^{-3}$ ), p-cymene ( $4 \pm 2 \mu\text{g m}^{-3}$ ), camphor ( $2 \pm 2 \mu\text{g m}^{-3}$ ) and $\alpha$ -terpinene ( $29 \pm 2 \mu\text{g m}^{-3}$ )											
0.230	0.895	6.35	0.782	11.1	1.49	5.12	1.34	8.21	33.2	2.15	70.8
Avg	0.271	1.06	5.77	0.607	9.73	1.46	4.77	1.38	7.43	31.3	65.8
SFNO trial 1 <sup>a</sup> : reactive VOCs = $430 \pm 10 \mu\text{g m}^{-3}$											
0.223	0.655	2.71	3.94	3.94	0.408	2.28	0.692	4.24	7.18	0.641	26.9
0.124	0.681	2.44	3.35	3.06	0.365	2.26	0.747	3.11	7.47	0.378	24.0
Avg	0.173	0.668	2.57	3.65	3.50	0.386	2.27	0.719	3.67	7.32	25.4
SFNO trial 2 <sup>a</sup> : reactive VOCs = $560 \pm 20 \mu\text{g m}^{-3}$											
0.104	0.403	2.51	1.03	2.72	0.250	2.85	0.454	3.76	10.8	0.467	24.5
CFNO <sup>a</sup> : reactive VOCs = $530 \pm 70 \mu\text{g m}^{-3}$											
<i>n.d.</i>	0.652	1.40	0.264	0.775	0.260	0.869	0.563	3.81	15.1	0.323	24.0

<sup>a</sup>percent individual SOA product yields <sup>b</sup>The reactive precursors comprise of  $\alpha$ -pinene, 3-carene, limonene,  $\beta$ -pinene,  $\beta$ -caryophyllene, terpinolene,  $\alpha$ -caryophyllene, and  $\alpha$ -terpinene.

**Table 4.4** Comparison of molar yields for  $\alpha$ -pinene SOA ozonolysis products in percentage (%)

	$\alpha$ -pinene concentration ( $\mu\text{g m}^{-3}$ )	Ozone concentration (ppbV)	pinalic-4-acid	norpinonic acid	pinonic acid	norpinic acid	$\alpha$ -pinene unknown	OH-norpinonic acid	pinic acid	OH-pinonic acid	pinonaldehyde	OH-pinonaldehyde	Total
Glasius et al., 2000	8408 <sup>a</sup>	905 <sup>a</sup>	n.d. <sup>a</sup>	0.32 <sup>a</sup>	2.1 <sup>a</sup>	0.09 <sup>a</sup>	n.d.	n.d.	1.9 <sup>a</sup>	1.7 <sup>a</sup>	2.1 <sup>a</sup>	0.51 <sup>a</sup>	8.7 <sup>a</sup>
	9021	815	n.d.	0.19	1.5	0.04	n.d.	n.d.	1.4	0.86	1.9	0.32	6.2
Yu et al., 1999	317	237	n.d.	2.1 <sup>b</sup>	1.7	0.08	n.d.	n.d.	1.8	2.1	0.8	2.4	11
	362	269	n.d.	4.8 <sup>b</sup>	1.6	0.09	n.d.	n.d.	3.9	1.3	0.3	1.1	13
	251	74	n.d.	2.8 <sup>b</sup>	1.3	0.05	n.d.	n.d.	2.8	2.1	0.9	2.0	12
This work	230	456	0.40	0.16	1.4	0.08	0.27	0.26	2.6	0.39	n.d.	n.d.	5.5
		529	0.36	0.11	0.91	0.07	0.22	0.20	1.9	0.34	n.d.	n.d.	4.1
	280	505	0.30	0.17	1.3	0.07	0.23	0.34	2.8	0.43	n.d.	n.d.	5.7
		563	0.42	0.26	1.3	0.08	0.38	0.29	2.7	0.56	n.d.	n.d.	6.0

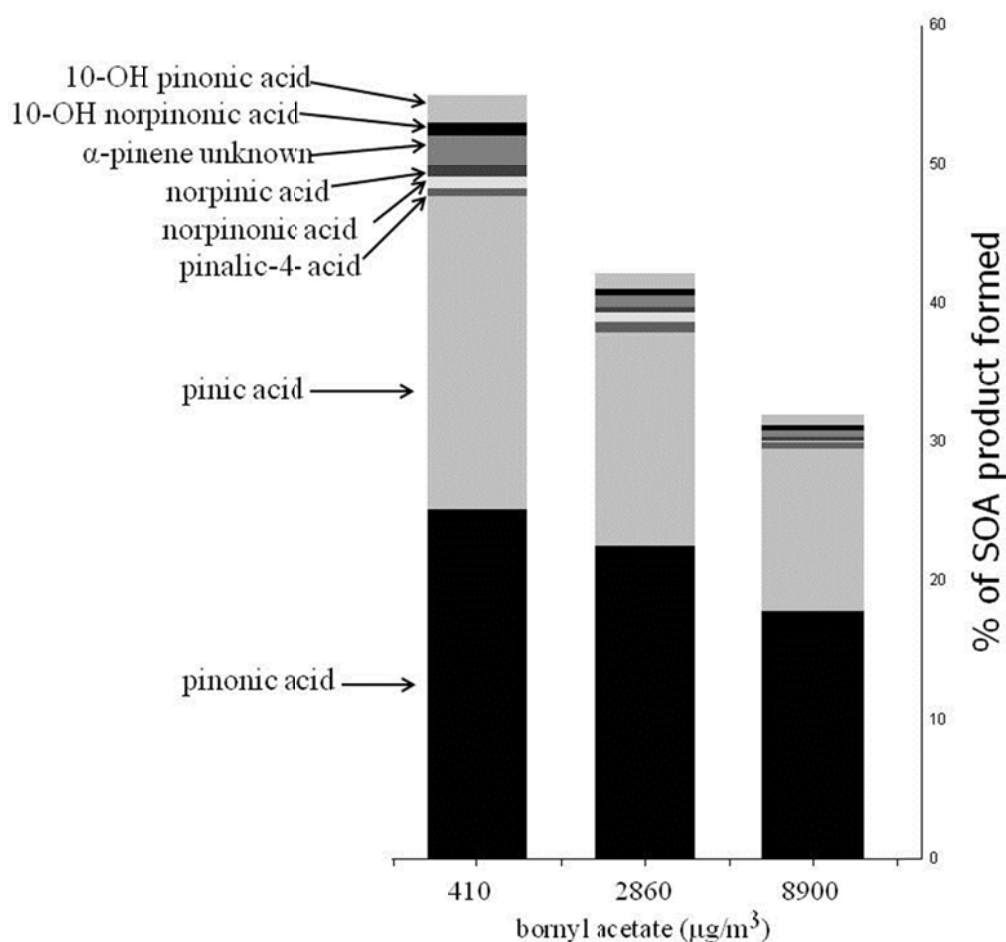
<sup>a</sup> No radical scavenger was used for this experiment <sup>b</sup> this work reported the yield from norpinonic acid as sum of norpinonic acid and an isomer.

#### 4.3.3.2 Speciation of SOA generated by ozonolysis of $\alpha$ -pinene + bornyl acetate mixtures

Six filter samples for SOA generated from 290-350  $\mu\text{g m}^{-3}$   $\alpha$ -pinene in the presence of bornyl acetate were collected, where the bornyl acetate concentration of ranged from 410-8900  $\mu\text{g m}^{-3}$ . We observe that with increasing concentration of bornyl acetate the number of products identified remain the same (Table 4.3). However, the amount of products characteristic of  $\alpha$ -pinene ozonolysis decreased. From Figure 4.1, which is a plot of the percent of the SOA product formed as a function of bornyl acetate concentration we see that the dominant products for all levels of bornyl acetate were pinic acid and pinonic, acid but the amount of all the products and total amount of SOA identified decreased with an increase in bornyl acetate concentration. The overall percentages of SOA products identified for these VOC mixtures were 59%, 42%, and 32% for bornyl acetate concentrations of 410  $\mu\text{g m}^{-3}$ , 2860  $\mu\text{g m}^{-3}$  and 8900  $\mu\text{g m}^{-3}$  respectively (Table 4.3).

Hatfield and Huff Hartz<sup>74</sup> have reported that the SOA yields from these mixtures remains the same even with increasing concentration of bornyl acetate. The mass of particulate matter measured by the SMPS relative to the mass of  $\alpha$ -pinene reacted did not change as the bornyl acetate concentration increased because bornyl acetate does not react with ozone. However, we found that the percent individual SOA product yields decreased as the concentration of bornyl acetate increased during SOA generation. One possible explanation for the decrease in amount of condensed phase products extracted and identified while SOA yields remained the same would be if bornyl acetate is present in high enough concentration where it would partition in condensed phase. Thus contribution from condensed phase of bornyl acetate would lead to underestimation of SOA collected on the filters and hence lower the amount of the products detected. However the saturation concentration of bornyl acetate at highest concentration of 8960  $\mu\text{g m}^{-3}$  is  $6.41 \times 10^3 \text{ mg/m}^3$ ,<sup>219</sup> thus at even the highest bornyl acetate concentration, less than

<0.1% of the bornyl acetate will partition to the condensed phase. This is not a high enough mass concentration to explain the decreases in the observed mass yields.



**Figure 4.1** Decrease in SOA product concentrations with increase in bornyl acetate concentrations

Another possible explanation for the observed decrease in the individual mass yields with an increase in bornyl acetate concentration is if bornyl acetate reacted with OH radicals, generated as a product of  $\alpha$ -pinene ozonolysis, to generate SOA, but the bornyl acetate SOA products were too volatile to be observed. If this were the case, then an increase in bornyl acetate concentration could cause a decrease in the individual mass yields of the  $\alpha$ -pinene SOA products. Bornyl acetate doesn't react with ozone under our experimental conditions because the bornyl acetate/ozone rate constant is negligible.<sup>74</sup> OH radicals are generated by reaction of  $\alpha$ -pinene

with ozone, where the Criegee intermediate isomerizes to a vinyl hydroperoxide and decomposes to carbonyl products and OH radical.<sup>220</sup> 2-butanol reacts with OH radicals and prevents further OH reaction with precursors; however when the concentration of bornyl acetate is high, bornyl acetate can compete with 2-butanol for the OH radical. Bornyl acetate reacts with OH radicals<sup>221</sup> generating SOA yields of approximately 5%. Coeur et al.<sup>221</sup> observed many SOA products but were successful in identifying a single keto product namely, 1,7,7-trimethyl-6-acetyloxy-bicyclo[2.2.1]-heptan-2,3-dione. However, we do not observe formation of this product or any other products that can be attributed to bornyl acetate. From the calculation of the pseudo-first order rate constants for the reaction of OH radical with between 2-butanol,  $\alpha$ -pinene, and bornyl acetate, we found that with increasing bornyl acetate concentration, approximately 0.7%, 4.4%, and 12.5% of bornyl acetate reacts with OH radicals. This calculation indicates that at the highest bornyl acetate concentration, a fraction of the radical scavenging during SOA formation is done by bornyl acetate instead of 2-butanol alone. While we do not observe changes in SOA yields and we do not observe bornyl acetate/OH SOA products in the condensed phase, due to the observed decrease in  $\alpha$ -pinene SOA products with increasing bornyl acetate concentration, we cannot rule out that bornyl acetate affects the radical chemistry during SOA formation (particularly HO<sub>2</sub>/RO<sub>2</sub> reaction pathways).

Statistical analysis were performed to compare the mass-based yields for individual SOA products generated from  $\alpha$ -pinene ozonolysis to the mass-based yields of individual SOA products generated from  $\alpha$ -pinene ozonolysis in the presence of bornyl acetate (Table 4.3). For each mixture, an independent, two sample t-test was performed, and the null hypotheses tested was that the averages of the percent individual SOA product yields for individual SOA products in the presence and absence of bornyl acetate were that same. A probability value (p) of lower

than 0.05 is considered significant, and it indicates that it is unlikely that the amount of SOA products generated in the presence and absence of bornyl acetate are the same. For  $\alpha$ -pinene SOA generated in the presence of the lowest bornyl acetate concentration, two products showed significant differences: pinalic-4-acid ( $p = 0.01$ ) and 10-OH norpinonic acid ( $p = 0.003$ ). The mass based yield for pinalic-4-acid decreased from 0.9% to 0.6 % while for 10-OH norpinonic acid the mass based yield increased from 0.5% to 0.9%. However, both these products are present in low concentrations, and we can't rule out variability due to errors introduced during SOA sampling process and extraction process, which can be as high as 50%.<sup>84,208</sup> When the percent individual SOA product yields from the mixture containing bornyl acetate ( $2860 \mu\text{g m}^{-3}$ ) concentration are compared to the  $\alpha$ -pinene the percent individual SOA product yields measure in the absence of bornyl acetate, the significance t-test gives  $p < 0.05$  for norpinic acid ( $p = 0.04$ ) and pinic acid ( $p = 0.002$ ). Upon the addition of  $2860 \mu\text{g m}^{-3}$  bornyl acetate during  $\alpha$ -pinene SOA generation, the mass based yield for pinic acid decreased from 29% to 15% and mass based yield for norpinic acid decreased from 0.6% to 0.4%. At highest concentration of bornyl acetate ( $8900 \mu\text{g m}^{-3}$ ) all products but 10-OH pinonic acid ( $p = 0.06$ ) have  $p < 0.05$ . The presence of bornyl acetate during  $\alpha$ -pinene ozonolysis significantly decreases the percent individual SOA product yields of the  $\alpha$ -pinene SOA products.

The decrease in percent individual SOA product yields for  $\alpha$ -pinene SOA products suggests that bornyl acetate when present at these concentrations can hinder mechanisms leading to generation of  $\alpha$ -pinene. As shown in Table 4.3, the total recovery of condensed phase  $\alpha$ -pinene SOA products in comparison to the total amount of mass on the filter decreases from 60% to 32%. However, the overall SOA yield does not change as the bornyl acetate concentration changes<sup>74</sup>. One plausible explanation is that as the bornyl acetate concentration increases,

products other than the  $\alpha$ -pinene SOA products shown in Table 4.3 form. In recent study Taatjes et al.,<sup>222</sup> the second-order reaction rates between Criegee biradicals with three carbonyl containing compounds were reported: acetone ( $2.3 \times 10^{-13} \text{ cm}^3 \text{ molecule}^{-1} \text{ s}^{-1}$ ) and acetaldehyde ( $9.5 \times 10^{-13} \text{ cm}^3 \text{ molecule}^{-1} \text{ s}^{-1}$ ) and hexafluoroacetone ( $3.0 \times 10^{-11} \text{ cm}^3 \text{ molecule}^{-1} \text{ s}^{-1}$ ). The carbonyl oxygen reacts with Criegee biradical to form trioxolane ring which can undergo rearrangement to form a formate. Other reactions have been suggested for formation involving addition of acid to Criegee intermediate by Heaton et al.,<sup>223</sup> from both this research findings the products formed will be an adduct of bornyl acetate (molecular formula  $\text{C}_{12}\text{H}_{20}\text{O}_3$ ) and the  $\alpha$ -pinene Criegee intermediates (molecular formula  $\text{C}_9\text{H}_{14}\text{O}_2$ ), the resulting adduct can have a molecular formula of  $\text{C}_{21}\text{H}_{34}\text{O}_5$ . However in this study no different products characteristic to bornyl acetate present in the mixture are detected. This work suggests that a reaction between carbonyl oxygen on bornyl acetate and Criegee biradical may exist and can be competitive with decomposition of Criegee biradical. This reaction may lead to lower amount of SOA products but keeping the SOA yield constant.

#### 4.3.3.3 Speciation of SOA generated by ozonolysis of VOC mixtures containing camphene

Three filter samples were collected for SOA generated from VOC mixtures containing camphene (Table 4.3). One filter was collected for SOA generated from a VOC mixture that contained  $\alpha$ -pinene ( $290 \pm 20 \text{ } \mu\text{g m}^{-3}$ ), bornyl acetate ( $400 \pm 20 \text{ } \mu\text{g m}^{-3}$ ), and camphene ( $180 \pm 10 \text{ } \mu\text{g m}^{-3}$ ). Two SOA filter samples were collected from SOA generated from a VOC mixture of  $\alpha$ -pinene ( $280 \pm 10 \text{ } \mu\text{g m}^{-3}$ ), bornyl acetate ( $400 \pm 20 \text{ } \mu\text{g m}^{-3}$ ), borneol ( $23 \pm 1 \text{ } \mu\text{g m}^{-3}$ ), and camphene ( $177 \pm 8 \text{ } \mu\text{g m}^{-3}$ ). The total percent individual SOA product yields of SOA products identified from mixture of  $\alpha$ -pinene, bornyl acetate, and camphene was 57% and for VOC

mixture containing  $\alpha$ -pinene, bornyl acetate, borneol, and camphene was 60%. Hatfield and Huff Hartz,<sup>74</sup> observed no change in SOA yield as function of camphene addition to the VOC mixture.

In addition to the SOA products from  $\alpha$ -pinene, two additional SOA products were observed to be generated from ozonolysis of camphene containing VOC mixtures. The mass fragmentation patterns for these compounds are shown in Figure A-IV 4 and Figure A-IV 7. The first product, camphene unknown 1, in CI-ACN mode only ion observed is 229 m/z which is attributed to molecular ion  $(M+1)^{+}$ . In EI mode the fragments are observed at m/z values of 228 and 213 which correspond to  $M^{+}$  and  $(M-15)^{+}$  respectively. The EI mass spectrum also shows presence of fragments at m/z 73 and 43 which can be attributed to trimethyl silyl group and  $\text{CH}_3\text{CO-}$  or  $-\text{CH}_2\text{CHO}$  group respectively. The underivatized mass of 156 m/z is calculated for the product assuming it has one replaceable hydrogen atom in form of an alcohol. From the mass fragmentation patterns and the underivatized mass, the estimated molecular formula for the compound is  $\text{C}_9\text{H}_{16}\text{O}_2$ . The mass-based yield of this compound is found to be 1.4 % for VOC mixture containing  $\alpha$ -pinene, bornyl acetate, and camphene and 0.970% for VOC mixture of  $\alpha$ -pinene, bornyl acetate, borneol, and camphene.

The mass spectrum of second unknown compound, camphene unknown 2, showed peaks in the CI mode at m/z values of 227, 301, 317, and 389 which are attributed to  $(M-15)^{+}$ ,  $(M-15)^{+}$ ,  $(M+1)^{+}$ , and  $(M+73)^{+}$  respectively. In EI mode, an intense ion at m/z value of 301 is observed, and it is correlated to  $(M-15)^{+}$ . The mass fragmentation pattern is similar to the norpinic acid mass fragmentation pattern, and this compound eluted after norpinic acid, hence we can assume that the structure is similar to norpinic acid and has molecular formula of  $\text{C}_8\text{H}_{12}\text{O}_4$ . The mass based yield of the  $\text{C}_8\text{H}_{12}\text{O}_4$  compound is found to be 2.9 % for VOC mixture containing



$\alpha$ -pinene, bornyl acetate, and camphene and 3.0% for VOC mixture of  $\alpha$ -pinene, bornyl acetate, borneol, and camphene.

There are only two reports of SOA products generated from ozonolysis of camphene<sup>224,225</sup> and the products identified from camphene are camphenilone ( $C_9H_{14}O_4$ ) and 6,6-dimethyl- $\epsilon$ -caprolactone-2,5-methylene ( $C_{10}H_{18}O_2$ ). Neither of these products was observed in our chromatogram, the reason for this being not known. These compounds will be discussed as camphene unknown 1 and camphene unknown 2 in the following text.

To find if the individual SOA product yields for  $\alpha$ -pinene based compounds change in presence of camphene, statistical t-tests was performed. The SOA products generated from VOC mixture of  $\alpha$ -pinene, bornyl acetate, and camphene are compared with SOA products generated from  $\alpha$ -pinene only experiments. The probability values are found to be lower than 0.05 for all the products except 10-OH pinonic acid ( $p = 0.93$ ). SOA products showing decrease in the mass yields include pinalic-4-acid, pinonic acid,  $\alpha$ -pinene unknown, and pinic acid. The other SOA products norpinonic acid, norpinic acid, and 10-OH norpinonic acid show an increase in their percent individual SOA product yields as compared to the percent individual SOA product yields for these products from  $\alpha$ -pinene only experiments (Table 4.4). The sum of the percent individual SOA product yields for SOA products from this VOC precursor mixture is 54%.

Next we do statistical comparison of the product yields generated from VOC mixture of  $\alpha$ -pinene, bornyl acetate, borneol, and camphene to product yields from  $\alpha$ -pinene only experiments. The probability values for  $\alpha$ -pinene unknown ( $p=0.4$ ), pinic acid ( $p=0.4$ ), and 10-OH pinonic acid ( $p=0.07$ ) are found to be greater than 0.05. For other five products, pinalic-4-acid ( $p=0.002$ ), norpinonic acid ( $p=0.047$ ), pinonic acid ( $p=0.007$ ), norpinic acid (0.04), and 10-OH norpinonic acid ( $p=0.02$ ), the probability values are lower than 0.05. For pinalic-4-acid

and pinonic acid the percent individual SOA product yields decrease while for norpinonic acid, norpinic acid, and 10-OH norpinonic acid the percent individual SOA product yields were found to increase (Table 4.3). The sum of the percent individual SOA product yields for SOA products from VOC mixture of  $\alpha$ -pinene, bornyl acetate, borneol, and camphene is 53%.

To summarize, the condensed phase of SOA generated from VOC mixtures that contained camphene showed two new products that have not been previously reported in the literature. These products were not generated from the oxidation containing VOC mixtures that do not contain camphene. The molecular formula for camphene unknown 1 and camphene unknown 2 are tentatively suggested as  $C_9H_{16}O_2$  and  $C_8H_{12}O_4$  respectively. Upon addition of camphene to the VOC mixture, the percent individual SOA product yields for  $\alpha$ -pinene characteristic SOA products are found to vary and the variation for each of the camphene containing mixtures is mentioned in above paragraphs.

#### **4.3.3.4 Speciation of SOA generated by ozonolysis of $\alpha$ -pinene and $\beta$ -pinene mixtures**

One SOA filter sample collected from SOA generated a VOC mixture of  $\alpha$ -pinene ( $280 \pm 10 \mu\text{g m}^{-3}$ ) and  $\beta$ -pinene ( $30 \pm 1 \mu\text{g m}^{-3}$ ) was analyzed (Table 4.3). The SOA products generated from ozonolysis of this mixture were similar to those generated by ozonolysis of  $\alpha$ -pinene, and no characteristic SOA products from oxidation of  $\beta$ -pinene were observed.  $\beta$ -pinene produces less SOA on a per mass basis than  $\alpha$ -pinene, and the  $\beta$ -pinene concentration was nearly ten times lower than  $\alpha$ -pinene concentration. Therefore, only low concentrations of characteristic  $\beta$ -pinene SOA products would be produced.

The percent individual SOA product yields for the  $\alpha$ -pinene SOA products in the presence and absence of  $\beta$ -pinene were compared. The student's t-test gave probability values lower than

0.05 for pinalic-4-acid ( $p=0.002$ ) and pinonic acid ( $p=0.02$ ), indicating that these products were statistically lower when  $\alpha$ -pinene SOA was generated in the presence of  $\beta$ -pinene. The percent individual SOA product yields for other products did not show significant variation ( $p>0.05$ ).

Jaoui and Kamens,<sup>177</sup> have studied formation of SOA products from oxidation of VOC mixture containing  $\alpha$ -pinene and  $\beta$ -pinene. The authors reported concentrations of the SOA products formed during the ozonolysis reaction of this mixture the authors find that pinic acid and pinonic acid are major products that are formed, which is consistent with our studies. The authors also reported detection of pinalic-4-acid, norpinonic acid, 10-OH pinonic acid, and norpinic acid, which is also in agreement with our studies. The authors also report that the most of the products characteristic of  $\beta$ -pinene ozonolysis occurred in the gas phase rather than in the condensed phase.

#### 4.3.3.5 Speciation generated by ozonolysis of reactive VOC mixtures

A total of three SOA filter samples were analyzed with a VOC precursor mixture containing  $280\pm 10 \mu\text{g m}^{-3}$   $\alpha$ -pinene,  $30\pm 1 \mu\text{g m}^{-3}$   $\beta$ -pinene, and  $190\pm 10 \mu\text{g m}^{-3}$  for 3-carene. Hatfield and Huff Hartz<sup>74</sup> found that the SOA yields from this mixture increased due to the addition of a significant concentration of 3-carene, which reacts with ozone and produces SOA with similar yields as  $\alpha$ -pinene. In addition to the SOA products from  $\alpha$ -pinene, one additional SOA product was detected in these filter samples. The mass fragmentation pattern of this product is shown in Figure A-IV 3. The mass fragmentation pattern in CI mode shows presence of one dominant ion at  $m/z$  value of 229, attributed to  $(M+1)^+$ . In EI mode, the ions with  $m/z$  228 ( $M$ )<sup>+</sup>, and 213 ( $M-15$ )<sup>+</sup> are observed along with ion fragments at  $m/z$  values of 73 (trimethyl silyl) and 43 ( $\text{CH}_3\text{CO}$ - or  $-\text{CH}_2\text{CHO}$ ). The mass fragmentation patterns for this SOA product are similar to nor-3-caralic

acid which has been reported by Ma et al.<sup>212</sup> as the ozonolysis products of 3-carene. The molecular structure of nor-3-caralic acid is  $C_8H_{12}O_3$  with an underivatized molecular mass of  $156\text{ g mol}^{-1}$ . No other characteristic products of 3-carene were observed, but due to structural similarity, we cannot rule out coelution with  $\alpha$ -pinene products.

One filter was analyzed containing SOA generated from a VOC mixture with the addition of limonene. The resulting VOC precursor mixture contained  $280 \pm 10\text{ }\mu\text{g m}^{-3}$   $\alpha$ -pinene,  $30 \pm 1\text{ }\mu\text{g m}^{-3}$   $\beta$ -pinene,  $150 \pm 10\text{ }\mu\text{g m}^{-3}$  3-carene, and  $30 \pm 1\text{ }\mu\text{g m}^{-3}$  limonene. Hatfield and Huff Hartz<sup>74</sup> found that the SOA yields from this mixture increased slightly with addition of  $30 \pm 1\text{ }\mu\text{g m}^{-3}$  limonene. Despite this slight increase in yield, the filter analysis showed that no characteristic SOA products from limonene. Limonene was present in small concentration as compared to other reactive species like  $\alpha$ -pinene (9 times the concentration of limonene) and 3-carene (5 times the concentration of limonene) which may explain absence of any characteristic products of limonene which were observed in Chapter 3.

To compare the variation between the SOA product yield upon addition of limonene to the VOC mixture a significance testing was done, for product yields from  $\alpha$ -pinene,  $\beta$ -pinene, 3-carene mixture and for  $\alpha$ -pinene,  $\beta$ -pinene, 3-carene and limonene mixture. The probability values for pinalic-4-acid ( $p=0.02$ ), nor-3-caralic acid ( $p=0.02$ ), pinonic acid ( $p=0.02$ ), norpinic acid ( $p=0.03$ ) and 10-OH norpinonic acid ( $p=0.0001$ ) were found to be lower than 0.05. For these products, the percent individual SOA product yields, upon the addition of limonene, were found to decrease for pinalic-4-acid (0.3% from 0.9%), and pinonic acid (9.5% from 15%) while an increase was observed for nor-3-caralic acid (4.4% from 3%), norpinic acid (1 % from 0.6%), and 10-OH norpinonic acid (6.7% from 0.5%) (Table 4.4). The increase in mass yield of 10-OH norpinonic acid was nearly tenfold. One explanation for this is that a SOA product characteristic

of limonene, like 10-OH norlimononic acid, coeluted with 10-OH norpinonic acid and may contribute towards the increase in amount of this product. However, the concentration of limonene is lowest in the mixture and also the SOA product 10-OH nor limononic acid is not observed for limonene only experiments mentioned in Chapter 3. Further investigation involving binary mixture of  $\alpha$ -pinene and limonene may be needed to investigate this variation in amounts of 10-nor limonoic acid.

#### 4.3.3.6 Speciation for SOA generated by ozonolysis of SFNO surrogates

Two SOA filter samples were collected from two SFNO surrogate experiments. The purpose of the surrogate mixtures was to determine if the yields and SOA products from a complex mixture could be replicated if the mixture was made from the individual constituents of the mixture. SOA from the first surrogate experiment (SFNO Surrogate 1) was generated from a mixture of eleven different VOCs:  $\alpha$ -pinene, bornyl acetate, camphene, 3-carene, limonene, borneol,  $\beta$ -pinene,  $\beta$ -caryophyllene, terpinolene,  $\alpha$ -caryophyllene, and p-cymene. SOA from the second surrogate mixture (SFNO Surrogate 2) was generated from a mixture of 13 VOCs, including all of the VOCs in SFNO surrogate 1 plus camphor and  $\alpha$ -terpinene. The ozone-reactive species in SFNO Surrogate 1 are  $\alpha$ -pinene, 3-carene, limonene,  $\beta$ -pinene,  $\beta$ -caryophyllene, terpinolene, and  $\alpha$ -caryophyllene. In SFNO Surrogate 2,  $\alpha$ -terpinene is also reactive. For SFNO surrogate 1 and SFNO surrogate 2 characteristic SOA products were observed. All the SOA products generated from SFNO Surrogate 1 and SFNO Surrogate 2 are in good agreement with each other (Table 4.3). The SOA product distribution for the surrogates is statistically similar (p values for all products  $>0.05$ ) to the SOA product distributions for VOC mixture containing  $\alpha$ -pinene,  $\beta$ -pinene, 3-carene, and limonene.

#### 4.3.3.7 Speciation generated by ozonolysis of SFNO

A total of three SOA filter samples were collected for the ozonolysis of SFNO, and two of these experiments were carried out at lower concentration (trial 1) of SFNO in the chamber than the other (trial 2). The concentration of reactive VOCs in the chamber was  $430 \pm 10 \mu\text{g m}^{-3}$  for trial 1 and  $560 \pm 20 \mu\text{g m}^{-3}$  for trial 2. Comparison of the percent individual SOA product yields for SNO and surrogates is made, some SOA products showed a significant decrease in observed mass yields, norpinonic acid ( $p=0.03$ ), and camphene unknown 2 ( $p=0.009$ ), and significant increase is observed in the mass-based yield of pinic acid (10.8% from 7.3%,  $p=0.02$ ).

The SOA generated in SFNO trial 2 has same reactive VOC concentration as the SFNO surrogate 2, and it also generated similar SOA yields.<sup>74</sup> However, when comparing the SOA products we observe that all SOA products were found to have smaller percent individual mass yields for SFNO trial 2 than in the surrogate experiments. This decrease of SOA product mass yields in commercially available essential oil as compared to the surrogates may be due disruption of reaction mechanisms of certain pathways of SOA formation. The other explanation for the decrease SOA product mass yield in SFNO is the formation of tracer or marker condensation products by the commercially available essential oil, which might use up an intermediate thus generating lower individual SOA product yield of the product however such tracer/marker products were not detected. The chamber SOA yield could remain constant in spite of a decrease in percent individual SOA product yields of individual products if non-reactive species with high saturation concentration are present in SFNO and contribute to the condensed phase.

#### 4.3.3.8 Speciation generated by ozonolysis of CFNO

One filter sample was collected from the SOA generation from CFNO. The sum of percent individual product yields for CFNO (24%) was found to be similar to total SOA mass yield generated from equivalent concentration of reactive precursors present in SFNO (24.5%, SFNO trial 2). Both filters were sampled from SOA generated using approximately the same amount of reactive precursor mixture (CFNO;  $530 \mu\text{g}/\text{m}^3$ , SFNO trial 2:  $560 \mu\text{g}/\text{m}^3$ ) and both FNOs gave similar SOA yields (CFNO: 0.237, SFNO: 0.243, both averaged for three trials).<sup>74</sup> The fir needle oils contain similar amounts of  $\alpha$ -pinene (CFNO: 12.3%, SFNO: 13.8%). However, the distribution for individual SOA products was different for CFNO and SFNO. The individual SOA percent mass yields for following products were found to decrease when CFNO was used as SOA precursor in comparison to SFNO: pinalic-4-acid (n.d vs. 0.104), nor-3-caralic acid (1.401 vs, 2.51), pinonic acid (0.775 vs. 2.72), camphene unknown 2 (0.869 vs 2.85), and 10-OH pinonic acid (0.323 vs. 0.467). The individual SOA percent mass yields for other products increased when the CFNO was used as the SOA precursor in comparison to SFNO: nor-pinonic acid (0.652 vs. 0.403), camphene unknown 1 (0.264 vs. 0.081), norpinic acid ( 0.260 vs. 0.250),  $\alpha$ -pinene unknown (0.563 vs. 0.454), 10-OH norpinonic acid (3.81 vs, 3.76) and pinic acid (15.1 vs. 10.8).

The variation in product distribution may be attributed to the difference in VOC composition between CFNO and SFNO. The decrease in amount of products cannot be explained alone on basis of concentration variation of  $\alpha$ -pinene, the  $\alpha$ -pinene concentration is found to be similar for SFNO (12.3%) and CFNO (13.8%). So in the following paragraphs comparison between SFNO oxidation products for other VOCs added to the VOC mixtures will be made.

In CFNO the concentration of non reactive species borneol and bornyl acetate is found to be lower 0.58% and 5.0% respectively, as compared to SFNO which has 1.9% and 32% of each respectively. Hence in the natural concentrations borneol and bornyl acetate are present in CFNO should not lead to decrease in amount  $\alpha$ -pinene characteristic products which was observed for SOA products generated from ozonolysis of mixtures containing higher concentration bornyl acetate. Camphene is present in lower concentrations in SFNO (21%) as compared to CFNO (8%), but the individual SOA product yield for camphene unknown 1 increases, but the individual SOA product yield for camphene unknown 2 is found to decrease, as expected. The 3-carene percentage is higher in CFNO (15%) than in SFNO (11%), but the individual SOA product yield for 3-carene was found to be lower in CFNO. The  $\beta$ -pinene concentration for CFNO (35%) are higher than SFNO (~2%) concentrations hence no decrease in pinalic-4-acid and pinonic acid was not observed, suggesting contribution of  $\beta$ -pinene towards this product formation. A decrease was observed when sample of  $\alpha$ -pinene  $\beta$ -pinene was analyzed for SOA products.

#### 4.4 Conclusions

The composition of the fraction of SOA products that can sampled by filters, extracted by solvents, and analyzed by GCMS was determined. Eleven SOA products were found, and eight were attributed to  $\alpha$ -pinene, the major ozone reactive monoterpene in the SOA precursor mixtures, two were attributed to camphene, and one was attributed to limonene. The amount of SOA mass identified, the types of products and the distribution of products from  $\alpha$ -pinene was similar to prior work.<sup>83,84</sup>



When  $\alpha$ -pinene forms SOA via ozonolysis, an increase in concentration of bornyl acetate leads to lower concentrations of the  $\alpha$ -pinene SOA products that were filtered, extracted, and analyzed by our method. The total mass of individual SOA products identified for the VOC mixture containing bornyl acetate decreases from 59% to 42% and to 31% as the concentration of bornyl acetate increases from  $410 \mu\text{g m}^{-3}$ ,  $2860 \mu\text{g m}^{-3}$ , to  $8900 \mu\text{g m}^{-3}$ , respectively. Because the SOA yield of  $\alpha$ -pinene in the presence of bornyl acetate does not change<sup>74</sup>, this implies that bornyl acetate enhances the formation of SOA oligomers.

SOA precursor mixtures containing camphene generated two products unique camphene-containing mixtures and have been tentatively identified to have molecular formulas of  $\text{C}_9\text{H}_{16}\text{O}_2$  and  $\text{C}_8\text{H}_{12}\text{O}_4$ . These products have not been previously reported for ozonolysis of camphene.

SOA precursor mixtures containing 3-carene yielded an SOA product of nor-3-caralic acid, which is unique to 3-carene and can be used as a tracer for 3-carene containing VOC mixtures. However, no unique SOA products were found in mixtures containing small amounts of  $\beta$ -pinene and limonene, possibly due to the low concentration of these precursors in the mixtures.

When SOA was generated from SFNO and SFNO all eleven SOA products were found. When SOA was generated from CFNO, ten SOA products were found; pinalic-4-acid was not detected. SOA speciation studies for each SFNO surrogate yielded products which were similar to the products generated by ozonolysis VOC mixture containing  $\alpha$ -pinene,  $\beta$ -pinene, 3-carene and limonene, no new products were observed. The SOA products from surrogates were characteristic of the dominant reactive species present in them, i.e.  $\alpha$ -pinene,  $\beta$ -pinene, limonene and 3-carene. However, when comparing the average percent individual SOA product yields of the two surrogates with SFNO trial 2 experiment, all three experiments introduce similar amount of reactive VOCs in the chamber, and this shows the percent yield of SOA products formed from

SFNO ozonolysis were lower than those generated by surrogate VOC mixtures. This reduction in the amount of SOA products of SFNO may be contributed to alteration of reaction pathways to form higher molecular weight oligomers, which explains the constant SOA yield and no detection of new products.

Comparing the SOA product distribution for experiments for CFNO and SFNO trial 2 shows that the lower amounts of certain SOA species is generated from CFNO which may due to difference in composition of two essential oils. In CFNO, the dominant reactive monoterpenes in  $\beta$ -pinene,  $\gamma$ -3-carene,  $\alpha$ -pinene, limonene (in terms of decreasing % composition in CFNO). While for SFNO the dominating monoterpene was  $\alpha$ -pinene, which is known for its higher SOA yields than  $\beta$ -pinene.

Overall we found, that as reported by previous work Glasius et al.,<sup>83</sup> and Yu et al.,<sup>84</sup> the dominating species generated from ozonolysis of  $\alpha$ -pinene containing VOC mixture is pinic acid. This work suggests, via indirect evidence that an alteration in reaction pathways or formation of new products by VOC precursors, occurs. While SOA generated from precursor mixtures takes on the characteristics of SOA generated from single precursors in terms of types of products and yield, the role of non-reactive VOCs and the composition of the reactive mixture may impact the concentrations of individual products. If the concentrations of the individual products impact the toxicity and/or the cloud properties of PM derived from biogenic SOA, then SOA generated from precursor mixtures might be a way to distinguish differences between single-precursor SOA and SOA that is generated from a complex mixture of VOCs and more likely to occur in the atmosphere.

## CHAPTER 5

### EFFECT OF $\text{NH}_4^+$ AGING OF SOA GENERATED FROM LEMON AND CHAMOMILE AIR FRESHENER AND SIBERIAN FIR NEEDLE OIL

#### 5.1 Introduction

Aerosols can affect the climate by radiative forcing as discussed in Chapter 1 (section 1.3.2.2). The radiative forcing of aerosols is categorized into the direct and the indirect effect. If the solar radiation is either scattered or absorbed by the particles it is called as the direct effect. On the other hand, when the microscopic properties of cloud are changed by aerosols by taking part in cloud formation process, and thus altering the cloud albedo, is called the indirect effect. In this chapter we will be focusing on a process which has the potential to impact the direct effect: aging of SOA generated from lemon and chamomile air freshener, which is limonene-based air freshener and Siberian fir needle oil (SFNO) in the presence of  $\text{NH}_4^+$ . The absorbance of the  $\text{NH}_4^+$ -treated SOA in UV-visible region is then correlated to aging time and components of these precursor mixtures.

##### 5.1.1 Elemental carbon and organic carbon as absorbing species

Carbonaceous aerosols are a large fraction of atmospheric aerosol and are present in elemental and organic form.<sup>14</sup> Many studies of aerosol absorption have focused on absorption of solar radiation by elemental or “black” carbon. The focus on elemental carbon is justified as light absorption by elemental carbon is continuous, i.e., it covers the visible spectra. The optical properties of elemental carbon are determined by the aerosol size and refractive index.<sup>28</sup>

The particulate organic carbon in the atmosphere tends to scatter incident solar radiation, which leads to negative radiative forcing. It is observed that only certain organic compounds

absorb light. The absorption of these compounds is highly wavelength specific and is greater at near-UV and blue wavelengths. They appear brownish and hence they are termed as “brown” carbon.<sup>226</sup> “Brown” carbon is important because it absorbs in visible region, and nearly 40% of solar energy is between wavelengths 400-600 nm.<sup>29</sup>

### 5.1.2 Chemical composition of light absorbing species in aerosols

The identity of the light absorbing organic compounds in aerosols is not yet completely known. However, a significant proportion of the aerosols are water soluble components classified as humic-like substances (HULIS), which have properties similar to humic acid.<sup>227,228</sup> Blough and Del Vecchio<sup>229</sup> reported a class of chromophoric dissolved organic matter present in the marine environment and terrestrial environments. These chromophoric dissolved organic matter have similar properties to HULIS,<sup>230</sup> because both are made of refractory and water soluble macromolecules which absorb light.<sup>231</sup>

Jacobson<sup>232</sup> identified nitrated and aromatic aerosols as the likely absorbing compounds in the UV-visible region. Bond<sup>233</sup> suggested that the different levels of aromatization among the organic compounds can be used to explain the wavelength-specific absorption of the aerosols. Hence, the criterion for a good chromophoric organic compound is the presence of conjugation.

The production of macromolecules from SOA take place when condensation reaction continue in condensed phase as aerosol ages, building macromolecules or oligomers out of monomeric units.<sup>234</sup> Production of macromolecules will not only depend on the source of SOA but also on the reactions between and among the SOA constituents and particulate matter (PM). The production of macromolecules can take place by two routes. One route occurs when SOA constituents can react with oxidants (OH, O<sub>3</sub>) or inorganic species (NH<sub>4</sub><sup>+</sup>, H<sub>2</sub>SO<sub>4</sub> etc.) present in

PM. For example, nitro PAHs were found as the products of the nitration of anthracene and pyrene on the surface of soot samples following exposure to a mixed flow of  $\text{NO}_3$  and  $\text{N}_2\text{O}_5$ . Absorption experiments indicate that the nitration of PAHs alters the optical properties of the particles to which they are adsorbed, giving rise to absorption intensity in the near UV and visible portions of the spectrum, as discussed by Kwamena and Abbatt.<sup>235</sup> Holmes and Petrucci<sup>236</sup> showed that the reaction of OH radical with levoglucosan, a proxy for biomass burning, lead to formation of two oligomers. One a lactone and other an ester generated from transesterification of the lactone functionality, the esters further lead to formation of polyesters, thus indicating that precursor for HULIS, can be generated from OH radical reaction with biomass burning aerosols.

As a second route for macromolecule formation, bond-forming reactions within or with other SOA products yielding dimers and oligomers can occur.<sup>237</sup> Examples of these reactions are aldol condensation of volatile aldehydes to less volatile species<sup>238,239</sup> and direct condensation of non-volatile oxidation products. Some of the condensation products were reported to absorb radiation in the visible region.<sup>240,242</sup> As the aerosol ages, the condensation reactions continue in the condensed phase, resulting in macromolecules or oligomers out of the monomeric units.<sup>234</sup>

### **5.1.3 Role of inorganic ions in absorption of radiation by aerosols**

Organic compounds that contain multiple carbonyl groups can be excellent building blocks for chromophores in aged SOA. These carbonyl organic compounds bond with inorganic counterparts like sulfate ion and ammonium ion in aerosols present in the atmosphere resulting in absorbing species. In following text reactions and examples leading to generation of absorbing species from carbonyl groups are mentioned.

SOA yields were observed to increase when inorganic acidic seed aerosols (sulfate or nitrate) are used in terpene-ozone reactions. These increase in the SOA yields have been attributed to heterogeneous aldol reaction.<sup>238,242</sup> Nozière and Esteve<sup>243</sup> have shown that sulfuric acid catalyzed condensation of acetaldehyde, acetone, and 2-butanone can lead to formation of chromophoric species.

Nozière et al.<sup>244</sup> reported that ammonium and carbonate ions act as catalysts for organic reactions in atmospheric aerosols. The reactions involved formation of C-C and C-O bonds by aldol condensation and acetal formation, thus revealing a new aspect of interactions between organic and inorganic materials in the natural environment. Product identification studies for liquid-phase reactions of glyoxal catalyzed with ammonium ion have revealed that the products are formed via a Brønsted acid pathway or an iminium pathway.<sup>245</sup> Shapiro et al.<sup>246</sup> have also reported the formation of light absorbing secondary organic material in acidic conditions formed by reaction between glyoxal and ammonium sulfate or ammonium nitrate. Galloway et al.<sup>247</sup> have reported identification of imidazole products when glyoxal uptake studies were performed using ammonium sulfate as a seed aerosol. All of the above studies use glyoxal as an organic species, which is smallest dicarbonyl present in the atmosphere. From these studies it would be fair to conclude that the di- or polycarbonyls present in the SOA generated by monoterpenes would react with ammonium ion, generating conjugated species like imidazoles or highly oxygenated polymers which would absorb radiation.<sup>247</sup>

#### 5.1.4 UV-visible absorbance by ammonium aged SOA

Bones et al.<sup>247</sup> performed UV-visible studies for aged SOA in presence and absence of  $\text{NH}_4^+$ . The SOA was generated by the ozonolysis of different monoterpenes  $\alpha$ -pinene,  $\beta$ -pinene,  $\gamma$ -

terpinene, limonene, and myrcene. In this work, the authors found that limonene SOA, when aged in presence of  $\text{NH}_4^+$ , reproducibly changed from colorless to orange. The treated limonene SOA generated absorption maxima at 430 nm and 505 nm, which increased over hours and days. For the monoterpenes  $\alpha$ -pinene,  $\beta$ -pinene, and myrcene, the authors did not report any significant color change due to  $\text{NH}_4^+$  presence in the visible region, but the absorbance in the UV region changed.  $\gamma$ -terpinene, which has the structure similar to limonene, showed absorbance extending from the UV region to 500 nm. Finally, SOA generated from each monoterpene, whether  $\text{NH}_4^+$  treated or untreated, showed a significant increase in absorbance at 250 nm. The suggested chromophores generated by the reaction between limonene- $\text{O}_3$  SOA in presence of  $\text{NH}_4^+$  are a conjugated imine or enamine, or an aromatic pyridinium ion or imidazole ring, and the reaction mechanisms are discussed in detail by Bones et al.<sup>247</sup>

To compare the total absorbance across near ultraviolet region (300-400 nm) and visible region (400-700 nm), the average absorption coefficients for different  $\text{NH}_4^+$  treated monoterpene SOA were calculated. The absorption coefficient,  $\beta$ , was calculated by dividing the average absorbance by the concentration of SOA, in grams per liter, and the pathlength of the absorption cell. The  $\beta$  values for SOA generated from different terpenes after 20 hours of aging in presence of  $\text{NH}_4^+$  are listed in Table 5.1. The absorption coefficient values ( $\beta$ ), for wavelengths 400-700 nm, depended on the SOA monoterpene precursor, where limonene >  $\gamma$ -terpinene > myrcene >  $\alpha$ -pinene >  $\beta$ -pinene. For wavelengths 300-400 nm, the absorption coefficient values also depended on the SOA monoterpene precursor:  $\gamma$ -terpinene > limonene > myrcene >  $\alpha$ -pinene >  $\beta$ -pinene. The UV average absorption coefficients tended to be greater than the visible absorption coefficients.

**Table 5.1** Average absorption coefficient for monoterpenes reported by Bones et al.<sup>247</sup> for sample treated with 0.008 mol L<sup>-1</sup> NH<sub>4</sub><sup>+</sup> for 20 hours

Wavelength 300-400 nm		Wavelength 400-700 nm	
monoterpenes	Average absorption coefficient (Lg <sup>-1</sup> cm <sup>-1</sup> )	monoterpene	Average absorption coefficient (Lg <sup>-1</sup> cm <sup>-1</sup> )
limonene	0.095	limonene	0.025
γ-terpinene	0.210	γ-terpinene	0.004
myrcene	0.090	myrcene	0.002
α-pinene	0.020	α-pinene	0.001
β-pinene	0.010	β-pinene	0.001

From the average absorption coefficients reported by Bones et al., we can observe that NH<sub>4</sub><sup>+</sup>-aged limonene SOA produces a stronger chromophore as compared to NH<sub>4</sub><sup>+</sup>-aged α-pinene SOA.

**The goal of these experiments is to determine if a precursor mixture that contains more limonene than α-pinene generates ammonium-aged SOA with stronger chromophores than SOA from a precursor mixture containing more α-pinene than limonene.** These

experiments give us more information about the composition of SOA from precursor mixtures, especially whether SOA derived from mixtures generates compounds that age in the presence of ammonium ion and generate chromophores like the sum of the SOA derived from the individual precursors, or whether different compounds are produced with different absorption characteristics. In addition, a precursor mixture is a more realistic method for SOA generation, because the SOA in the atmosphere is generated from mixtures of precursors and non-reactive species, rather than single monoterpenes.

## 5.2 Experimental details

### 5.2.1 Generation of SOA from SFNO

SOA was generated in 5.5 m<sup>3</sup> SIUC smog chamber, and details for the smog chamber and instruments connected to the chamber are given in Chapter 3 (section 3.2.1 to 3.2.5). To



summarize the SOA generation process, 250  $\mu\text{L}$  of radical scavenger, 2-butanol, was volatilized in the smog chamber. After volatilization of 2-butanol, ozone was added to the chamber (1000-2000 ppb). At this time, a filter sample of the chamber air was collected using a Pallflex Tissuquartz filters (47 mm) enclosed in a Gelman stainless steel filter holder, and this sample serves as the blank filter. The sample the of chamber air, a vacuum was applied at a flow rate of  $40 \pm 1 \text{ L min}^{-1}$  (Gast, part # 0823-1010-SG608X), and the flow rate for filter sample collection was monitored using an Omega flow meter (FL-2017). Once the ozone concentration stabilized, 50  $\mu\text{L}$  of SFNO or limonene-based air freshener was volatilized in the chamber which initiates the particle formation. To avoid formation of liquid droplets within the injection port (which impairs the reproducibility of the experiments), five serial injections of 10  $\mu\text{L}$  each were performed. To allow sufficient time for volatilization, the syringe was left inside the injection port for three minutes for first four injections and 15 minutes for the last injection. PM concentrations were monitored using the SMPS (TSI, Model# 3936). SMPS comprised of a long dynamic mobility analyzer (DMA, 3080) and a condensation particle counter (CPC, 3010). After the injection of VOC, the reaction was monitored for  $300 \pm 30 \text{ min}$ , and then a second filter sample was collected. This filter, referred to as SOA filter sample in following text, was collected for around 120 minutes until approximately 90% of the volume of the chamber was passed through the filter.

### 5.2.2 Generation of SOA from limonene-based air freshener

The SOA was generated from the ozonolysis of limonene-based air freshener and SFNO. The filter samples were stored in the freezer for one week at  $-18 \text{ }^{\circ}\text{C}$ . The SOA yields and physical parameters during SOA generation from limonene-based air freshener are given in Table 3.5 and

Appendix II (AII-Table2) respectively, and the discussion on comparison of SOA yields can be found in the related sections (Chapter 3, section 3.3.2).

For filter extraction, the halves of the combined filter samples and blanks were transferred to Falcon™ centrifuge tubes, and 10.0 mL of distilled water was added to each test tube. The tubes were vortexed for 30 seconds and sonicated for three minutes. After sonication, 150  $\mu\text{L}$  of 1 M ammonium sulfate, previously prepared by dissolving 13.5634 g of anhydrous ammonium sulfate (Acros chemicals, purity>99%) in 40 mL of distilled water and finally diluting to 100 mL with distilled water in a volumetric flask, was added to half of the test tubes, resulting in treated and untreated sample for each of the filters. The final concentration of ammonium ion in the centrifuge tube was  $0.03 \text{ mol L}^{-1}$ . To settle the filter paper debris, the centrifuge tubes were centrifuged using Eppendorf Centrifuge 5810 R, at 3000 rpm for five minutes. The solutions were filtered using a  $0.2 \mu\text{m}$  nylon filter (Fisher Scientific) which reduces particles that could contribute to scattering, filtration was done before recording spectra at every time point. The SOA concentration given in Table 5.2 is the amount of SOA in 10 mL of extraction solvent water. For this calculation, it was assumed that all the SOA on the filter was transferred into the aqueous phase. The SOA concentration shown in the Table 5.2 was calculated by dividing the half of the average SOA collected from two experiments with volume of extraction solvent. The SOA concentrations used in these experiments are similar to the concentrations used by Bones et al.<sup>247</sup> The samples were stored in dark at room temperature during the aging process.

### 5.2.3 UV-visible spectroscopy

The UV-visible absorbance data were recorded using a double beam Perkin Elmer Lambda25 instrument, in Dr. Punit Kohli's Lab, the software used to collect data was UV Winlab

5.1.4.0630. Prior to scanning samples, an instrument autozero was performed, and distilled water was used as the reference. Each extract was placed in a quartz cuvette, with path length of 1 cm, and scanned between 200 nm to 700 nm (resolution of 1 nm). The absorbance spectrum for each aqueous extract of a filter was recorded immediately after addition of ammonium sulfate to the sample (0 hours) and at subsequent time points of 12, 24, 36, 48, 66, 138, and 162 hours. For the remainder of this chapter, whenever it is mentioned that the UV-spectra was recorded for a filter, it corresponds to the aqueous extract of the filter.

## 5.3 Results

### 5.3.1 SOA yields from SFNO

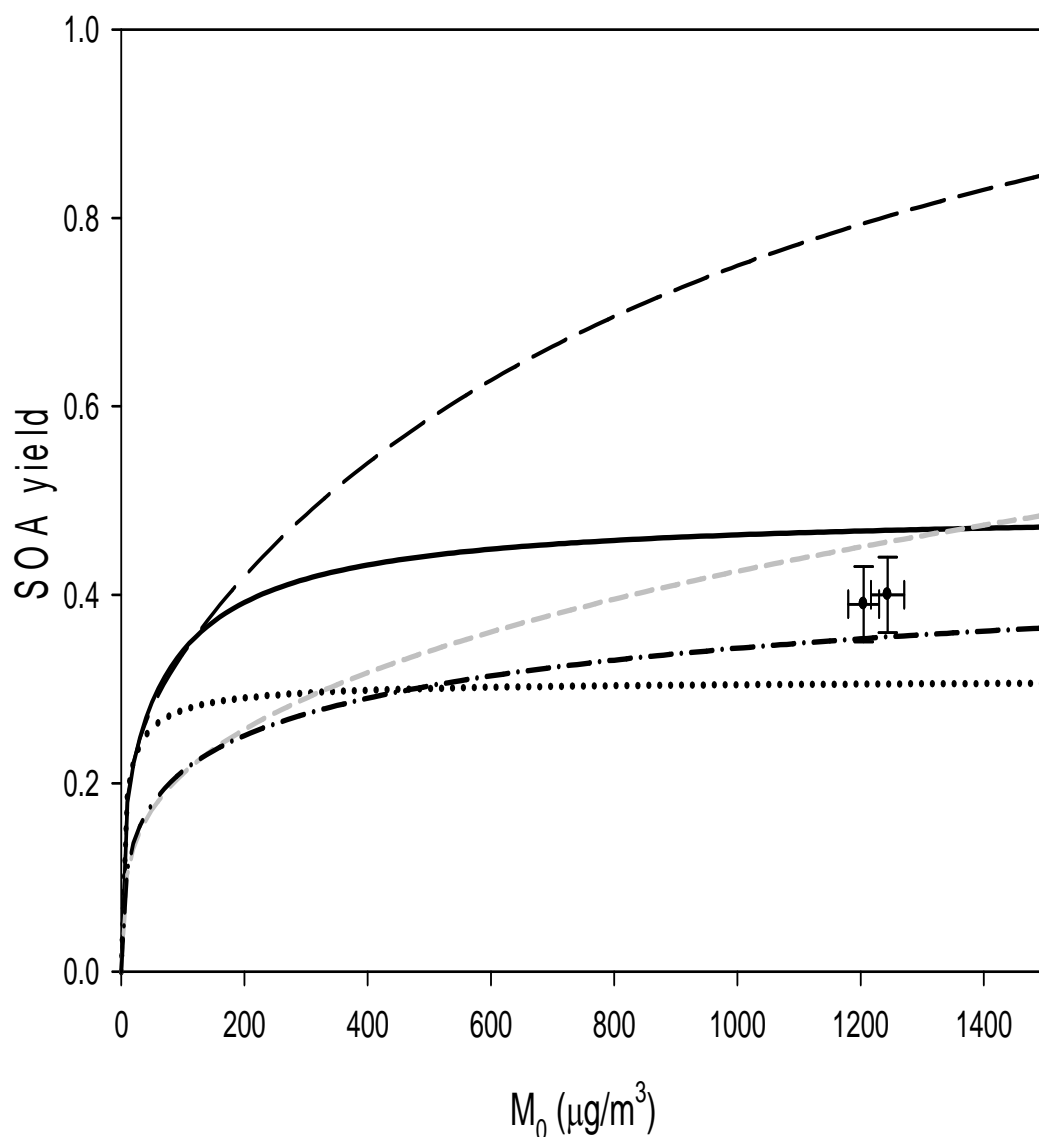
Two SOA generation experiments were carried out using SFNO as precursor. The experimental parameters are summarized in Table 5.2 below. The SOA yields from two experiments were calculated as  $0.39 \pm 0.04$  and  $0.40 \pm 0.03$ . Hatfield and Huff Hartz<sup>74</sup> have reported SOA yields for increasing concentrations of SFNO used. These studies were performed to calculate the according to VBS theory. The authors reported a SOA yield of  $0.31 \pm 0.01$  for SFNO experiment with reactive concentration of  $1860 \pm 60 \mu\text{g m}^{-3}$  at ozone concentration of approximately 500 ppb. The higher SOA yields obtained in this chapter can be explained due to higher concentration of reactive precursor used  $3100 \pm 125 \mu\text{g m}^{-3}$ . Also, the ozone concentration used in these experiments was more than three times used by Hatfield and Huff Hartz.<sup>74</sup>

The SOA yields are plotted against the  $M_0$  and are shown in Figure 5.1. The SOA yields are represented by black dots and the error bars represent the absolute uncertainty in SOA yield and  $M_0$ . The yields are compared to yields predicted by the VBS theory parameters mentioned

Hatfield and Huff Hartz.<sup>74</sup> The solid black line represents the theoretical SOA yields for SFNO at corresponding  $M_0$ , the calculations were done on basis of mass based yields given in Hatfield and Huff Hartz.<sup>74</sup> The other curves were plotted by using mass-based yields for  $\alpha$ -pinene published by different research groups. The black dashed line represents the work by Chan *et al.*,<sup>247</sup> the gray dashed line represents the work done by Pathak *et al.*,<sup>89</sup> the black dash dot line is generated using mass based yield values from Presto and Donahue<sup>250</sup> and the black dotted line represents the work by Shilling *et al.*<sup>251</sup> Hatfield and Huff Hartz<sup>74</sup> showed that the SOA yields from SFNO agree with  $\alpha$ -pinene SOA yields of Shilling *et al.*<sup>251</sup> when  $M_0$  is less than  $200 \mu\text{g m}^{-3}$ . Above  $200 \mu\text{g m}^{-3}$  the VBS curve agrees with the work of Presto and Donahue<sup>250</sup> obtained for  $\alpha$ -pinene. The SOA yields are lower than predicted by VBS curve from Hatfield and Huff Hartz.<sup>74</sup> The lower experimental SOA yields may be result of higher concentration (approximately 1600 ppb) of ozone used than SOA generation studies by Hatfield and Huff Hartz<sup>74</sup> (approximately 500 ppb). Also, the mass based yields,  $\alpha$ , (not to be confused with aerosol yield,  $Y$ ) calculated by Hatfield and Huff Hartz<sup>74</sup> were for  $M_0$  values ranging from  $22.4 \pm 0.8 \mu\text{g m}^{-3}$  to  $577 \pm 9 \mu\text{g m}^{-3}$  and do not cover the range of experimental values for  $M_0$ ,  $1205 \pm 25 \mu\text{g m}^{-3}$  and  $1244 \pm 27 \mu\text{g m}^{-3}$ .

The mass of SOA collected on the filter was calculated from the integrated SMPS mass concentration during filter sampling, the sampling flow rate, and the sampling time. The chamber blanks have negligible SOA mass on the filters (calculated to be  $< 0.0001 \text{ g}$ ). The values shown in parenthesis represent the range of SOA mass collected on filter. The range of masses shown in Table 5.2 is calculated by the propagation of error associated with SMPS, sampling time, the uncertainty in density of SOA,<sup>162,247</sup> and the positive and negative artifacts arising from the use of quartz filters.<sup>208</sup>

For each SOA generation experiment, two filter samples (one chamber blank and one sample filter) were collected. For each precursor mixture, two experiments were performed, making total of eight filter samples: four chamber blanks and four SOA filters. The chamber blank samples from the limonene-based air freshener SOA and SFNO SOA were combined, respectively; and sample filters from each precursor mixture were combined, so that concentration of SOA in the final extract would be in same range as reported in Bones et al. Then, the filters were then cut in half, thus for each type of precursor mixture, an ammonium ion-treated sample and blank was compared to an untreated sample and blank. The final concentration of SFNO SOA in each treated and untreated aliquot was equal to  $0.305 \text{ g L}^{-1}$ , and the concentration of limonene based air freshener SOA in each treated and untreated test tube was  $0.175 \text{ g L}^{-1}$ .



**Figure 5.1.** SOA yield vs  $M_0$  for Siberian fir needle oil. The experiments carried out for SOA generation (details Table 5.1) are represented by the two filled circles; the error in each parameter is shown. The error in SOA yields are calculated by propagation of uncertainties associated with VOC concentrations and  $M_0$ . The error in  $M_0$  is the standard error associated with curve-fit used for wall loss corrections used in this experiment. The additional lines represent the volatility basis set fit for  $\alpha$ -pinene SOA. Black dashed line: Chan et al.;<sup>246</sup> black solid line: Hatfield and Huff Hartz;<sup>74</sup> gray dashed line Pathak et al.;<sup>89</sup> black dash dot line: Presto and Donahue;<sup>250</sup> black dotted line: Shilling et al.<sup>251</sup>

**Table 5.2** Experimental parameters and amount of SOA collected on filters for SFNO<sup>a</sup>

Reactive VOC concentration ( $\mu\text{g m}^{-3}$ ) <sup>b</sup>	$M_0$ ( $\mu\text{g m}^{-3}$ ) <sup>c</sup>	SOA yield <sup>d</sup>	Initial ozone concentration (ppb) <sup>e</sup>	Average temperature (K) <sup>f</sup>	Relative humidity (%) <sup>g</sup>	Pressure (atm) <sup>h</sup>	Mass of SOA collected on filter (g) <sup>i</sup>
3100±125	1205±25	0.39±0.0 <sub>4</sub>	1720±7	293.9±0.3	8.17±2.2	0.951±0.001	0.0031 (0.0026-0.0044)
3100±125	1244±27	0.40±0.0 <sub>3</sub>	1618±4	296.6±0.3	0.62±0.2	0.935±0.031	0.0030 (0.0026-0.0042)

<sup>a</sup>The details on SOA yields for limonene based air freshener and physical parameters are mentioned in Table 3.5 and Appendix II (Table AI-II). <sup>b</sup>The uncertainties in VOC concentration calculated by propagation of uncertainty associated with syringe used for VOC injection, density of VOC and uncertainty in volume of bag (estimated 10%).

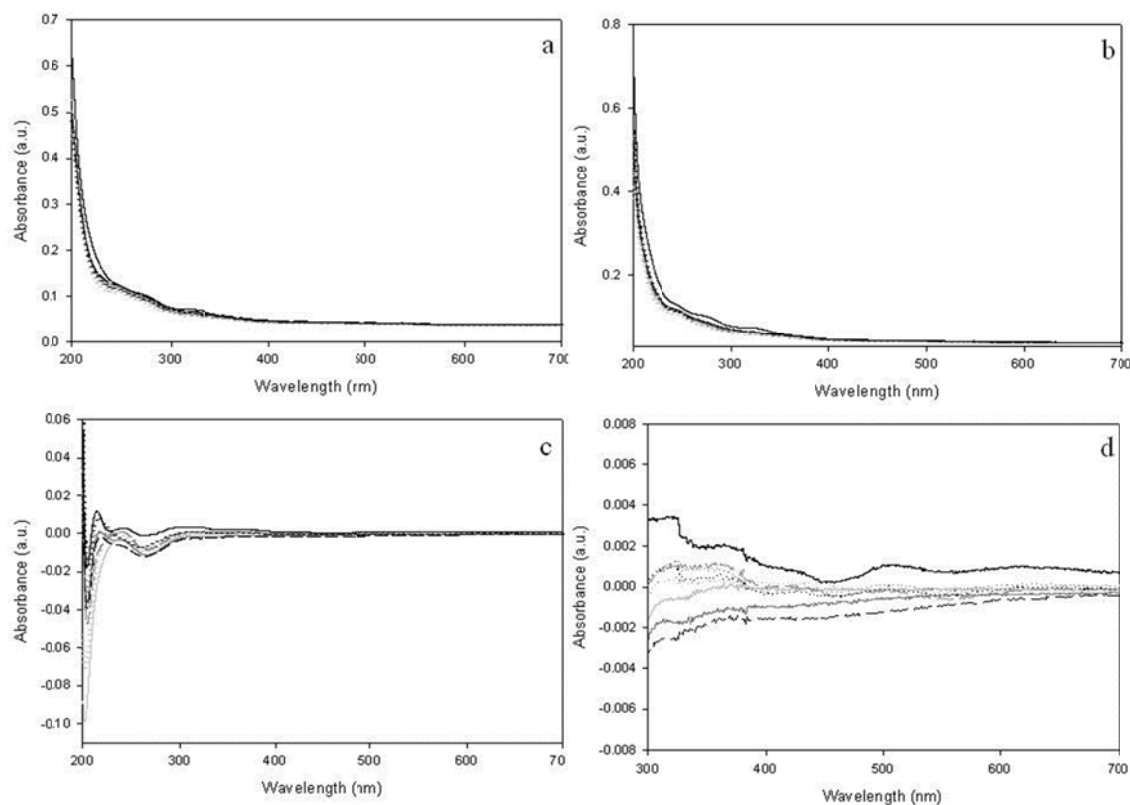
<sup>c</sup>The error in  $M_0$ , is the standard error associated with curve fit used for wall-loss corrections used in these experiments. <sup>d</sup>The uncertainties associated with SOA yield are calculated by error propagation using uncertainties in VOC concentration and standard error in  $M_0$ . <sup>e</sup>The ozone concentration is calculated by averaging ozone concentration readings obtained from Teledyne Instruments (Model 450), twenty minutes prior to injection of VOC, the uncertainty in the measurement is the standard deviation between these values. <sup>f</sup>The temperature is calculated by averaging temperature recorded during course of chamber experiment by the four thermocouples, humidity meter, and pressure sensor; the error in temperature measurement is calculated by error propagation of the standard deviation for measurement obtained from each device. <sup>g</sup>The relative humidity reported is the average of RH readings recorded during the course of experiment, the error in the measurement is the standard deviation among the readings.

<sup>h</sup>The pressure value reported is obtained by averaging the readings recorded by the pressure sensor during the course of the experiment and the error is the standard deviation among the recorded readings. <sup>i</sup>The values in the parenthesis represent the range for amount of SOA collected on the filter, this range is calculated by propagation of error associated with SMPS, CPC, amount and time for which vacuum is applied, uncertainty in density of particle (literature have reported densities of particles ranging from 0.9 g cm<sup>-3</sup> (Kostenidou et al.)<sup>251</sup> to 1.4 g cm<sup>-3</sup> (Ng et al.)<sup>162</sup>) and positive artifact due absorption of gases on quartz filters<sup>205</sup>. <sup>j</sup>The mean expected SOA concentration in the extract is shown, as the filters were cut in half, this concentration is half of total SOA collected from chamber 10 mL of extraction solvent.

### 5.3.2 Absorbance spectra for blank filters

The absorbance spectra for  $\text{NH}_4^+$  treated and untreated blank filters, blank filters were pre annealed quartz filters and no air was sampled using this filter, are shown in Figure 5.2. Figure 5.2a shows the absorbance as a function of time for the untreated blank filter solution and Figure 5.2b shows the absorbance for  $\text{NH}_4^+$  treated blank filter sample as a function of time. Figure 5.2c shows the difference between the absorbance of each treated and untreated filter at each time point. Figure 5.2 d is an expanded view of Figure 5.2c between wavelengths of 300-700 nm. We do not observe any peaks for treated and untreated blank filter samples. Table 5.3 summarizes the average absorbance values for treated and untreated samples. The absorbance for both treated and untreated blank filters increased at wavelengths  $< 250$  nm which is consistent with findings from Bones et al.<sup>247</sup> The differences in absorbance between treated and untreated filter samples in both near UV and visible region fluctuated around zero and are smaller than the absorbances from SOA filters (section 5.3.5 and section 5.3.6). Furthermore, no distinctive absorbance peaks were observed in the visible region of the spectra. We can conclude the treatment of  $\text{NH}_4^+$  on blank filters does not lead to generation of chromophores.





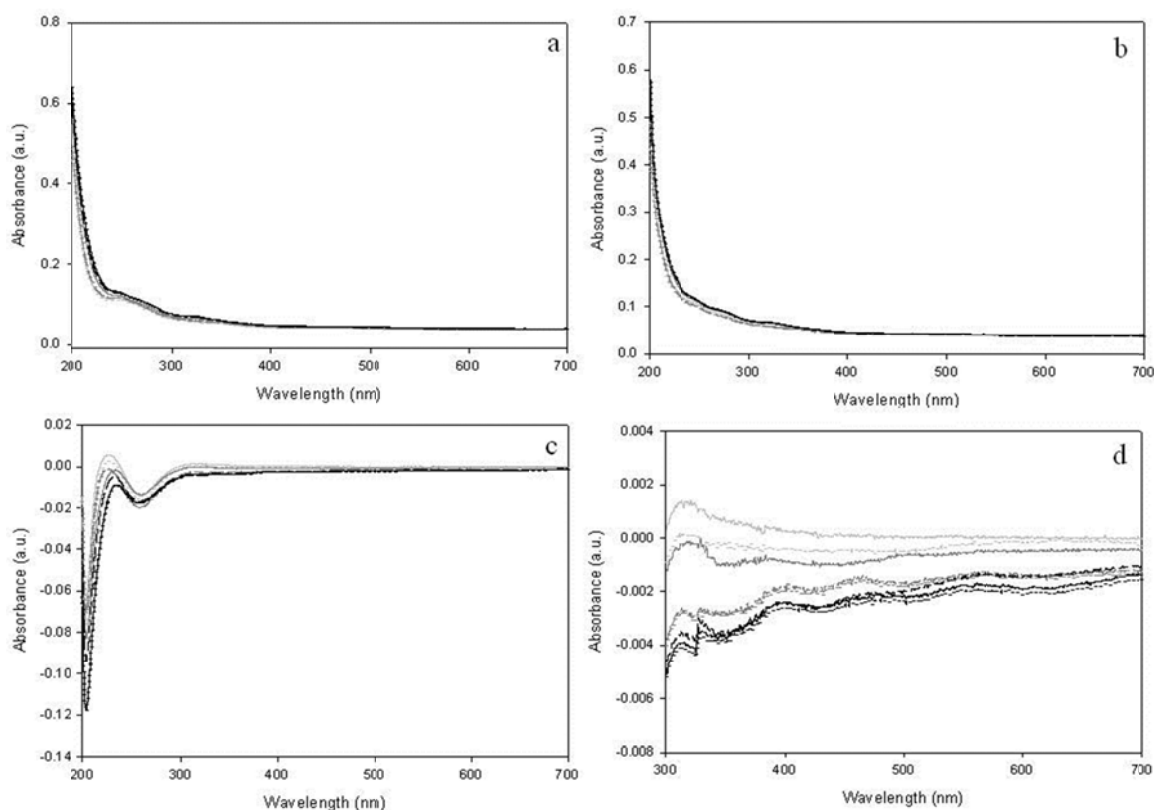
**Figure 5.2** UV-visible absorption spectra of (a) untreated blank filter (b)  $\text{NH}_4^+$  treated blank filter (c) difference in UV-visible absorption of treated and untreated blank filters (d) expanded view for part c, from wavelength 300 nm to 700 nm. Curves in each plot represent UV-visible spectra at different times after addition of  $\text{NH}_4^+$ , black solid line represents 162 hours, dotted black line represents 138 hours, dash black line represents 66 hours, dark gray solid line represents 48 hours, dotted dark gray line represents 36 hours, dash dark gray line represents 24 hours, gray solid line represents 12 hours, and dotted gray line represents 0 hours.

**Table 5.3** Average absorbance for treated and untreated blank filter samples

Aging time	Wavelength 300-400 nm			Wavelength 400-700 nm		
	Average absorbance untreated filters	Average absorbance for $\text{NH}_4^+$ treated filters	Difference	Average absorbance untreated filters	Average absorbance for $\text{NH}_4^+$ treated filters	Difference
0 hour	0.0510	0.0512	0.0002	0.0382	0.0383	-0.0001
12 hours	0.0543	0.0540	-0.0003	0.0390	0.0389	-0.0001
24 hours	0.0550	0.0557	0.0007	0.0404	0.0401	-0.0003
36 hours	0.0540	0.0546	0.0006	0.0392	0.0391	-0.0001
48 hours	0.0580	0.0570	-0.0010	0.0410	0.0405	-0.0005
66 hours	0.0590	0.0570	-0.0020	0.0420	0.0411	-0.0009
138 hours	0.0568	0.0572	0.0004	0.0407	0.0405	-0.0002
162 hours	0.0595	0.0617	0.0022	0.0410	0.0417	0.0007

### 5.3.3 Limonene-based air freshener chamber blanks

Figure 5.3 shows UV-visible absorbance spectra for aqueous filter extracts of chamber blanks for limonene-based air freshener experiments, as a function of time. The chamber blanks are collected prior to injection of air freshener in the chamber and hence do not contain any SOA. Figure 5.3a shows the absorbance spectra for the untreated chamber blank, Figure 5.3b shows the absorbance spectra for  $(\text{NH}_4)_2\text{SO}_4$  treated chamber blanks, and Figure 5.3c shows difference between the absorbance of treated and untreated chamber blanks. Figure 5.3d is an expanded view of Figure 5.3c for absorbance between 300 nm to 700 nm.



**Figure 5.3** UV-visible absorption spectra of (a) untreated chamber blank of lemon and chamomile filter (b)  $\text{NH}_4^+$  treated chamber blank of lemon and chamomile filter (c) difference in UV-visible absorption of treated and untreated chamber blank of lemon and chamomile filter (d) expanded view for part c, from wavelength 300 nm to 700 nm. Curves in each plot represent UV-visible spectra at different times after the addition of  $\text{NH}_4^+$ , black solid line represents 162 hours, dotted black line represents 138 hours, dash black line represents 66 hours, dark gray solid line represents 48 hours, dotted dark gray line represents 36 hours, dash dark gray line represents 24 hours, gray solid line represents 12 hours, and dotted gray line represents 0 hours.

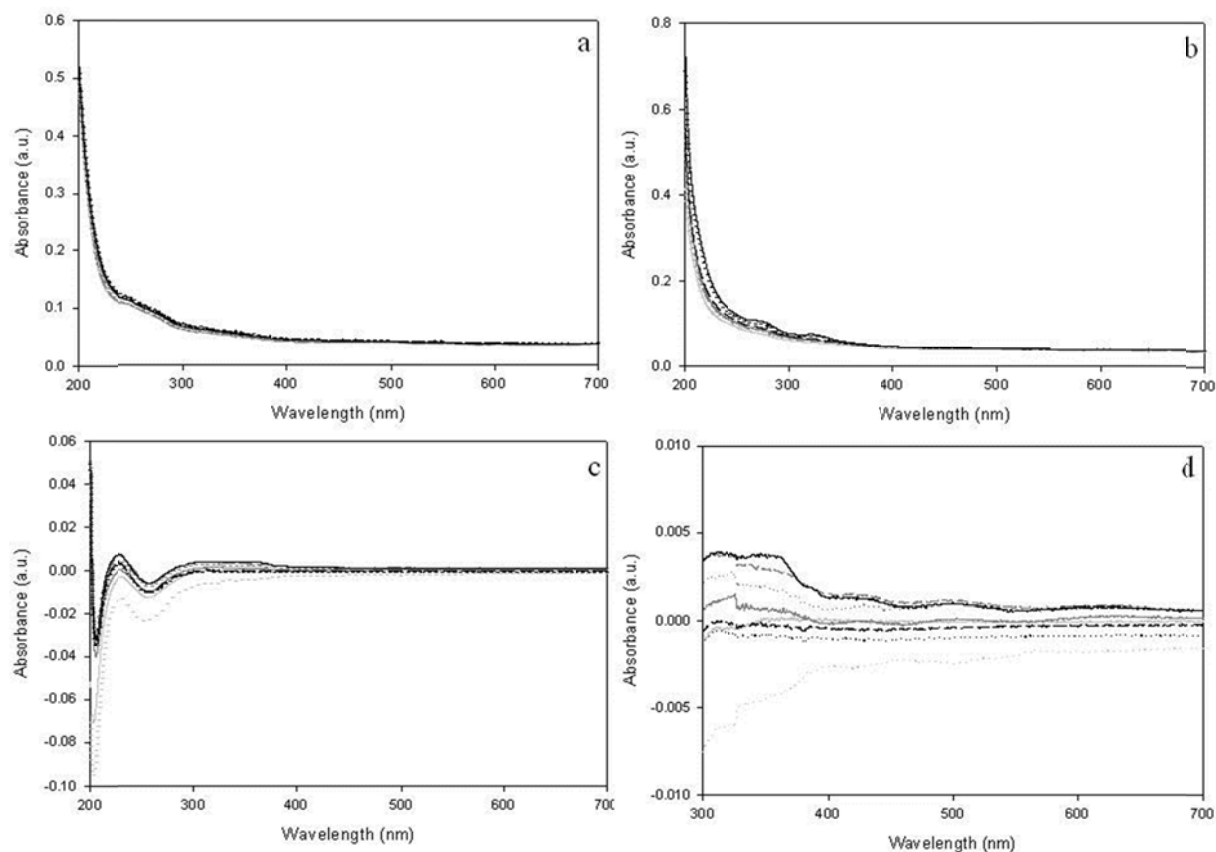
From the figures, we observe that there were no distinct absorption peaks for the visible region of absorbance spectrum. Table 5.4 shows the average absorbance calculated for aqueous solutions both  $\text{NH}_4^+$  treated and untreated limonene-based chamber blank. The  $\text{NH}_4^+$  treated filters tend to absorb less than the untreated filters, and the magnitude of this difference increases with increasing aging time. From Table 5.4 and Table 5.6, the increase in absorbance for the  $\text{NH}_4^+$  treated chamber blank filters were found to be lower than increase in absorbance of the  $\text{NH}_4^+$  treated limonene based air freshener SOA in both near UV and visible region.

**Table 5.4** Average absorbance for treated and untreated chamber blanks for limonene-based air freshener

Aging time	Wavelength 300-400 nm			Wavelength 400-700 nm		
	Average absorbance untreated filters	Average absorbance for $\text{NH}_4^+$ treated filters	Difference	Average absorbance untreated filters	Average absorbance for $\text{NH}_4^+$ treated filters	Difference
0 hour	0.0512	0.0510	-0.0002	0.0384	0.0381	-0.0003
12 hours	0.0526	0.0533	0.0007	0.0385	0.0384	-0.0001
24 hours	0.0536	0.0509	-0.0027	0.0397	0.0381	-0.0016
36 hours	0.0548	0.0521	-0.0027	0.0408	0.0392	-0.0016
48 hours	0.0560	0.0533	-0.0007	0.0396	0.0390	-0.0006
66 hours	0.0593	0.0560	-0.0030	0.0409	0.0392	-0.0017
138 hours	0.0595	0.0588	-0.0036	0.0412	0.0391	-0.0021
162 hours	0.0608	0.0573	-0.0035	0.0425	0.0406	-0.0019

### 5.3.4 Siberian fir needle oil chamber blanks

The UV-visible absorbance spectra for the aqueous filter extract for SFNO chamber blanks are shown in Figure 5.4. Figure 5.4a represents the UV-visible spectra for untreated chamber blank. Figure 5.4b represents the spectra for treated chamber blanks. Figure 5.4c is the difference in absorbance between treated and untreated filter, Figure 5.4d is the expanded view of Figure 5.4c.



**Figure 5.4** UV-visible absorption spectra of (a) untreated chamber blank of SFNO filter (b)  $\text{NH}_4^+$  treated chamber blank of SFNO filter (c) difference in UV-visible absorption of treated and untreated chamber blank of SFNO filter (d) expanded view for part c, from wavelength 300 nm to 700 nm. Curves in each plot represent UV-visible spectra at different times after addition of  $\text{NH}_4^+$ , black solid line represents 162 hours, dotted black line represents 138 hours, dash black line represents 66 hours, dark gray solid line represents 48 hours, dotted dark gray line represents 36 hours, dash dark gray line represents 24 hours, gray solid line represents 12 hours, and dotted gray line represents 0 hours.

No characteristic absorbance maxima were observed for the SFNO chamber blanks. The increase in absorbance of  $\text{NH}_4^+$  treated SFNO chamber blanks is small in comparison to the  $\text{NH}_4^+$  treated SFNO SOA filters. The difference between the absorbance of treated and untreated chamber blanks for SFNO fluctuates like random noise on either side of zero as is observed for the blank filters (Section 5.3.2). Hence we conclude that the change in absorbance in the  $\text{NH}_4^+$  treated chamber blanks is negligible.

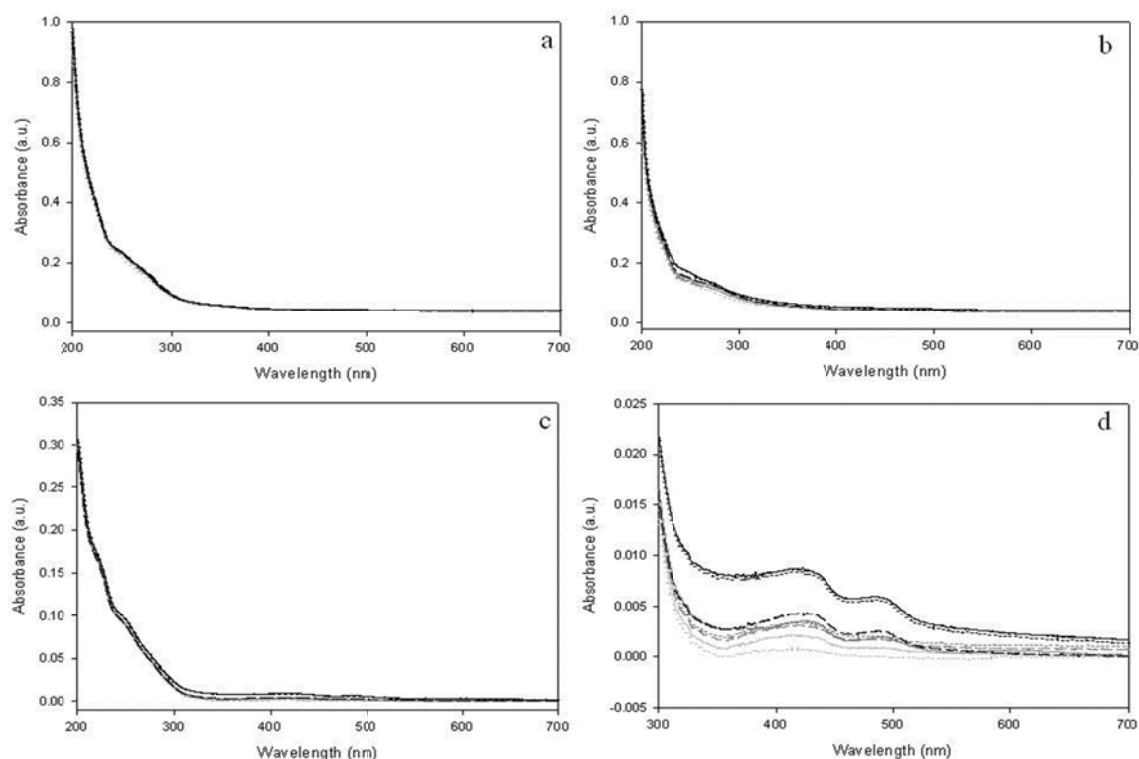
**Table 5.5** Average absorbance for treated and untreated chamber blanks for Siberian fir needle oil

Aging time	Wavelength 300-400 nm			Wavelength 400-700 nm		
	Average absorbance untreated filters	Average absorbance for $\text{NH}_4^+$ treated filters	Difference	Average absorbance untreated filters	Average absorbance for $\text{NH}_4^+$ treated filters	Difference
0 hour	0.0522	0.0506	-0.0046	0.0400	0.0379	-0.0021
12 hours	0.0506	0.0504	-0.0002	0.0379	0.0378	-0.0001
24 hours	0.0508	0.0536	0.0028	0.0379	0.0388	0.0009
36 hours	0.0520	0.0538	0.0017	0.0383	0.0390	0.0007
48 hours	0.0543	0.0549	0.0006	0.0392	0.0393	0.0001
66 hours	0.0576	0.0573	-0.0003	0.0407	0.0404	-0.0003
138 hours	0.0587	0.0582	-0.0005	0.0415	0.0399	-0.0016
162 hours	0.0554	0.0614	0.0059	0.0398	0.0406	0.0008

All three blank filters (one blank filter and two chamber blanks) show no characteristic absorbance maxima and slight-to-no increase in the average absorbance over period of time, indicating that  $\text{NH}_4^+$  aging has no effect on the aqueous extracts of quartz filters. Hence, there is a little or no contribution from the blank filters by addition of  $\text{NH}_4^+$ .

### 5.3.5 Limonene-based air freshener SOA filter samples

Figure 5.5a represents UV-visible spectra for the aqueous extract of untreated SOA filter generated by ozonolysis of limonene-based air freshener as a function of time. Figure 5.5b represents spectra for treated SOA filter sample as a function of  $\text{NH}_4^+$  aging time. Figure 5.5c represents the spectra generated from difference between absorbance of  $\text{NH}_4^+$ -treated and untreated filters. Figure 5.5d is expanded view of Figure 5.5c between wavelengths of 300-700 nm. The absorbance below 250 nm rapidly increased for both  $\text{NH}_4^+$ -treated and untreated filters, as was the case for the chamber blank.



**Figure 5.5** UV-visible absorption spectra of (a) untreated lemon and chamomile SOA filter (b)  $\text{NH}_4^+$  treated lemon and chamomile SOA filter (c) difference in UV-visible absorption of treated and untreated lemon and chamomile SOA filter (d) expanded view for part c, from wavelength 300 nm to 700 nm. Curves in each plot represent UV-visible spectra at different times after addition of  $\text{NH}_4^+$ , black solid line represents 162 hours, dotted black line represents 138 hours, dash black line represents 66 hours, dark gray solid line represents 48 hours, dotted dark gray line represents 36 hours, dash dark gray line represents 24 hours, gray solid line represents 12 hours, and dotted gray line represents 0 hours.

According to Figure 5.5d, the absorbance of the  $\text{NH}_4^+$ -treated filter was higher than the untreated filter sample. The figure also showed two absorbance maxima observed at wavelengths of 423 nm and 486 nm. Bones et al.<sup>247</sup> reported two absorbance maxima for limonene SOA at wavelengths of 430 nm and 505 nm, and these maxima were attributed to imidazole ring compounds or aromatic pyridinium ions formed by reaction of oxygenated SOA products with  $\text{NH}_4^+$ . The maxima for limonene-based air freshener SOA filter extracts were found to be blue shifted.

Table 5.6 shows the average absorbance for both treated and untreated filter samples for wavelength at near UV region and visible region. The average absorbance in the near UV region for  $\text{NH}_4^+$ -treated SOA filter, 0.0144, was more than the untreated filter, 0.0069. The average absorbance in visible region for the untreated filters steadily increased by 0.0022, while the average absorbance for  $\text{NH}_4^+$ -treated filter increased by 0.0062. Hence, when SOA from limonene-based air freshener was aged in presence of  $\text{NH}_4^+$ , the absorbance in the near UV and visible region increased steadily as the aging time increased. A higher increase in absorbance for  $\text{NH}_4^+$  treated SOA filters in both near UV and visible region and appearance of characteristic absorbance maxima in visible region is observed from these data. These observations imply that reaction between  $\text{NH}_4^+$  and limonene-based air freshener SOA generate chromophores which are similar to chromophores generated by aging of single VOC SOA in presence of  $\text{NH}_4^+$ .

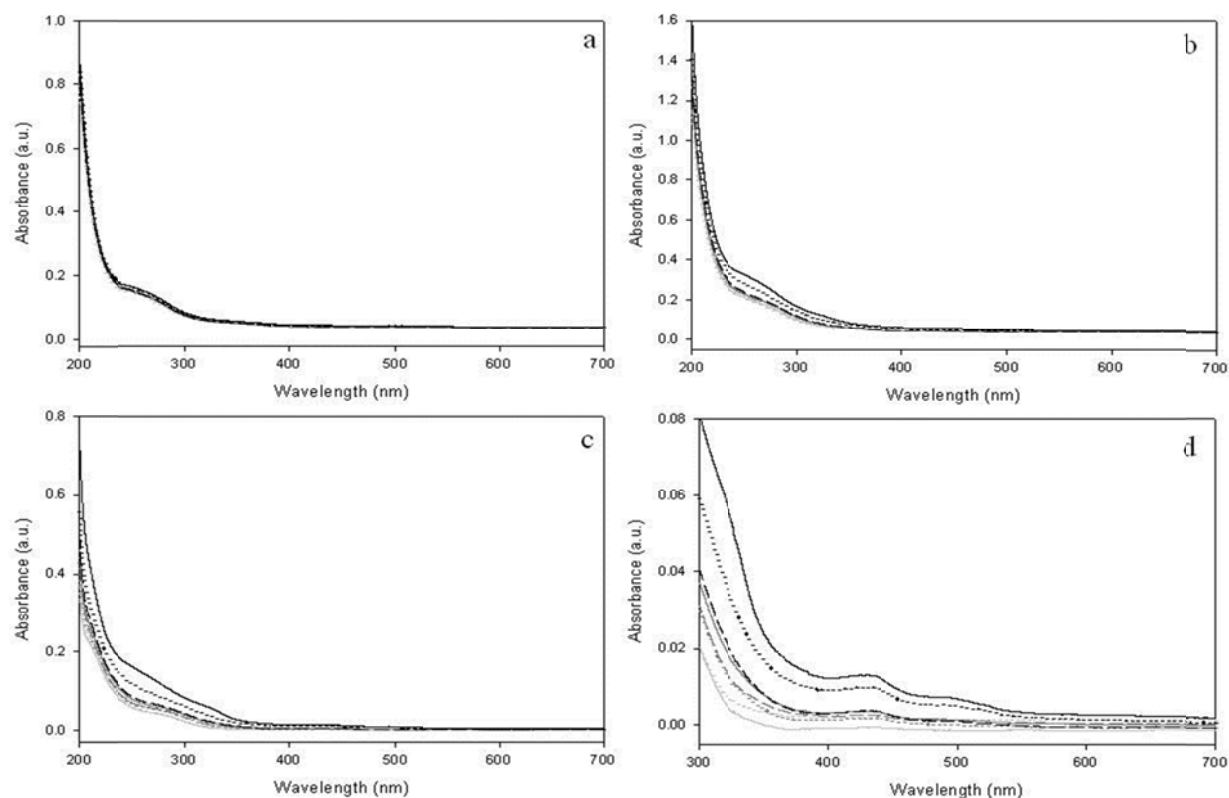
**Table 5.6** Average absorbance for treated and untreated SOA filter generated from ozonolysis of limonene-based air freshener

Aging time	Wavelength 300-400 nm			Wavelength 400-700 nm		
	Average absorbance untreated filters	Average absorbance for $\text{NH}_4^+$ treated filters	Difference	Average absorbance untreated filters	Average absorbance for $\text{NH}_4^+$ treated filters	Difference
0 hour	0.0522	0.0535	-0.0017	0.0380	0.0381	0.0001
12 hours	0.0578	0.0575	-0.0002	0.0384	0.0390	0.0006
24 hours	0.0552	0.0562	0.0010	0.0376	0.0390	0.0014
36 hours	0.0563	0.0577	0.0014	0.0388	0.0405	0.0017
48 hours	0.0576	0.0599	0.0024	0.0386	0.0398	0.0012
66 hours	0.0582	0.0607	0.0025	0.0383	0.0397	0.0014
138 hours	0.0579	0.0665	0.0085	0.0391	0.0428	0.0037
162 hours	0.0591	0.0679	0.0089	0.0402	0.0443	0.0041
Increase in absorption over 162 hours	0.0069	0.0144	-	0.0022	0.0062	-



### 5.3.6 Siberian fir needle oil SOA filter samples

The UV-visible absorbance spectra for aqueous filter extract for SOA of SFNO as a function of time are shown in Figure 5.6. Figure 5.6a represents the UV-visible spectra for untreated SFNO SOA filter. Figure 5.6b represents the spectra for  $\text{NH}_4^+$ -treated SOA filter samples for SFNO. Figure 5.6c is the difference in absorbance between treated and untreated filter SFNO SOA filters, Figure 5.6d is the expanded view of Figure 5.6c from wavelengths of 300-700 nm.



**Figure 5.6** UV-visible absorbance spectra of (a) untreated SFNO SOA filter (b)  $\text{NH}_4^+$  treated SFNO SOA filter (c) difference in UV-visible absorption of treated and untreated SFNO SOA filter (d) expanded view for part c, from wavelength 300 nm to 700 nm. The curves in each plot represent UV-visible spectra at different times after addition of  $\text{NH}_4^+$ , where the black solid line represents 162 hours, dotted black line represents 138 hours, dash black line represents 66 hours, dark gray solid line represents 48 hours, dotted dark gray line represents 36 hours, dash dark gray line represents 24 hours, gray solid line represents 12 hours, and dotted gray line represents 0 hours.

From the figures, there was a steady increase in the difference absorbance of  $\text{NH}_4^+$ -treated SOA sample generated from SFNO (Figure 5.6 c and d). Two absorbance maxima were observed at wavelengths of 423 and 486 nm, which is similar to the maxima generated by  $\text{NH}_4^+$ -treated limonene-based air freshener SOA. The smaller intensity of absorbance maxima, as compared to  $\text{NH}_4^+$ -treated limonene-based air freshener SOA, may be due to smaller amount of limonene present in the SFNO, 4.9% by mass, as compared to that of limonene based air freshener, 6.2%.<sup>182</sup>

**Table 5.7** Average absorbance for treated and untreated SOA filter generated from ozonolysis of Siberian fir needle oil

Aging time	Wavelength 300-400 nm			Wavelength 400-700 nm		
	Average absorbance untreated filters	Average absorbance for $\text{NH}_4^+$ treated filters	Difference	Average absorbance untreated filters	Average absorbance for $\text{NH}_4^+$ treated filters	Difference
0 hour	0.0520	0.0574	0.0054	0.0377	0.0390	0.0013
12 hours	0.0558	0.0586	0.0027	0.0395	0.0382	-0.0013
24 hours	0.0552	0.0641	0.0089	0.0387	0.0396	0.0010
36 hours	0.0545	0.0623	0.0078	0.0383	0.0382	-0.0001
48 hours	0.0520	0.0638	0.0118	0.0374	0.0383	0.0009
66 hours	0.0532	0.0659	0.0127	0.0384	0.0388	0.0004
138 hours	0.0569	0.0803	0.0234	0.0399	0.0435	0.0036
162 hours	0.0592	0.0937	0.0345	0.0417	0.0470	0.0053
Increase in absorption over 162 hours	0.0072	0.0363	-	0.0040	0.0080	-

From Table 5.7, we observe an increase in absorbance as a function of time for the SFNO-SOA filters in both near UV and visible region. In UV region, we find that the increase in absorbance was 0.0072 for untreated filter samples and 0.0363 for the  $\text{NH}_4^+$ -treated SFNO SOA filters. The average absorbance in visible region for the untreated filters steadily increased by 0.0040 over a period of 162 hours and during the same time period the average absorbance for

$\text{NH}_4^+$  treated filter increased by 0.0080. The difference in absorbance for  $\text{NH}_4^+$ -treated and untreated SFNO SOA filters did not increase sequentially in both the near UV and the visible regions with time. Thus, we observe that SFNO SOA treated with  $\text{NH}_4^+$  leads to generation of chromophores which have lower absorption than the  $\text{NH}_4^+$  treated SOA generated from limonene based air freshener. This lower absorption values for SFNO SOA as compared to limonene based SOA can be correlated to the lower concentration of limonene in SFNO as compared to limonene based air freshener.

## 5.4 Calculation and discussions

### 5.4.1 Calculation of average absorption coefficients

To generalize the results, the average absorption coefficients were calculated using the method by Bones et al.<sup>247</sup> (refer Table 5.1), and the weighted absorption coefficients calculated for ammonium aged limonene-based air freshener SOA and SFNO SOA are compared weighted absorption coefficients for ammonia-aged SOA generated from single monoterpene precursors. To our knowledge, the absorption coefficient values for ammonium ion aged SOA generated from limonene,  $\gamma$ -terpinene, myrcene,  $\alpha$ -pinene, and  $\beta$ -pinene have only been reported by Bones et al.<sup>247</sup>

### 5.4.2 Absorption coefficients for $\text{NH}_4^+$ aged limonene-based air freshener SOA

The composition for limonene-based air freshener is 6.23% limonene, 1.61%  $\beta$ -pinene, 0.986% myrcene, 0.191%  $\gamma$ -terpinene, and 0.178%  $\alpha$ -pinene by weight. The calculated weighted mean absorption coefficient for limonene based air freshener is calculated by summing the reported absorption coefficient for each monoterpene multiplied by the fraction of each component in the precursor mixture. The calculated absorption coefficients for limonene-based

air freshener are  $0.0074 \text{ L g}^{-1} \text{ cm}^{-1}$  in the near UV region and  $0.0016 \text{ L g}^{-1} \text{ cm}^{-1}$  in the visible region, for 20 hours after addition of 0.008 M ammonium ions. The  $\beta$  values are calculated by dividing the average absorbance with SOA concentration and pathlength the values are listed in Table 5.8.

The measured absorption coefficient values ( $\beta$ ) were calculated for visible and near UV region using two approaches. First, the absolute average absorbance was used to calculate the absorption coefficient, and second, the difference in average absorbance between ammonium treated and untreated SOA filters is used. The first approach (absolute) is identical to the method used by Bones et al.<sup>247</sup> However, our samples show significant non-specific scattering, which increases the overall absorbance due to the background. Thus, we also correct the average absorbance using the untreated SOA filter. For the limonene-based air freshener, the absorption coefficients calculated using the absolute average absorbance values and were found to increase steadily for both visible and near UV region. The  $\beta$  values calculated using absolute average absorbance after 24 hours are  $0.2229 \text{ L g}^{-1} \text{ cm}^{-1}$  and  $0.3211 \text{ L g}^{-1} \text{ cm}^{-1}$  in visible and near UV region. Both  $\beta$  values are higher than the theoretical values calculated using the work of Bones et al.<sup>247</sup>, possibly due to the background scattering. The  $\beta$  values, using the average absorbance difference between the ammonium-treated and untreated filters, were calculated after 24 hours, and these values are  $0.0080 \text{ L g}^{-1} \text{ cm}^{-1}$  in the visible and  $0.0057 \text{ L g}^{-1} \text{ cm}^{-1}$  UV region. The measured  $\beta$  values for the visible and near UV region are higher than the calculated values reported above. This suggests the presence of other precursors which may contribute to absorbance of SOA upon aging in presence of ammonium ions. More investigation is needed for aging studies of individual components of this precursor mixture. From Table 5.8, we observe that there is an increase in absorption coefficients with increasing aging time, however, the

absorption coefficients for the UV region at time points of 0 and 12 hours is negative for the measurement with difference in absorbance of treated and untreated filters, which is due to higher absorbance of the untreated filter when compared to treated filters in this region and at that time point, the exact reason for increased absorbance of the untreated filters is not known, but can be due to some other absorbing species present in the SOA air freshener. We compare the absorption coefficient values for our data with Bones et al.<sup>247</sup> for 20 hours as it was the latest time point for which the authors had plotted the absorbance coefficient values for use of 0.008 M ammonium ion concentration as this is the highest concentration of ammonium sulfate data used by authors.

**Table 5.8:** Calculated and measured average absorbance coefficients ( $\beta$ ) for lemon and chamomile air freshener

Aging time	Average absorption coefficient, 300-400 nm ( $\text{Lg}^{-1}\text{cm}^{-1}$ )	Average absorption coefficient, 400-700 nm ( $\text{Lg}^{-1}\text{cm}^{-1}$ )	Average absorption coefficient, 300-400 nm ( $\text{Lg}^{-1}\text{cm}^{-1}$ )	Average absorption coefficient, 400-700 nm ( $\text{Lg}^{-1}\text{cm}^{-1}$ )
	Measured using absolute absorbance of treated SOA filters		Measured using difference between treated and untreated SOA filters	
0 hours	0.3057	0.2177	-0.0097	0.0006
12 hours	0.3286	0.2229	-0.0011	0.0034
24 hours	0.3211	0.2229	0.0057	0.0080
36 hours	0.3297	0.2314	0.0080	0.0097
48 hours	0.3423	0.2274	0.0137	0.0069
66 hours	0.3469	0.2269	0.0143	0.0080
138 hours	0.3800	0.2446	0.0486	0.0211
162 hours	0.3880	0.2531	0.0509	0.0234
Calculated according to Bones et al. <sup>a</sup>	0.0074	0.0016	-	-

<sup>a</sup>The  $\text{NH}_4^+$  concentration was 0.008 M and spectra was recorded after 20 hours

### 5.4.3 Absorption coefficients for $\text{NH}_4^+$ aged SFNO SOA

SFNO contains 13.8%  $\alpha$ -pinene, 4.9% limonene, 1.86%  $\beta$ -pinene, 0.46% myrcene and 0.056%  $\gamma$ -terpinene by weight. The calculated absorption coefficient for SFNO in near UV region is  $0.0083 \text{ L g}^{-1} \text{ cm}^{-1}$  and in visible region is  $0.0014 \text{ L g}^{-1} \text{ cm}^{-1}$ . These are the expected values for the absorption coefficient after 20 hours of 0.008 M ammonium ion aging. These calculated values are compared with the values measured from our data. The measured values are summarized in Table 5.9.

**Table 5.9:** Average absorbance coefficients for Siberian fir needle oil

Aging time	Average absorption coefficient, 300-400 nm ( $\text{Lg}^{-1}\text{cm}^{-1}$ )	Average absorption coefficient, 400-700 nm ( $\text{Lg}^{-1}\text{cm}^{-1}$ )	Average absorption coefficient, 300-400 nm ( $\text{Lg}^{-1}\text{cm}^{-1}$ )	Average absorption coefficient, 400-700 nm ( $\text{Lg}^{-1}\text{cm}^{-1}$ )
	Measured using absolute absorbance of treated SOA filters		Measured using difference between treated and untreated SOA filters	
0 hours	0.1882	0.1279	0.0177	0.0013
12 hours	0.1921	0.1252	0.0089	-0.0013
24 hours	0.2102	0.1298	0.0292	0.0010
36 hours	0.2043	0.1252	0.0256	-0.0001
48 hours	0.2092	0.1256	0.0387	0.0009
66 hours	0.2161	0.1272	0.0416	0.0004
138 hours	0.2633	0.1426	0.0767	0.0036
162 hours	0.3072	0.1541	0.1131	0.0053
Calculated according to Bones et al. <sup>a</sup>	0.0083	0.0014	-	-

<sup>a</sup>The  $\text{NH}_4^+$  concentration was 0.008 M and spectra was recorded after 20 hours

The values of  $\beta$  at 24 hours for SFNO are  $0.210 \text{ L g}^{-1} \text{ cm}^{-1}$  in the near UV region and  $0.130 \text{ L g}^{-1} \text{ cm}^{-1}$  for visible region. These values are much higher than the expected values, and given that the background absorbs, this may suggest that non-specific light-scattering contributes to the measured absorption coefficient. Hence, we use the difference in absorbance of treated and untreated filters to calculate the  $\beta$  values. At 24 hours, the calculated absorbance coefficients are

0.029 L g<sup>-1</sup> cm<sup>-1</sup> and 0.003 L g<sup>-1</sup> cm<sup>-1</sup> in near UV and visible region respectively. The absorbance coefficient for visible region was found to be twice of the calculated value of 0.001 L g<sup>-1</sup> cm<sup>-1</sup>.

The  $\beta$  value in the UV region is also higher than the expected value. This might be due to presence of other absorbing species forming during aging process in presence of ammonium ion.

#### **5.4.4 Comparison of absorption coefficients for NH<sub>4</sub><sup>+</sup> aged SFNO SOA and limonene-based air freshener SOA**

To compare the absorbance of ammonium ion aged SOA generated from different precursor mixtures, the absorption coefficients ( $\beta$  values) are compared. In the near UV region, the absorption coefficient for SFNO 0.1131 L g<sup>-1</sup> cm<sup>-1</sup> is greater than the absorption coefficient for the limonene-based air freshener 0.0509 L g<sup>-1</sup> cm<sup>-1</sup>. This was not expected, because ammonium ion-aged limonene and  $\gamma$ -terpinene SOA have higher absorption coefficients in the near UV region, and limonene and  $\gamma$ -terpinene are present in higher concentration in the limonene-based air freshener than in the SFNO. In the visible region, the  $\beta$  value for limonene-based air freshener increased steadily with final value of 0.0234 L g<sup>-1</sup> cm<sup>-1</sup> after 162 hours, while for SFNO the  $\beta$  values varied before steadily increasing, and at 162 hours, the value was 0.0053 L g<sup>-1</sup> cm<sup>-1</sup>. The difference in values can be attributed to the difference in the composition of the precursor mixtures. The limonene-based air freshener contains more limonene than SFNO, and ammonium ion aged limonene SOA has a higher absorption coefficient in visible region. However, both precursor mixtures contain reactive VOCs other than the five monoterpenes reported by Bones et al. In fact, only 9% of the total precursor mass in the air freshener and 21% of the total precursor mass in the SFNO has known ammonium ion aged SOA absorption coefficients. Since higher absorption coefficients were measured in comparison to the calculated

absorption coefficient, this suggests that there are additional SOA precursors which generate SOA and react with  $\text{NH}_4^+$  to produce absorbing aerosol. Both SFNO and limonene based air freshener contain other ozone reactive species (likely candidates to generate aged absorbing aerosol) like terpinolene ( $\text{O}_3 = 1.9 \times 10^{-15} \text{ cm}^3 \text{ molecule}^{-1} \text{ s}^{-1}$ ), myrcene ( $\text{O}_3 = 4.7 \times 10^{-16} \text{ cm}^3 \text{ molecule}^{-1} \text{ s}^{-1}$ ),  $\beta$ -phellandrene ( $\text{O}_3 = 4.7 \times 10^{-17} \text{ cm}^3 \text{ molecule}^{-1} \text{ s}^{-1}$ ) and  $\alpha$ -terpineol ( $\text{O}_3 = 3.0 \times 10^{-16} \text{ cm}^3 \text{ molecule}^{-1} \text{ s}^{-1}$ ) which have rate constants and SOA forming abilities similar to monoterpenes investigated by Bones et al.<sup>247</sup>

## 5.5 Conclusions

SFNO and limonene-based air freshener both show formation of chromophores upon aging in the presence of ammonium ion. Two absorption maxima, at 423 nm and 486 nm, are observed. Both maxima are blue shifted when compared to wavelengths reported by Bones et al.<sup>247</sup> The blue shift may be due to use of higher concentration of ammonium sulfate, leading to higher ionic strength. The measured limonene-based air freshener gave a higher absorption coefficient in the visible region than SFNO was expected because the concentration of the species which leads to the highest absorbance, limonene, is higher in the air freshener. This confirms our hypothesis that if limonene generates stronger chromophore upon aging than  $\alpha$ -pinene, the precursor mixtures containing more limonene should generate strong chromophores as well. However, on the UV region, the absorption coefficient was higher for SFNO, which may be due to higher total concentration of monoterpenes which generate chromophores upon aging than the air freshener.



## CHAPTER 6

### SUMMARY AND CONCLUSION

#### 6.1 Research Aims

The focus of this dissertation was to investigate how VOCs that have the potential to alter the efficiency of SOA formation and type of products formed. The variations in VOCs that are emitted from trees and that act as SOA precursors were measured as a function of insect infestation. SOA generation from monoterpene ozonolysis and SOA product analysis were carried out for  $\alpha$ -pinene, limonene, several lab made VOC mixtures, and commercial VOC mixtures. The SOA generated from commercial VOC mixtures were investigated for the absorption characteristics in presence of ammonium ion.

#### 6.2 Research Findings

The total VOC emissions from bark beetle infested trees were higher than emissions from the healthy and non-infested trees. The infested lodgepole pine trees showed an increase in  $\beta$ -phellandrene emissions by a factor of thirty in comparison to noninfested lodgepole pine trees. Infested Engelmann spruce trees emitted higher concentrations of 3-carene,  $\alpha$ -pinene, and  $\beta$ -pinene than noninfested Engelmann spruce trees. Each monoterpene can react at atmospherically relevant time scales to generate SOA and contribute to the regional PM concentrations, causing deleterious health effects and impact the radiative forcing in the atmosphere.

In this dissertation, SOA generation from limonene, lab made VOC mixtures containing limonene, and a commercially available limonene-based air freshener was discussed. SOA yields from the air freshener, surrogates, and VOC mixtures containing similar amounts of limonene

agreed within experimental error. The SOA yields generated from mixtures of precursors depend on the most dominant VOC present in the mixture. Filters containing condensed phase SOA generated from limonene, lab made VOC mixtures containing limonene, and limonene-based air freshener were extracted and analyzed. The ozonolysis products for lab made VOC mixtures containing limonene were found to be similar to the ozonolysis products of limonene. No products characteristic of other VOCs were detected for these mixtures, because limonene was the most ozone reactive VOC in the mixture and was in concentrations of more than five times than  $\beta$ -pinene, the next most reactive precursor. The ozonolysis of air freshener generated a product which was not identified in the SOA from any other VOC precursor mixtures or limonene. While the SOA yields of precursor mixtures are similar to the SOA yields of the single dominant precursor in the mixtures, the products of SOA mixtures may be contain additional compounds.

Filters samples containing the condensed phase portion of SOA generated from  $\alpha$ -pinene, VOC mixtures containing  $\alpha$ -pinene, SFNO, and CFNO yielded species that were characteristic of  $\alpha$ -pinene, but with additional products characteristic of the other VOCs in the precursor mixture. VOC mixtures that contained camphene generated two unique products. For mixtures containing 3-carene, nor-3-carene, a characteristic product of 3-carene, was identified. This identification was possible as the concentration of 3-carene was similar to  $\alpha$ -pinene in the precursor mixture. The presence of bornyl acetate during  $\alpha$ -pinene SOA generation leads to decrease in the mass of SOA products recovered without decreasing the amount of SOA formed. This is indirect evidence for the formation of oligomers. A similar observation was made when comparing the SOA products from SFNO, CFNO, and the surrogate mixtures, where the some of the individual SOA products were lower for SFNO.

The absorption coefficient for ammonium ion mediated aging of SOA generated from SFNO and limonene based air freshener was measured. The absorption coefficient of the SOA increased with an increase in aging time. The SOA generated from these two commercial VOC mixtures may generate chromophores upon atmospheric processing.

### **6.3 Future Direction**

The work from this dissertation can be furthered by investigating the impact of other oxidants like OH and NO<sub>x</sub> is similar on the SOA yields and oxidation product distributions. An investigation can be carried out for the variation in SOA yield and products formed by making binary VOC mixtures in lab with incremental increases in concentration of one of the VOCs in the mixture. Furthermore, SOA yields and products from  $\beta$ -phellandrene are not known, yet this VOC has the potential to impact VOC concentrations and PM levels in regions with widespread bark beetle infested lodgepole pine trees. Only atmospherically relevant VOCs and realistic mixture concentrations may help to control the number of VOCs to be analyzed.

## REFERENCES

1. *The world health report 2002- Reducing Risks, Promoting Healthy Life*; World Health Organization: Geneva, Switzerland, 2002;  
[http://www.who.int/whr/2002/en/whr02\\_en.pdf](http://www.who.int/whr/2002/en/whr02_en.pdf).
2. Monks, P. S.; Granier, C.; Fuzzi, S.; Stohl, A.; Williams, M. L.; Akimoto, H.; Amann, M.; Baklanov, A.; Baltensperger, U.; Bey, I.; Blake, N.; Blake, R. S.; Carslaw, K.; Cooper, O. R.; Dentener, F.; Fowler, D.; Fragkou, E.; Frost, G. J.; Generoso, S.; Ginoux, P.; Grewe, V.; Guenther, A.; Hansson, H. C.; Henne, S.; Hjorth, J.; Hofzumahaus, A.; Huntrieser, H.; Isaksen, I. S. A.; Jenkin, M. E.; Kaiser, J.; Kanakidou, M.; Klimont, Z.; Kulmala, M.; Laj, P.; Lawrence, M. G.; Lee, J. D.; Liousse, C.; Maione, M.; McFiggans, G.; Metzger, A.; Mieville, A.; Moussiopoulos, N.; Orlando, J. J.; O'Dowd, C. D.; Palmer, P. I.; Parrish, D. D.; Petzold, A.; Platt, U.; Poschl, U.; Prevot, A. S. H.; Reeves, C. E.; Reimann, S.; Rudich, Y.; Sellegri, K.; Steinbrecher, R.; Simpson, D.; ten Brink, H.; Theloke, J.; van der Werf, G. R.; Vautard, R.; Vestreng, V.; Vlachokostas, C.; von Glasow, R. Atmospheric composition change - global and regional air quality. *Atmos. Environ.* **2009**, *43* (33), 5268-5350.
3. Fowler, D.; Pilegaard, K.; Sutton, M. A.; Ambus, P.; Raivonen, M.; Duyzer, J.; Simpson, D.; Fagerli, H.; Fuzzi, S.; Schjoerring, J. K.; Granier, C.; Neftel, A.; Isaksen, I. S. A.; Laj, P.; Maione, M.; Monks, P. S.; Burkhardt, J.; Daemmgen, U.; Neirynck, J.; Personne, E.; Wichink-Kruit, R.; Butterbach-Bahl, K.; Flechard, C.; Tuovinen, J. P.; Coyle, M.; Gerosa, G.; Loubet, B.; Altimir, N.; Gruenhage, L.; Ammann, C.; Cieslik, S.; Paoletti, E.; Mikkelsen, T. N.; Ro-Poulsen, H.; Cellier, P.; Cape, J. N.; Horvath, L.; Loreto, F.;

- Niinemets, U.; Palmer, P. I.; Rinne, J.; Misztal, P.; Nemitz, E.; Nilsson, D.; Pryor, S.; Gallagher, M. W.; Vesala, T.; Skiba, U.; Brueggemann, N.; Zechmeister-Boltenstern, S.; Williams, J.; O'Dowd, C.; Facchini, M. C.; de Leeuw, G.; Flossman, A.; Chaumerliac, N.; Erisman, J. W. Atmospheric composition change: Ecosystems-atmosphere interactions. *Atmos. Environ.* **2009**, *43* (33), 5193-5267.
4. Isaksen, I. S. A.; Granier, C.; Myhre, G.; Berntsen, T. K.; Dalsoren, S. B.; Gauss, M.; Klimont, Z.; Benestad, R.; Bousquet, P.; Collins, W.; Cox, T.; Eyring, V.; Fowler, D.; Fuzzi, S.; Jockel, P.; Laj, P.; Lohmann, U.; Maione, M.; Monks, P.; Prevo, A. S. H.; Raes, F.; Richter, A.; Rognerud, B.; Schulz, M.; Shindell, D.; Stevenson, D. S.; Storelvmo, T.; Wang, W. C.; van Weele, M.; Wild, M.; Wuebbles, D. Atmospheric composition change: Climate-chemistry interactions. *Atmos. Environ.* **2009**, *43* (33), 5138-5192.
  5. Health topics: Air pollution; [http://www.who.int/topics/air\\_pollution/en/](http://www.who.int/topics/air_pollution/en/)
  6. Laj, P.; Klausen, J.; Bilde, M.; Plass-Duelmer, C.; Pappalardo, G.; Clerbaux, C.; Baltensperger, U.; Hjorth, J.; Simpson, D.; Reimann, S.; Coheur, P. F.; Richter, A.; De Maziere, M.; Rudich, Y.; McFiggans, G.; Tørseth, K.; Wiedensohler, A.; Morin, S.; Schulz, M.; Allan, J. D.; Attie, J. L.; Barnes, I.; Birmili, W.; Cammas, J. P.; Dommen, J.; Dorn, H. P.; Fowler, D.; Fuzzi, S.; Glasius, M.; Granier, C.; Hermann, M.; Isaksen, I. S. A.; Kinne, S.; Koren, I.; Madonna, F.; Maione, M.; Massling, A.; Moehler, O.; Mona, L.; Monks, P. S.; Müller, D.; Müller, T.; Orphal, J.; Peuch, V. H.; Stratmann, F.; Tanre, D.; Tyndall, G.; Rizi, A. A.; Van Roozendaal, M.; Villani, P.; Wehner, B.; Wex, H.; Zardini, A. A. Measuring atmospheric composition change. *Atmos. Environ.* **2009**, *43* (33), 5351-5414.
  7. US-EPA, Pollutants in Ambient Air; <http://www.epa.gov/apti/course422/ap2.html>

8. US-EPA, Criteria Air Pollutants; <http://www.epa.gov/air/caa/>
9. Forster, P., V. Ramaswamy, P. Artaxo, T. Berntsen, R. Betts, D.W. Fahey, J. Haywood, J. Lean, D.C. Lowe, G. Myhre, J. Nganga, R. Prinn, G. Raga, M. Schulz and R. Van Dorland, 2007: Changes in Atmospheric Constituents and in Radiative Forcing. In: Climate Change 2007: The Physical Science Basis. Contribution of Working Group I to the Fourth Assessment Report of the Intergovernmental Panel on Climate Change [Solomon, S., D. Qin, M. Manning, Z. Chen, M. Marquis, K.B. Averyt, M. Tignor and H.L. Miller (eds.)]. Cambridge University Press, Cambridge, United Kingdom and New York, NY, USA
10. Pope, C. A.; Dockery, D. W. Health effects of fine particulate air pollution: Lines that connect. *J. Air Waste Manage. Assoc.* **2006**, 56 (6), 709-742.
11. Davidson, C. I.; Phalen, R. F.; Solomon, P. A., Airborne particulate matter and human health: A review. *Aerosol Sci. Technol.* **2005**, 39 (8), 737-749.
12. Seinfeld, J. H.; Pandis, S. N. *Atmospheric Chemistry and Physics: From Air Pollution to Climate Change*; John Wiley & Sons: New York, 2006.
13. US-EPA, Supersites Project; <http://www.epa.gov/ttnamti1/files/ambient/super/ssback.pdf>
14. Lee, J. H.; Hopke, P. K.; Turner, J. R. Source identification of airborne PM<sub>2.5</sub> at the St. Louis-Midwest Supersite. *J. Geophys. Res., [Atmos.]* **2006**, 111 (D10).
15. US-EPA, understanding particulate matter;  
[http://www.epa.gov/airtrends/aqtrnd04/pmreport03/pmunderstand\\_2405.pdf](http://www.epa.gov/airtrends/aqtrnd04/pmreport03/pmunderstand_2405.pdf)
16. Pace, T. G. Session I: PM Composition and Sources (Ambient Composition: What are the Important Sources), EPA National EI Conference, New Orleans, LA, May 15, 2006.  
[http://www.epa.gov/ttn/chief/conference/ei15/training/pm\\_training.pdf](http://www.epa.gov/ttn/chief/conference/ei15/training/pm_training.pdf)

17. Turpin, B. J.; Saxena, P.; Andrews, E. Measuring and simulating particulate organics in the atmosphere: Problems and prospects. *Atmos. Environ.* **2000**, *34* (18), 2983-3013.
18. Asgharian, B.; Price, O. T. Deposition of ultrafine (nano) particles in the human lung. *Inhalation Toxicol.* **2007**, *19* (13), 1045-1054.
19. Oberdorster, G.; Oberdorster, E.; Oberdorster, J. Nanotoxicology: An emerging discipline evolving from studies of ultrafine particles. *Environ. Health Perspect.* **2005**, *113* (7), 823-839.
20. Peters, A.; Doring, A.; Wichmann, H. E.; Koenig, W. Increased plasma viscosity during an air pollution episode: A link to mortality? *Lancet* **1997**, *349* (9065), 1582-1587.
21. Weichenthal, S.; Dufresne, A.; Infante-Rivard, C. Indoor ultrafine particles and childhood asthma: Exploring a potential public health concern. *Indoor Air* **2007**, *17* (2), 81-91.
22. Brook, R. D.; Rajagopalan, S. Particulate matter, air pollution, and blood pressure. *J. Am. Soc. Hypertens.* **2009**, *3* (5), 332-350.
23. US-EPA, Particulate Matter (PM<sub>2.5</sub>) 1997, standard nonattainment area counties;  
<http://www.epa.gov/air/oaqps/greenbk/qnay.html>
24. US-EPA, Particulate matter (PM<sub>2.5</sub>) 2006, standard nonattainment area counties;  
<http://www.epa.gov/air/oaqps/greenbook/rnay.html>
25. *Indoor air chemistry: Cleaning agents, ozone and toxic air contaminants; Final Report: Contract No. 01-336*; Prepared for the California Air Resources Board and the California Environmental Protection Agency, **2006**; [http://www.arb.ca.gov/research/apr/past/01-336\\_a.pdf](http://www.arb.ca.gov/research/apr/past/01-336_a.pdf).
26. Destailats, H.; Lunden, M. M.; Singer, B. C.; Coleman, B. K.; Hodgson, A. T.; Weschler, C. J.; Nazaroff, W. W. Indoor secondary pollutants from household product emissions in

- the presence of ozone: A bench-scale chamber study. *Environ. Sci. Technol.* **2006**, *40* (14), 4421-4428.
27. Singer, B. C.; Coleman, B. K.; Destailats, H.; Hodgson, A. T.; Lunden, M. M.; Weschler, C. J.; Nazaroff, W. W. Indoor secondary pollutants from cleaning product and air freshener use in the presence of ozone. *Atmos. Environ.* **2006**, *40* (35), 6696-6710.
  28. Horvath, H. Atmospheric light-absorption: A review. *Atmos. Environ. Part a-General Topics* **1993**, *27* (3), 293-317.
  29. Bond, T. C.; Bergstrom, R. W., Light absorption by carbonaceous particles: An investigative review. *Aerosol Sci. Technol.* **2006**, *40* (1), 27-67.
  30. USEPA: Volatile organic compounds. <http://www.epa.gov/iaq/voc2.html#definition>
  31. Weschler, C. J. Changes in indoor pollutants since the 1950s. *Atmos. Environ.* **2009**, *43* (1), 153-169
  32. Fraser, M. P.; Cass, G. R.; Simoneit, B. R. T. Gas-phase and particle-phase organic compounds emitted from motor vehicle traffic in a Los Angeles roadway tunnel. *Environ. Sci. Technol.* **1998**, *32* (14), 2051-2060.
  33. Fortmann, R.; Roache, N.; Chang, J. C. S.; Guo, Z. Characterization of emissions of volatile organic compounds from interior alkyd paint. *J. Air Waste Manage. Assoc.* **1998**, *48* (10), 931-940.
  34. McDonald, J. D.; Zielinska, B.; Fujita, E. M.; Sagebiel, J. C.; Chow, J. C.; Watson, J. G. Emissions from charbroiling and grilling of chicken and beef. *J. Air Waste Manage. Assoc.* **2003**, *53* (2), 185-194.
  35. Andreae, M. O.; Merlet, P. Emission of trace gases and aerosols from biomass burning. *Global Biogeochem. Cycles* **2001**, *15* (4), 955-966.



36. Fall, R.; Karl, T.; Hansel, A.; Jordan, A.; Lindinger, W. Volatile organic compounds emitted after leaf wounding: On-line analysis by proton-transfer-reaction mass spectrometry. *J. Geophys. Res., [Atmos.]* **1999**, *104* (D13), 15963-15974.
37. Barker, M.; Hengst, M.; Schmid, J.; Buers, H. J.; Mittermaier, B.; Klemp, D.; Koppman, R. Volatile organic compounds in the exhaled breath of young patients with cystic fibrosis. *Eur. Respir. J.* **2006**, *27* (5), 929-936.
38. Liao, H.; Chen, W. T.; Seinfeld, J. H. Role of climate change in global predictions of future tropospheric ozone and aerosols. *J. Geophys. Res., [Atmos.]* **2006**, *111* (D12).
39. Guenther, A.; Hewitt, C. N.; Erickson, D.; Fall, R.; Geron, C.; Graedel, T.; Harley, P.; Klinger, L.; Lerdau, M.; McKay, W. A.; Pierce, T.; Scholes, B.; Steinbrecher, R.; Tallamraju, R.; Taylor, J.; Zimmerman, P. A global-model of natural volatile organic compound emissions. *J. Geophys. Res., [Atmos.]* **1995**, *100* (D5), 8873-8892.
40. Fuentes, J. D.; Lerdau, M.; Atkinson, R.; Baldocchi, D.; Bottenheim, J. W.; Ciccioli, P.; Lamb, B.; Geron, C.; Gu, L.; Guenther, A.; Sharkey, T. D.; Stockwell, W. Biogenic hydrocarbons in the atmospheric boundary layer: A review. *Bull. Am. Meteorol. Soc.* **2000**, *81* (7), 1537-1575.
41. Guenther, A. The contribution of reactive carbon emissions from vegetation to the carbon balance of terrestrial ecosystems. *Chemosphere* **2002**, *49* (8), 837-844.
42. Kesselmeier, J.; Kuhn, U.; Rottenberger, S.; Biesenthal, T.; Wolf, A.; Schebeske, G.; Andreae, M. O.; Ciccioli, P.; Brancaleoni, E.; Frattoni, M.; Oliva, S. T.; Botelho, M. L.; Silva, C. M. A.; Tavares, T. M. Concentrations and species composition of atmospheric volatile organic compounds (VOCs) as observed during the wet and dry season in Rondonia (Amazonia). *J. Geophys. Res., [Atmos.]* **2002**, *107* (D20).

43. Kanakidou, M.; Seinfeld, J. H.; Pandis, S. N.; Barnes, I.; Dentener, F. J.; Facchini, M. C.; Van Dingenen, R.; Ervens, B.; Nenes, A.; Nielsen, C. J.; Swietlicki, E.; Putaud, J. P.; Balkanski, Y.; Fuzzi, S.; Horth, J.; Moortgat, G. K.; Winterhalter, R.; Myhre, C. E. L.; Tsigaridis, K.; Vignati, E.; Stephanou, E. G.; Wilson, J. Organic aerosol and global climate modelling: A review. *Atmos. Chem. Phys.* **2005**, *5*, 1053-1123.
44. Kesselmeier, J.; Staudt, M. Biogenic volatile organic compounds (VOC): An overview on emission, physiology and ecology. *J. Atmos. Chem.* **1999**, *33* (1), 23-88.
45. Kimmerer, T. W.; Kozlowski, T. T. Ethylene, ethane, acetaldehyde, and ethanol-production by plants under stress. *Plant Physiol.* **1982**, *69* (4), 840-847.
46. Kimmerer, T. W.; Macdonald, R. C. Acetaldehyde and ethanol biosynthesis in leaves of plants. *Plant Physiol.* **1987**, *84* (4), 1204-1209.
47. Sharkey, T. D.; Loreto, F. Water stress, temperature, and light effects on the capacity for isoprene emission and photosynthesis of Kudzu leaves. *Oecologia* **1993**, *95* (3), 328-333.
48. Bertin, N.; Staudt, M. Effect of water stress on monoterpene emissions from young potted Holm oak (*Quercus ilex* L) trees. *Oecologia* **1996**, *107* (4), 456-462.
49. Frost, C.J.; Mescher M.C.; Carlson J.E.; De Moraes C.M. Plant defense priming against herbivores: Getting ready for a different battle. *Plant Physiol.* **2008**, *146*, 818-824.
50. Griffin, R. J.; Cocker, D. R.; Seinfeld, J. H.; Dabdub, D. Estimate of global atmospheric organic aerosol from oxidation of biogenic hydrocarbons. *Geophys. Res. Lett.* **1999**, *26* (17), 2721-2724.
51. Tsigaridis, K.; Kanakidou, M. Global modelling of secondary organic aerosol in the troposphere: a sensitivity analysis. *Atmos. Chem. Phys.* **2003**, *3*, 1849-1869.

52. Raffa, K. F. Induced defensive reactions in conifer-bark beetle systems. In *Phytochemical Induction by Herbivores*; Tallamy, D. W.; Raupp, M. J., Eds. Academic Press: New York, 1991; pp 245-276.
53. Prieme, A.; Knudsen, T. B.; Glasius, M.; Christensen, S. Herbivory by the weevil, *Strophosoma melanogrammum*, causes severalfold increase in emission of monoterpenes from young Norway spruce (*Picea abies*). *Atmos. Environ.* **2000**, *34* (5), 711-718.
54. Levin, H. Building materials and indoor air quality. *Occupational Medicine-State of the Art Reviews* **1989**, *4* (4), 667-693.
55. Corsi, R. L.; Lin, C.-C. Emissions of 2,2,4-trimethyl-1,3-pentanediol monoisobutyrate (TMPD-MIB) from latex paint: A critical review. *Environ. Sci. Technol.* **2009**, *39* (12), 1052-1080.
56. Lamorena, R. B.; Jung, S. G.; Bae, G. N.; Lee, W. The formation of ultra-fine particles during ozone-initiated oxidations with terpenes emitted from natural paint. *J. Hazard. Mater.* **2007**, *141* (1), 245-251.
57. Nazaroff, W. W.; Weschler, C. J. Cleaning products and air fresheners: Exposure to primary and secondary air pollutants. *Atmos. Environ.* **2004**, *38* (18), 2841-2865.
58. Singer, B. C.; Destailats, H.; Hodgson, A. T.; Nazaroff, W. W. Cleaning products and air fresheners: Emissions and resulting concentrations of glycol ethers and terpenoids. *Indoor Air* **2006**, *16* (3), 179-191.
59. Sensing opportunities in dormitory air;  
<http://www.nytimes.com/2007/01/03/business/media/03fresh.html>
60. Nazaroff, W. W. Inhalation intake fraction of pollutants from episodic indoor emissions. *Building and Environment* **2008**, *43* (3), 269-277.

61. Huang, Y.; Ho, K. F.; Ho, S. S. H.; Lee, S. C.; Yau, P. S.; Cheng, Y. Physical parameters effect on ozone-initiated formation of indoor secondary organic aerosols with emissions from cleaning products. *J. Hazard. Mater.* **2011**, *192* (3), 1787-1794.
62. Liu, X. Y.; Mason, M.; Krebs, K.; Sparks, L. Full-scale chamber investigation and simulation of air freshener emissions in the presence of ozone. *Environ. Sci. Technol.* **2004**, *38* (10), 2802-2812.
63. Weschler, C. J.; Shields, H. C. Indoor ozone/terpene reactions as a source of indoor particles. *Atmos. Environ.* **1999**, *33* (15), 2301-2312.
64. Weschler, C. J. Ozone in indoor environments: Concentration and chemistry. *Indoor Air* **2000**, *10* (4), 269-288.
65. Atkinson, R.; Arey, J. Atmospheric degradation of volatile organic compounds. *Chem. Rev.* (Washington, DC, U.S.) **2003**, *103* (12), 4605-4638.
66. US-EPA, Airtrends website; <http://www.epa.gov/airtrends/ozone.html>
67. Carslaw N. Simulating indoor atmospheres: Development of explicit chemical mechanism. *NATO Sci. Ser., IV* **2008**, 167-172, DOI:10.1007/978-1-4020-8846-9\_13.
68. Brown, S. S.; Ryerson, T. B.; Wollny, A. G.; Brock, A. C.; Peltier, R.; Sullivan A. P.; Weber, R. P.; Dubé, W. P.; Trainer, M.; Meagher, J.F.; Fehsenfeld, F.C.; Ravishankara A.R. Variability in nocturnal nitrogen oxide processing and its role in regional air quality. *Science* **2006**, *311*, 67-70.
69. Hao, L. Q.; Yli-Pirila, P.; Tiitta, P.; Romakkaniemi, S.; Vaattovaara, P.; Kajos, M. K.; Rinne, J.; Heijari, J.; Kortelainen, A.; Miettinen, P.; Kroll, J. H.; Holopainen, J. K.; Smith, J. N.; Joutsensaari, J.; Kulmala, M.; Worsnop, D. R.; Laaksonen, A. New particle

- formation from the oxidation of direct emissions of pine seedlings. *Atmos. Chem. Phys.* **2009**, *9* (20), 8121-8137.
70. Hao, L. Q.; Romakkaniemi, S.; Yli-Pirila, P.; Joutsensaari, J.; Kortelainen, A.; Kroll, J. H.; Miettinen, P.; Vaattovaara, P.; Tiitta, P.; Jaatinen, A.; Kajos, M. K.; Holopainen, J. K.; Heijari, J.; Rinne, J.; Kulmala, M.; Worsnop, D. R.; Smith, J. N.; Laaksonen, A. Mass yields of secondary organic aerosols from the oxidation of alpha-pinene and real plant emissions. *Atmos. Chem. Phys.* **2011**, *11* (4), 1367-1378.
  71. Kiendler-Scharr, A.; Wildt, J.; Dal Maso, M.; Hohaus, T.; Kleist, E.; Mentel, T. F.; Tillmann, R.; Uerlings, R.; Schurr, U.; Wahner, A. New particle formation in forests inhibited by isoprene emissions. *Nature* **2009**, *461* (7262), 381-384.
  72. van Reken, T. M.; Greenberg, J. P.; Harley, P. C.; Guenther, A. B.; Smith, J. N. Direct measurement of particle formation and growth from the oxidation of biogenic emissions. *Atmos. Chem. Phys.* **2006**, *6*, 4403-4413.
  73. Mentel, T. F.; Wildt, J.; Kiendler-Scharr, A.; Kleist, E.; Tillmann, R.; Dal Maso, M.; Fisseha, R.; Hohaus, T.; Spahn, H.; Uerlings, R.; Wegener, R.; Griffiths, P. T.; Dinar, E.; Rudich, Y.; Wahner, A. Photochemical production of aerosols from real plant emissions. *Atmos. Chem. Phys.* **2009**, *9* (13), 4387-4406.
  74. Hatfield, M. L.; Huff Hartz, K. E. Secondary organic aerosol from biogenic volatile organic compound mixtures. *Atmos. Environ.* **2011**, *45* (13), 2211-2219.
  75. Huang, H. L.; Sheu, S. C.; Wu, Y. Y.; Hsu, D. J. Comparison of Chinese herbal oils and lemon oil for formation of secondary organic aerosol. *Aerosol and Air Qual. Res.* **2011**, *11* (7), 854-859.

76. Bogdan, J.; Dlugogorski, Z.; Kennedy E. M.; and Mackie J.C. Identification and quantitation of volatile organic compounds from oxidation of linseed oil. *Ind. Eng. Chem. Res.* **2012**, *51* (16), 5645–5652.
77. Pankow, J. F. An absorption model of gas aerosol partitioning involved in the formation of secondary organic aerosol. *Atmos. Environ.* **1994**, *28* (2), 189-193.
78. Odum, J. R.; Hoffmann, T.; Bowman, F.; Collins, D.; Flagan, R. C.; Seinfeld, J. H. Gas/particle partitioning and secondary organic aerosol yields. *Environ. Sci. Technol.* **1996**, *30* (8), 2580-2585.
79. Donahue, N. M.; Robinson, A. L.; Stanier, C. O.; Pandis, S. N. Coupled partitioning, dilution, and chemical aging of semivolatile organics. *Environ. Sci. Technol.* **2006**, *40* (8), 2635-2643.
80. Stanier, C. O.; Donahue, N. M.; Pandis, S. N. Parameterization of secondary organic aerosol mass fractions from smog chamber data. *Atmos. Environ.* **2008**, *42* (10), 2276-2299.
81. Criegee, R. Unfälle mit Peroxyden. *Angew. Chem.* **1953**, *65* (15), 398-399. DOI: 10.1002/ange.19530651507
82. Welz, O.; Savee, J. D.; Osborn, D. L.; Vasu, S. S.; Percival, C. J.; Shallcross, D. E.; Taatjes, C. A. Direct kinetic measurements of Criegee intermediate ( $\cdot\text{CH}_2\text{OO}\cdot$ ) formed by reaction of  $\text{CH}_2\text{I}$  with  $\text{O}_2$ . *Science* **2012**, *335* (6065), 204-207.
83. Glasius, M.; Lahaniati, M.; Calogirou, A.; Di Bella, D.; Jensen, N. R.; Hjorth, J.; Kotzias, D.; Larsen, B. R. Carboxylic acids in secondary aerosols from oxidation of cyclic monoterpenes by ozone. *Environ. Sci. Technol.* **2000**, *34* (6), 1001-1010.

84. Yu, J. Z.; Cocker, D. R.; Griffin, R. J.; Flagan, R. C.; Seinfeld, J. H. Gas-phase ozone oxidation of monoterpenes: Gaseous and particulate products. *J. Atmos. Chem.* **1999**, *34* (2), 207-258.
85. Ma, Y.; Russell, A. T.; Marston, G. Mechanisms for the formation of secondary organic aerosol components from the gas-phase ozonolysis of alpha-pinene. *Phys. Chem. Chem. Phys.* **2008**, *10* (29), 4294-4312.
86. Jang, M.; Kamens, R. M. Newly characterized products and composition of secondary aerosols from the reaction of alpha-pinene with ozone. *Atmos. Environ.* **1999**, *33* (3), 459-474.
87. Koch, S.; Winterhalter, R.; Uherek, E.; Kolloff, A.; Neeb, P.; Moortgat, G. K. Formation of new particles in the gas-phase ozonolysis of monoterpenes. *Atmos. Environ.* **2000**, *34* (23), 4031-4042.
88. Jaoui, M.; Kamens, R. M. Gas phase photolysis of pinonaldehyde in the presence of sunlight. *Atmos. Environ.* **2003**, *37* (13), 1835-1851.
89. Pathak, R. K.; Stanier, C. O.; Donahue, N. M.; Pandis, S. N. Ozonolysis of alpha-pinene at atmospherically relevant concentrations: Temperature dependence of aerosol mass fractions (yields). *J. Geophys. Res., [Atmos.]* **2007**, *112* (D3).
90. Warren, B.; Austin, R. L.; Cocker, D. R., III. Temperature dependence of secondary organic aerosol. *Atmos. Environ.* **2009**, *43* (22-23), 3548-3555.
91. Stanier, C. O.; Pathak, R. K.; Pandis, S. N. Measurements of the volatility of aerosols from alpha-pinene ozonolysis. *Environ. Sci. Technol.* **2007**, *41* (8), 2756-2763.
92. Saathoff, H.; Naumann, K. H.; Moehler, O.; Jonsson, A. M.; Hallquist, M.; Kiendler-Scharr, A.; Mentel, T. F.; Tillmann, R.; Schurath, U. Temperature dependence of yields of

- secondary organic aerosols from the ozonolysis of alpha-pinene and limonene. *Atmos. Chem. Phys.* **2009**, 9 (5), 1551-1577.
93. Pathak, R.; Donahue, N. M.; Pandis, S. N. Ozonolysis of beta-pinene: Temperature dependence of secondary organic aerosol mass fraction. *Environ. Sci. Technol.* **2008**, 42 (14), 5081-5086.
  94. von Hessberg, C.; von Hessberg, P.; Poeschl, U.; Bilde, M.; Nielsen, O. J.; Moortgat, G. K. Temperature and humidity dependence of secondary organic aerosol yield from the ozonolysis of beta-pinene. *Atmos. Chem. Phys.* **2009**, 9 (11), 3583-3599.
  95. Jonsson, A. M.; Hallquist, M.; Ljungstrom, E. Impact of humidity on the ozone initiated oxidation of limonene, delta (3)-carene, and alpha-pinene. *Environ. Sci. Technol.* **2006**, 40 (1), 188-194.
  96. Pankow, J. F.; Chang, E. I. Variation in the sensitivity of predicted levels of atmospheric organic particulate matter (OPM). *Environ. Sci. Technol.* **2008**, 42 (19), 7321-7329.
  97. Barley, M.; Topping, D. O.; Jenkin, M. E.; McFiggans, G. Sensitivities of the absorptive partitioning model of secondary organic aerosol formation to the inclusion of water. *Atmos. Chem. Phys.* **2009**, 9 (9), 2919-2932.
  98. Prisle, N. L.; Engelhart, G. J.; Bilde, M.; Donahue, N. M. Humidity influence on gas-particle phase partitioning of alpha-pinene + O<sub>3</sub> secondary organic aerosol. *Geophys. Res. Lett.* **2010**, 37.
  99. Presto, A. A.; Huff Hartz, K. E.; Donahue, N. M. Secondary organic aerosol production from terpene ozonolysis. 1. Effect of UV radiation. *Environ. Sci. Technol. Environ. Sci. Technol.* **2005**, 39 (18), 7036-7045.



100. Cao, G.; Jang, M. Effects of particle acidity and UV light on secondary organic aerosol formation from oxidation of aromatics in the absence of NO<sub>x</sub>. *Atmos. Environ.* **2007**, *41* (35), 7603-7613.
101. Zhang, J.; Huff Hartz, K. E.; Pandis, S. N.; Donahue, N. M. Secondary organic aerosol formation from limonene ozonolysis: Homogeneous and heterogeneous influences as a function of NO<sub>x</sub>. *J. Phys. Chem. A* **2006**, *110* (38), 11053-11063.
102. Atkinson, R.; Aschmann, S. M.; Arey, J.; Shorees, B. Formation of OH radicals in the gas-phase reactions of O<sub>3</sub> with a series of terpenes. *J. Geophys. Res., [Atmos.]* **1992**, *97* (D5), 6065-6073.
103. Atkinson, R.; Aschmann, S. M. OH radical production from the gas phase reactions of O<sub>3</sub> with a series of alkenes under atmospheric conditions. *Environ. Sci. Technol.* **1993**, *27* (7), 1357-1363.
104. Wegener, R.; Brauers, T.; Koppmann, R.; Bares, S. R.; Rohrer, F.; Tillmann, R.; Wahner, A.; Hansel, A.; Wisthaler, A. Simulation chamber investigation of the reactions of ozone with short-chained alkenes. *J. Geophys. Res., [Atmos.]* **2007**, *112* (D13), 17.
105. Chew, A. A.; Atkinson, R. OH radical formation yields from the gas-phase reactions of O<sub>3</sub> with alkenes and monoterpenes. *J. Geophys. Res., [Atmos.]* **1996**, *101*, 28649-28653.
106. Keywood, M. D.; Varutbangkul, V.; Bahreini, R.; Flagan, R. C.; Seinfeld, J. H. Secondary organic aerosol formation from the ozonolysis of cycloalkenes and related compounds. *Environ. Sci. Technol.* **2004**, *38* (15), 4157-4164.
107. Docherty, K. S.; Ziemann, P. J. Effects of stabilized Criegee intermediate and OH radical scavengers on aerosol formation from reactions of beta-pinene with O<sub>3</sub>. *Aerosol Sci. Technol.* **2003**, *37* (11), 877-891.

108. Jonsson, A. M.; Hallquist, M.; Ljungstrom, E. The effect of temperature and water on secondary organic aerosol formation from ozonolysis of limonene, delta (3)-carene and  $\alpha$ -pinene. *Atmos. Chem. Phys.* **2008**, *8* (21), 6541-6549.
109. Na, K.; Song, C.; Switzer, C.; Cocker, D. R., III. Effect of ammonia on secondary organic aerosol formation from  $\alpha$ -pinene ozonolysis in dry and humid conditions. *Environ. Sci. Technol.* **2007**, *41* (17), 6096-6102.
110. Charlson, R. J.; Schwartz, S. E.; Hales, J. M.; Cess, R. D.; Coakley, J. A.; Hansen, J. E.; Hofmann, D. J. Climate forcing by anthropogenic aerosols. *Science* **1992**, *255* (5043), 423-430.
111. Akimoto, H. Global air quality and pollution. *Science* **2003**, *302* (5651), 1716-1719.
112. Hoffmann, T.; Odum, J. R.; Bowman, F.; Collins, D.; Klockow, D.; Flagan, R. C.; Seinfeld, J. H. Formation of organic aerosols from the oxidation of biogenic hydrocarbons. *J. Atmos. Chem.* **1997**, *26* (2), 189-222.
113. Griffin, R. J.; Cocker, D. R.; Flagan, R. C.; Seinfeld, J. H. Organic aerosol formation from the oxidation of biogenic hydrocarbons. *J. Geophys. Res., [Atmos.]* **1999**, *104* (D3), 3555-3567.
114. Griffin, R. J.; Cocker, D. R.; Seinfeld, J. H.; Dabdub, D. Estimate of global atmospheric organic aerosol from oxidation of biogenic hydrocarbons. *Geophys. Res. Lett.* **1999**, *26* (17), 2721-2724.
115. Tsigaridis, K.; Kanakidou, M. Secondary organic aerosol importance in the future atmosphere. *Atmos. Environ.* **2007**, *41* (22), 4682-4692.
116. Henze, D. K.; Seinfeld, J. H.; Ng, N. L.; Kroll, J. H.; Fu, T. M.; Jacob, D. J.; Heald, C. L. Global modeling of secondary organic aerosol formation from aromatic hydrocarbons:

- High vs. low yield pathways. *Atmos. Chem. Phys.* **2008**, 8 (9), 2405-2420.
117. Hallquist, M.; Wenger, J. C.; Baltensperger, U.; Rudich, Y.; Simpson, D.; Claeys, M.; Dommen, J.; Donahue, N. M.; George, C.; Goldstein, A. H.; Hamilton, J. F.; Herrmann, H.; Hoffmann, T.; Iinuma, Y.; Jang, M.; Jenkin, M. E.; Jimenez, J. L.; Kiendler-Scharr, A.; Maenhaut, W.; McFiggans, G.; Mentel, T. F.; Monod, A.; Prevot, A. S. H.; Seinfeld, J. H.; Surratt, J. D.; Szmigielski, R.; Wildt, J. The formation, properties and impact of secondary organic aerosol: Current and emerging issues. *Atmos. Chem. Phys.* **2009**, 9 (14), 5155-5236.
  118. Geron, C.; Rasmussen, R.; Arnts, R. R.; Guenther, A. A review and synthesis of monoterpene speciation from forests in the United States. *Atmos. Environ.* **2000**, 34 (11), 1761-1781.
  119. Pureswaran, D. S.; Gries, R.; Borden, J. H. Quantitative variation in monoterpenes in four species of conifers. *Biochem. Syst. Ecol.* **2004**, 32 (12), 1109-1136.
  120. Lerdau, M.; Dilts, S. B.; Westberg, H.; Lamb, B. K.; Allwine, E. J. Monoterpene emission from ponderosa pine. *J. Geophys. Res., [Atmos.]* **1994**, 99 (D8), 16609-16615.
  121. Snyder, M. A. Selective herbivory by Abert's squirrel mediated by chemical variability in ponderosa pine. *Ecology* **1992**, 73 (5), 1730-1741.
  122. Langenheim, J. H. Higher plant terpenoids: A phytocentric overview of their ecological roles. *J. Chem. Ecol.* **1994**, 20 (6), 1223-1280.
  123. Lewinsohn, E.; Gijzen, M.; Muzika, R. M.; Barton, K.; Croteau, R. Oleoresinosis in Grand Fir (*Abies Grandis*) saplings and mature trees-modulation of this wound response by light and water stresses. *Plant Physiol.* **1993**, 101 (3), 1021-1028.
  124. Hobson, K. R.; Wood, D. L.; Cool, L. G.; White, P. R.; Ohtsuka, T.; Kubo, I.; Zavarin, E.

- Chiral specificity in responses by the bark beetle *Dendroctonus Valens* to host kairomones. *J. Chem. Ecol.* **1993**, *19* (9), 1837-1846.
125. Lorio, P. L.; Stephen, F. M.; Paine, T. D. Environment and ontogeny modify loblolly pine response to induce acute water deficits and bark beetle attack. *For. Ecol. Manage.* **1995**, *73* (1-3), 97-110.
  126. Heijari, J.; Blande, J. D.; Holopainen, J. K. Feeding of large pine weevil on Scots pine stem triggers localised bark and systemic shoot emission of volatile organic compounds. *Environ. Exp. Bot.* **2011**, *71* (3), 390-398.
  127. Wood, S. L. A revision of bark beetle genus *Dendroctonus* Erichson (Coleoptera: Scolytidae). *Great Basin Nat.* **1963**, *23*, 117.
  128. Raffa, K. F.; Aukema, B. H.; Erbilgin, N.; Klepzig, K. D.; Wallin, K. F. Interactions among conifer terpenoids and bark beetles across multiple levels of scale: An attempt to understand links between population patterns and physiological processes. In *Recent Advances in Phytochemistry*; J. Romeo, Ed. Elsevier: Amsterdam, **2005**; Vol. 39, pp 80-118.
  129. Smith, R. H. Toxicity of pine resin vapors to 3 species of *Dendroctonus* bark beetles. *J. Econ. Entomol.* **1963**, *56* (6), 827-&.
  130. Berryman, A. A.; Raffa, K. F.; Millstein, J. A.; Stenseth, N. C. Interaction dynamics of bark beetle aggregation and conifer defense rates. *Oikos* **1989**, *56* (2), 256-263.
  131. Safranyik, L.; Shrimpton, D.M.; Whitney, H.S. An interpretation of the interaction between lodgepole pine, the mountain pine beetle and its associated blue stain fungi in western Canada. **1975**, pp 406-428. In D.M. Baumgartner, ed. Management of lodgepole pine ecosystems. Washington State University Cooperative Extension Service, Pullman,

WA.

132. Solheim, H. Early stages of blue-stain fungus invasion of lodgepole pine sapwood following mountain beetle attack *Canadian Journal of Botany-Revue Canadienne De Botanique* **1995**, 73 (1), 70-74.
133. Mathre, D. E. Pathogenicity of ceratocystis, IPS + ceratocystis minor to *Pinus Ponderosa*. *Contributions from Boyce Thompson Institute* **1964**, 22 (7), 363-&.
134. Amman, G. D. Mountain pine beetle Coleoptera scolytidae brood production in relation to thickness of lodgepole pine phloem. *J. Econ. Entomol.* **1972**, 65 (1), 138-141.
135. Miller, R. H.; Berryman, A. A.; Ryan, C. A. Biotic elicitors of defense reactions in lodgepole pine. *Phytochemistry* **1986**, 25 (3), 611-612.
136. Raffa, K. F.; Berryman, A. A. Physiological-aspects of lodgepole pine wound responses to a fungal symbiont of the mountain pine beetle, *Dendroctonus Ponderosae* (Coleoptera,Scolytidae). *Can. Entomol.* **1983**, 115 (7), 723-734.
137. Huber, D. P. W.; Aukema, B. H.; Hodgkinson, R. S.; Lindgren, B. S. Successful colonization, reproduction, and new generation emergence in live interior hybrid spruce *Picea engelmannii* x *glauca* by mountain pine beetle *Dendroctonus ponderosae*. *Agricultural and Forest Entomology* **2009**, 11 (1), 83-89.
138. Taylor, S. W.; Carroll, A. L.; Alfaro, R. I.; Safranyik, L. Forest, Climate and Mountain Pine Beetle Outbreak Dynamics in Western Canada. In *The Mountain Pine Beetle: A Synthesis of Biology, Management and Impacts in Lodgepole Pine*; Safranyik, L; Wilson, B. Eds.; Natural Resources Canada: Victoria, BC, **2006**; pp 67-94

139. Kurz, W. A.; Dymond, C. C.; Stinson, G.; Rampley, G. J.; Neilson, E. T.; Carroll, A. L.; Ebata, T.; Safranyik, L. Mountain pine beetle and forest carbon feedback to climate change. *Nature* **2008**, *452* (7190), 987-990
140. Westfall, J.; Ebata, T.; 2007 *Summary of forest health conditions in British Columbia*; Ministry of Forests and Range, Forest Practices Branch: Victoria, British Columbia, Canada, **2008**;  
[http://www.for.gov.bc.ca/ftp/HFP/external/!publish/Aerial\\_Overview/2008/Aerial%20Overview%202008.pdf](http://www.for.gov.bc.ca/ftp/HFP/external/!publish/Aerial_Overview/2008/Aerial%20Overview%202008.pdf).
141. Logan, J. A.; Powell, J. A Ghost forests, global warming, and the mountain pine beetle. *Amer. Entomol.* **2001**, *47*(3), 160–173.
142. Williams, D. W.; Liebhold, A. M. Climate change and the outbreak ranges of two North American bark beetles. *Agr. For. Ent.* **2002**, *4*, 87–99.
143. Borys, R. D.; Wetzel, M. A. Storm Peak Laboratory: A research, teaching, and service facility for the atmospheric sciences. *Bull. Am. Meteorol. Soc.* **1997**, *78* (10), 2115-2123.
144. Hallar, A. G.; Lowenthal, D. H.; Chirokova, G.; Borys, R. D.; Wiedinmyer, C. Persistent daily new particle formation at a mountain top location. *Atmos. Environ.* **2011**, *45* (24), 4111-4115.
145. Raguso, R. A.; Pellmyr, O. Dynamic headspace analysis of floral volatiles: a comparison of methods. *Oikos* **1998**, *81* (2), 238-254.
146. Amin, H.; Atkins P.T.; Russo R.S.; Brown A.W.; Sive B.; Hallar A.G.; Huff Hartz K.E. Effect of bark beetle infestation on secondary organic aerosol precursor emissions, *Environ. Sci. Technol.*, **2012**, in press.
147. Adams, R. P. *Identification of Essential Oil Components by Gas Chromatography/Mass*

*Spectrometry*; Allured Publishing: Carol Stream, IL, 2007.

148. Sturaro, A.; Parvoli, G.; Doretto, L. Artifacts produced by Propak-Q sorvent tubes on solvent desorption. *Chromatographia* **1992**, *33* (1-2), 53-57.
149. Sive, B. C.; Zhou, Y.; Troop, D.; Wang, Y. L.; Little, W. C.; Wingenter, O. W.; Russo, R. S.; Varner, R. K.; Talbot, R. Development of a cryogen-free concentration system for measurements of volatile organic compounds. *Anal. Chem.* **2005**, *77* (21), 6989-6998.
150. Russo, R. S.; Zhou, Y.; Haase, K. B.; Wingenter, O. W.; Frinak, E. K.; Mao, H.; Talbot, R. W.; Sive, B. C. Temporal variability, sources, and sinks of C<sub>1</sub>-C<sub>5</sub> alkyl nitrates in coastal New England. *Atmos. Chem. Phys.* **2010**, *10* (4), 1865-1883.
151. Gara, R. I.; Little, W. R.; Rhoades, D. F. Emission of ethanol and monoterpenes by fungal infected lodgepole pine trees. *Phytochemistry* **1993**, *34* (4), 987-990.
152. Jost, R. W.; Rice, A. V.; Langor, D. W.; Boluk, Y. Monoterpene emissions from lodgepole and jack pine bark inoculated with mountain pine beetle-associated fungi. *J. Wood Chem. Technol.* **2008**, *28* (1), 37-46.
153. Surratt, J. D.; Gomez-Gonzalez, Y.; Chan, A. W. H.; Vermeylen, R.; Shahgholi, M.; Kleindienst, T. E.; Edney, E. O.; Offenberg, J. H.; Lewandowski, M.; Jaoui, M.; Maenhaut, W.; Claeys, M.; Flagan, R. C.; Seinfeld, J. H. Organosulfate formation in biogenic secondary organic aerosol. *J. Phys. Chem. A* **2008**, *112* (36), 8345-8378.
154. Lee, A.; Goldstein, A. H.; Keywood, M. D.; Gao, S.; Varutbangkul, V.; Bahreini, R.; Ng, N. L.; Flagan, R. C.; Seinfeld, J. H. Gas-phase products and secondary aerosol yields from the ozonolysis of ten different terpenes. *J. Geophys. Res., [Atmos.]* **2006**, *111* (D7), 18.
155. Lee, A.; Goldstein, A. H.; Kroll, J. H.; Ng, N. L.; Varutbangkul, V.; Flagan, R. C.; Seinfeld, J. H. Gas-phase products and secondary aerosol yields from the photooxidation

- of 16 different terpenes. *J. Geophys. Res., [Atmos.]* **2006**, *111* (D17).
156. Lamb, B.; Gay, D.; Westberg, H.; Pierce, T. A biogenic hydrocarbon emission inventory for the USA using a simple forest canopy model. *Atmos. Environ. Part a-General Topics* **1993**, *27* (11), 1673-1690.
  157. Millet, D. B.; Donahue, N. M.; Pandis, S. N.; Polidori, A.; Stanier, C. O.; Turpin, B. J.; Goldstein, A. H. Atmospheric volatile organic compound measurements during the Pittsburgh air quality study: Results, interpretation, and quantification of primary and secondary contributions. *J. Geophys. Res., [Atmos.]* **2005**, *110* (D7).
  158. Andersson-Skold, Y.; Simpson, D. Secondary organic aerosol formation in northern Europe: A model study. *J. Geophys. Res., [Atmos.]* **2001**, *106* (D7), 7357-7374.
  159. Moufida, S.; Marzouk, B. Biochemical characterization of blood orange, sweet orange, lemon, bergamot and bitter orange. *Phytochemistry* **2003**, *62* (8), 1283-1289.
  160. Brown, S. K.; Sim, M. R.; Abramson, M. J.; Gray, C. N. Concentrations of volatile organic compounds in indoor air: A review. *Indoor Air-International Journal of Indoor Air Quality and Climate* **1994**, *4* (2), 123-134.
  161. Li, T. H.; Turpin, B. J.; Shields, H. C.; Weschler, C. J. Indoor hydrogen peroxide derived from ozone/d-limonene reactions. *Environ. Sci. Technol.* **2002**, *36* (15), 3295-3302.
  162. Ng, N. L.; Kroll, J. H.; Keywood, M. D.; Bahreini, R.; Varutbangkul, V.; Flagan, R. C.; Seinfeld, J. H.; Lee, A.; Goldstein, A. H. Contribution of first- versus second-generation products to secondary organic aerosols formed in the oxidation of biogenic hydrocarbons. *Environ. Sci. Technol.* **2006**, *40* (7), 2283-2297.
  163. Fry, J. L.; Kiendler-Scharr, A.; Rollins, A. W.; Brauers, T.; Brown, S. S.; Dorn, H. P.; Dube, W. P.; Fuchs, H.; Mensah, A.; Rohrer, F.; Tillmann, R.; Wahner, A.; Wooldridge,



- P. J.; Cohen, R. C. SOA from limonene: Role of NO<sub>3</sub> in its generation and degradation. *Atmos. Chem. Phys.* **2011**, *11* (8), 3879-3894.
164. Leungsakul, S.; Jaoui, M.; Kamens, R. M. Kinetic mechanism for predicting secondary organic aerosol formation from the reaction of d-limonene with ozone. *Environ. Sci. Technol.* **2005**, *39* (24), 9583-9594.
165. Chen, X.; Hopke, P. K. A chamber study of secondary organic aerosol formation by limonene ozonolysis. *Indoor Air* **2010**, *20* (4), 320-328.
166. Grosjean, D.; Williams, E. L.; Grosjean, E.; Andino, J. M.; Seinfeld, J. H. Atmospheric oxidation of biogenic hydrocarbons: Reaction of ozone with  $\beta$ -pinene, d-limonene, and trans-caryophyllene. *Environ. Sci. Technol.* **1993**, *27* (13), 2754-2758.
167. Calogirou, A.; Larsen, B. R.; Kotzias, D. Gas-phase terpene oxidation products: A review. *Atmos. Environ.* **1999**, *33* (9), 1423-1439.
168. Larsen, B. R.; Di Bella, D.; Glasius, M.; Winterhalter, R.; Jensen, N. R.; Hjorth, J. Gas-phase OH oxidation of monoterpenes: Gaseous and particulate products. *J. Atmos. Chem.* **2001**, *38* (3), 231-276.
169. Jaoui, M.; Corse, E.; Kleindienst, T. E.; Offenberg, J. H.; Lewandowski, M.; Edney, E. O. Analysis of secondary organic aerosol compounds from the photooxidation of d-limonene in the presence of NO<sub>x</sub> and their detection in ambient PM<sub>2.5</sub>. *Environ. Sci. Technol.* **2006**, *40* (12), 3819-3828.
170. Walser, M. L.; Desyaterik, Y.; Laskin, J.; Laskin, A.; Nizkorodov, S. A. High-resolution mass spectrometric analysis of secondary organic aerosol produced by ozonation of limonene. *Phys. Chem. Chem. Phys.* **2008**, *10* (7), 1009-1022.
171. Ziemann, P. J. Aerosol products, mechanisms, and kinetics of heterogeneous reactions of

- ozone with oleic acid in pure and mixed particles. *Faraday Discuss.* **2005**, *130*, 469-490.
172. Docherty, K. S.; Wu, W.; Lim, Y. B.; Ziemann, P. J. Contributions of organic peroxides to secondary aerosol formed from reactions of monoterpenes with O<sub>3</sub>. *Environ. Sci. Technol.* **2005**, *39* (11), 4049-4059.
173. Bateman, A. P.; Nizkorodov, S. A.; Laskin, J.; Laskin, A. Time-resolved molecular characterization of limonene/ozone aerosol using high-resolution electrospray ionization mass spectrometry. *Phys. Chem. Chem. Phys.* **2009**, *11* (36), 7931-7942.
174. Li, Y. J.; Lee, A. K. Y.; Lau, A. P. S.; Chan, C. K. Accretion reactions of octanal catalyzed by sulfuric acid: Product identification, reaction pathways, and atmospheric implications. *Environ. Sci. Technol.* **2008**, *42* (19), 7138-7145.
175. Waring, M. S.; Wells, J. R.; Siegel, J. A. Secondary organic aerosol formation from ozone reactions with single terpenoids and terpenoid mixtures. *Atmos. Environ.* **2011**, *45* (25), 4235-4242.
176. Nojgaard, J. K.; Bilde, M.; Stenby, C.; Nielsen, O. J.; Wolkoff, P. The effect of nitrogen dioxide on particle formation during ozonolysis of two abundant monoterpenes indoors. *Atmos. Environ.* **2006**, *40* (6), 1030-1042.
177. Jaoui, M.; Kamens, R. M. Gaseous and particulate oxidation products analysis of a mixture of  $\alpha$ -pinene plus  $\beta$ -pinene/O<sub>3</sub>/air in the absence of light and  $\alpha$ -pinene plus  $\beta$ -pinene/NO<sub>x</sub>/air in the presence of natural sunlight. *J. Atmos. Chem.* **2003**, *44* (3), 259-297.
178. Weschler, C. J.; Shields, H. C. Experiments probing the influence of air exchange rates on secondary organic aerosols derived from indoor chemistry. *Atmos. Environ.* **2003**, *37* (39-40), 5621-5631.
179. Wainman, T.; Zhang, J. F.; Weschler, C. J.; Lioy, P. J. Ozone and limonene in indoor air:

- A source of submicron particle exposure. *Environ. Health Perspect.* **2000**, *108* (12), 1139-1145.
180. Rohr, A. C.; Weschler, C. J.; Koutrakis, P.; Spengler, J. D. Generation and quantification of ultrafine particles through terpene/ozone reaction in a chamber setting. *Aerosol Sci. Technol.* **2003**, *37* (1), 65-78.
  181. Sarwar, G.; Corsi, R. The effects of ozone/limonene reactions on indoor secondary organic aerosols. *Atmos. Environ.* **2007**, *41* (5), 959-973.
  182. Hatfield, M.L. Particulate matter yields and secondary organic aerosol production from atmospheric biogenic precursor mixtures. M.S. Thesis, Southern Illinois University Carbondale, Carbondale, IL 2010
  183. Omega pressure sensor manual; <http://www.omega.com/temperature/z/pdf/z103.pdf>.
  184. Shu, Y. G.; Atkinson, R. Rate constants for the gas-phase reactions of O<sub>3</sub> with a series of terpenes and OH radical formation from the O<sub>3</sub> reactions with sesquiterpenes at 296±2 K. *Int. J. Chem. Kinet.* **1994**, *26* (12), 1193-1205.
  185. Nolte, C. G.; Schauer, J. J.; Cass, G. R.; Simoneit, B. R. T. Trimethylsilyl derivatives of organic compounds in source samples and in atmospheric fine particulate matter. *Environ. Sci. Technol.* **2002**, *36* (20), 4273-4281.
  186. Huff Hartz, K. E.; Weitkamp, E. A.; Sage, A. M.; Donahue, N. M.; Robinson, A. L. Laboratory measurements of the oxidation kinetics of organic aerosol mixtures using a relative rate constants approach. *J. Geophys. Res., [Atmos.]* **2007**, *112* (D4), 13.
  187. Dipropylene glycol methyl ether as a solvent;  
<http://www.lyondellbasell.com/Products/ByMarket/PersonalCare/NailCare/ARCOSOLV>  
DPM/

188. Methoxy-prpoxy-2-propanol as a solvent;  
<http://www.thegoodscentscopy.com/data/rw1234861.html>
189. US-EPA, EPI websuite; available <http://www.epa.gov/oppt/exposure/pubs/episuite.htm>
190. Leather, K. E.; McGillen, M. R.; Percival, C. J. Temperature-dependent ozonolysis kinetics of selected alkenes in the gas phase: an experimental and structure-activity relationship (SAR) study. *Phys. Chem. Chem. Phys.* **2010**, *12* (12), 2935-2943.
191. Orav, A.; Kailas, T.; Ivask, K. Composition of the essential oil from *Achillea millefolium* L. from Estonia. *J. Essent. Oil Res.* **2001**, *13* (4), 290-294.
192. Mierendorff, H.G.; Stahl-Biskup, E.; Posthumus M.A.; van Beek, T.A. Composition of commercial Cape chamomile oil. *Flavor and Fragrance Journal* **2003**, *18*, 510-514.
193. Verzera, A.; Trozzi, A.; Zappala, M.; Condurso, C.; Cotroneo, A. Essential oil composition of *Citrus meyerii* Y. Tan. and *Citrus medica* L. cv. Diamante and their lemon hybrids. *J. Agric. Food Chem.* **2005**, *53* (12), 4890-4894.
194. Steinemann, A. C. Fragranced consumer products and undisclosed ingredients. *Environmental Impact Assessment Review* **2009**, *29* (1), 32-38.
195. Forester, C. D.; Ham, J. E.; Wells, J. R. Gas-phase chemistry of dihydromyrcenol with ozone and OH radical: Rate constants and products. *Int. J. Chem. Kinet.* **2006**, *38* (7), 451-463.
196. Atkinson, R.; Arey, J.; Aschmann, S. M.; Corchnoy, S. B.; Shu, Y. H. Rate constants for the gas-phase reactions of cis-3-hexen-1-ol, cis-3-hexenyl acetate, trans-2-hexenal, and linalool with OH and NO<sub>3</sub> radicals and O<sub>3</sub> at 296±2 K, and OH radical formation yields from the O<sub>3</sub> reactions. *Int. J. Chem. Kinet.* **1995**, *27* (10), 941-955.
197. Atkinson, R.; Hasegawa, D.; Aschmann, S. M. Rate constants for the gas-phase reactions

- of O<sub>3</sub> with a series of monoterpenes and related compounds at 296±2 K. *Int. J. Chem. Kinet.* **1990**, 22 (8), 871-887.
198. Forester, C. D.; Ham, J. E.; Wells, J. R.  $\beta$ -Ionone reactions with ozone and OH radical: Rate constants and gas-phase products. *Atmos. Environ.* **2007**, 41 (38), 8758-8771
  199. Ham, J. E.; Proper, S. P.; Wells, J. R. Gas-phase chemistry of citronellol with ozone and OH radical: Rate constants and products. *Atmos. Environ.* **2006**, 40 (4), 726-735.
  200. Wells, J.R. Gas-phase chemistry of  $\alpha$ -terpineol with ozone and OH radical: Rate constants and products. *Environ. Sci. Technol.* **2005**, 39, 6937-6943.
  201. Ma, Y.; Marston, G. Formation of organic acids from the gas-phase ozonolysis of terpinolene. *Phys. Chem. Chem. Phys.* **2009**, 11 (21), 4198-4209.
  202. Pathak, R.; Donahue, N. M.; Pandis, S. N. Ozonolysis of beta-pinene: Temperature dependence of secondary organic aerosol mass fraction. *Environ. Sci. Technol.* **2008**, 42 (14), 5081-5086.
  203. Chen, X.; Hopke, P. K. A chamber study of secondary organic aerosol formation by linalool ozonolysis. *Atmos. Environ.* **2009**, 43 (25), 3935-3940.
  204. Jonsson, A. M.; Hallquist, M.; Ljungstrom, E. Influence of OH scavenger on the water effect on secondary organic aerosol formation from ozonolysis of limonene, delta 3-carene, and  $\alpha$ -pinene. *Environ. Sci. Technol.* **2008**, 42 (16), 5938-5944.
  205. Rontani, J. F.; Aubert, C. Electron ionization mass spectral fragmentation of C-19 isoprenoid aldehydes and carboxylic acid methyl and trimethylsilyl esters. *Rapid Commun. Mass Spectrom.* **2003**, 17 (9), 949-956.
  206. Rontani, J. F.; Aubert, C. Trimethylsilyl transfer during electron ionization mass spectral fragmentation of some omega-hydroxycarboxylic and omega-dicarboxylic acid

- trimethylsilyl derivatives and the effect of chain length. *Rapid Commun. Mass Spectrom.* **2004**, *18* (17), 1889-1895.
207. Jaoui, M.; Kleindienst, T. E.; Lewandowski, M.; Offenberg, J. H.; Edney, E. O. Identification and quantification of aerosol polar oxygenated compounds bearing carboxylic or hydroxyl groups. 2. Organic tracer compounds from monoterpenes. *Environ. Sci. Technol.* **2005**, *39* (15), 5661-5673.
208. Subramanian, R.; Khlystov, A. Y.; Cabada, J. C.; Robinson, A. L. Positive and negative artifacts in particulate organic carbon measurements with denuded and undenuded sampler configurations. *Aerosol Sci. Technol.* **2004**, *38*, 27-48.
209. McLafferty, F.W.; Tureček, F. *Interpretation of Mass Spectra*, 4<sup>th</sup> ed., University Science Books: CA, 1993.
210. Atkinson, R. J. Ozone variability over the southern hemisphere. *Aust. Meteorol. Mag.* **1997**, *46* (3), 195-201.
211. Goldstein, A. H.; Galbally, I. E. Known and unexplored organic constituents in the earth's atmosphere. *Environ. Sci. Technol.* **2007**, *41* (5), 1514-1521.
212. Ma, Y.; Russell, A. T.; Marston, G. Mechanisms for the formation of secondary organic aerosol components from the gas-phase ozonolysis of  $\alpha$ -pinene. *Phys. Chem. Chem. Phys.* **2008**, *10* (29), 4294-4312.
213. Jaoui, M.; Kamens, R. M. Mass balance of gaseous and particulate products analysis from  $\alpha$ -pinene/NO<sub>x</sub>/air in the presence of natural sunlight. *J. Geophys. Res., [Atmos.]* **2001**, *106* (D12), 12541-12558.
214. Gao, Y. Q.; Hall, W. A.; Johnston, M. V. Molecular composition of monoterpene secondary organic aerosol at low mass loading. *Environ. Sci. Technol.* **2010**, *44* (20),

7897-7902.

215. Jaoui, M.; Edney, E. O.; Kleindienst, T. E.; Lewandowski, M.; Offenberg, J. H.; Surratt, J. D.; Seinfeld, J. H. Formation of secondary organic aerosol from irradiated  $\alpha$ -pinene/toluene/NO<sub>x</sub> mixtures and the effect of isoprene and sulfur dioxide. *J. Geophys. Res., [Atmos.]* **2008**, *113* (D9).
216. Forester, C. D.; Wells, J. R. Hydroxyl radical yields from reactions of terpene mixtures with ozone. *Indoor Air* **2011**, *21* (5), 400-409.
217. Gao, S.; Keywood, M.; Ng, N. L.; Surratt, J.; Varutbangkul, V.; Bahreini, R.; Flagan, R. C.; Seinfeld, J. H. Low molecular weight and oligomeric components in secondary organic aerosol from the ozonolysis of cycloalkenes and  $\alpha$ -pinene. *J. Phys. Chem. A* **2004**, *108* (46), 10147-10164.
218. Hall, W. A.; Johnston, M. V. Oligomer content of  $\alpha$ -pinene secondary organic aerosol. *Aerosol Sci. Technol.* **2011**, *45* (1), 37-45.
219. Vapor pressure of 0.6 mm of Hg  
<http://www.sigmaaldrich.com/catalog/product/fluka/45855?lang=en&region=US>
220. Presto, A. A.; Donahue, N. M. Ozonolysis fragment quenching by nitrate formation: The pressure dependence of prompt OH radical formation. *J. Phys. Chem. A* **2004**, *108* (42), 9096-9104.
221. Coeur, C.; Jacob, V.; Foster, P. Aerosol formation from the gas-phase reaction of hydroxyl radical with the natural hydrocarbon bornyl acetate. *Atmos. Environ.* **1999**, *33* (10), 1615-1620.
222. Taatjes, C. A.; Welz, O.; Eskola, A. J.; Savee, J. D.; Osborn, D. L.; Lee, E. P. F.; Dyke, J. M.; Mok, D. W. K.; Shallcross, D. E.; Pervical, C. J. Direct measurement of Criegee

- intermediate (CH<sub>2</sub>OO) reactions with acetone, acetaldehyde, and hexafluoroacetone. *Phys. Chem. Chem. Phys.* **2012**, in press, Advance Article, DOI:10.1039/c2cp40294g.
223. Heaton, K. J.; Dreyfus, M. A.; Wang, S.; Johnston, M. V. Oligomers in the early stage of biogenic secondary organic aerosol formation and growth. *Environ. Sci. Technol.* **2007**, *41* (17), 6129-6136.
  224. Hakola, H.; Arey, J.; Aschmann, S. M.; Atkinson, R. Product formation from the gas-phase reactions of OH radicals and O<sub>3</sub> with a series of monoterpenes. *J. Atmos. Chem.* **1994**, *18* (1), 75-102.
  225. Jay, K.; Stieglitz, L. Gas-phase ozonolysis of camphene in presence of SO<sub>2</sub>. *Atmos. Environ.* **1989**, *23* (6), 1219-1221.
  226. Andreae, M. O.; Gelencser, A. Black carbon or brown carbon? The nature of light-absorbing carbonaceous aerosols. *Atmos. Chem. Phys.* **2006**, *6*, 3131-3148.
  227. Gelencser, A.; Meszaros, T.; Blazso, M.; Kiss, G.; Krivacsy, Z.; Molnar, A.; Meszaros, E. Structural characterisation of organic matter in fine tropospheric aerosol by pyrolysis-gas chromatography-mass spectrometry. *J. Atmos. Chem.* **2000**, *37*(2), 173-183.
  228. Mukai, H.; Ambe, Y. Characterization of humic acid-like brown substance in airborne particulate matter and tentative identification of its origin. *Atmos. Environ.* **1986**, *20* (5), 813-819.
  229. Blough, N. V., and Del Vecchio, R. Chromophoric DOM in the coastal environment, in *Biogeochemistry of Marine Dissolved Organic Matter*, edited by D. A. Hansell and C. A. Carlson, Academic Press, San Diego, California **2002**, 509-546.
  230. Graber, E. R.; Rudich, Y. Atmospheric HULIS: How humic-like are they? A comprehensive and critical review. *Atmos. Chem. Phys.* **2006**, *6*, 729-753.



231. Santos, P. S. M.; Otero, M.; Duarte, R.; Duarte, A. C. Spectroscopic characterization of dissolved organic matter isolated from rainwater. *Chemosphere* **2009**, 74 (8), 1053-1061
232. Jacobson, M. Z. Isolating nitrated and aromatic aerosols and nitrated aromatic gases as sources of ultraviolet light absorption. *J. Geophys. Res., [Atmos.]* **1999**, 104 (D3), 3527-3542.
233. Bond, T. C. Spectral dependence of visible light absorption by carbonaceous particles emitted from coal combustion. *Geophys. Res. Lett.* **2001**, 28 (21), 4075-4078.
234. Barsanti, K. C.; Pankow, J. F. Thermodynamics of the formation of atmospheric organic particulate matter by accretion reactions - 2. Dialdehydes, methylglyoxal, and diketones. *Atmos. Environ.* **2005**, 39 (35), 6597-6607.
235. Kwamena, N. O. A.; Abbatt, J. P. D. Heterogeneous nitration reactions of polycyclic aromatic hydrocarbons and n-hexane soot by exposure to  $\text{NO}_3/\text{NO}_2/\text{N}_2\text{O}_5$ . *Atmos. Environ.* **2008**, 42 (35), 8309-8314.
236. Holmes, B. J.; Petrucci, G. A. Oligomerization of levoglucosan by Fenton chemistry in proxies of biomass burning aerosols. *J. Atmos. Chem.* **2007**, 58 (2), 151-166.
237. Kroll, J. H.; Seinfeld, J. H. Chemistry of secondary organic aerosol: Formation and evolution of low-volatility organics in the atmosphere. *Atmos. Environ.* **2008**, 42 (16), 3593-3624.
238. Czoschke, N. M.; Jang, M.; Kamens, R. M. Effect of acidic seed on biogenic secondary organic aerosol growth. *Atmos. Environ.* **2003**, 37 (30), 4287-4299.
239. Li, Y. J.; Lee, A. K. Y.; Lau, A. P. S.; Chan, C. K. Accretion reactions of octanal catalyzed by sulfuric acid: Product identification, reaction pathways, and atmospheric implications. *Environ. Sci. Technol.* **2008**, 42 (19), 7138-7145.

240. Noziere, B.; Dziedzic, P.; Cordova, A. Formation of secondary light-absorbing "fulvic-like" oligomers: A common process in aqueous and ionic atmospheric particles? *Geophys. Res. Lett.* **2007**, *34* (21), L03812, DOI:10.1029/2004GL021942.
241. Noziere, B.; Dziedzic, P.; Cordova, A. Products and kinetics of the liquid-phase reaction of glyoxal catalyzed by ammonium ions  $\text{NH}_4^+$ . *J. Phys. Chem. A* **2009**, *113* (1), 231-237.
242. Czoschke, N. M.; Jang, M. S. Acidity effects on the formation of  $\alpha$ -pinene ozone SOA in the presence of inorganic seed. *Atmos. Environ.* **2006**, *40* (23), 4370-4380.
243. Noziere, B.; Esteve, W. Organic reactions increasing the absorption index of atmospheric sulfuric acid aerosols. *Geophys. Res. Lett.* **2005**, *32* (3), L21812, DOI:10.1029/2007GL031300.
244. Noziere, B.; Dziedzic, P.; Cordova, A. Common inorganic ions are efficient catalysts for organic reactions in atmospheric aerosols and other natural environments. *Atmos. Chem. Phys. Discuss.*, **2009**, *9*, 1–21.
245. Shapiro, E. L.; Szprengiel, J.; Sareen, N.; Jen, C. N.; Giordano, M. R.; McNeill, V. F. Light-absorbing secondary organic material formed by glyoxal in aqueous aerosol mimics. *Atmos. Chem. Phys.* **2009**, *9* (7), 2289-2300.
246. Galloway, M. M.; Chhabra, P. S.; Chan, A. W. H.; Surratt, J. D.; Flagan, R. C.; Seinfeld, J. H.; Keutsch, F. N. Glyoxal uptake on ammonium sulphate seed aerosol: reaction products and reversibility of uptake under dark and irradiated conditions. *Atmos. Chem. Phys.* **2009**, *9* (10), 3331-3345.
247. Bones, D. L.; Henricksen, D. K.; Mang, S. A.; Gonsior, M.; Bateman, A. P.; Nguyen, T. B.; Cooper, W. J.; Nizkorodov, S. A., Appearance of strong absorbers and fluorophores in limonene- $\text{O}_3$  secondary organic aerosol due to  $\text{NH}_4^+$  mediated chemical aging over long

- time scales. *J. Geophys. Res., [Atmos.]* **2010**, *115*
248. Chan, M. N.; Chan, A. W. H.; Chhabra, P. S.; Surratt, J. D.; Seinfeld, J. H. Modeling of secondary organic aerosol yields from laboratory chamber data. *Atmos. Chem. Phys.* **2009**, *9* (15), 5669-5680
249. Presto, A. A.; Donahue, N. M. Investigation of  $\alpha$ -pinene plus ozone secondary organic aerosol formation at low total aerosol mass. *Environ. Sci. Technol.* **2006**, *40* (11), 3536-3543.
250. Shilling, J. E.; Chen, Q.; King, S. M.; Rosenoern, T.; Kroll, J. H.; Worsnop, D. R.; DeCarlo, P. F.; Aiken, A. C.; Sueper, D.; Jimenez, J. L.; Martin, S. T. Loading dependent elemental composition of  $\alpha$ -pinene SOA particles. *Atmos. Chem. Phys.* **2009**, *9* (3), 771-782.
251. Kostenidou, E.; Pathak, R. K.; Pandis, S. N. An algorithm for the calculation of secondary organic aerosol density combining AMS and SMPS data. *Aerosol Sci. Technol.* **2007**, *41* (11), 1002-1010.

## **APPENDICES**

## Appendix I

### TOTAL VOCs FROM INDIVIDUAL SCENT TRAP SAMPLES COLLECTED OVER THE PERIOD OF BARK BEETLE PROJECT

**A-I Table 1.** Total VOC concentration (ng L<sup>-1</sup>) at site 1 for lodgepole pine, sampled by scent trap and detected by GCMS. Values given are the average over three replicate injections and corrected for blanks and the propagated uncertainty in the average.

	S1T1		S1T2		S1T3	
	Trunk	Canopy	Trunk	Canopy	Trunk	Canopy
8/1/09						
8 AM	12±2	10.7±1.2	106±10	-	-	-
11 AM	16±2	7.8±1.1	69±5	-	-	-
2 PM	13±2	12.7±1.3	231±17	-	-	-
8/15/09						
8 AM	-	-	97±3	12±1	nd	nd
11 AM	-	-	34±1	14±1	nd	0.04±0.01
2 PM	-	-	26±1	9±1	0.8±0.2	0.05±0.02
8/23/09						
8 AM	3.4±0.8	1.4±0.3	90±3	0.2±0.1	0.7±0.2	0.4±0.2
11 AM	0.8±0.2	nd	199±5	nd	0.6±0.2	nd
2 PM	1.1±0.2	nd	228±5	0.4±0.2	1.2±0.2	25.4±0.1
8/29/09						
8 AM	8.3±1.0	1.7±0.2	88±3	4.7±0.4	7.1±0.7	1.6±0.2
11 AM	2.5±0.3	0.6±0.2	116±3	1.5±0.3	2.3±0.4	1.5±0.3
2 PM	3.3±0.4	0.6±0.2	167±5	2.9±0.4	1.3±0.2	0.4±0.2
9/4/09						
8 AM	1.3±0.2	1.7±0.3	34±2	2.6±0.3	0.8±0.2	0.6±0.1
11 AM	1.3±0.2	1.8±0.3	71±4	1.8±0.3	1.0±0.2	1.3±0.3
2 PM	0.9±0.3	nd	6±1	nd	nd	nd
9/11/09						
8 AM	3.0±0.3	0.7±0.1	25±1	2.4±0.2	2.8±0.2	0.5±0.1
11 AM	0.73±0.09	0.6±0.1	65±2	0.6±0.1	4.0±0.3	0.9±0.1
2 PM	0.8±0.1	0.55±0.09	44±2	0.5±0.1	1.0±0.1	0.6±0.1

nd indicates that all of the VOCs were below the detection limit. - indicates that no samples were collected at this site for the date and time listed.

**A-I Table 2.** Total VOC concentration ( $\text{ng L}^{-1}$ ) at site 2 for lodgepole pine, sampled by scent trap and detected by GCMS. The values are the average over three replicate injections and corrected for blanks and the propagated uncertainty in the average.

	S2T6		S2T7		S2T8	
	trunk	canopy	trunk	canopy	trunk	canopy
7/31/09						
11 AM	65 $\pm$ 5	15 $\pm$ 2	10 $\pm$ 1	17 $\pm$ 2	-	-
8/2/09						
8 AM	570 $\pm$ 40	11 $\pm$ 1	22 $\pm$ 2	16 $\pm$ 2	17 $\pm$ 2	-
11 AM	820 $\pm$ 60	21 $\pm$ 2	13 $\pm$ 2	9 $\pm$ 1	-	9 $\pm$ 1
2 PM	28 $\pm$ 3	9 $\pm$ 1	15 $\pm$ 1	9 $\pm$ 1	-	-
8/16/09						
8 AM	nd	0.08 $\pm$ 0.05	27 $\pm$ 1	0.03 $\pm$ 0.01	-	-
11 AM	19.6 $\pm$ 0.5	0.05 $\pm$ 0.03	nd	nd	-	-
2 PM	13.3 $\pm$ 0.5	0.16 $\pm$ 0.09	0.10 $\pm$ 0.05	nd	-	-
8/22/09						
8 AM	13.7 $\pm$ 5	nd	0.5 $\pm$ 0.2	nd	2.8 $\pm$ 0.3	nd
11 AM	44 $\pm$ 1	5.8 $\pm$ 0.9	nd	2.3 $\pm$ 0.8	8.1 $\pm$ 0.4	nd
2 PM	30 $\pm$ 1	1.8 $\pm$ 0.2	0.9 $\pm$ 0.2	1.8 $\pm$ 0.7	3.1 $\pm$ 0.4	nd
8/30/09						
8 AM	326 $\pm$ 7	0.7 $\pm$ 0.2	1.6 $\pm$ 0.2	nd	-	-
11 AM	57 $\pm$ 2	1.5 $\pm$ 0.3	0.5 $\pm$ 0.2	0.3 $\pm$ 0.2	-	-
2 PM	82 $\pm$ 2	1.1 $\pm$ 0.3	2.5 $\pm$ 0.3	3.2 $\pm$ 0.3	-	-
9/7/09						
8 AM	40 $\pm$ 2	0.8 $\pm$ 0.2	0.2 $\pm$ 0.1	1.0 $\pm$ 0.3	0.7 $\pm$ 0.4	1.1 $\pm$ 0.2
11 AM	99 $\pm$ 5	1.3 $\pm$ 0.2	2.5 $\pm$ 0.3	nd	2.2 $\pm$ 0.3	0.4 $\pm$ 0.2
2 PM	87 $\pm$ 4	0.7 $\pm$ 0.2	1.0 $\pm$ 0.2	1.0 $\pm$ 0.3	3.0 $\pm$ 0.8	0.4 $\pm$ 0.2
9/12/09						
8 AM	3.4 $\pm$ 0.2	nd	1.4 $\pm$ 0.1	1.3 $\pm$ 0.2	-	-
11 AM	18 $\pm$ 1	2.2 $\pm$ 0.2	1.9 $\pm$ 0.1	1.3 $\pm$ 0.2	-	-
2 PM	1.4 $\pm$ 0.2	-	1.6 $\pm$ 0.2	10.6 $\pm$ 0.4	-	-
9/20/09						
8 AM	5.3 $\pm$ 1.3	-	nd	nd	0.46 $\pm$ 0.08	nd
11 AM	3.7 $\pm$ 1.2	6.5 $\pm$ 0.36	nd	nd	0.19 $\pm$ 0.08	nd
2 PM	13 $\pm$ 2	-	nd	0.5 $\pm$ 0.2	0.63 $\pm$ 0.09	nd
9/27/09						
8 AM	9 $\pm$ 1	0.3 $\pm$ 0.1	0.3 $\pm$ 0.1	9.7 $\pm$ 1.8	6 $\pm$ 1	1.6 $\pm$ 0.2
11 AM	9.7 $\pm$ 0.9	10 $\pm$ 2	0.19 $\pm$ 0.08	1.0 $\pm$ 0.2	0.2 $\pm$ 0.1	0.2 $\pm$ 0.1
2 PM	12 $\pm$ 1	0.3 $\pm$ 0.1	3.5 $\pm$ 1.3	0.3 $\pm$ 0.1	0.3 $\pm$ 0.1	0.8 $\pm$ 0.2
10/02/09						
8 AM	30.3 $\pm$ 0.8	30.5 $\pm$ 0.7	nd	76 $\pm$ 3	-	-
11 AM	nd	24.9 $\pm$ 0.6	8.9 $\pm$ 0.5	29.4 $\pm$ 0.7	-	-
2 PM	15.9 $\pm$ 0.8	11.0 $\pm$ 0.7	45 $\pm$ 1	17.2 $\pm$ 0.6	-	-

	S2T6		S2T7		S2T8	
	trunk	canopy	trunk	canopy	trunk	canopy
	10/12/09					
8 AM	1.1±0.4	3.5±0.5	17±1	nd	nd	nd
11 AM	8.5±1.1	nd	1.6±0.3	4.8±0.5	2.1±0.3	nd
2 PM	34±2	1.8±0.4	nd	nd	0.13±0.10	nd
	10/19/09					
8 AM	204±5	nd	0.6±0.3	1.4±0.2	-	-
11 AM	nd	0.8±0.3	19±3	nd	-	-
2 PM	nd	nd	nd	nd	-	-
	10/26/09					
8 AM	nd	44±3	nd	nd	nd	nd
11 AM	32±4	nd	nd	nd	1.0±0.5	nd
2 PM	nd	nd	nd	nd	nd	nd

nd indicates that all of the VOCs were below the detection limit. - indicates that no samples were collected at this site for the date and time listed.

**A-I Table 3.** Total VOC concentration ( $\text{ng L}^{-1}$ ) at site 3 for lodgepole pine, sampled by scent trap and detected by GCMS. The values are the average over three replicate injections and corrected for blanks and the propagated uncertainty in the average.

	S3T9		S3T10		S3T11	
	trunk	canopy	trunk	canopy	trunk	canopy
9/19/09						
8 AM	nd	6.1 $\pm$ 0.5	120 $\pm$ 3	-	nd	nd
11 AM	nd	nd	33 $\pm$ 1	-	nd	nd
2 PM	nd	nd	3.4 $\pm$ 0.3	-	0.9 $\pm$ 0.3	nd
10/1/09						
8 AM	23.4 $\pm$ 0.6	21.6 $\pm$ 0.5	97 $\pm$ 2	-	13.7 $\pm$ 0.5	12.0 $\pm$ 0.4
11 AM	45.3 $\pm$ 1.0	26.1 $\pm$ 0.6	34 $\pm$ 0.8	-	24.1 $\pm$ 0.7	9.3 $\pm$ 0.4
2 PM	17.0 $\pm$ 0.7	13.3 $\pm$ 0.7	106 $\pm$ 3	-	29.7 $\pm$ 0.8	0.6 $\pm$ 0.1
10/9/09						
8 AM	1.2 $\pm$ 0.3	47.5 $\pm$ 1.8	5.5 $\pm$ 0.3	-	77.8 $\pm$ 2.4	nd
11 AM	37.5 $\pm$ 1.5	nd	14.3 $\pm$ 0.7	-	3.5 $\pm$ 0.6	nd
2 PM	28.8 $\pm$ 2.4	24.0 $\pm$ 1.6	21 $\pm$ 2	-	48.6 $\pm$ 1.9	58 $\pm$ 2
10/17/09						
8 AM	33.2 $\pm$ 3.7	1.3 $\pm$ 0.2	66 $\pm$ 5	-	nd	0.7 $\pm$ 0.2
11 AM	46.4 $\pm$ 4.1	nd	60 $\pm$ 2	-	43.2 $\pm$ 2.4	nd
2 PM	nd	32.3 $\pm$ 3.3	67 $\pm$ 2	-	nd	nd
10/24/09						
8 AM	89.3 $\pm$ 9.0	nd	6 $\pm$ 2	-	nd	nd
11 AM	nd	52.3 $\pm$ 9.6	21 $\pm$ 3	-	nd	16 $\pm$ 4
2 PM	6.3 $\pm$ 3.9	43.8 $\pm$ 9.6	16 $\pm$ 4	-	nd	nd
10/31/09						
8 AM	21.9 $\pm$ 1.3	-	17.2 $\pm$ 0.6	-	nd	nd
11 AM	20.7 $\pm$ 1.1	-	252 $\pm$ 6	-	nd	nd
2 PM	nd	-	156 $\pm$ 4	-	36.2 $\pm$ 1.5	nd

nd indicates that all of the VOCs were below the detection limit. - indicates that no samples were collected at this site for the date and time listed.



**A-I Table 4.** Total VOC concentration ( $\text{ng L}^{-1}$ ) for Engelmann spruce, sampled by scent trap and detected by GCMS. The values are the average over three replicate injections and corrected for blanks and the propagated uncertainty in the average.

	S2T4 trunk	S2T5 trunk
	08/02/2009	
2 PM	31.8 $\pm$ 0.6	-
	08/16/2009	
8 AM	15.1 $\pm$ 0.9	nd
11 AM	55.6 $\pm$ 2.4	nd
2 PM	35.5 $\pm$ 1.8	0.21 $\pm$ 0.11
	08/30/2009	
8 AM	71.05 $\pm$ 1.7	7.4 $\pm$ 1.0
2 PM	102.5 $\pm$ 2.7	4.3 $\pm$ 0.3
	09/12/2009	
8 AM	9.2 $\pm$ 0.3	1.3 $\pm$ 0.2
11 AM	35.5 $\pm$ 1.2	1.7 $\pm$ 0.2
2 PM	40.3 $\pm$ 1.4	1.4 $\pm$ 0.2
	10/02/2009	
8 AM	25.9 $\pm$ 0.7	9.2 $\pm$ 0.6
11 AM	6.0 $\pm$ 0.7	13.3 $\pm$ 0.5
2 PM	67.0 $\pm$ 1.2	16.7 $\pm$ 0.7
	10/19/2009	
8 AM	nd	nd
11 AM	45.2 $\pm$ 2.7	nd
2 PM	14.6 $\pm$ 2.8	nd

nd indicates that all of the VOCs were below the detection limit.

- indicates that no samples were collected at this site for the date and time listed.

**APPENDIX II**  
**PHYSICAL PARAMETERS FOR SMOG CHAMBER EXPERIMENTS IN CHAPTER 3**

**A-II Table 1.** VOC precursor concentrations and calculated SOA yields from limonene and other VOC mixtures

Reactive precursor	$k_1^b \times 10^5$ (s <sup>-1</sup> )	$k_2^b \times 10^5$ (s <sup>-1</sup> )	Pressure <sup>e</sup> (atm)	Temperature <sup>f</sup> (K)	Relative humidity <sup>g</sup> (%)
Limonene (367±48 µg m <sup>-3</sup> )					
Limonene	140±10	5.84±0.21	0.984±0.00 1	293.1±0.3	3.0±1.8
Limonene	190±10	2.92±0.08	0.991±0.00 03	292.6±0.5	3.0±0.4
Limonene	190±10	4.21±0.06	0.976±0.00 2	0295.2±1.4	35.9±8
Mixture 2A. Limonene (374±48 µg m <sup>-3</sup> ) and p-cymene (8.4±1 µg m <sup>-3</sup> )					
Limonene	190±5	3.90±0.64	0.978±0.00 05	294.4±0.3	7.5±0.7
Limonene	140±4	3.50±0.08	0.976±0.00 02	292.6±0.0	6.5±0.6
Mixture 2B. Limonene (310±40 µg m <sup>-3</sup> ) and p-cymene (72±9 µg m <sup>-3</sup> )					
Limonene	130±4	7.27±0.11	0.984±0.00 04	295.3±1.3	7.2±0.9
Mixture 2C. Limonene (372±47 µg m <sup>-3</sup> ) and p-cymene (87±11 µg m <sup>-3</sup> )					
Limonene	120±4	4.43±0.09	0.976±0.00 1	294.2±0.2	8.5±0.4
Mixture 2D. Limonene (374±48 µg m <sup>-3</sup> ) and p-cymene (85±11 µg m <sup>-3</sup> )					
Limonene	150±7	5.36±0.13	0.990±0.00 1	294.1±0.6	10.2±0.5
Mixture 3. Limonene (379±48 µg m <sup>-3</sup> ), p-cymene (10±1 µg m <sup>-3</sup> ), α-pinene (10±1 µg m <sup>-3</sup> ) and β-pinene (30±4 µg m <sup>-3</sup> )					
limonene + α-pinene +β-pinene	150±8	4.83±0.13	0.983±0.00 1	294.2±0.2	10.4±0.4
limonene +α-pinene +β-pinene	120±6	4.34±0.14	0.978±0.00 02	294.3±0.2	10.2±0.9

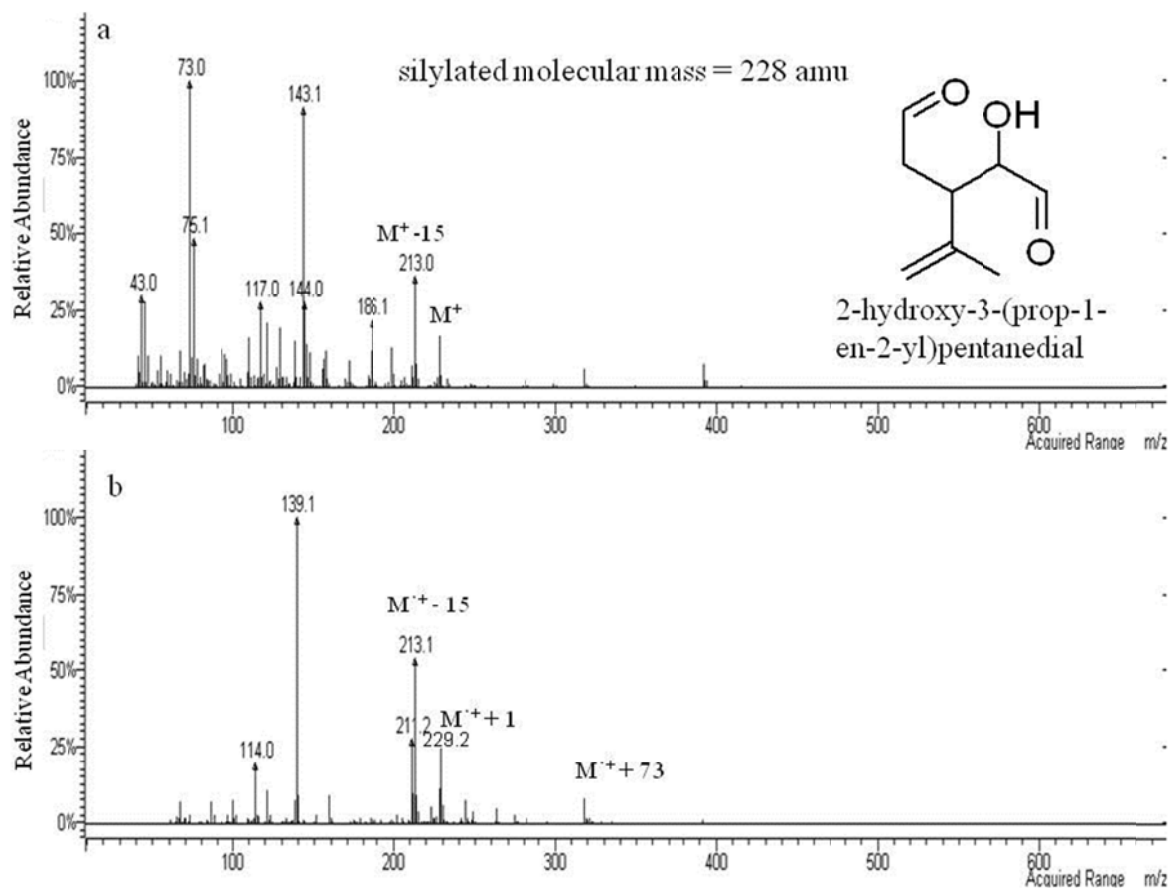
Mixture 4A. Limonene ( $377 \pm 47 \mu\text{g m}^{-3}$ ), Linalool ( $236 \pm 29 \mu\text{g m}^{-3}$ ), p-cymene ( $9 \pm 1 \mu\text{g m}^{-3}$ ), $\alpha$ -pinene ( $10 \pm 1 \mu\text{g m}^{-3}$ ) and $\beta$ -pinene ( $33 \pm 4 \mu\text{g m}^{-3}$ )					
Limonene + $\alpha$ -pinene + $\beta$ -pinene	160 $\pm$ 8	4.68 $\pm$ 0.14	0.974 $\pm$ 0.00 1	294.1 $\pm$ 0.2	13.1 $\pm$ 0.5
Limonene + $\alpha$ -pinene + $\beta$ -pinene	120 $\pm$ 7	5.57 $\pm$ 0.16	0.979 $\pm$ 0.00 1	294.6 $\pm$ 0.8	12.9 $\pm$ 0.9
Reactive precursor	$k_1^b \times 10^5$ (s <sup>-1</sup> )	$k_2^b \times 10^5$ (s <sup>-1</sup> )	Pressure <sup>e</sup> (atm)	Temperature <sup>f</sup> (K)	Relative humidity <sup>g</sup> (%)
Mixture 4B. Limonene ( $368 \pm 46 \mu\text{g m}^{-3}$ ), Linalool ( $238 \pm 30 \mu\text{g m}^{-3}$ ), p-cymene ( $11 \pm 1 \mu\text{g m}^{-3}$ ), $\alpha$ -pinene ( $11 \pm 1 \mu\text{g m}^{-3}$ ) and $\beta$ -pinene ( $36 \pm 4 \mu\text{g m}^{-3}$ )					
Limonene + $\alpha$ -pinene + $\beta$ -pinene	180 $\pm$ 7	5.43 $\pm$ 0.10	0.985 $\pm$ 0.00 1	292.9 $\pm$ 0.2	9.8 $\pm$ 0.4
Limonene + $\alpha$ -pinene + $\beta$ -pinene	200 $\pm$ 10	3.83 $\pm$ 0.13	0.981 $\pm$ 0.00 1	295.2 $\pm$ 0.2	6.2 $\pm$ 1.0
Mixture 4C. Limonene ( $370 \pm 46 \mu\text{g m}^{-3}$ ), Linalool ( $1138 \pm 140 \mu\text{g m}^{-3}$ ), p-cymene ( $11 \pm 1 \mu\text{g m}^{-3}$ ), $\alpha$ -pinene ( $10 \pm 1 \mu\text{g m}^{-3}$ ) and $\beta$ -pinene ( $29 \pm 4 \mu\text{g m}^{-3}$ )					
Limonene + $\alpha$ -pinene + $\beta$ -pinene	160 $\pm$ 10	4.75 $\pm$ 0.21	0.978 $\pm$ 0.00 1	294.3 $\pm$ 0.2	7.4 $\pm$ 1.2
Limonene + $\alpha$ -pinene + $\beta$ -pinene	230 $\pm$ 20	3.07 $\pm$ 0.14	0.980 $\pm$ 0.00 1	294.7 $\pm$ 0.2	7.8 $\pm$ 1.2
Mixture 5. Limonene ( $368 \pm 46 \mu\text{g m}^{-3}$ ) and Linalool ( $234 \pm 29 \mu\text{g m}^{-3}$ )					
Limonene	160 $\pm$ 9	4.05 $\pm$ 0.12	0.979 $\pm$ 0.00 1	292.8 $\pm$ 0.2	11.5 $\pm$ 0.8

**A-II Table 2.** VOC precursor concentrations and calculated SOA yields from limonene and other VOC mixtures

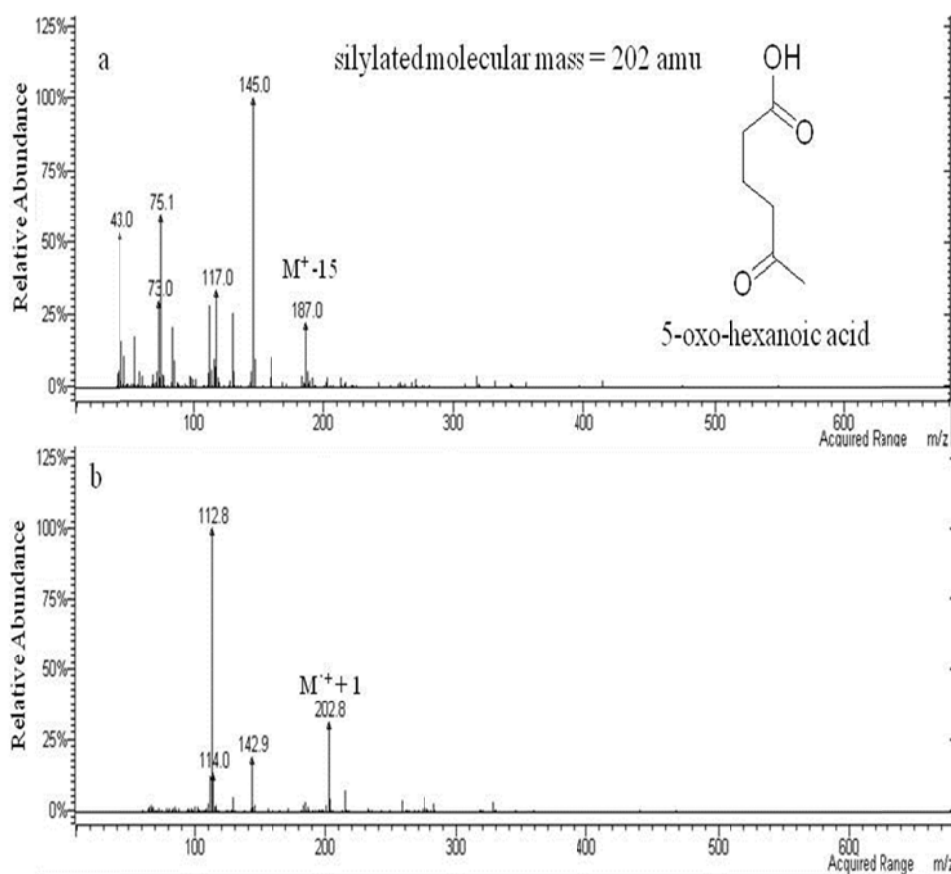
Reactive precursor	$k_1^b \times 10^5$ (s <sup>-1</sup> )	$k_2^b \times 10^5$ (s <sup>-1</sup> )	Pressure <sup>e</sup> (atm)	Temperature <sup>f</sup> (K)	Relative humidity <sup>g</sup> (%)
Surrogate 1. Limonene (375±47 µg m <sup>-3</sup> ), Linalool (225±28 µg m <sup>-3</sup> ), Estragole (107±13 µg m <sup>-3</sup> ), γ-terpinine (85±11 µg m <sup>-3</sup> ), α-terpineol (52±6 µg m <sup>-3</sup> ), β-pinene (31±4 µg m <sup>-3</sup> ), terpinolene (22±3 µg m <sup>-3</sup> ), p-cymene (11±1 µg m <sup>-3</sup> ), α-pinene (9±1 µg m <sup>-3</sup> ) and anethole (20±3 µg m <sup>-3</sup> )					
Limonene +α-pinene +β-pinene +terpinolene	140±10	4.39±0.19	0.981±0.001	294.7±0.2	7.8±0.8
Surrogate 2. Limonene (368±46 µg m <sup>-3</sup> ), Linalool (239±30 µg m <sup>-3</sup> ), Estragole (110±14 µg m <sup>-3</sup> ), γ-terpinine (84±10 µg m <sup>-3</sup> ), α-terpineol (50±6 µg m <sup>-3</sup> ), β-pinene (40±5 µg m <sup>-3</sup> ), terpinolene (23±3 µg m <sup>-3</sup> ), p-cymene (10±1 µg m <sup>-3</sup> ), α-pinene (10±1 µg m <sup>-3</sup> ) and anethole (20±3 µg m <sup>-3</sup> )					
Limonene +α-pinene +β-pinene +terpinolene	160±10	2.78±0.14	0.983±0.001	294.3±0.2	5.6±0.9
Surrogate 3. Limonene (350±43 µg m <sup>-3</sup> ), Linalool (1086±134 µg m <sup>-3</sup> ), Estragole (76±9 µg m <sup>-3</sup> ), γ-terpinine (22±3 µg m <sup>-3</sup> ), α-terpineol (24±3 µg m <sup>-3</sup> ), β-pinene (99±12 µg m <sup>-3</sup> ), terpinolene (23±3 µg m <sup>-3</sup> ), p-cymene (62±8 µg m <sup>-3</sup> ), α-pinene (16±2 µg m <sup>-3</sup> ) and anethole (43±5 µg m <sup>-3</sup> )					
Limonene +α-pinene +β-pinene +terpinolene	165±10	3.98±0.14	0.982±0.001	294.3±0.2	7.99±0.9
Surrogate 3. Limonene (201±25 µg m <sup>-3</sup> ), Linalool (623±77 µg m <sup>-3</sup> ), Estragole (43±5 µg m <sup>-3</sup> ), γ-terpinine (12±2 µg m <sup>-3</sup> ), α-terpineol (14±2 µg m <sup>-3</sup> ), β-pinene (57±7 µg m <sup>-3</sup> ), terpinolene (13±2 µg m <sup>-3</sup> ), p-cymene (35±4 µg m <sup>-3</sup> ), α-pinene (9±1 µg m <sup>-3</sup> ) and anethole (24±3 µg m <sup>-3</sup> )					
limonene +α-pinene +β-pinene +terpinolene	185±15	3.37±0.14	0.983±0.001	294.3±0.2	7.61±0.9

Reactive precursor	$k_1^b \times 10^5$ (s <sup>-1</sup> )	$k_2^b \times 10^5$ (s <sup>-1</sup> )	Pressure <sup>e</sup> (atm)	Temperature <sup>f</sup> (K)	Relative humidity <sup>g</sup> (%)
Limonene based air freshener-Trial 1: limonene (201±25 µg m <sup>-3</sup> ), β-pinene (53±6 µg m <sup>-3</sup> ), terpinolene (5±1 µg m <sup>-3</sup> ), α-pinene (6±1 µg m <sup>-3</sup> ) <sup>h</sup>					
limonene +α-pinene +β-pinene +terpinolene	150±8	4.05±0.12	0.981±0.001	294.3±0.2	7.6±0.9
limonene +α-pinene +β-pinene +terpinolene	140±9	4.14±0.10	0.981±0.001	294.6±0.3	6.6±1.1
limonene +α-pinene +β-pinene +terpinolene	80±7	3.51±0.03	0.982±0.001	296.7±0.6	6.3±0.8
Limonene based air freshener-Trial 2: limonene (322±40 µg m <sup>-3</sup> ), β-pinene (89±9 µg m <sup>-3</sup> ), terpinolene (8±1 µg m <sup>-3</sup> ), α-pinene (10±1 µg m <sup>-3</sup> ) <sup>h</sup>					
limonene +α-pinene +β-pinene +terpinolene	80±3	2.27±0.07	0.983±0.002	294.2±0.2	5.1±0.6
limonene +α-pinene +β-pinene +terpinolene	130±6	2.17±0.08	0.982±0.001	294.7±0.2	6.3±2.0
limonene +α-pinene +β-pinene +terpinolene	200±20	1.82±0.12	0.982±0.001	294.8±0.2	4.3±0.6
Limonene based air freshener-Trial 3: limonene (477±46 µg m <sup>-3</sup> ), β-pinene (126±10 µg m <sup>-3</sup> ), terpinolene (11±1 µg m <sup>-3</sup> ), α-pinene (14±1 µg m <sup>-3</sup> )					
limonene +α-pinene +β-pinene +terpinolene	295±30	2.72±0.07	0.981±0.001	294.3±0.2	5.3±2.0
limonene +α-pinene +β-pinene +terpinolene	306±31	2.73±0.07	0.980±0.001	294.6±0.2	4.6±0.6

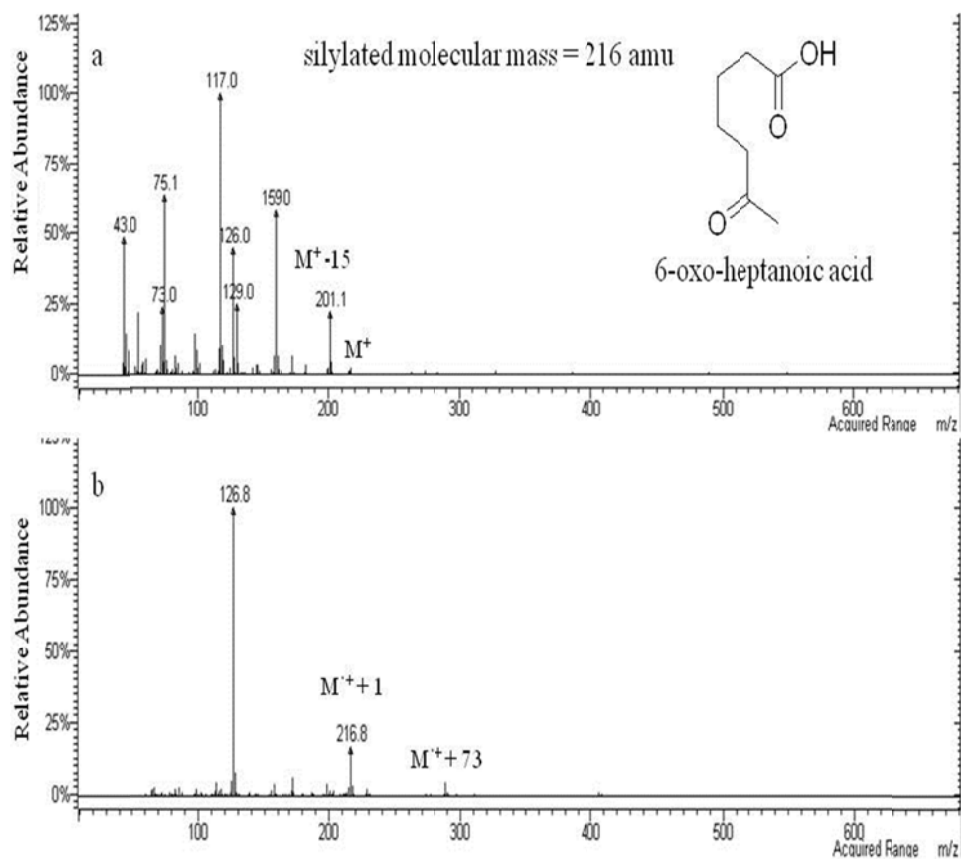
## Appendix III

MASS SPECTRAL FRAGMENTATION PATTERNS FOR SOA PRODUCTS  
IDENTIFIED FROM LIMONENE VOC MIXTURES: CHAPTER 3

**Figure AIII-1** EI (a) and CI (b) mass spectra for trimethylsilyl derivative of 2-hydroxy-3-(prop-1-en-2-yl)pentanedial

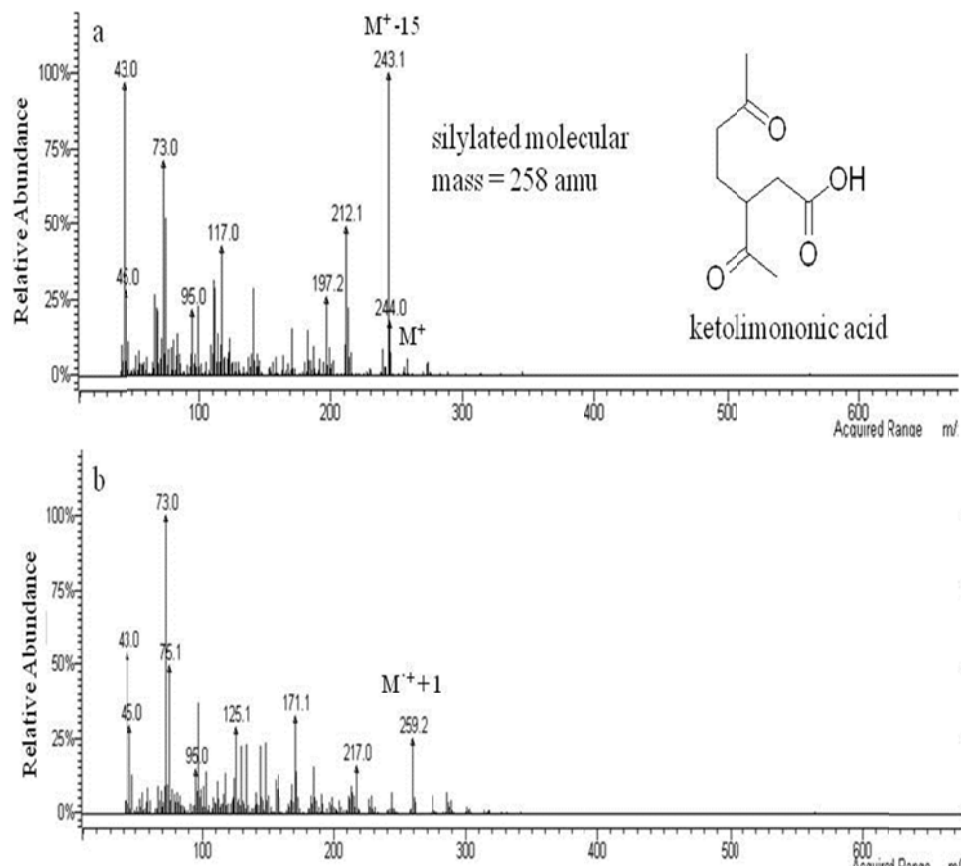


**Figure AIII-2** EI (a) and CI (b) mass spectra for trimethylsilyl derivative of 5-oxo-hexanoic acid

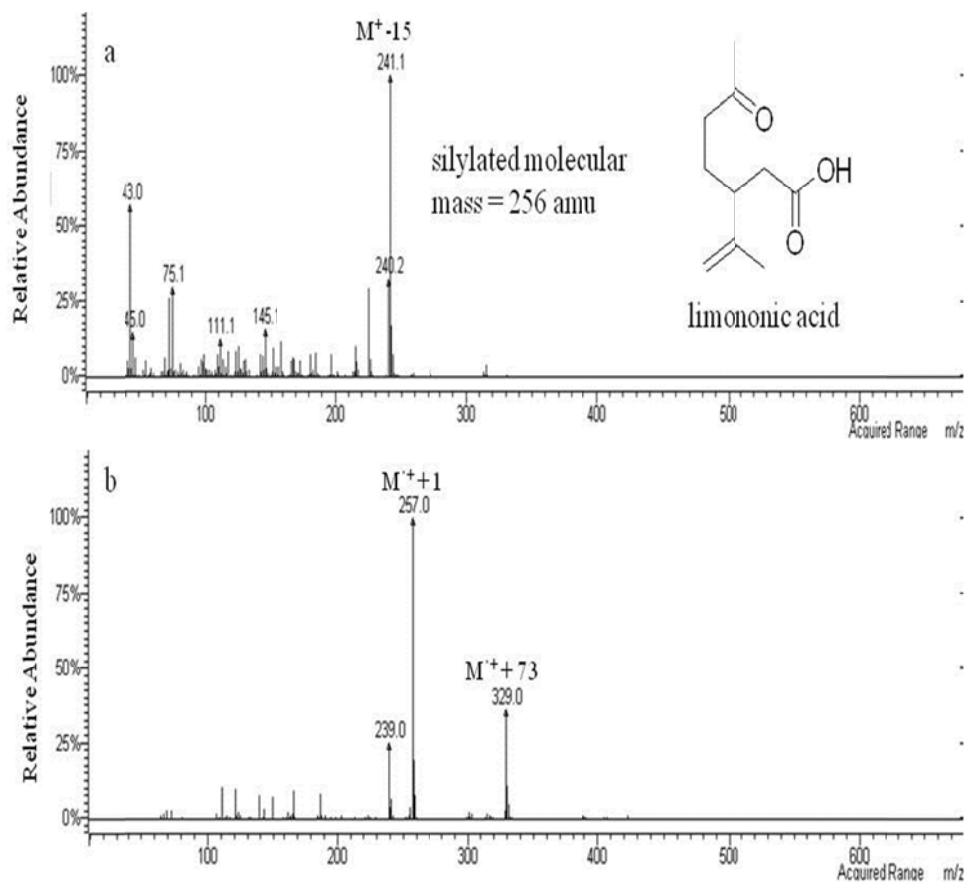


**Figure AIII-3** EI (a) and CI (b) mass spectra for trimethylsilyl derivative of 6-oxo-heptanoic acid.

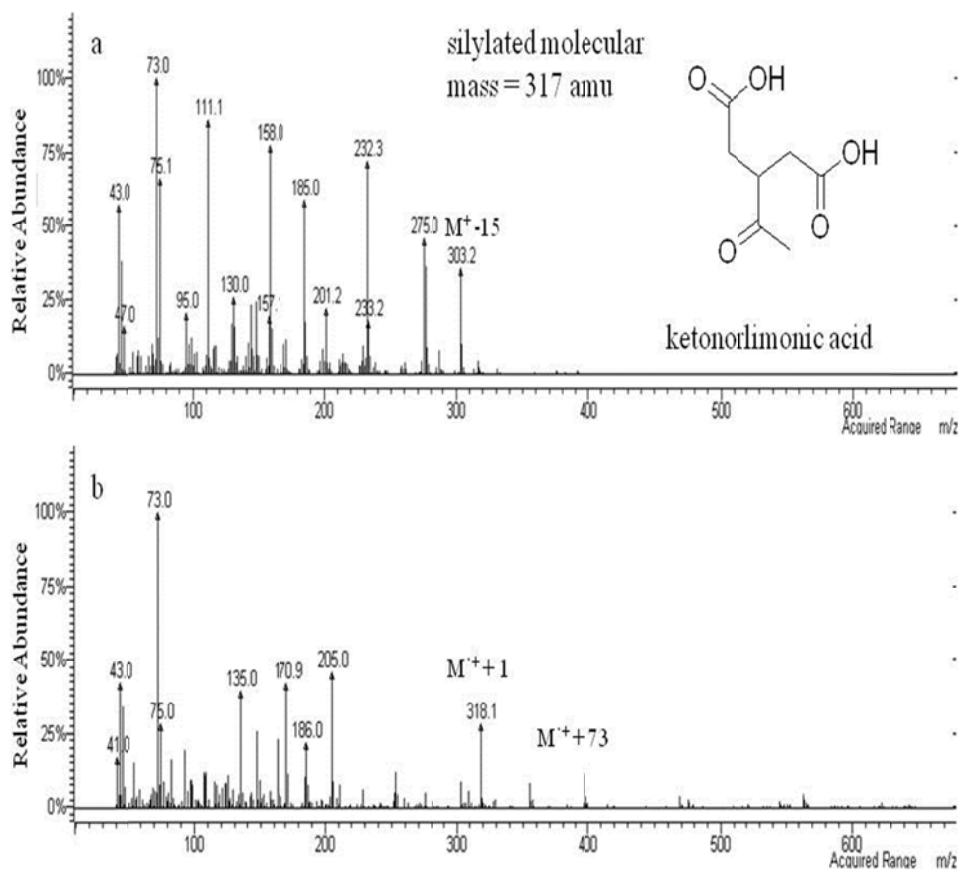




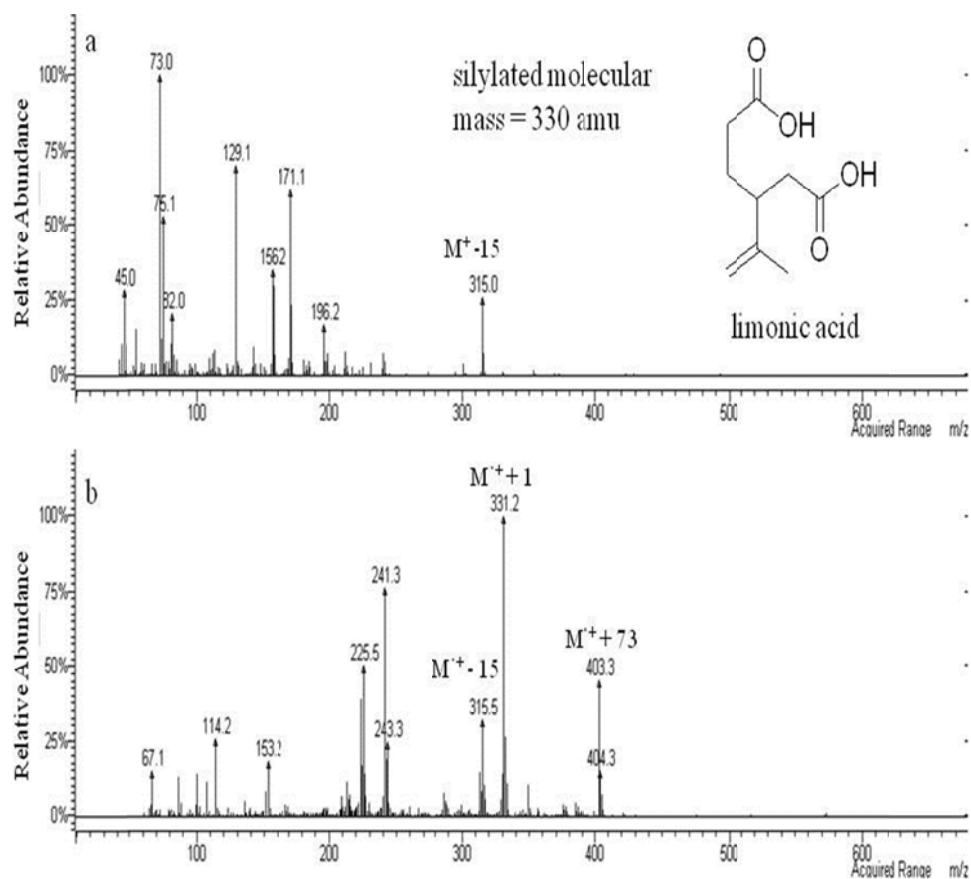
**Figure AIII-4** EI (a) and CI (b) mass spectra for trimethylsilyl derivative of ketolimononic acid



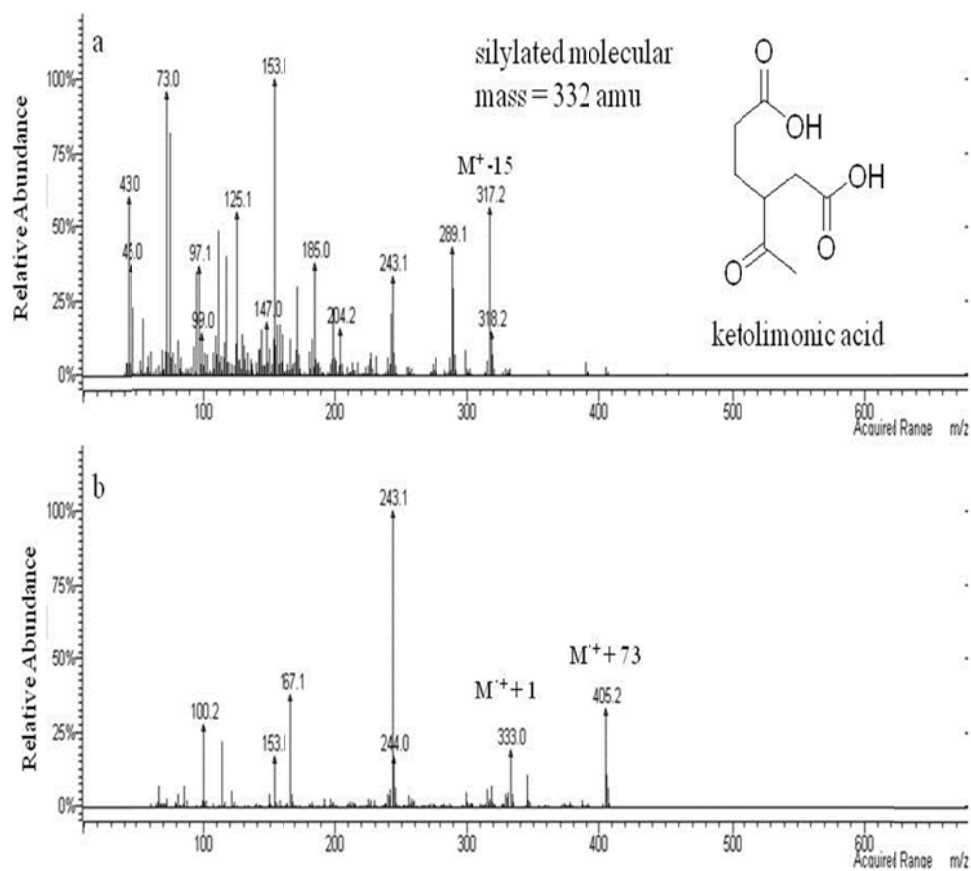
**Figure AIII-5** EI (a) and CI (b) mass spectra for trimethylsilyl derivative of limononic acid.



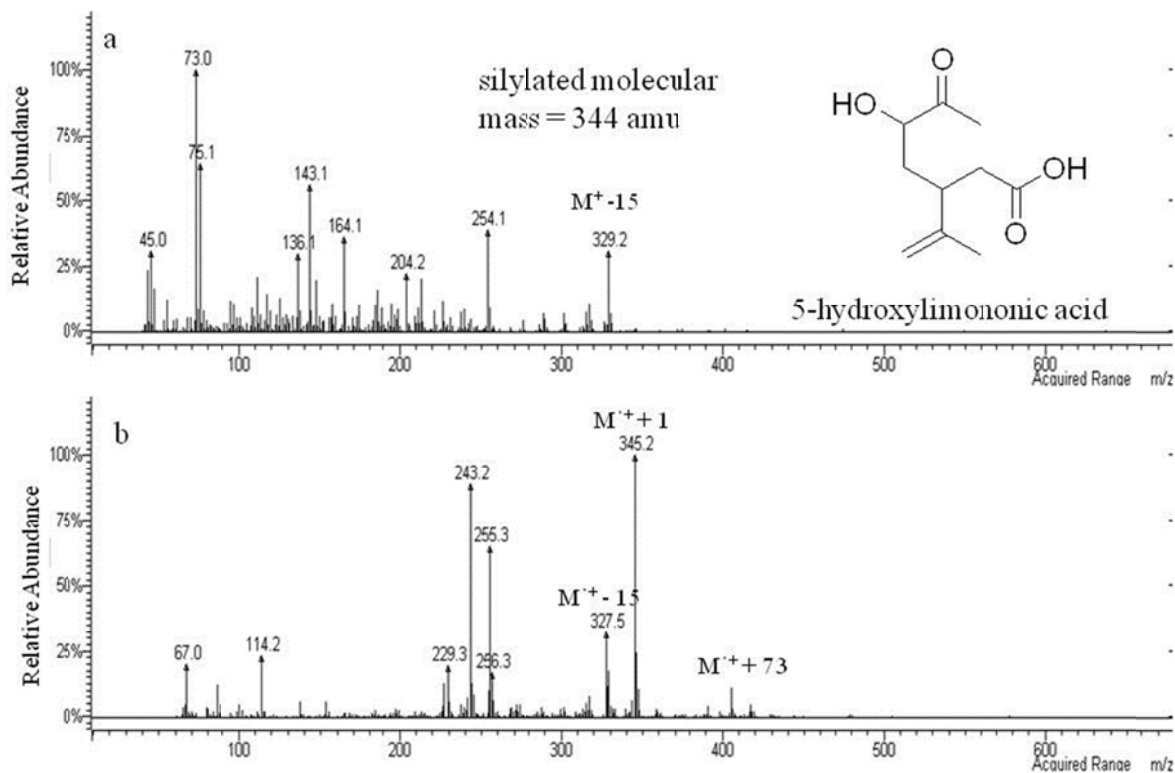
**Figure AIII-6** EI (a) and CI (b) mass spectra for trimethylsilyl derivative of ketonorlimonic acid.



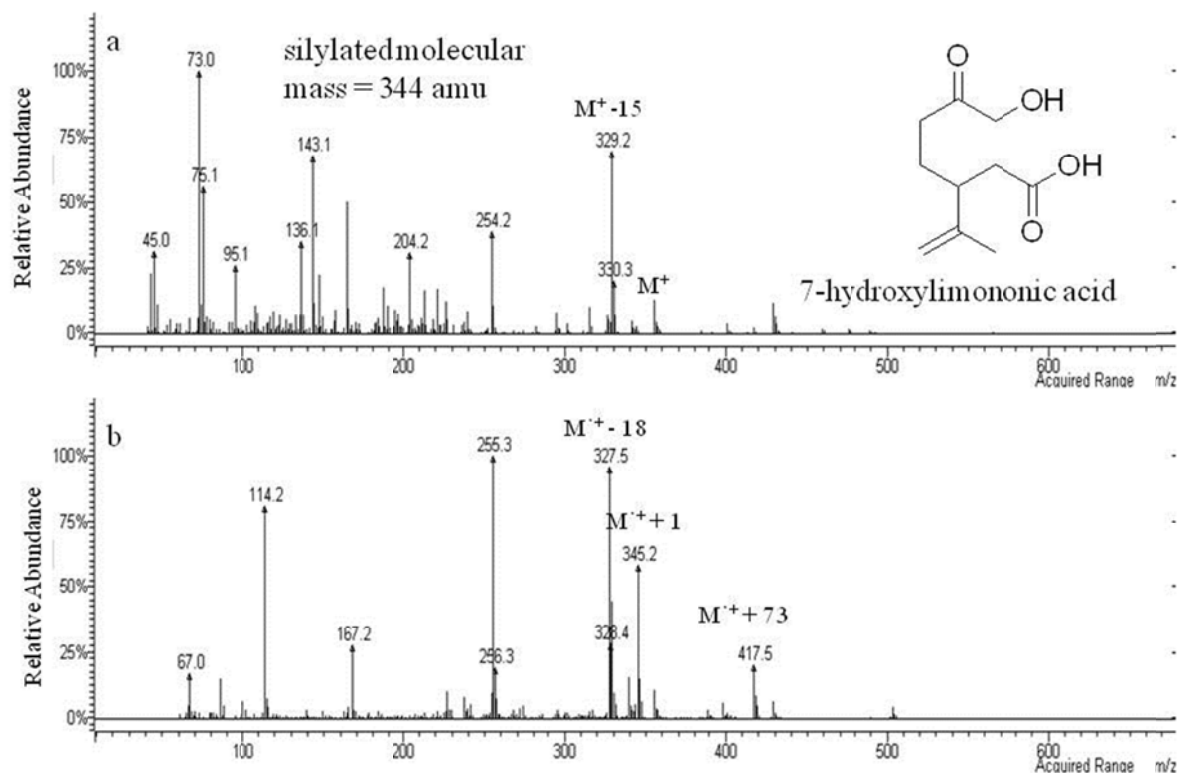
**Figure AIII-7** EI (a) and CI (b) mass spectra for trimethylsilyl derivative of limonic acid.



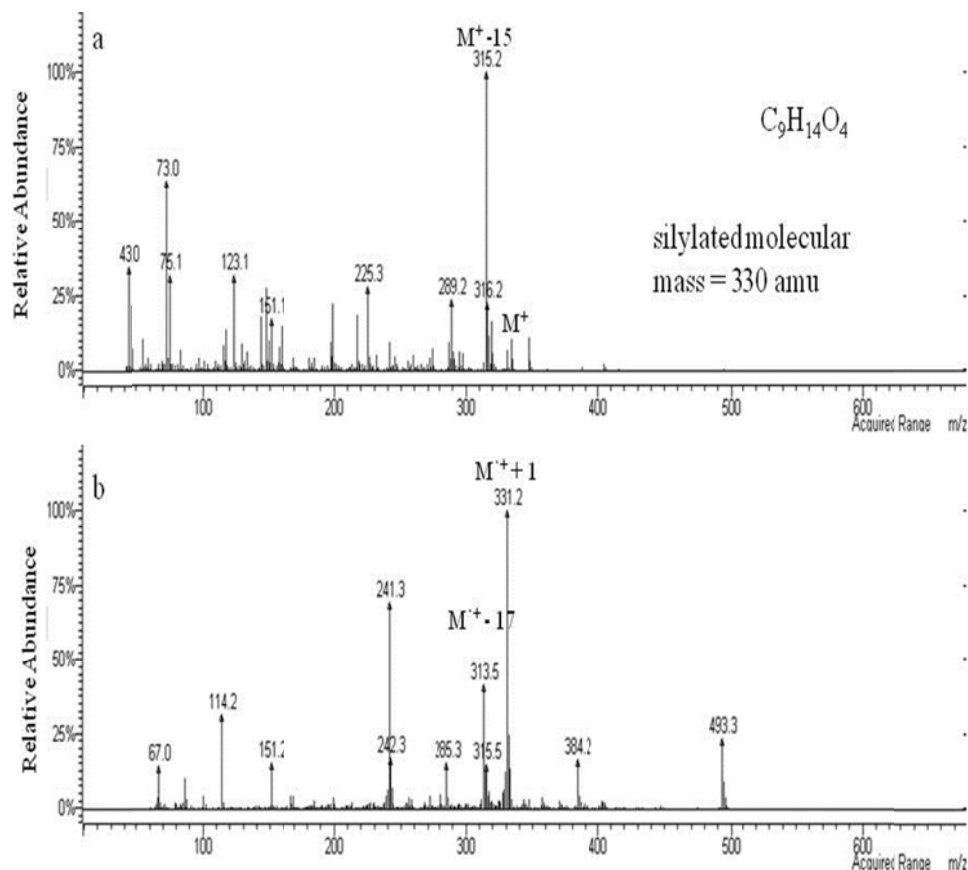
**Figure AIII-8** EI (a) and CI (b) mass spectra for trimethylsilyl derivative of ketolimonic acid.



**Figure AIII-9** EI (a) and CI (b) mass spectra for trimethylsilyl derivative of 5-hydroxylimononic acid.

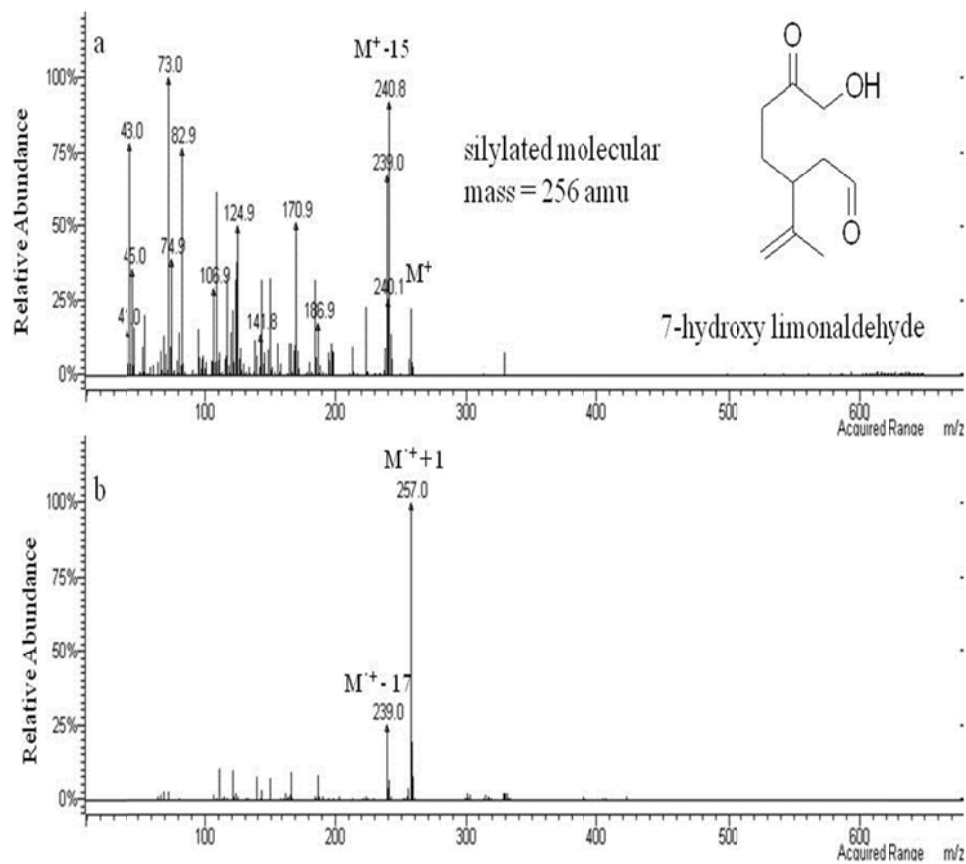


**Figure AIII-10** EI (a) and CI (b) mass spectra for trimethyl silyl derivative of 7-hydroxylimononic acid.

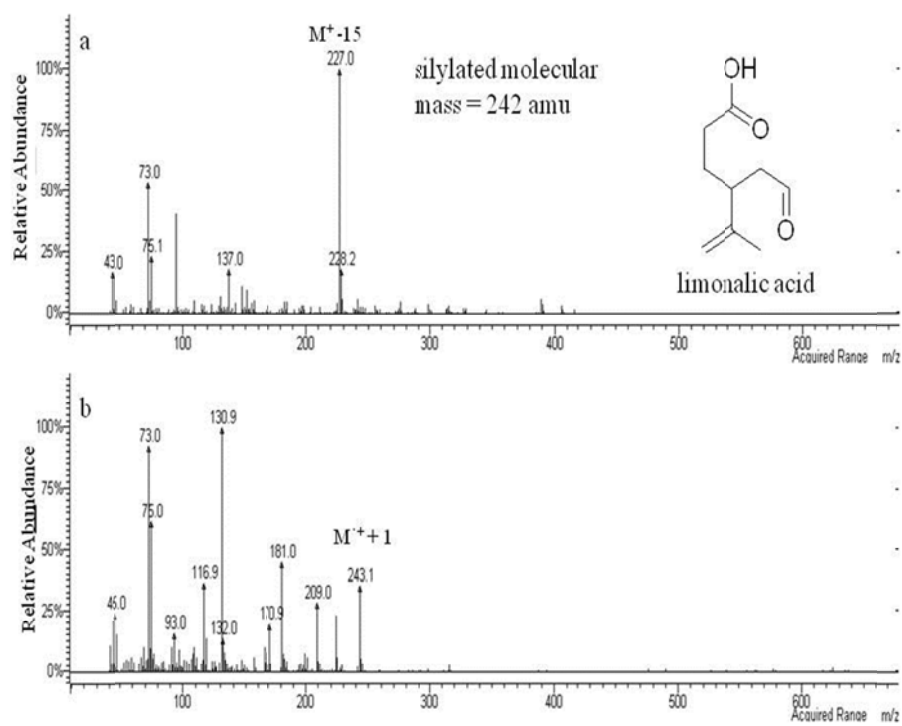


**Figure AIII-11** EI (a) and CI (b) mass spectra for trimethylsilyl derivative of a compound with molecular formula of  $C_9H_{14}O_4$ . From molecular formula and molecular mass of silylated compound obtained from mass spectrum it can be concluded that it is a diprotic acid

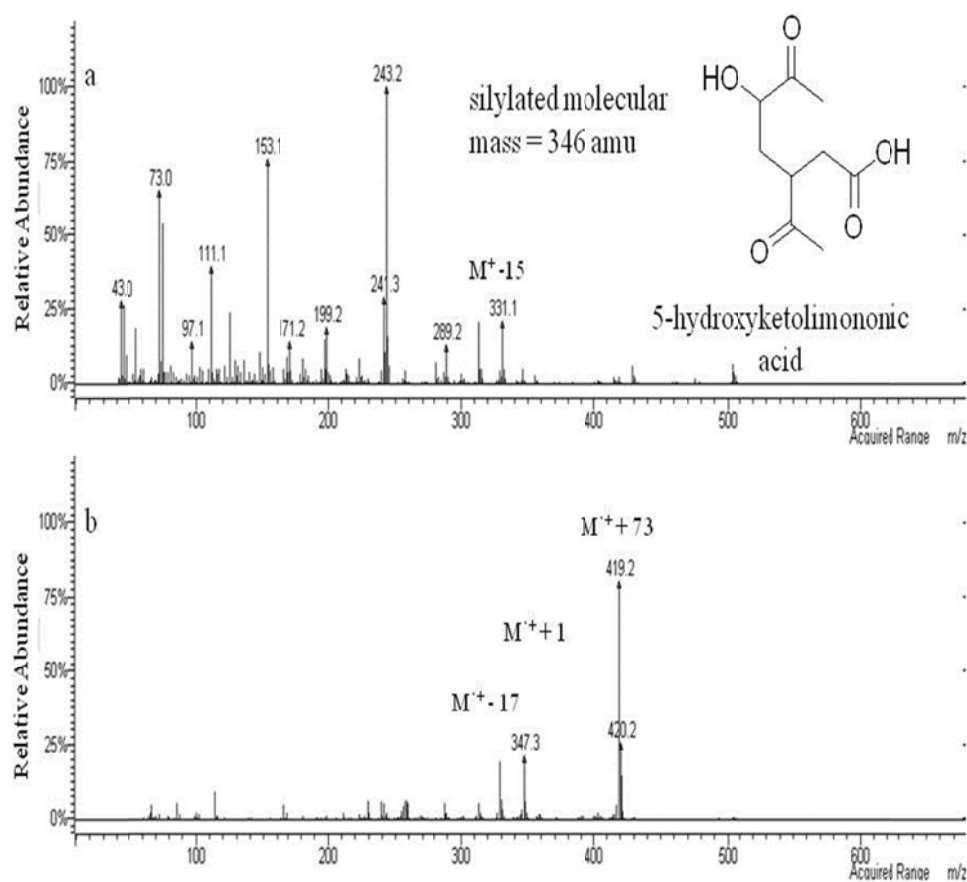




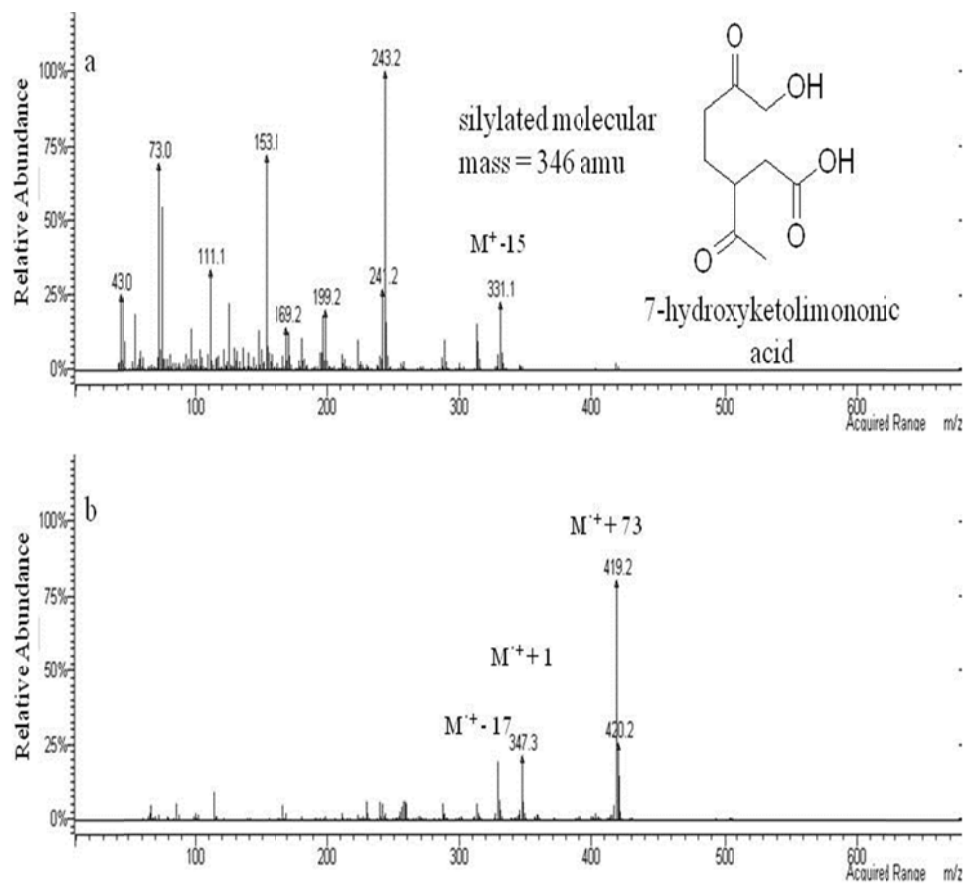
**Figure AIII-12** EI (a) and CI (b) mass spectra for trimethylsilyl derivative of 7-hydroxy limonaldehyde



**Figure AIII-13** EI (a) and CI (b) mass spectra for trimethylsilyl derivative of limonic acid

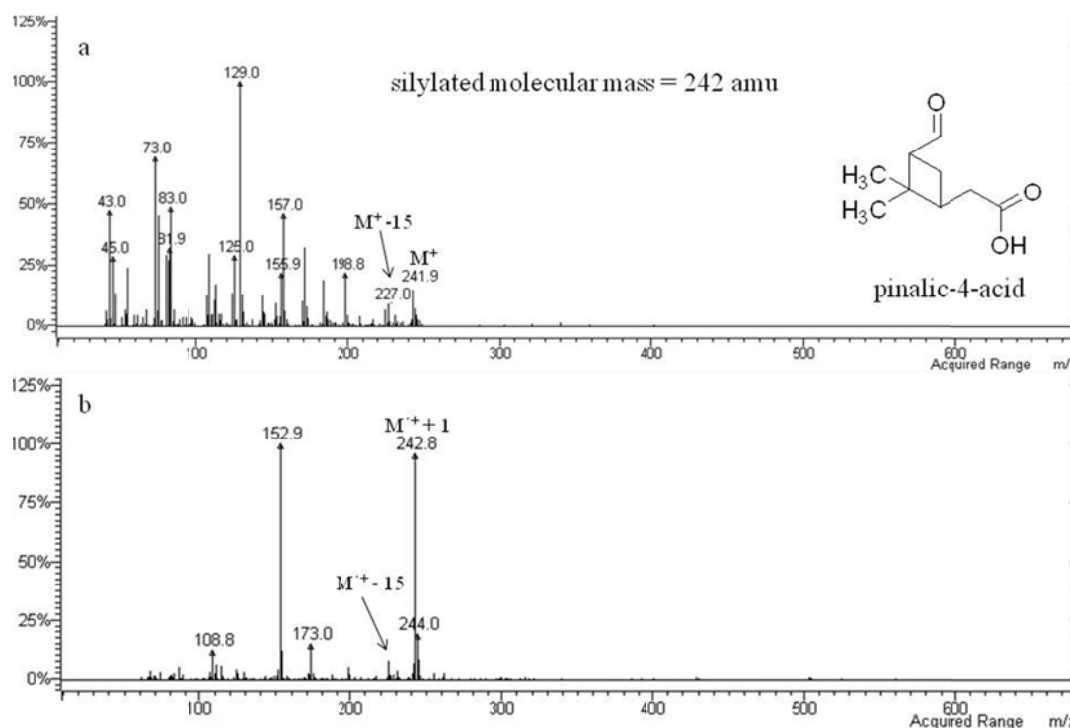


**Figure AIII-14** EI (a) and CI (b) mass spectra for trimethylsilyl derivative of 5-hydroxy ketolimononic acid

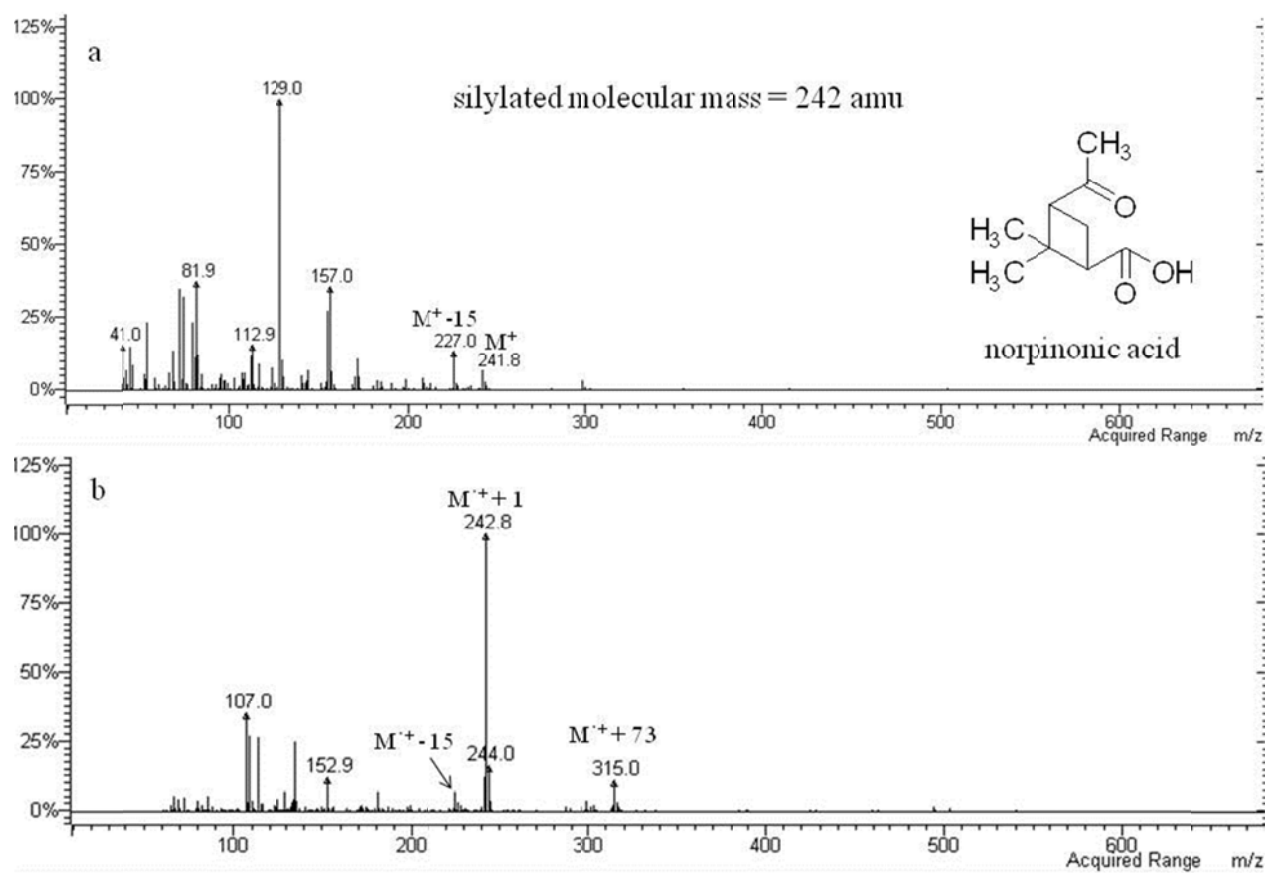


**Figure AIII-15** EI (a) and CI (b) mass spectra for trimethylsilyl derivative of 7-hydroxy ketolimononic acid

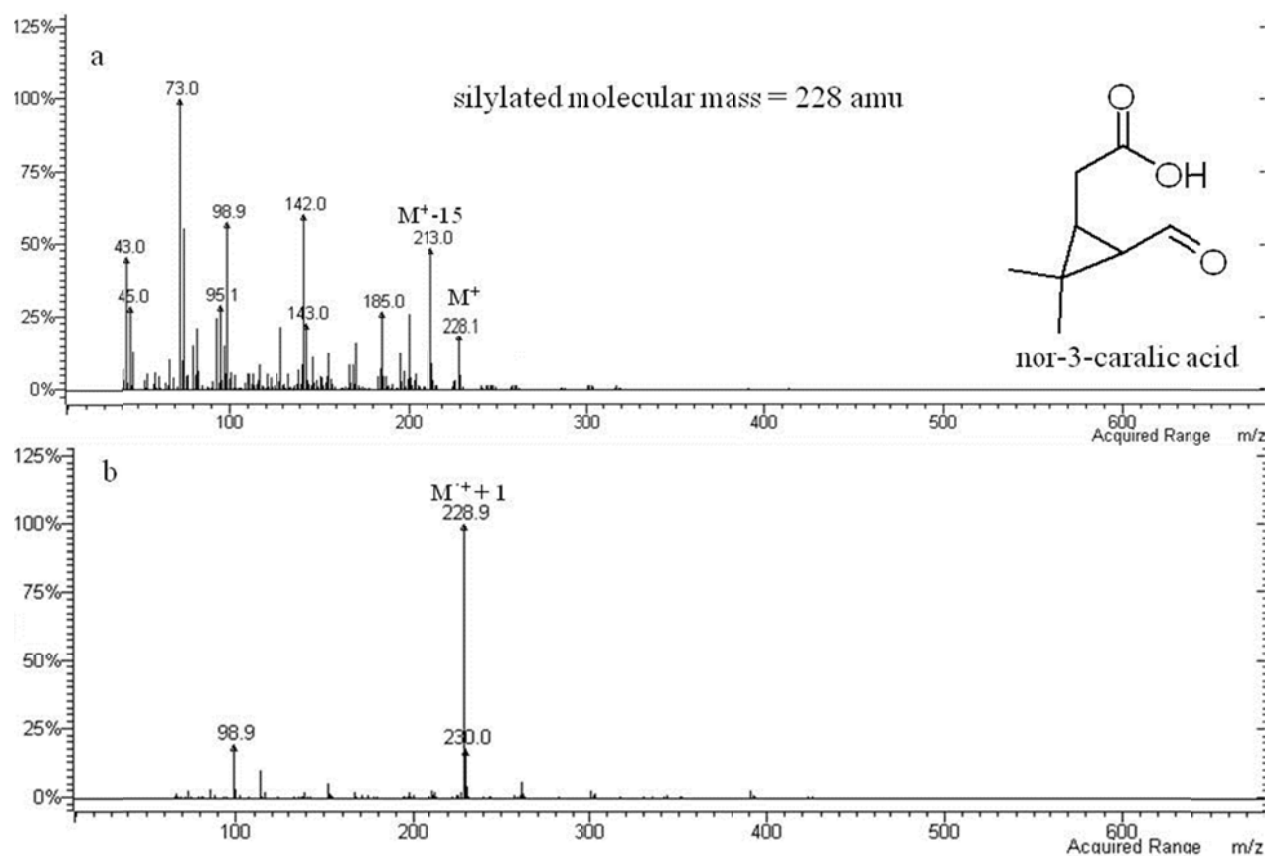
## Appendix IV

MASS SPECTRAL FRAGMENTATION PATTERNS FOR SOA PRODUCTS  
IDENTIFIED FROM  $\alpha$ -PINENE VOC MIXTURES: CHAPTER 4

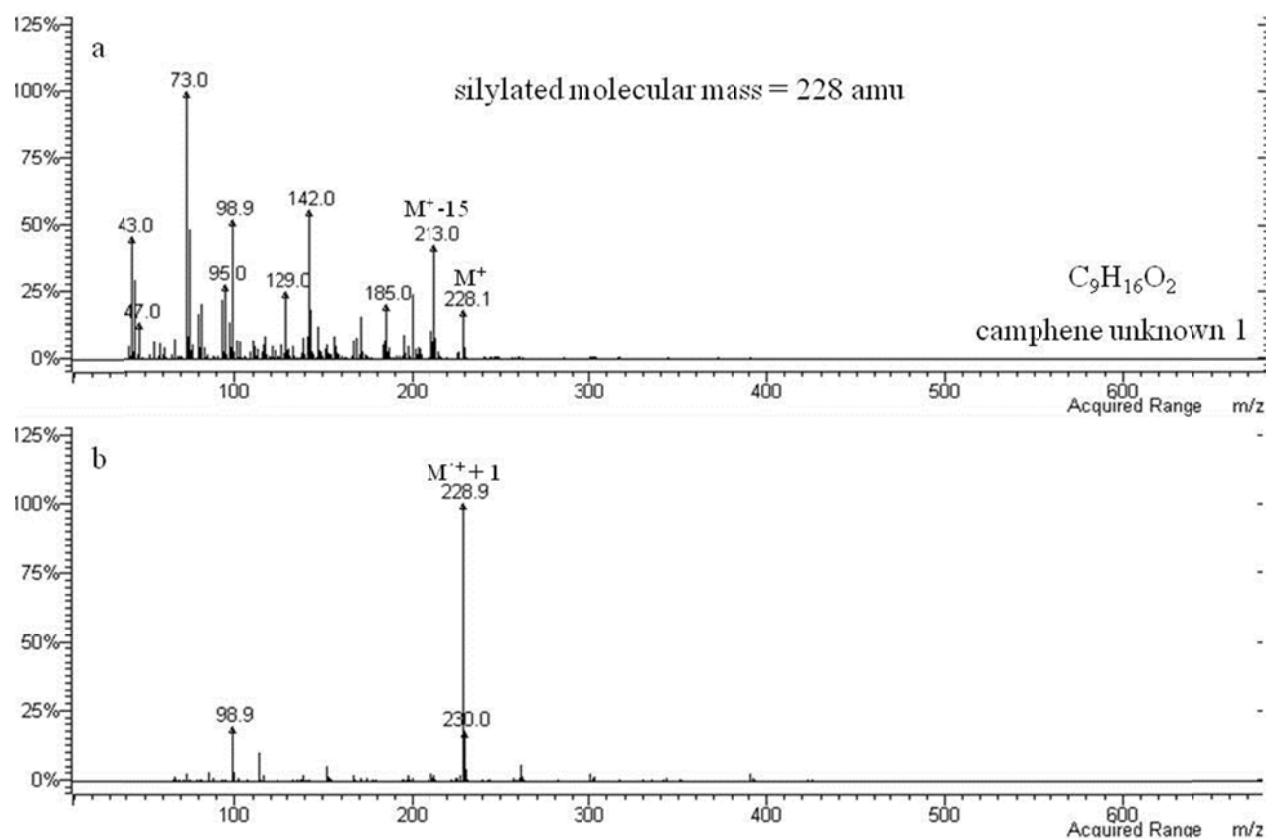
**Figure A-IV 1** EI (a) and CI (b) mass spectra for trimethylsilyl derivative of pinalic-4-acid



**Figure A-IV 2** EI (a) and CI (b) mass spectra for trimethylsilyl derivative of norpinonic acid

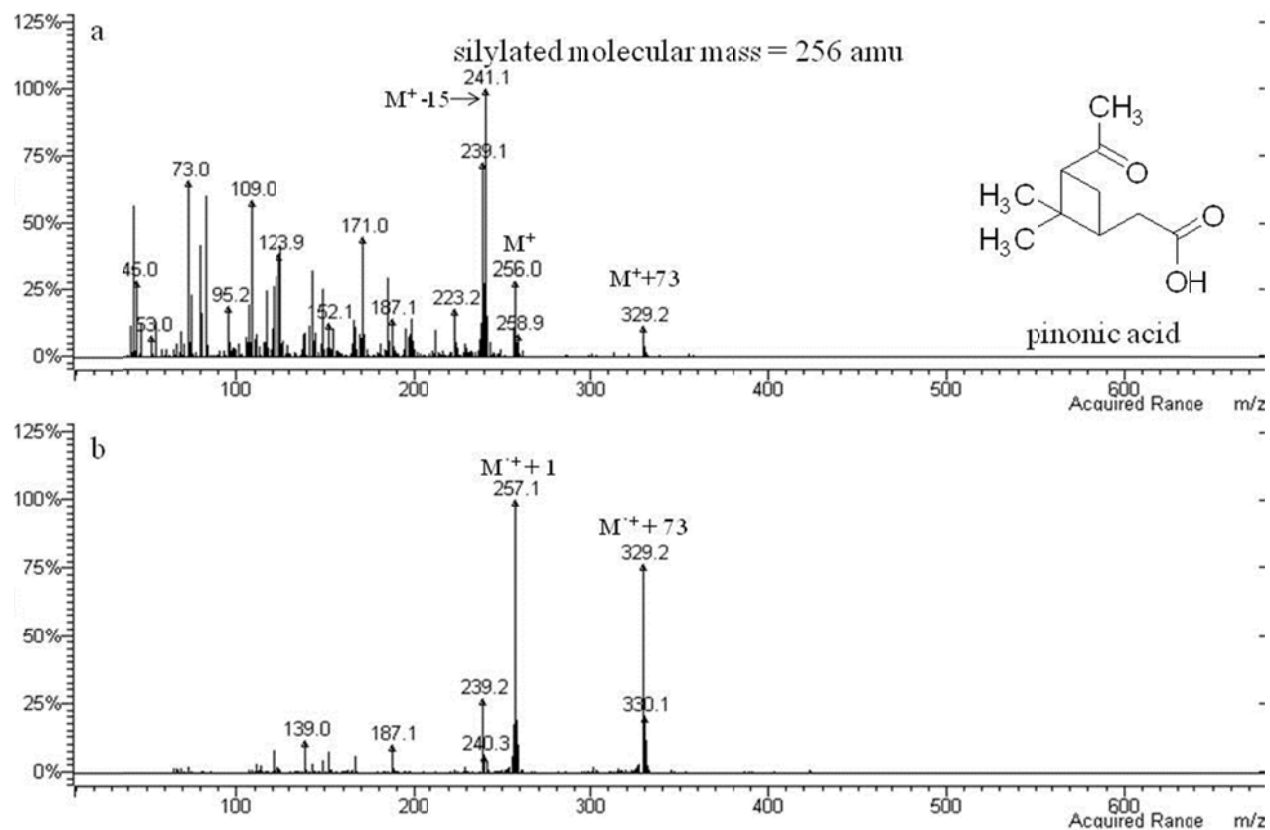


**Figure A-IV 3** EI (a) and CI (b) mass spectra for trimethylsilyl derivative of nor-3-caralic acid

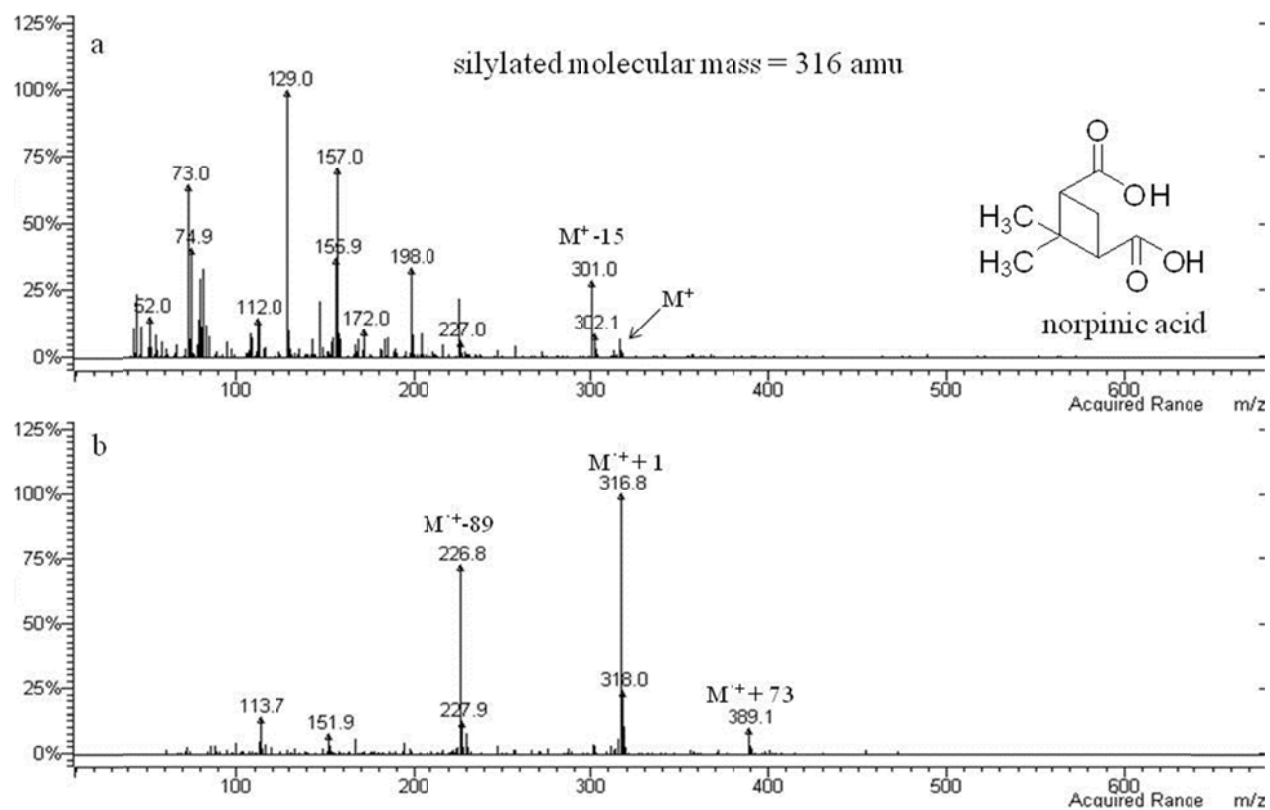


**Figure A-IV 4** EI (a) and CI (b) mass spectra for trimethylsilyl derivative of camphene unknown 1, suggested molecular formula  $C_9H_{16}O_2$

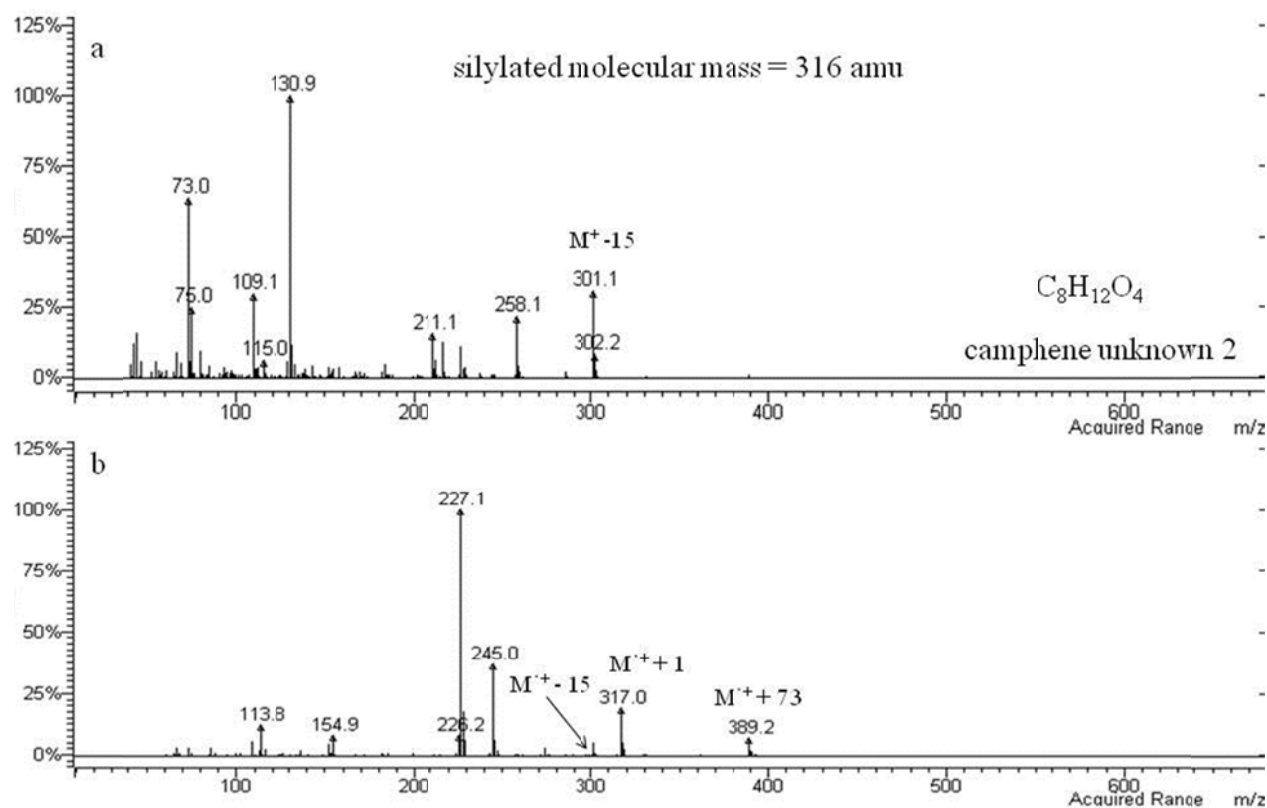




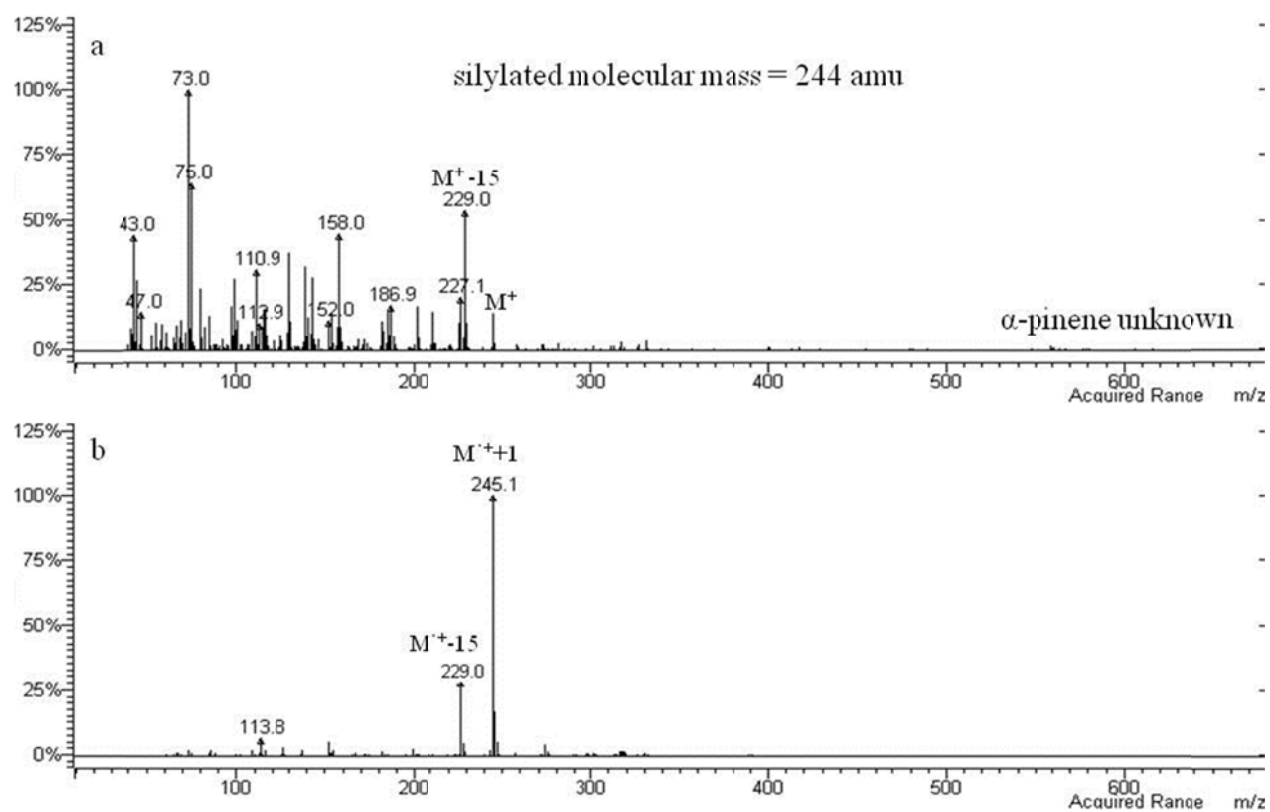
**Figure A-IV 5** EI (a) and CI (b) mass spectra for trimethylsilyl derivative of pinonic acid



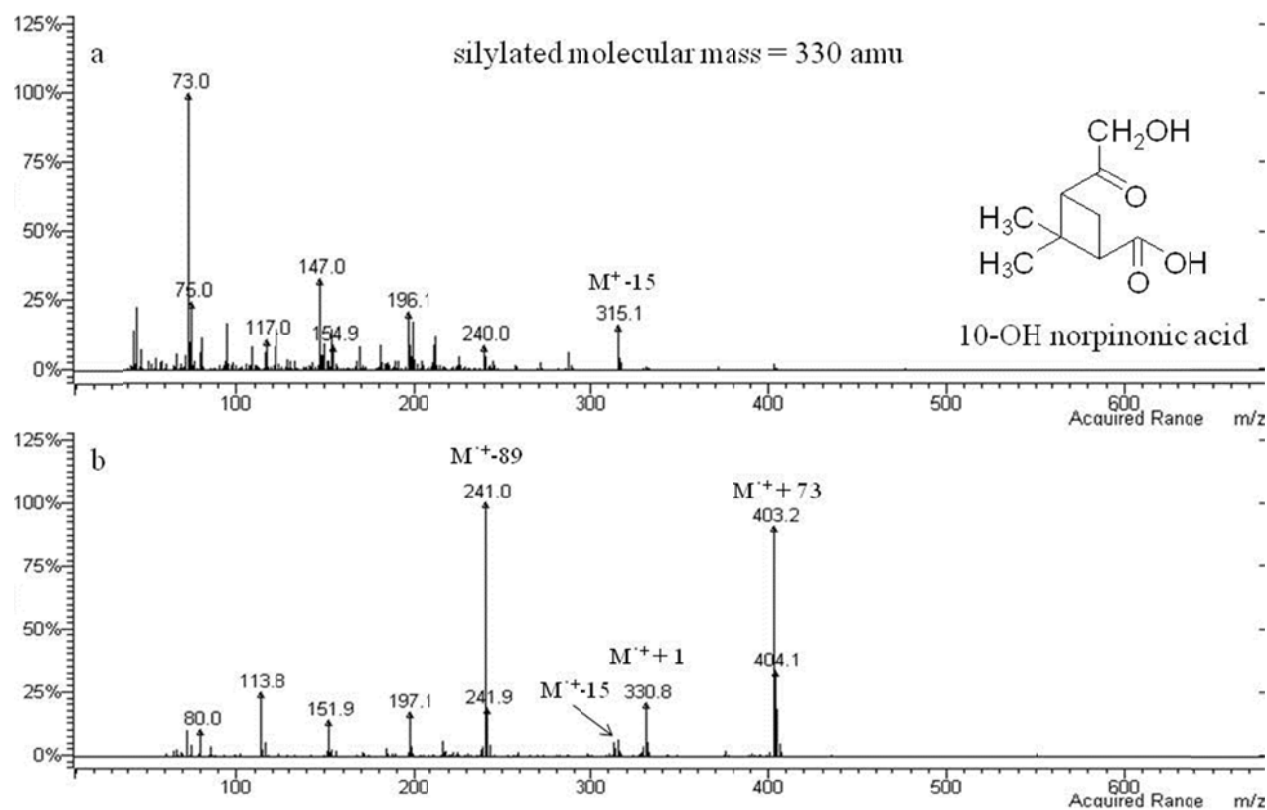
**Figure A-IV 6** EI (a) and CI (b) mass spectra for trimethylsilyl derivative of norpinic acid



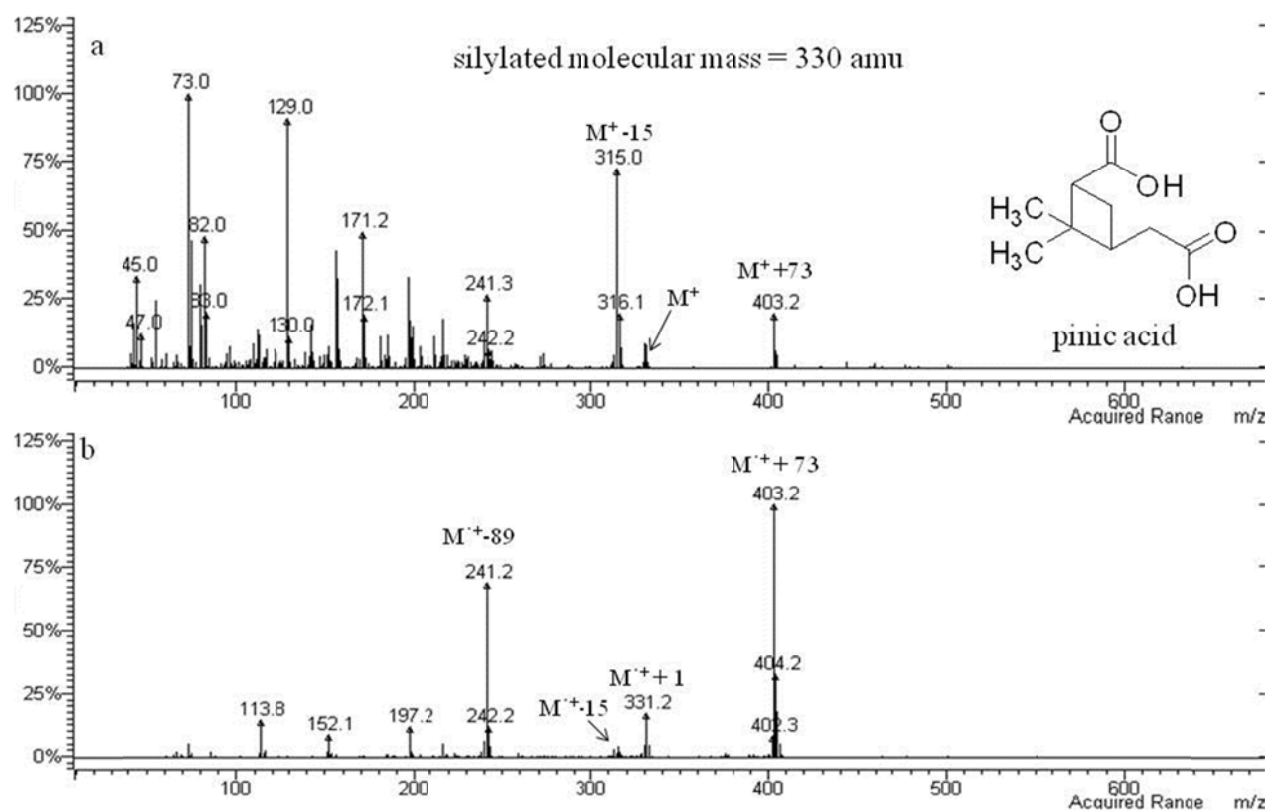
**Figure A-IV 7** EI (a) and CI (b) mass spectra for trimethylsilyl derivative of camphene unknown 2, suggested molecular formula  $C_8H_{12}O_4$



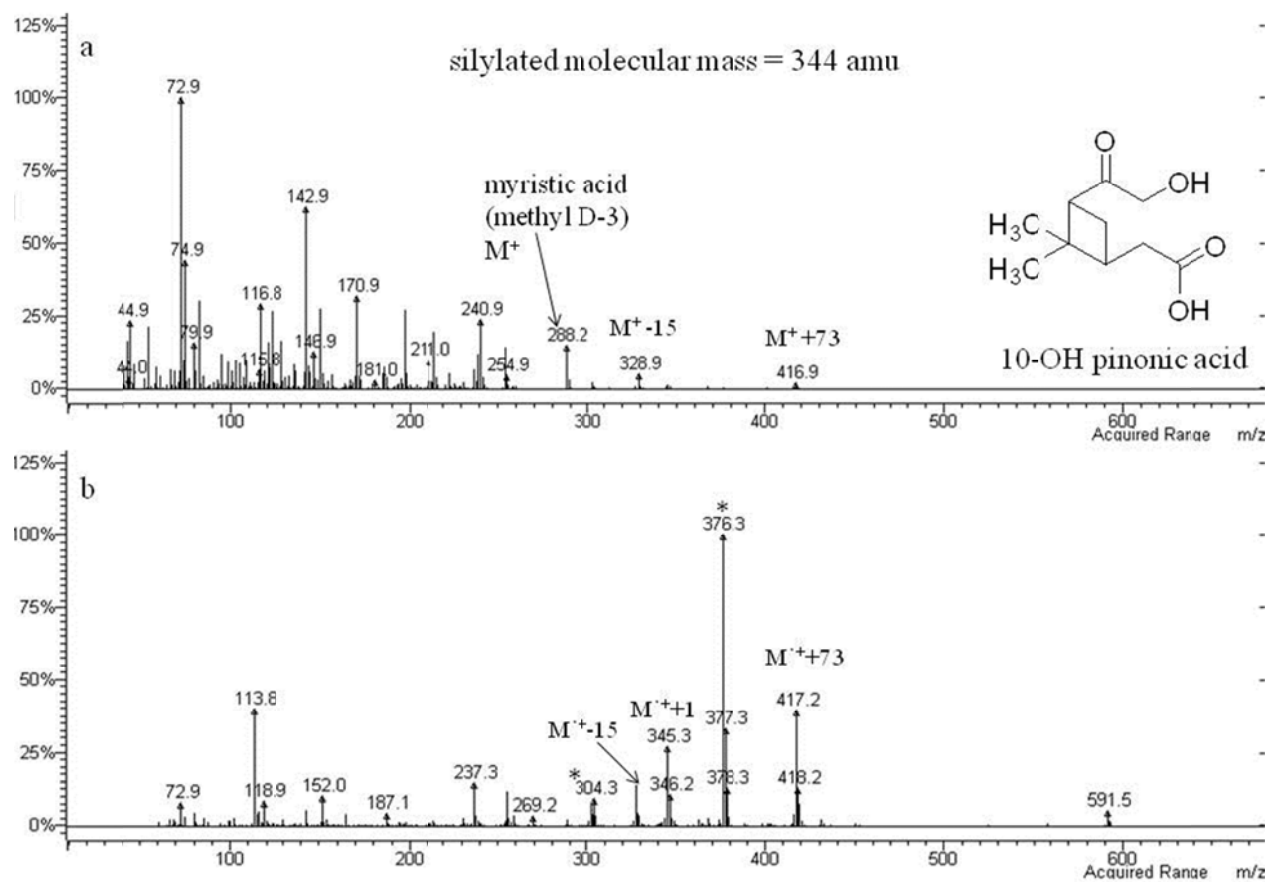
**Figure A-IV 8** EI (a) and CI (b) mass spectra for trimethylsilyl derivative of  $\alpha$ -pinene unknown



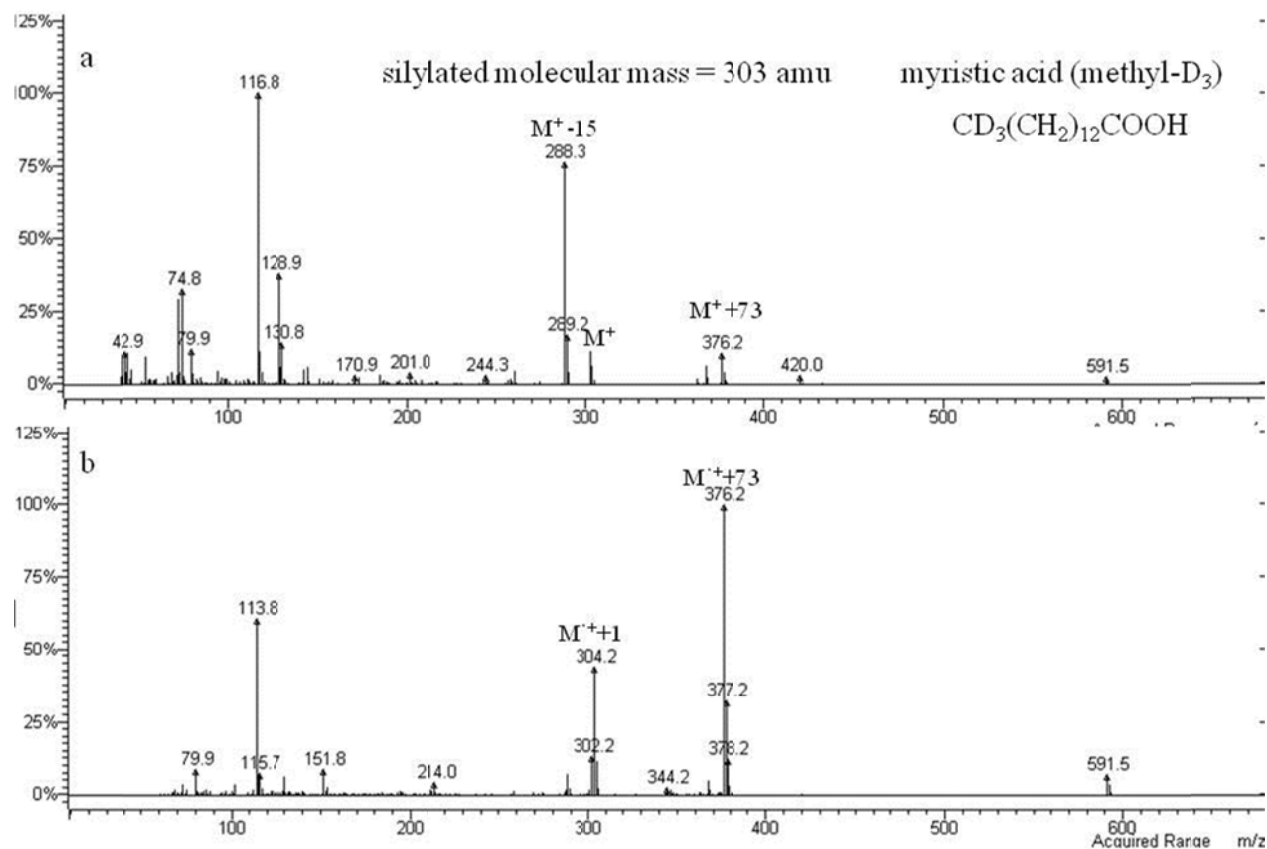
**Figure A-IV 9** EI (a) and CI (b) mass spectra for trimethylsilyl derivative of 10-OH norpinonic acid



**Figure A-IV 10** EI (a) and CI (b) mass spectra for trimethylsilyl derivative of pinic acid



**Figure A-IV 11** EI (a) and CI (b) mass spectra for trimethylsilyl derivative of 10-OH pinonic acid

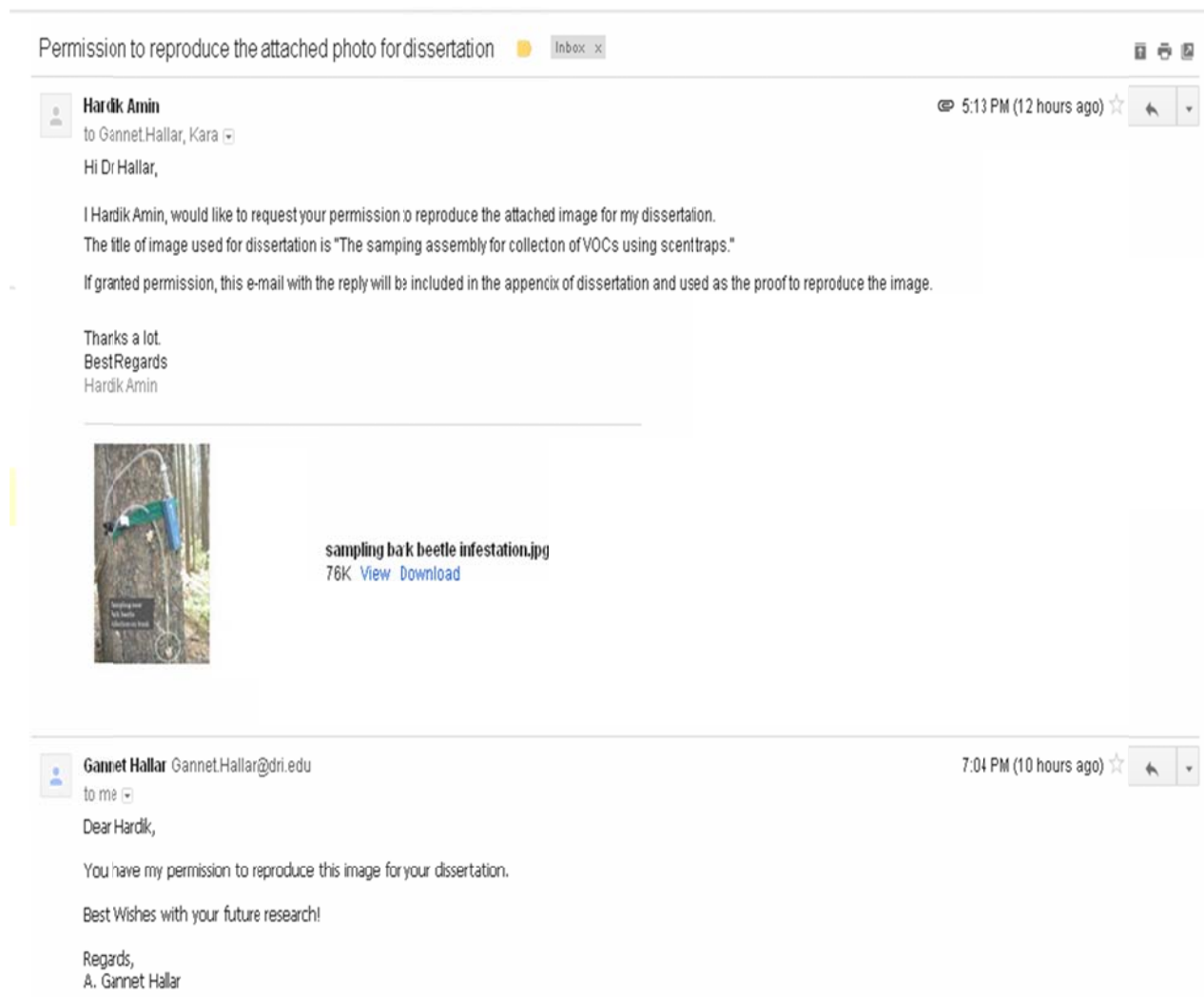


**Figure A-IV 12** EI (a) and CI (b) mass spectra for trimethylsilyl derivative of myristic acid (methyl D-3)



## Appendix V

### PERMISSION TO REPRODUCE FIGURE 2.2 “THE SAMPLING ASSEMBLY FOR COLLECTION OF VOCs USING SCENT TRAPS”



The permission to reproduce the Figure 2.2 “The sampling assembly for collection of VOCs using scent traps”, was obtained from Dr. Gannet Hallar. Dr. Hallar was a collaborator on the project and co-authored a research publication in which the above image was included.

## VITA

Graduate School  
Southern Illinois University

Hardik Surendra Amin

hardikamin82@gmail.com

Ramnarain Ruia College, University of Mumbai  
B.Sc., Chemistry, December 2003

Ramnarain Ruia College, University of Mumbai  
M.Sc., Inorganic Chemistry, December 2005

Crocker Nuclear Laboratory/IMPROVE Program, UC Davis, CA.  
Postdoctoral Scholar, June 2012-current  
Advisor: Dr. Ann Dillner

Special Honors and Awards:

C. David Schmulbach Award for Outstanding Teaching Assistant, SIUC (2008)

Travel grant by American Association for Aerosol Research for attending Annual Conference, Orlando, FL (10/2008)

Merit Scholarship for academic excellence by Masters Student, Dr. A.P. Rao foundation, Ramnarain Ruia College, Mumbai, India

Dissertation Title:

Speciation Studies for Biogenic Volatile Organic Compounds and Secondary Organic Aerosol Generated by Ozonolysis of Volatile Organic Compound Mixtures

Major Professor: Kara E. Huff Hartz

Publications:

Sheetal Nikam, **Hardik Amin**, Pulkeshi Desai and Kiran Mangaonkar, "Stability &

Antimicrobial studies of Mn(II), Fe(III), Co(II), Ni(II) & Cu(II) metal chelates of N,N'-

bis(salicyldehyde)-1,8-Naphthalenediamine." *Asian Journal of Chemistry*, 17(4), 2451-2454

(2005)

**Hardik Amin**, P. Tyson Atkins, Craig Dodson and A. Gannet Hallar and Kara Huff Hartz

“Effects of Bark Beetle Infestation on Secondary Organic Aerosol Precursors in Western United States” *Environ. Sci. Technol.*, **2012**, in press.

**Hardik Amin**, Kara E. Huff Hartz, “SOA Formation and Speciation Studies for Ozonolysis of Limonene Dominated mixed VOC systems” *To be submitted to Indoor Air*.

**Hardik Amin**, Meagan Hatfield, Kara E. Huff Hartz, “Speciation Studies for Ozonolysis of  $\alpha$ -pinene VOC mixtures” *To be submitted to Atmos. Environ.*

Conference Proceedings (talks):

**Hardik Amin** and Kara Huff Hartz, “Speciation and formation of SOA generated from ozonolysis of realistic terpene mixtures” ACS Midwest /Great Lakes Regional Meeting, St Louis, MO (10/2011)

**Hardik Amin**, Meagan Hatfield, John Junge, Audrey Wagner and Kara Huff Hartz, “Speciation of the ozonolysis products of household volatile organic compounds” American Association for Aerosol Research Annual Conference, Orlando, FL (10/2008)